

Glaciation or not? An analytic review of features of glaciation and sediment gravity flows: introducing a methodology for field research

Mats O. Molén¹

¹Umeå FoU AB

November 21, 2022

Abstract

For more than 150 years, geological features claimed to be evidence for pre-Pleistocene glaciations have been debated. Advancements in recent decades, in understanding features generated by glacial and mass flow processes, are here reviewed. It is timely to make renewed comparisons and to re-visit the interpretations of data used to support pre-Pleistocene glaciations. Similarities and differences of Quaternary glaciogenic and sediment gravity flow features, which are most often referred to as proxies and evidence of ancient glaciations, are documented, discussed and closely examined, in order to uncover the origin of more ancient deposits. It is necessary to use multiple proxies to develop a correct interpretation of ancient strata. Analyses and evaluation of data are from a) Quaternary glaciations and glaciers, b) formations which have been assigned to pre-Pleistocene glaciations, and c) formations with comparable features associated with mass-flow deposition (and occasionally tectonics). The aim is not to reinterpret specific formations and past climate changes, but to enable data to be evaluated using a broader and more inclusive conceptual framework. To achieve this goal, detailed descriptions of field evidences are documented from papers that may suggest different interpretations of these data. This is not in an intention to present revised interpretations of these papers, but to collect data and develop a foundation for enhanced analysis of geologic processes and features. Regularly occurring features interpreted to be glaciogenic and are contemporaneous with pre-Pleistocene diamictites which have been interpreted to be tillites, have often been shown to have few or no Quaternary glaciogenic equivalents. These same features commonly form by sediment gravity flows or other non-glacial processes, which may have led to misinterpretations of ancient deposits. These features include, for example, appearances and documented data from the extent and thickness of diamictite deposits, environmental and depositional affinity of fossils in close connection to diamictites, grading and bedding of diamictites, fabrics, size of erratics, polished and striated clasts and surfaces (“pavements”), boulder pavements, lineations, valleys, glaciofluvial deposits, dropstones, laminated sediments, glaciomarine sediments, periglacial structures, soft sediment tectonics, and surface microtextures. The analysis of these features provide detailed documentation that may be used to help identify the origin for many pre-Pleistocene diamictites. Recent decades of progress in research relating to glacial and sediment gravity flow processes has resulted in proposals by geologists, based on more detailed field data, more often of an origin by mass movements and tectonism than glaciation. The most coherent data of this review, i.e. appearances of features produced by glaciation, sediment gravity flows and a few other geological processes, are summarized in a Diamict Origin

Item marked with *** have to be changed later. It is a reference where the article is in press and final volume is not known.

1 **Glaciation or not? An analytic review of features of glaciation**
2 **and sediment gravity flows: introducing a methodology for**
3 **field research**

4 Mats O. Molén

5 Umeå FoU AB, Vallmov 61, S-903 52 Umeå, Sweden

6 Table of contents

7 1. Introduction

8 1.1. Structure of the current paper

9 1.2. Historical sketch

10 1.3. Bias in diamictite research

11 1.4. Geologic features produced by sediment gravity flows

12 2. Similarities and differences between glaciogenic and other geologic features

13 2.1. Geographical extent, dating, climate and fossils

14 2.1.1. Geographical extent

15 2.1.2. Correlations and dating

16 2.1.3. Fossil vegetation

17 2.1.3.1. Association between vegetation and glaciogenic sediments

18 2.1.3.2. Ecology

19	2.2. Till structure
20	2.2.1. More mass flows and marine sediments than basal glaciogenic sediments
21	2.2.2. No rock flour and density of deposits
22	2.2.3. Correlation between clast size and thickness of strata
23	2.2.4. Grading in sediments
24	2.2.5. Bedding and amalgamation
25	2.2.6. Presence of soft sediment structures
26	2.2.7. Clasts pressed into underlying surface
27	2.2.8. Channels below “tillites”
28	2.2.9. Fabrics
29	2.2.10. Flutes
30	2.2.11. Impact structures, meteorites
31	2.3. Erratics
32	2.3.1. Erratics, transport and inclinations – similarities
33	2.3.2. Erratics, transport and inclinations – differences
34	2.3.2.1. Size dependence
35	2.3.2.2. Jigsaw puzzle texture
36	2.4. Polished, faceted and striated clasts
37	2.5. Striated, grooved and polished surfaces/pavements
38	2.5.1. Presence of striated, grooved and polished surfaces/pavements
39	2.5.2. Formation of striated, grooved and polished surfaces/pavements
40	2.5.3. Differences displayed by striated, grooved and polished surfaces/pavements
41	2.6. Striated, grooved and polished surfaces, rock polish
42	2.7. Striated, grooved and polished surfaces, iceberg keel scour marks
43	2.8. Boulder pavements
44	2.9. Erosional landforms, lineations
45	2.10. Erosional landforms – plucking

46	2.11. Glacial and non-glacial valleys and fjords
47	2.11.1. Glacial and non-glacial valleys – general appearance
48	2.11.2. Glacial and non-glacial valleys – shape
49	2.11.3. Glacial and non-glacial valleys – fjords
50	2.12. Glaciofluvial deposits
51	2.12.1. Eskers
52	2.12.2. Tunnel valleys
53	2.12.3. Raised channels, eskers and tunnel valleys
54	2.13. Dropstones
55	2.13.1. Dropstones, similarities
56	2.13.1.1. Transport by sediment gravity flows
57	2.13.1.2. Transport by vegetation, animals and floatation
58	2.13.3. Dropstones, differences
59	2.14. Laminated sediments
60	2.15. Glaciomarine (and lake) diamictites
61	2.16. Periglacial structures
62	2.17. Soft sediment deformation, tectonism
63	2.18. SEM studies
64	3. Discussion
65	4. Conclusion
66	5. Appendix: Diamict Origin Table
67	6. References
68	Supplementary material: Tables.
69	ABSTRACT

70 For more than 150 years, geological features claimed to be evidence for pre-Pleistocene
71 glaciations have been debated. Advancements in recent decades, in understanding features
72 generated by glacial and mass flow processes, are here reviewed. It is timely to make renewed
73 comparisons and to re-visit the interpretations of data used to support pre-Pleistocene
74 glaciations. Similarities and differences of Quaternary glaciogenic and sediment gravity flow
75 features, which are most often referred to as proxies and evidence of ancient glaciations, are
76 documented, discussed and closely examined, in order to uncover the origin of more ancient
77 deposits. It is necessary to use multiple proxies to develop a correct interpretation of ancient
78 strata.

79 Analyses and evaluation of data are from a) Quaternary glaciations and glaciers, b) formations
80 which have been assigned to pre-Pleistocene glaciations, and c) formations with comparable
81 features associated with mass-flow deposition (and occasionally tectonics). The aim is not to
82 reinterpret specific formations and past climate changes, but to enable data to be evaluated
83 using a broader and more inclusive conceptual framework. To achieve this goal, detailed
84 descriptions of field evidences are documented from papers that may suggest different
85 interpretations of these data. This is not in an intention to present revised interpretations of
86 these papers, but to collect data and develop a foundation for enhanced analysis of geologic
87 processes and features.

88 Regularly occurring features interpreted to be glaciogenic and are contemporaneous with pre-
89 Pleistocene diamictites which have been interpreted to be tillites, have often been shown to
90 have few or no Quaternary glaciogenic equivalents. These same features commonly form by
91 sediment gravity flows or other non-glacial processes, which may have led to
92 misinterpretations of ancient deposits. These features include, for example, appearances and
93 documented data from the extent and thickness of diamictite deposits, environmental and
94 depositional affinity of fossils in close connection to diamictites, grading and bedding of

95 diamictites, fabrics, size of erratics, polished and striated clasts and surfaces (“pavements”),
96 boulder pavements, lineations, valleys, glaciofluvial deposits, dropstones, laminated
97 sediments, glaciomarine sediments, periglacial structures, soft sediment tectonics, and surface
98 microtextures. The analysis of these features provide detailed documentation that may be
99 used to help identify the origin for many pre-Pleistocene diamictites. Recent decades of
100 progress in research relating to glacial and sediment gravity flow processes has resulted in
101 proposals by geologists, based on more detailed field data, more often of an origin by mass
102 movements and tectonism than glaciation. The most coherent data of this review, i.e.
103 appearances of features produced by glaciation, sediment gravity flows and a few other
104 geological processes, are summarized in a Diamict Origin Table.

105 *Keywords:*

106 tillite

107 sediment gravity flow (SGF)

108 striation

109 groove

110 dropstone

111 paleoclimate

112 fossil vegetation

113 glaciogenic proxies

114 surface microtexture

115 Late Paleozoic Ice Age

116 *Terminology*

117 *Dropstone and lonestone:* Dropstone is a genetic label for a clast that has been dropped into

118 water from ice. This label may also be used for clasts dropped by other agents, like from
119 floating vegetation. In the current paper the label dropstone will refer to any outsized clasts
120 which have been interpreted in the literature to be dropped from ice, even if that interpretation
121 may not be valid. A non-genetic term for outsized clasts is lonestone. This term would be
122 better to use than dropstone, but as lonestones are commonly interpreted to be dropstones and
123 the terms sometimes even are used interchangeable, the label dropstone is used whenever it
124 has been done so by earlier researchers. Otherwise, the interpretation of the origin has to be
125 discussed for every clast that is referred to.

126 *Groove*: Commonly defined in width as >10 mm up to a few meters or more. Marine
127 geologists may label any large linear erosional (V-shaped) forms as grooves (Nwoko et al.,
128 2020a), even if they are kilometers in width, but in the current paper the definition is used for
129 erosion by tools.

130 *Striation*: Commonly defined as <10 mm in width. Marine geologists may label large
131 erosional (wide and flat-bottomed) channels made by megaclasts on the sea bottom as
132 striations (Nwoko et al., 2020a), but that definition is not used in the current paper.

133 *Tillite and "tillite"*: This label is a genetic term, and by definition a lithified till. Any ancient
134 diamictite which has been classified as tillite by former researchers, even if the evidence from
135 recent geological research indicates a non-glacial origin of the deposit, will here also be
136 labeled tillite. If the word diamictite should be used instead of tillite, then the current or most
137 common interpretation of the deposit will be missed. Therefore, for the discussions
138 concerning the interpretation of the origin of a deposit, the term will be marked within
139 quotation marks, i.e. "tillite," independent of the most recent interpretation.

140 **1. Introduction**

141 *1.1. Structure of the current paper*

142 The basic assumption for the current paper is that the recent is better known than the past.
143 This is an actualistic approach, i.e., the principle that the same processes and natural laws
144 applied in the past are the same as those active today. By not using models or longstanding
145 interpretations, but recent field studies and experiments, this actualistic approach is followed.
146 Recent progress in studies of sediment gravity flow (SGF) (used interchangeably with mass
147 flow), glaciogenic and a few other processes which may be relevant, are applied when
148 documenting the origin of ancient deposits. Where there is a lack of published data,
149 documentation is compiled or otherwise acknowledged as missing. It may be questioned that
150 mainly Quaternary examples of geologic features are used in comparison to features from the
151 much longer pre-Quaternary time scales, but as it is assumed that natural laws have not
152 changed, this will not be much of a problem.

153 Diamictites are often interpreted to have been formed in a cold climate environment based on
154 the general structure of the deposits, associated geologic features, and polar wander paths.
155 Geochemical data may be used to strengthen the interpretation of glaciation, but these display
156 apparent shortcomings (Frimmel, 2010; Bahlburg and Dobrzinski, 2011; Garzanti and
157 Resentini, 2016; Macdonald, 2020; Caetano-Filho et al., 2021; Mikhailova et al., 2021;
158 Rogov et al., 2021; Scotese et al., 2021; Retallack et al., 2021). Similarities in outcrop of
159 most of the features of glaciation may, however, be produced by different geologic processes
160 (Isbell et al., 2021), mainly SGFs, and therefore more detailed criteria are needed for
161 interpretation. The current paper analyzes and reviews a broad range of such geologic
162 features. The intention is to design questions for field research, rather than to present
163 solutions to all problems of interpretation. Only the appearance of geologic features which are
164 described in great detail will be documented, and former general inferred interpretations of
165 glaciation may not be followed. Different processes which may create similar features are
166 documented in a way of using process-related or “process-sedimentological” principles “to
167 consider alternative hypotheses” (Shanmugam, 2012). Relevant field data is summed up in a

168 Diamict Origin Table, as a guide to the interpretation of the geologic features which have
169 been documented and discussed (Appendix).

170 Even if there is an awareness of the importance of gathering data from different research
171 disciplines, it may be difficult to evaluate what data shall be used while constructing and
172 interpreting models. Areas which have been described to have formed by ancient glaciations
173 have to be discussed from data compilation from many research disciplines. It may also be
174 insufficient to use interpretations from different research disciplines or articles as facts, if the
175 research data may be better described from a different geological and climatological aspect
176 than is currently done.

177 The current paper concentrates on features which are most often reported and also
178 documented in detail in association with “tillites,” and these are compared to similar features
179 from Quaternary glaciations and SGFs that mimic (or are) these features. Therefore,
180 unintentionally, this work may have become controversial, not because of the compilation of
181 research data, but because of longstanding interpretations of many ancient deposits. The
182 documentation is to a large part biased by reference to well documented and extensive
183 outcrops. The main exception is the documentation of outsized clasts, because limestones are
184 often interpreted to be dropstones and therefore are commonly suggested to be evidence for
185 glaciation (e.g., Rodríguez-López et al., 2016; López-Gamundí et al., 2021; Le Heron et al.,
186 2021a; Bronikowska et al., 2021).

187 *1.2. Historical sketch*

188 Ever since diamictites were first interpreted to be pre-Pleistocene ice age deposits, by Ramsay
189 in 1855 for some Permian boulder deposits in England (Harland and Herod, 1975; Hoffman,
190 2011), there has been much controversy over their interpretation. The first steps of SGF

191 research can be said to have started in 1827, with the introduction of the term flysch (Studer,
192 1827). The first mention of a submarine fan was in 1955 (Menard, 1955), and the first
193 mention of a turbidite-fan link in ancient fans was in 1962 (Bouma, 1962; Shanmugam,
194 2016). The importance of SGFs in the geologic record has often been underestimated
195 (Shanmugam, 2016, 2020, 2021b), even if SGF deposits have often been documented in
196 papers concerning diamictites. Lately, hyperpycnal flows have been recognized to transform,
197 after deposition, into a full spectrum of SGF deposits, including cohesive debris flows and
198 rhythmites, which adds one more dimension to this research area (Zavala and Arcuri, 2016;
199 Shanmugam, 2019, 2021b; Zavala, 2019, 2020).

200 Since the early 1970s, starting with an earlier paper by Crowell (1957), it has been recognized
201 that many “ice-age remains” have been deposited by different kinds of SGFs, for example by
202 turbidity currents but especially by cohesive debris flows. For example, in the Tertiary of
203 Alaska, twelve major glaciations were reinterpreted as formed largely by SGFs (Plafker et al.,
204 1977; Eyles and Eyles, 1989). Schermerhorn published a comprehensive review which
205 documented the evidence for a SGF origin of ancient diamictites, shown in his classic work
206 on Late Precambrian diamictites (Schermerhorn, 1974a, 1976a, 1976b, 1977). The current
207 paper is partly inspired by the work of Schermerhorn, but is also influenced by published
208 work on fan deposits and SGFs (Shanmugam, 2016; Peakall et al., 2020). Many researchers
209 in addition to Schermerhorn have compared tills, glaciomarine sediments and different kinds
210 of SGFs, but the work may have been hampered by the assumption that outcrops with
211 equivocal origin are ice-age deposits (Hambrey and Harland, 1981; Boulton and Deynoux,
212 1981; Anderson, 1983; Wright et al., 1983; Eyles, 1993). The documentation in
213 Schermerhorn’s classic paper (1974a) has to a large part gone unnoticed, even though this
214 article may be referred to in passing (e.g., Le Heron et al., 2017). Eyles (1993) wrote: “ ...
215 unfortunately, the inclusion of strata that were indisputable of a glacial origin weakened the
216 essential correctness of Schermerhorn’s argument.”

217 Pre-Pleistocene formations which are, or have been, interpreted to have formed by glaciations
218 are documented from the Archean, the Paleoproterozoic, the Neoproterozoic, and during all
219 periods of the Phanerozoic (Hambrey and Harland, 1981; Caputo and Santos, 2020; Youbi et
220 al., 2021) sometimes even in the tropics and indicating low elevations (Soreghan et al., 2014),
221 including during five different episodes of the Cretaceous (Alley et al., 2020). The most
222 accepted and geologically important glaciations are in the Paleoproterozoic, the
223 Neoproterozoic, the Upper Ordovician, and the Late Paleozoic Ice Age (LPIA; recently dated
224 to 372-259 million years; Pauls et al., 2021) (Hambrey and Harland, 1981).

225 *1.3. Bias in diamictite research*

226 Glaciogenic proxies are documented in order to find stratigraphic intervals displaying
227 glaciations, as there, on the basis of uniformitarianism, had been many glaciations throughout
228 earth history (e.g., Williams, 2005). The current interpretation of a stratigraphic interval
229 commonly biases the research questions and which observations and measurements are made,
230 and frequently it is mainly data supposed to be relevant for the current interpretation that are
231 reported. These circumstances have resulted in that alternative interpretations were not always
232 fully investigated. Therefore the features which are described in the literature often contain
233 too few details to establish if the deposits have originated from glacial action, SGF or by any
234 other means. For example, a clast or a surface with striations is often reported to have been
235 glacially striated if present in connection to a diamictite (Atkins, 2003). In other words,
236 features which may be formed in different environments are reported, but diagnostic features
237 may not be documented or discussed. Single or even groups of features which display
238 appearances partly similar to and interpreted to be glaciogenic features, may subsequently be
239 shown to be very different from Pleistocene and more recent glaciogenic features. In short,
240 the question of the origin of diamictites has become a part of a scientific paradigm (Kuhn,
241 1970; Shanmugam, 2016) connected to long-term climatic correlations (Young, 2013; Shields

242 et al., 2022).

243 As recent research uncovers growing evidence of non-glacial transport, diamictites worldwide
244 have more often been interpreted as glaciomarine and often considered as parts of interglacial
245 periods. This includes approximately 95% of all “glaciogenic” deposits, i.e. sediments which
246 may contain an abundance of marine fossils, and to a large part are made up of SGF deposits
247 (Eyles 1993; González and Glasser, 2008; Isbell et al., 2016; López-Gamundí et al., 2016,
248 2021; Assine et al., 2018; Vesely et al., 2018; Rosa et al., 2019; Sterren et al., 2021; Isbell et
249 al., 2021; Molén and Smit, 2022). These interpretations make it more difficult to discover if
250 the deposits had been produced primarily by glaciation or are non-glacial marine. In this case
251 often the only “unequivocal” evidence for glacial influence is considered to be dropstones,
252 especially if outsized clasts occur in rhythmites, but also if SGF deposits or stratified
253 diamictites display outsized clasts (e.g., Ezpeleta et al., 2020). Apart from dropstones, striated
254 clasts and surfaces (“pavements”) are commonly referred to as evidence for glaciation
255 without discussing alternative interpretations in depth (e.g., different examples in Molnia,
256 1983a; Miall, 1983, 1985; Eyles, 1993; Hoffman et al., 1998; Carto and Eyles, 2012a;
257 Rodríguez-López et al., 2016; Le Heron et al., 2017; Le Heron and Vandyk, 2019).

258 *1.4. Geologic features produced by sediment gravity flows*

259 Gravity-induced slope processes include variations of rock fall, slides, slumps, debris flows
260 and turbidites. In some outcrops there is an almost complete visible sectioned sequence,
261 horizontally and/or vertically, which shows how mass movements have changed from e.g.,
262 slides, to debris flows, and finally to turbidity currents (Ogata et al., 2019; Rodrigues et al.,
263 2020; Kennedy and Eyles, 2021). Sedimentary and erosional features which commonly form
264 from such processes, especially those originating from cohesive debris flows, share many
265 similarities in appearance to glaciogenic features and are present in many diamictites which

266 had been interpreted to be glaciogenic (e.g., Molén, 2017, 2021). Another process which
267 shows similarities to slope processes are land derived hyperpycnal flows. Such flows can in
268 some cases last for months. Even though they have a different origin from slope processes,
269 they display similarities in the sedimentation process and the deposits may be reworked and
270 transform into a full spectrum of SGFs (Zavala and Arcuri, 2016; Shanmugam, 2019, 2021b;
271 Zavala, 2019, 2020). Hyperpycnal flow deposits are therefore included here in what is
272 commonly described as SGF deposits.

273 Below is a list of features that commonly originate by especially cohesive debris flows, but
274 which also may originate from other slope processes like turbidites and slides that commonly
275 co-occur with debris flows. These geologic features are important to acknowledge as there are
276 differences between features of glaciation and SGFs which will be outlined herein. The
277 features below are well known in the geologic community within the discipline of slope
278 processes, but the details are often not well known outside of this community. All the features
279 listed have to be acknowledged. An assemblage of these are commonly present in close
280 connection to diamictites, i.e. they are parts of ancient diamictites and other erosional and
281 depositional features which have been interpreted to be glaciogenic, and are by definition also
282 present in areas displaying non-glacial SGF deposits. If the features in the list below are
283 studied more in detail, it may be possible to demonstrate if an area or outcrop was formed
284 mainly by SGFs or by glaciation. A subsample of references from a complete research
285 discipline, which may be the most important from the discipline of SGF research, which all
286 document many of the features in the list below, are Middleton and Hampton (1976),
287 Shanmugam et al. (1994), Schneider and Fisher (1998), Major et al. (2005), Moscardelli et al.
288 (2006), Talling et al. (2007, 2012, 2015), Watt et al. (2012), Dakin et al. (2013), Pickering
289 and Hiscott (2015), Shanmugam (2016, 2020, 2021), Peakall et al. (2020), Cardona et al.
290 (2020), Baas et al. (2021); Dufresne et al. (2021).

291 a) diamict texture, but deposits often may be in streaks and display some sorting and grading,

- 292 b) grooves and striations on clasts and surfaces/pavements, especially below debris flows that
293 may hold clasts in fixed positions,
- 294 c) lonestones which may be interpreted as dropstones,
- 295 d) sharp and irregular fronts,
- 296 e) a great degree of scatter and variable thickness of the deposits,
- 297 f) variable erosion and depth of deformation of the underlying substratum (e.g, sharp,
298 undulating, interdigitating, ripple-type, grooved),
- 299 g) deposition in or at the end of channels,
- 300 h) reworking at the top of the deposits by bottom currents,
- 301 I) conformably draping by mass flow beds of rapid deposition (mainly turbidites),
- 302 j) soft sediment structures, like load casts, clastic dykes, boudinage, folds and convolute
303 bedding,
- 304 k) scour and fill structures,
- 305 l) rhythmites,
- 306 m) climbing ripples,
- 307 n) contorted rip-up soft slabs of sandstone or other sediments,
- 308 o) mud-flakes or clasts which have often been pressed down into the underlying sediments
309 from above, and therefore the beds also display holes or depressions below debrites, where
310 embedded clasts have been eroded out,
- 311 p) a thickness-to-width ratio commonly thicker than 1:50,
- 312 q) more than 3-5% clay, or otherwise may transform distally into hyperconcentrated flow or
313 sediment-laden floods,
- 314 r) an appearance of crossbedding,
- 315 s) a basement which has been rounded with a superficial appearance of having been glaciated,
316 e.g. displaying bedrock forms similar to roches moutonnées, even with evidence of plucking,
- 317 t) brecciation of the substratum, which may also display cataclasis,
- 318 u) a thin basal layer of debris, i.e. a traction carpet or liquefied sandstone,

- 319 v) rip up soft sedimentary megaclasts with intact stratigraphy,
- 320 x) entrainment of sediments, including processes that may be defined as plucking, during the
- 321 complete path of movement,
- 322 y) laminar behavior,
- 323 z) uphill movement,
- 324 za) no or rare evidence of fossils,
- 325 zb) an upper hummocky terrain,
- 326 zc) drop formed landforms which are erosional remnants.

327 **2. Similarities and differences between glaciogenic and other geologic features**

328 Ancient outcrops commonly are visually restricted, and therefore it may be difficult to
329 document appearances of features from the action of glaciers or any other processes. Many
330 different geological features which may be misinterpreted in restricted outcrops, are
331 documented below. Some researchers state that it may be impossible to confidently identify a
332 specific environment of deposition by macroscopically features and textural criteria
333 (Kilfeather et al., 2010), but as is documented in the current paper there are more unequivocal
334 criteria than is usually recognized.

335 If there is glaciogenic material which has never been processed by but only transported by a
336 glacier, such as supraglacial till, it will not acquire many of the characteristics imposed by
337 glacial forces. The same holds for flow tills, if they are supraglacial mass flows that have
338 never been covered by a glacier. This may also hold for some aspects of squeezed flow till
339 (Hicock, 1991; Hicock and Dreimanis, 1992b). Flow tills are in any case difficult to
340 differentiate from non-glaciogenic mass flows, especially if they are formed subaqueously
341 (Evenson et al., 1977). Englacial till which has been deposited as melt-out till also may not
342 acquire many glaciogenic features. However, all material that is deposited in a subglacial

343 environment will display evidence of this process (Mahaney, 2002; Molén, 2014).

344 Furthermore, supraglacial tills and other tills that have not been transported at the base of a
345 glacier are usually a minor part of glaciogenic sediments, and they are easily removed by later
346 erosion, in contrast to basal till.

347 Many features which are interpreted to be evidence of glaciation form in a wide range of
348 environments (e.g., Eyles, 1993; Eyles and Boyce, 1998; Atkins, 2003; Thompson, 2009). If
349 clasts from one environment are incorporated by a new process, e.g., tectonic material that is
350 mixed with finer material and beach/slope material in a debris flow, the origin of the deposit
351 may be difficult to uncover (e.g., Festa et al., 2019). This mixing of different materials is
352 common in SGFs, and up to 50% of the material may be entrained through erosion from the
353 substrate along the path of the flow (e.g., Thompson, 2009; Carto and Eyles, 2012a, 2012b;
354 Ortiz-Karpf et al., 2017; Ogata et al., 2019; Nugraha et al., 2020; Rodrigues et al., 2020).
355 Eyles and Eyles (2000) described a “cement-mixer-model” of how different sediments could
356 mix.

357 Each of the features reviewed in the sections 2.1.-2.18. is commonly referred to when
358 exploring evidence of glaciation. There is, however, an increasing understanding that similar
359 features, which more or less mimic the typical glacial features, also can originate as a
360 consequence of different kinds of SGFs and other non-glacial processes. In addition, there are
361 many geologic features from “ancient ice-ages” which have rarely or never been formed by
362 Pleistocene or younger glaciers. These features may be at odds with a glaciogenic
363 interpretation, but often at the same time indicate a SGF or/and tectonic origin. Also, there are
364 some general problems in regard to “tillites” that do not apply to SGFs, e.g. climate and
365 correlations, which are also discussed below.

366 *2.1. Geographical extent, dating, climate and fossils*

367 2.1.1. Geographical extent

368 SGFs occur worldwide, independent of latitude, and are therefore present in the same areas as
369 the more geographically restricted glaciers. Mountain glaciers are areally restricted, but are
370 present worldwide if above the equilibrium-line altitude (e.g., Mahaney, 1990).

371 The geographic extents of deposits from “ancient ice-ages” are often comparatively small and
372 “tillites” are often dispersed as separate outcrops (e.g., Lindsay, 1966; Finkl and Fairbridge,
373 1979; Fairbridge and Finkl, 1980; Deynoux and Trompette, 1981b; Le Heron et al., 2018a).

374 There are two exceptions. The first is the Ordovician deposits in northern Africa which cover
375 between 8×10^6 (Biju-Duval et al., 1981) and 20×10^6 km² (Fairbridge, 1979). The size
376 difference depends on whether the Arabian diamictites are included or not. If the lesser
377 Ordovician outcrops in South Africa, Europe and South America are included, the maximum
378 hypothetical glaciated area is c. 40×10^6 km² (Le Heron et al., 2005, 2018a; Ghienne et al.,
379 2007). The second exception is the LPIA outcrops which cover maybe 30×10^6 km² if
380 deposits from separate basins in South America, Antarctica, Australia, India, South Africa,
381 Congo and Madagascar are included (Gravenor, 1979). Parts of the Arabic Peninsula,
382 Ethiopia, Chad and a few other areas may also be included in the LPIA (e.g., Bussert, 2010,
383 2014; Le Heron, 2018). The LPIA has lately been alternatively interpreted as many smaller
384 glaciations, to a large part marine and including SGFs, and parts of the area have even been
385 described as formed in a large glacial lake (Horan, 2015; Dietrich et al., 2019; Fedorchuk et
386 al., 2019; López-Gamundí et al., 2021; Isbell et al., 2021; Ives and Isbell, 2021).

387 Neoproterozoic diamictites are commonly present in downwarping or deep basins, otherwise
388 close to rifts, and rarely on stable bedrock (Schermerhorn, 1974a; Eyles, 1993; Arnaud, 2008;
389 Frimmel, 2018; Kennedy and Eyles, 2019, 2021), and many Precambrian “tillites” can be
390 correlated with tectonic movements apparently connected to continental breakup (Eyles,

391 1993; Williams, 2005; Carto and Eyles, 2012a, 2012b; Delpomdor et al., 2016; Gómez-Peral
392 et al., 2017; Kennedy and Eyles, 2019, 2021; Molén 2021). Recent active areas of
393 tectonism/volcanism may display similar geologic features as in Precambrian “tillites” (Carto
394 and Eyles, 2012a). Peperites are mixed with Neoproterozoic diamictites in Argentina and
395 Paleoproterozoic diamictites in Canada, indicating that volcanism was the triggering process
396 for the origin of some diamictites (Young et al., 2004b; Pazos et al., 2008). Deposits from
397 Phanerozoic ice-ages have accumulated on more stable bedrock than during the Precambrian
398 (Schermerhorn, 1974a), but the LPIA formations in both southern Africa and South America,
399 have been deposited in tectonically controlled former sinking basins or close to areas of
400 tectonic movements (Johnson et al., 1997; Barbolini et al., 2018; Hansen et al., 2019; Dietrich
401 and Hofmann, 2019; Fedorchuk et al., 2019; Limarino and López-Gamundí, 2021; Creixell et
402 al., 2021; Veroslavsky, 2021; Molén and Smit, 2022). The overall geological framework of
403 the Ordovician glaciated area was a continuous transgression over a slowly subsiding cratonic
404 platform (Ghienne, 2003), and there is evidence of recurrent magmatic activity in the area
405 from the Precambrian to the Holocene (Ghuma and Rogers, 1978; El-Makhrouf, 1988; Young
406 et al., 2004a; Permenter and Oppenheimer, 2007; Liégeois, 2006). Consequently, even the
407 Paleozoic glaciations may in some aspects be connected to tectonism. Quaternary glaciations
408 commonly were and are on more stable bedrock.

409 Many ancient sedimentary deposits which are interpreted to be glacially influenced are
410 hundreds of meters to many kilometers thick (Volkheimer, 1969; Schermerhorn, 1974a;
411 Woolfe, 1994; Visser, 1989a; Vesely and Assine, 2014; Ali et al., 2018; Kennedy and Eyles,
412 2019; Rosa et al., 2019), as are mass flow deposits (Kuenen, 1964; Komar, 1970). As an
413 example, a median thickness value for 197 mass flows (mainly Pliocene and younger) is 66
414 m, but thicknesses of hundreds of meters are common and there are examples of kilometers
415 (Moscardelli and Wood, 2016; Ogata et al., 2019; Alves and Gamboa, 2020). Large mass
416 movements may even generate isostatic uplift or downwarping of the lithosphere (Kneller et

417 al, 2016). Sedimentation will in general be more massive in areas where there is rapid
418 subsidence in tectonically active basins (Kennedy and Eyles, 2021). SGF deposits may be
419 complex, multi-layered units which may have been deposited during an event or a very short
420 time period (e.g., Shanmugam, 2012, 2021b).

421 Even though the examples below are mostly from sediments deposited on oceanic crust,
422 marine fossils are present almost worldwide, from former transgressions, and marine fossils
423 are present next to geologic features which are interpreted to be glaciogenic (see examples in
424 sections 2.1., 2.13, 2.15). Massive debris flows may travel 200 km without depositing any
425 sediment (Talling et al., 2007), and therefore the resulting deposits may appear to be isolated
426 “tillite” mounds. Many SGFs travel long distances, e.g., 900-2000 km outside off the coast of
427 northwestern Africa (Georgiopoulou et al., 2010; Moscardelli and Wood, 2016), and there
428 have been suggestions of 4000 km for less dense turbidity currents (Pickering and Hiscott,
429 2015). Such flows affected extensive areas, e.g., 95 000 km² for the Storegga Slide
430 (Haflidason et al., 2004) and 132 000 km² in the Canada Basin (Moscardelli and Wood,
431 2016). The largest known Late Pleistocene debris flow influenced an area of 45 000 km²
432 (Embley, 1982) and the largest known recent turbidity current influenced an area of 500 000
433 km² (Heezen and Hollister, 1971), but SGFs are usually much more restricted in areal extent
434 than these two deposits, with a median value less than 100 km² (Moscardelli and Wood,
435 2016).

436 In contrast to “tillites” and SGF deposits, separate till beds, with characteristic structure and
437 mineral content, can be traced over hundreds of kilometers and are often less than five meters
438 thick (Schermerhorn, 1974a). Most layers are less than 100 m and usually not more than 10 m
439 thick. In Canada the thickness of the till is 2-10 m (Eyles et al., 1983), in Norway the mean
440 till layer is 5 m (Haldorsen, 1983), in Finland 2-3 m and in Sweden 5-15 m (Flint, 1971). At
441 the southern limit of the North American inland ice sheet, separate till beds are superposed

442 and in total often thicker, e.g., from 10 to 52 m in a 300 km wide band (Flint, 1971), but in
443 Europe the tills often thin out at the southern limits (Piotrowski et al., 2001). The thickest
444 known accumulation of till beds from the Pleistocene is 400 m (Flint, 1971; Schermerhorn,
445 1974a).

446 The late Cenozoic exceptions, which exhibit thick glacial sequences, are in places with
447 glaciomarine sedimentation, at the continental shelf of Antarctica and the Yakataga
448 Formation of the Gulf of Alaska (Anderson, 1983). Most of these deposits have originated by
449 SGFs but under the influence of nearby glaciers (Eyles and Lagoe, 1998).

450 Valley glaciers commonly merge into larger glaciers. Similarly “glacial” paleo-flows may be
451 in one main direction and a few smaller merging valley flow directions (Visser, 1981). This is
452 similar to what may take place during large slides/SGFs (e.g., Hafliðason et al., 2004). Also,
453 SGFs may diverge, bend and split into many smaller flows (Moscardelli et al., 2006;
454 Sobiesiak et al., 2018; Kumar et al., 2021), somewhat similar to what may take place if a
455 glacier is spreading out over a more planar surface.

456 Erosion has reduced the extent of many Pleistocene glaciogenic deposits. This explanation
457 must not, however, be used only to defy the small and discontinuous extent of ancient
458 deposits without documentation of evidence of erosion subsequent to a glacial period.

459 *2.1.2. Correlations and dating*

460 In general, there are always intricate problems with correlations, especially if these are long
461 distance (Blauw, 2012; Gaucher et al., 2015). Commonly diamictites do not contain material
462 that may be isotopically dated. Diamictites and “glaciogenic features” have therefore
463 sometimes been interpreted to be glacial, only if they are of the “correct” age. Furthermore,

464 diamictites which commonly are regarded as glaciogenic today have earlier been regarded as
465 not glaciogenic, because they have been considered to have been in the wrong
466 paleogeographic area (Caputo and Santos, 2020). In some cases, diamictites have been
467 redated, even four times, in order to correlate these to other deposits which have been
468 interpreted to be glaciogenic. There are examples of redating from the Neoproterozoic
469 throughout the Phanerozoic and occasionally even into the Pleistocene (Dow et al., 1971;
470 Schenk, 1972; Schermerhorn, 1974a; McClure, 1980; Rehmer, 1981; Carto and Eyles, 2012b;
471 de Wit, 2016a, 2016b; Moxness et al., 2018; Caputo and Santos, 2020; Hore et al., 2020). All
472 these reinterpretations show that there are many difficulties and unknowns in the studies of
473 diamictites and other geologic features which have been referred to as being glaciogenic.

474 *2.1.3. Fossil vegetation*

475 Fossil vegetation, including coal deposits, is often present adjacent to or in between deposits
476 from “ancient ice-ages” (e.g., Plumstead, 1964; Lindsay, 1970a; Finkl and Fairbridge, 1979;
477 Rocha-Campos and Santos, 1981; Gravenor and Rocha-Campos, 1983; Gravenor et al., 1984;
478 Stavrakis and Smyth, 1991; Woolfe, 1994; Fedorchuk et al., 2019; Kent and Muttoni, 2020).
479 Even if the time scales are long, these sedimentary proximities are so common that they have
480 to be discussed.

481 Plants are better climatic indicators than rocks and would indicate any deviation from a polar
482 climate. However, the ecology of plants often is interpreted from geology and not from plant
483 physiology or ecology, which may be circular reasoning. For example, old editions of books
484 may describe the *Glossopteris* flora as subtropical or tropical, but not so in more recent
485 editions (e.g., Dott and Batten, 1976, compared to e.g., Prothero and Dott, 2003).

486 Current experiments and observations show different levels of ^{13}C and ^{12}C in living plants,

487 depending on e.g. latitude, temperature, precipitation and species (Cernusak et al., 2008;
488 Kohn, 2010; White, 2015; Porter et al., 2017; Stein et al., 2021). Furthermore, there are
489 different sensitivities to pCO₂ and other environmental factors for different plants (Klein and
490 Ramon, 2019; Wilson et al., 2020; Stein et al., 2021), and many plants are insensitive to
491 environmental drivers for isotope discrimination including pCO₂, water and temperature
492 (Stein et al., 2021). Some researchers have even sampled data only from plant studies that
493 show isotope discrimination, to calculate former pCO₂ (Stein et al., 2021). All these different
494 data make ancient pCO₂ model calculations based on plant fossil carbon-isotope data
495 suspicious.

496 *2.1.3.1. Association between vegetation and glaciogenic sediments*

497 Macrofossils are rarely found in diamictites. However, in the LPIA of South Africa, fossils of
498 plants of *Gangamopteris* of the *Glossopteris* flora have been found within the diamictites and
499 squeezed in between the Dwyka “tillite” and the underlying “ice-polished bedrock” (du Toit,
500 1926; Sandberg, 1928). Coalified plant fragments occur within massive “tillites,” and coal
501 seams are often present on or between “tillites” (du Toit, 1926; Sandberg, 1928; Adie, 1975;
502 Anderson and McLachlan, 1976; John, 1979; Bond, 1981a, 1981b; Le Blanc Smith and
503 Eriksson, 1979; Visser, 1983a, 1989a; Stavrakis, 1986; Stavrakis and Smyth, 1991; Von
504 Brunn, 1994; Hancox and Götz, 2014; Caputo and Santos, 2020). Coal seams that may be
505 interbedded with “glaciogenic” diamictites have in many instances coalesced with other coal
506 seams to form one thick coal seam (Stavrakis and Smyth, 1991). Interlayering of diamictite
507 and coal beds is often considered to be a result of reworking of diamictites (Hancox and Götz,
508 2014), but that explanation does not hold well for plant fossils within massive diamictites and
509 coalesced strata. Geologic evidence of long time periods are commonly missing. Coal seams
510 that are interbedded between diamictites are often thin, and complete sequences may appear
511 to be a kind of debrites (Hancox and Götz, 2014).

512 In the LPIA of Antarctica, diamictites intrude strata upward as diapirs (nearest plant fossils
513 are c. 0.5 m above the “tillite”; Cuneo et al. , 1993), and boulders and conglomerates from the
514 upper strata protrude downward into the diamictite. Furthermore, “glaciotectonic structures”
515 are present both in the “tillite” and the lower part of the coal bearing strata (mainly
516 sandstones and conglomerates; Isbell, 2010). In some places the boundary between the beds
517 are gradational, and in other places the deposits are interfingering (Cuneo et al. , 1993; Isbell,
518 2010). Considered as a whole, these evidences indicate a short time period. Isbell (2010)
519 concluded that the evidence suggested “temperate glacial conditions.”

520 Deposits containing fossil plants close to diamictites may be considered to be hyperpycnites,
521 i.e. deposits formed by dense water flows laden with sediment and large plant parts. These
522 may be sorted into dense and diluted parts, with or without plant material, but plant material
523 may also be transported with turbidities, cyclones and tsunamis (Zavala and Arcuri, 2016;
524 Shanmugam, 2019, 2021b; Zavala, 2019, 2020; Dou et al., 2021). Plant parts have been
525 transported into deep marine basins at estimated paleodepths of approximately 400-600 m
526 (Pickering and Corregidor, 2005).

527 The evidence from the absence of plant fossils within most Paleozoic diamictite deposits may
528 be an indication of water depth or transport distance, i.e. in deeper water, or during longer
529 transport, plant material and other organisms may be sorted out. The $\delta^{13}\text{C}_{\text{carb}}$ in the Dwyka
530 Group diamictites appear to be of primarily algal origin, which may be an indication of water
531 depth (Scheffler et al., 2003). Fossils are seldom reported from within debris flow deposits.
532 On the other hand, Holocene glaciogenic deposits may hold an abundance of trees and other
533 plants, if forests have grown nearby (Ryder and Thomson, 1986; Fleisher et al., 2006). This
534 would not be considered to be uncommon in areas with Alpine glaciation or at the
535 southernmost parts of continental glaciers, but less common if there was polar climate.

536 2.1.3.2. *Ecology*

537 The vegetation present next to “glaciogenic” facies of the LPIA deposits does not include
538 typical cold-climate plants (Anderson and McLachlan, 1976; McLoughlin, 2011; Hancox and
539 Götz, 2014; Caputo and Santos, 2020). The LPIA fossil plants, i.e. the *Glossopteris* flora, do
540 not display any typical appearances of cold climate peats or other cold climate environments,
541 and no indication that they could have thrived in polar climates (Srivastava and Agnihotri,
542 2010; McLoughlin, 2011; Isbell et al., 2016; Götz et al., 2018; Gastaldo et al., 2020a, 2020b;
543 Mays et al., 2020; Tripathy et al., 2021). The main argument for a cold climate adaptation of
544 the vegetation (if this question even is raised) is the close connection to sedimentary deposits
545 which are regarded to be from an ice age. Similar plant fossils are present even at a
546 paleolatitude of 75-85°S, even if there are not always diamictites close by, and the estimated
547 range of productivity of these far southern forests is similar to that of modern forests (Cuneo
548 et al., 1993; Isbell et al., 2016; Miller et al., 2016; Decombeix et al., 2021). There also are
549 indications that at least some plants were evergreen (Gulbranson et al., 2014), and no
550 evidence of frost rings (Taylor et al., 1992). But growth rings would be expected from a shift
551 from light to dark seasons, or amount of precipitation (e.g., Glock, et al., 1960; LaMarche,
552 1969; McLoughlin, 2011). Even if all these fossil plants are not close to diamictites in time or
553 space, they are in a paleopolar area. It would seem as reasonable to argue that because there
554 are temperate or possible subtropical plant fossils present close to many diamictites, as these
555 are also present where there is no diamictites, such deposits cannot be glaciogenic and might
556 instead be SGF deposits. Although the *Glossopteris* flora species are gymnosperms, and not
557 angiosperms which have been better studied, leaf size and appearance may be an indicator of
558 paleoclimate. Hence, the physiology of the fossil plants, displaying complete (non-toothed)
559 and also large sized leaves, suggests that the *Glossopteris* flora of Gondwana could even be
560 considered to be evidence for a tropical or subtropical climate zone (e.g., Gastaldo et al.,
561 2020a; DeVore and Pigg, 2020).

562 The Paleozoic ferns, gymnosperms and other plants are present in many climatic zones. The
563 same genus or even species of plants that are present next to Paleozoic “tillites,” are also
564 present in many places with non-glacial climate (e.g., compare Gateway to the Paleobiology
565 Database, 2020, to Barbolini, 2014). For example, *Glossopteris* flora, which is present over
566 most of Gondwana (McLoughlin, 2011), have been discovered in the Late Permian of Jordan,
567 i.e. in the northern, tropical/subtropical part of Gondwana (Blomenkemper et al., 2020), in
568 Mongolia (Naugolnykh and Uranbileg, 2018), and also in deposits at the Permian-Triassic
569 border of Pakistan which are considered to have been laid down during a greenhouse climate
570 (Schneebeil-Hermann et al., 2015). Meyerhoff et al. (1996), Srivastava and Agnihotri (2010),
571 McLoughlin (2011), and Mays et al. (2020) describe more examples of *Glossopteris* flora
572 outside of the Gondwana area, but there is skepticism whether all these fossils really are
573 *Glossopteris* (Mays et al., 2020). Coal-forming plants showing affinities to plants which are
574 present in North America and Europe and are interpreted to be from tropical or subtropical
575 areas, are also present in Gondwana, but these fossils have not been clearly described or are
576 reassigned to other species, which may make the interpretation of paleoclimate from these
577 fossils at least equivocal (Charrier, 1986; Spiekermann et al., 2020). However, well
578 documented *Sigillaria* is present in northern Gondwana (Seward, 1932) and lepidodendroid
579 lycopsids (*Lepidodendrales*) in the Devonian of Australia (Peyrot, et al., 2019).

580 From the evidence of the vegetation, it may be possible that the climate during the LPIA was
581 similar to the Middle/Late Permian, Mesozoic and early Cenozoic “near-tropical”
582 “Greenhouse World” climate, the latter displaying no large glaciers and mean annual
583 temperatures from maybe +5°C to +20°C (or at least no long periods of time with
584 temperatures below the freezing point) close to the poles (Leonard et al., 1981; Sloan and
585 Barron, 1990; Bickert and Heinrich, 2011; Rose et al., 2013; Mori et al., 2016; Bernardi et al.,
586 2018; Decombeix et al., 2021), with e.g., dinosaurs (Mori et al., 2016; Fiorillo et al., 2019;
587 Takasaki et al., 2019) and subtropical and temperate forests growing close to the poles

588 (Wolfe, 1977; Morris, 1985; Francis, 1990; Kerr, 1993, 2008; Wilf et al., 2009; Cerda et al.,
589 2012). There is a lack of evidence of continuous glaciation in Gondwana during the LPIA,
590 even if the South Pole was situated close by from the Late Proterozoic until the Early Triassic
591 (e.g., Horan, 2015). And there are very few and no unequivocal evidences of glaciation in the
592 northern hemisphere during the LPIA (Isbell et al., 2012, 2013, 2016; Montañez and Poulsen,
593 2013; Craddock et al., 2019; Griffis et al., 2019; Fedorchuk et al., 2019, 2021; Rosa and
594 Isbell, 2021). The LPIA is immediately followed by a period of “Triassic Hothouse extremes”
595 (Götz et al., 2018). Even during the Neogene the Antarctic continental mean summer
596 temperatures were +5°C, i.e. possible 30°C warmer than today (Rees-Owen et al., 2018).

597 All the evidence from fossils show that there is no need to ascribe a polar climate to polar
598 areas, as may be done when referring to polar wander paths and also to the recent climate at
599 the poles.

600 *2.2. Till structure*

601 In many aspects SGF deposits may be indistinguishable from subglacial tills (section 1.4. and
602 e.g., Mountjoy et al., 1972; Schermerhorn, 1974a; Kurtz and Anderson, 1979; Lowe, 1982;
603 Visser, 1983a; Wright et al., 1983).

604 Transverse and irregular moraine forms are not common in diamictites, but are regularly
605 present in Pleistocene and younger tills. However, compressional transverse ridges,
606 hummocky terrain, and flow lines similar to those on the surfaces of some glaciers, are
607 formed by SGFs (e.g., Haflidason et al., 2004; Pickering and Hiscott, 2015; Nugraha et al.,
608 2020; Dufresne et al., 2021; Procter et al., 2021).

609 *2.2.1. More mass flows and marine sediments than basal glaciogenic sediments*

610 “Tillites,” in comparison to glaciogenic deposits from the Holocene and Pleistocene, more
611 often have been disturbed by SGFs, or have been interpreted to be deposited mainly by glacial
612 marine sedimentation (i.e. 95%, section 1.3.), and, therefore, it is especially difficult to
613 distinguish such deposits from non-glaciogenic SGF deposits (e.g., Aalto, 1971; Martin,
614 1981a; Von Brunn and Stratten, 1981; Gravenor et al., 1984; Molén and Smit, 2022). The
615 natural explanation for this – erosion of higher lying terrestrial source areas – has not been
616 substantiated by reports concerning possible evidence of erosion of “tillites,” and there may
617 still be much sedimentary material close to the central areas of “glaciation” (Biju-Duval et al.,
618 1981; Gravenor and Rocha-Campos, 1983; Visser, 1988, 1989a; Le Heron et al., 2010).

619 Often ancient basal “tillites”/diamictites are overlain and/or underlain by SGF deposits or
620 marine strata (e.g., Banerjee, 1966; Visser, 1983b; González and Glasser, 2008; Caputo and
621 Santos, 2020) – a less common observation in Pleistocene deposits. Slides, slumps and debris
622 flows often trigger turbidity flows that will retain some coarse sediment and will be deposited
623 on top of, or downslope from, the denser flow (Hampton, 1972; Middleton and Hampton,
624 1976; Embley, 1980, Lowe. 1982). This can explain why diamictites often are surrounded by,
625 or draped with, shale or rhythmites with limestones (e.g., Molén, 2017, 2021; Rampino, 2017;
626 López-Gamundí et al., 2021).

627 *2.2.2. No rock flour and density of deposits*

628 Till contains a large component of rock flour, i.e. material with a grain size $<2 \mu\text{m}$, as
629 opposed to many “tillites” (Frakes, 1979; Molén, 2017). For example, the Saharan and Saudi
630 Arabian Ordovician diamictites which are interpreted to be glaciogenic are composed of
631 similar sized material as the underlying sandstones, i.e. sand/silt and no (or very little)
632 grinded rock flour (Le Heron et al., 2005, 2006; Yassin and Abdullatif, 2017). Diamictites in
633 China also are sandy to silty (Chen et al., 2021).

634 Deposits formed by direct sedimentation from dense suspension are among the most loosely
635 packed natural sediments (Lowe, 1982), i.e. different from subglacially deposited material.
636 However, SGF deposits appear to consolidate quickly, which may mimic compression of
637 sediments by glaciers in tills (Moscardelli et al., 2006). Also, as diamictites are lithified, the
638 cementing agent might obscure indices of the former ratio of pore spaces.

639 *2.2.3. Correlation between clast size and thickness of strata*

640 The largest boulders in “tillites” are often present in the thickest sedimentary horizons
641 (Schermerhorn, 1974a; Martin et al., 1985; Eyles and Januszczak, 2007). This indicates
642 transport by SGFs (Dott, 1963; Kuenen, 1964; Larsen and Steel, 1978; Derbyshire, 1979;
643 Lowe, 1982; Walton and Palmer, 1988; Middleton and Neal, 1989; Eyles and Januszczak,
644 2007; Kennedy and Eyles, 2021). Ice distribute boulders more randomly.

645 *2.2.4. Grading in sediments*

646 There is much grading in diamictites which have been or are interpreted to be “tillites,”
647 including lodgement/basal “tillites,” i.e. a) graded bedding, upwards fining, or the largest
648 boulders deposited at the bottom of the sequences (Kulling, 1951; Lindsay, 1968; Bowen,
649 1969; Schermerhorn, 1975; Visser and Kingsley, 1982; Visser, 1982; Deynoux, 1985b;
650 Gravenor and Von Brunn, 1987; Le Heron et al., 2018b, Le Heron et al., 2021b), b) “tillites”
651 grading upwards to shales, dropstone bearing shales or fluvial sediment (Dow et al., 1971;
652 Frakes and Crowell, 1969; Visser et al., 1987; Mustard and Donaldson, 1987b;
653 López-Gamundí, 2010), c) reverse grading from “sandstone with rounded dropstones” to
654 “clast-rich diamictite” (Hoffman et al., 2021), and d) conglomerates or breccias grade
655 upwards to, or are directly overlain, by diamictites which have been interpreted to be “tillites”
656 or SGFs (Kulling, 1951; Lindsay, 1966, 1970; Lindsey, 1969; Cahen and Lepersonne, 1981;

657 Deynoux and Trompette, 1981b; Visser, 1981, 1983b, 1997; Mustard and Donaldson, 1987a,
658 1987b; Isbell et al., 2008; Festa et al., 2016; Kennedy and Eyles, 2021; Molén, 2021).

659 The occurrence of breccias might indicate that the process of movement was triggered by
660 tectonism, or that the bedrock broke to pieces by the impact of a SGF (Dakin et al., 2013;
661 Molén, 2021). Grading is an indication of transportation by SGFs (section 1.4; Cecioni, 1957;
662 Eriksson, 1991), but may be present in glaciogenic deposits. Even if there is not any evidence
663 of grading in all stratigraphic successions, many pre-Pleistocene “glaciogenic” and also SGF
664 deposits display a general sequence, with a few or many of the following facies, starting from
665 the bottom: breccia, conglomerate or clast supported diamictite, massive diamictite, stratified
666 diamictite, sand or siltstone, and rhythmites with finer material displaying lonestones (e.g.,
667 Molén, 2017, 2021; Le Heron et al., 2021b López-Gamundi et al., 2021; Molén and Smit,
668 2022). Furthermore, massive diamictites which have been studied in more detail, have been
669 shown to be stratified, and may indicate a non-glacial origin (Stavrakis, 1986; Stavrakis and
670 Smyth, 1991; Von Brunn, 1994; Visser, 1997; Visser et al. 1997; Huber et al. 2001;
671 Haldorsen et al. 2001; Isbell et al., 2008; Dietrich and Hofmann, 2019; pers. commun., Johan
672 N. J. Visser, 2020; Molén and Smit, 2022).

673 *2.2.5. Bedding and amalgamation*

674 Sandstones which have been interpreted to be “tillites” may be faintly bedded and display
675 structures similar to dish structures (Biju-Duval et al., 1981; Gravenor and Rocha-Campos,
676 1983; Deynoux 1985b), which might indicate deposition by debris flows (Middleton and
677 Hampton, 1976; Lowe, 1982; Visser, 1983a). But, fissility textures in tills, and dewatering of
678 two component glaciomarine facies, may occasionally display an appearance similar to dish
679 structures.

680 Ancient diamictites often display amalgamation of debris flow deposits (Kennedy and Eyles,
681 2021), which Domack and Hoffman (2011) interpreted as amalgamation of tillites. The
682 number of “tillite” beds also had been interpreted as the number of glaciations (Ali et al.,
683 2018).

684 *2.2.6. Presence of soft sediment structures*

685 In SGFs, large rip-up contorted slabs of soft sediments are commonly transported (Crowell,
686 1957; Lindsay, 1966; Lowe, 1979; Shanmugam, 2012, 2021b; Vesely et al., 2018; Rosa et al.,
687 2019; Rodrigues et al., 2020; Isbell et al., 2021), but sometimes such “clasts” have been taken
688 as evidence for glaciation (Deynoux and Trompette, 1981b; Runkel et al., 2010). Even though
689 soft-sediment rafted material may occasionally be transported by and not become shattered by
690 glaciers, “tillites” often contain contorted transported sheets of sediment, thus indicating a
691 more probable transport by SGFs (Lindsay, 1966; Bowen, 1969; Frakes et al., 1969; Visser,
692 1983b; Deynoux, 1985b; Molén, 2017; Kennedy and Eyles, 2019, 2021).

693 Other structures which are commonly present in SGF deposits, but also in a lesser amount in
694 what is or have been considered to be glaciogenic sediments/tillites are: rotational structures,
695 necking structures (squeezing of material between clasts), wisps, flame structures, sediment
696 diapirs, load casts, intra-clasts of diamictite (not to confuse with intra-tills; Evans et al.,
697 2006), and dykes (e.g., Shanmugam, 2012, 2017b, 2021b; Isbell et al., 2016; Moxness et al.,
698 2018; Molén, 2021; Kennedy and Eyles, 2019; Caputo and Santos, 2020; Molén and Smit,
699 2022).

700 *2.2.7. Clasts pressed into underlying surface*

701 Clasts in “tillites” have been pressed down into the underlying surface, which actually is not

702 always considered to had been soft (Lindsay, 1970a, 1970b; Hambrey, 1983; Caputo and
703 Santos, 2020). This can be better explained by a SGF over unconsolidated sediment than a
704 glacial origin (Molén, 2017).

705 *2.2.8. Channels below or next to “tillites”*

706 In the sedimentary strata just below or next to “tillites” there are occasionally erosional
707 channels (Lindsay, 1970a; Biju-Duval et al., 1981; Schatz et al., 2011; Molén, 2017). These
708 structures indicate that water, debris flows or slides eroded the underlying sediments before
709 deposition took place, but these may not be incompatible with a glaciogenic origin (Mountjoy
710 et al., 1972; Karlsrud and Edgers, 1982; Walton and Palmer, 1988; Eyles and Eyles, 1989;
711 Eyles 1990; Eriksson, 1991; Talling et al., 2007; Dakin et al., 2013; Shanmugam, 2016; Baas
712 et al., 2021).

713 *2.2.9. Fabrics*

714 The long axes of pebbles in Pleistocene tills often show a 10-20° dip in the direction of the
715 ice movement, but there may also be a transverse fabric present (Lindsay, 1968, 1970a,
716 1970b; van der Meer et al., 2003; Evans et al., 2016).

717 In SGFs the fabric of outsized clasts can be similar to a till fabric, including a bimodal fabric
718 and transverse oriented clasts, but it also display differences changing with the height in the
719 sedimentary sequence (Lindsay, 1968; Best, 1992; Kim et al., 1995; Major, 1998; Kennedy
720 and Eyles, 2019). In many SGF deposits the fabric is planar or sub-parallel to bedding
721 (Evenson et al., 1977; Hill et al., 1982; Gravenor, 1986; Eriksson, 1991; Rodrigues et al.,
722 2020), but it may be (sub)vertical, in places displaying protruding large clasts, or, about 30%
723 of the clasts have a dip in excess of 20° (Lawson, 1979; Visser, 1996; Dasgupta, 2003; Liu et

724 al., 2021). The variation of the fabric sometimes makes it possible to find support for an
725 origin by SGF. It is more difficult to provide conclusive evidence for a glacial origin of a
726 diamictite only from fabrics, if the deposits are not in widespread horizons, even if doubts
727 about the origin may not be strong (Lindsay, 1968; Lawson, 1979; Hicock and Dreimanis,
728 1992b; Piotrowski et al., 2001, 2002).

729 Pre-Pleistocene “tillite” fabrics typically display no systematic patterns and appearances
730 which are indicative of tills, i.e. there are many varied directions and dips (Bigarella et al.,
731 1967; Lindsey, 1969; Lindsay, 1970a, 1970b; Lindsay et al., 1970; Rehmer, 1981; Young,
732 1981a; Gravenor and Rocha-Campos, 1983; Miall, 1983; Deynoux, 1983, 1985b; Visser et
733 al., 1987, 1997; Visser 1996). Many “tillite” fabrics seem to be more or less planar, but
734 sometimes the dips are not reported (Visser, 1983b).

735 *2.2.10. Flutes*

736 Flutes may be formed behind obstacles in any environment. In glacial environments,
737 obstacles are commonly at least 0.3-0.5 m higher than a lodged till surface, the flute is
738 commonly lower and thinner than the obstacle, and the length may be many kilometers
739 (Woodworth-Lynas, 1996). These are different from flutes described from areas which are
740 interpreted to have been produced by glaciation, e.g. different appearance next to obstacles or
741 no evidence of obstacles (e.g., Rosa et al., 2019; Le Heron et al., 2019).

742 *2.2.11. Impact structures, meteorites*

743 Deformed en echelon-fractures, hinged and crushed stones, which are followed by brittle
744 fracture, such as so-called “bread-cut-to-slices” structures are typical for impact-cratering
745 events (Oberbeck et al., 1993a, 1993b, 1994; Rampino, 2017). Such evidence has been

746 proxies to reinterpret “tillites” as originating by impact-generated debris flows (Rampino,
747 1994, 2017). Other criteria for impacts are shocked clast and minerals, and distinctive surface
748 microtextures on quartz grains (Rampino, 1994, 2017; Mahaney, 2002).

749 *2.3. Erratics*

750 *2.3.1. Erratics, transport and inclinations – similarities*

751 Except for by glaciation, erratics can be transported by e.g. mass flows, tsunamis and
752 cyclones (Carter, 1975; Malahoff et al., 1979; Elfström, 1987; Shanmugam, 2012, 2021b;
753 Lascelles and Lowe, 2021). The largest clasts transported by tsunamis are 40x27x6 m
754 (Lascelles and Lowe, 2021; see also Shanmugam, 2012, 2021b). Probably the largest known
755 erratics in “tillites” are 40 m, 100 m, and 320 m long, respectively, and the structures in the
756 surrounding diamictites indicate that these clasts have been transported by SGFs
757 (Schermerhorn, 1975; Molén, 2017). Large clasts are often deposited at the margin of mass
758 flow deposits (Ortiz-Karpf et al., 2017).

759 Large slide blocks are often more than one kilometer long and hundreds of meters high. The
760 largest known blocks are hundreds of square kilometers in area. Some of these have been
761 moved many tens to hundreds of kilometers (Maxwell, 1959; Wilson, 1969; Mountjoy et al.,
762 1972; Schermerhorn, 1975; Moore et al., 1989, 1995; Alves, 2015; Ortiz-Karpf et al., 2017;
763 Hodgson et al., 2018; Sobiesiak et al., 2018; Soutter et al., 2018; Alves and Gamboa, 2020;
764 Nwoko et al., 2020a, 2020b; Puga Bernabéu et al., 2020; Kennedy and Eyles, 2021; Kumar et
765 al., 2021). This long distance transport of material, whether debris flows or slides, is possible
766 because of processes labeled hydroplaning, shear wetting or substrate liquefaction (de Blasio,
767 2006; Moscardelli et al., 2006; Sobiesiak et al. 2016, 2018; Alves and Gamboa, 2020).

768 Turbidity currents and other mass flows have transported debris many hundreds (Wilson,
769 1969; Komar, 1970; Embley, 1976; Embley and Morley, 1980; Wright et al., 1983;
770 Middleton and Neal, 1989; Stoopes and Sheridan, 1992; Shanmugam, 2016) to thousands
771 (Kuenen, 1964; Stevenson et al., 2014) of kilometers. Far-transported clasts may become
772 incorporated in existing sediments, whereafter the deposits turn unstable and move as dense
773 SGFs, which after deposition displays characteristics similar to tills (Crowell, 1957; Jansa
774 and Carozzi, 1970; Walton and Palmer, 1988; Eyles 1990).

775 Slopes beneath Pleistocene and younger glaciers may vary, but often it is close to zero over
776 large areas, i.e. close to 0.001° . Slopes recorded for coarse grained turbidity flows (containing
777 gravel sized clasts) are commonly as low as $0.02\text{-}0.05^\circ$ (Kuenen, 1964; Komar, 1970; Wright
778 et al., 1983; Stevenson et al., 2014; Sobiesiak et al., 2018). For debris flows the angle
779 commonly is below 1° but in places less than 0.1° (Mountjoy, 1972; Carter, 1975; Middleton
780 and Hampton, 1976; Embley, 1976, 1982; Shanmugam, 2021b), but even debris flows may
781 move over an area with lower slopes than 0.05° (Stevenson et al., 2014). Subaqueous
782 landslides have been recorded to travel on slopes of approximately 1° for almost 1000 km
783 (Yincan et al., 2017). If these slopes are compared with those in ancient “tillites,” some of the
784 gentler slopes in “tillites” are steeper than for glaciers, thus indicating a possibility of SGF
785 transport, for example, in the Ordovician in Sahara 1° (Fairbridge, 1971), and in different
786 places in South America $0.25\text{-}1^\circ$ (Caputo and Crowell, 1985).

787 Even though all researchers may not be aware of how common this is (de Wit, 2016a, 2016b),
788 SGFs and slides may climb upwards (e.g., Pickering and Hiscott, 2015; Nugraha et al., 2020),
789 sometimes for horizontal distances of more than 100 km (Stevenson et al., 2014). A recent
790 slide started from above the sea surface, then moved submerged for 1.5 km down to a depth
791 of 80-90 m below sea level, before it re-emerged on land and was deposited at a height of 15
792 m above sea level (Dufresne et al., 2018). A submarine slide moved uphill 500 m against a

793 16° slope (Tucholke, 1992), and another travelled upwards for 140 km to a height of 300 m
794 (Moore et al., 1989). One slide (or “debris avalanche”) traveled uphill to a height of 100 m at
795 a velocity of approximately 52 m/s (Watt et al., 2012). Submarine hills and overbank levee
796 sites which are covered by turbidites may be more than 180 m above the surrounding bottom
797 of the sea (Abbot and Embley, 1982; Mountjoy et al., 2018), but heights between 5-120 m are
798 commonly recorded (some covers may just be because of the thickness of the flows), and for
799 debris flows 20 m uphill flow has been documented (Stevenson et al., 2014).

800 *2.3.2. Erratics, transport and inclinations – differences*

801 *2.3.2.1. Size dependence*

802 In glaciers there is no clear maximum size for transported clasts, as the competence of ice
803 sheets is almost limitless. The Pleistocene glaciers transported scores of large clasts (both
804 sedimentary and magmatic, e.g., Bukhari et al., 2021; Fig. 1). Even if there has been no large
805 systematic study, Quaternary glaciations have accumulated innumerable quantities of large
806 clasts in boulder size, which are evident almost everywhere. The accumulation of large
807 boulders in Fig. 1D, in this single spot (which is not exceptional, but common), is more
808 abundant than the total number of boulders present in many “tillites” covering large areas.
809 Both in “tillites” and SGFs boulders are rarer (e.g., Molén, 2021). In Pleistocene deposits
810 great areas are covered with thousands upon thousands of boulders even with diameters larger
811 than one meter (Fig. 1). Erratics with diameters larger than 5-10 m are not rare, and some
812 erratics are hundreds of meters (Embleton and King, 1968) and even many kilometers in
813 length (Stalker, 1975, 1976). The largest known block, which might have been transported
814 with glacier ice, measures 4000x2000x120 m (Sugden and John, 1982).

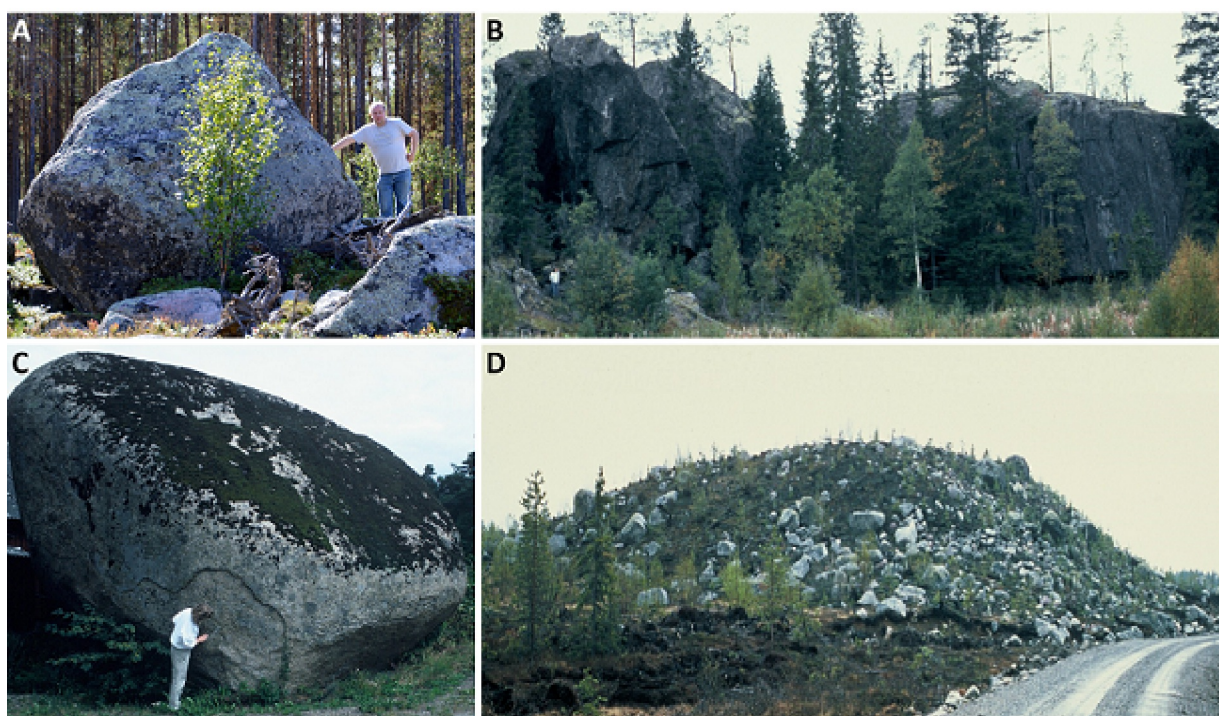
815 In all deposits from ancient “ice-ages” the erratics are usually not larger than a few meters in

816 diameter, and even erratics one meter in diameter are rare (e.g., Kulling, 1951; Flint, 1961;
817 Schwarzbach, 1961; Hambrey and Harland, 1981; Visser and Kingsley, 1982; Visser, 1982,
818 1983b; Caputo and Crowell, 1983; Martin et al., 1985; Deynoux, 1985b; Haldorsen et al.,
819 2001; Zimmerman et al., 2011; Bechstädt et al., 2018; Vesely et al., 2021). Blocks larger than
820 five meters in diameter have rarely been reported. A common maximum clast size is 1.5-2 m,
821 but often the largest erratics have a diameter less than 25-50 cm, and over large areas the size
822 is only around 5 cm (e.g., Von Brunn and Stratten 1981; Le Blanc Smith and Eriksson, 1979;
823 Visser, 1983b; Chen et al., 2020, 2021; Le Heron et al., 2021b; Vesely et al., 2021; Molén
824 2021).

825 In beds from the same area, which have been deposited by verified SGFs, or at least showing
826 indication of quick deposition, the clast size is often larger than in supposed “tillites” or other
827 glaciogenic material which has not been deposited by SGF processes (Molén, 2021). When
828 these differences are documented, which is not often done, there is a clear systematic trend.
829 For example, in LPIA deposits in South America, the “glaciogenic” beds commonly carry
830 clasts of cobble size, while gravity or water flow deposits carry boulders of many meters in
831 size (Rosa et al., 2019; López-Gamundí et al., 2021). And in the Neoproterozoic Namibian
832 deposits the largest clast, many meters in size, are in massive debris flows or slides, even
833 though these clasts at the same time had been interpreted to be dropstones (Domack and
834 Hoffman, 2011). This systematic difference is opposite to what is expected, because glaciers
835 can in general transport larger clasts than SGFs, without showing any evidence of flow
836 structures.

837 If a SGF moves at a low velocity, if there is less water and less turbulent movement involved,
838 and if the SGF is denser, i.e. a high-strength cohesive debris flow, then the final deposit ought
839 to display an appearance more similar to a till than deposits from other mass movements. This
840 might be the explanation of why deposits from “ancient ice-ages” do not contain many large

841 erratics. If a deposit from a dense SGF should not exhibit easily recognizable and extensive
842 evidence of turbulence, SGF currents and tectonic slide and slip structures, it might be that a
843 size of 1-3 m in diameter is most often the maximum size of the clasts that can be transported
844 (Komar, 1970; Clark, 1991; Talling et al., 2012; Dakin et al., 2013; Peakall et al., 2020). This
845 size of clasts is often the maximum size that has been observed moving with slow (Shepard
846 and Dill, 1966; Carter, 1975; Middleton and Hampton, 1976) and fast (Elfström, 1987) SGFs.
847 When the clasts are larger, a stronger current and/or higher buoyancy in the matrix is
848 necessary, and the sedimentary structures (e.g., fluvial, bedding and different kinds of slide
849 and load structures) will more clearly indicate that there has been a SGF, and the difference
850 between the deposit and a till is clear cut.



851 Fig. 1. This is the common appearance of tills and other glaciogenic material in most parts of
852 Sweden, i.e. there are innumerable large boulders everywhere. A. Clast in the jökulhaup or
853 sandur of Mettjaur, Västerbotten county, Sweden. This size of clasts is common. B. The
854 probably largest erratic clast in Europe, the Botsmark rock (split into pieces probably by a
855 local postglacial earthquake; Mörner, 2008). There is till under this piece of a mountain, so it

856 has not only been transported on top of the underlying bedrock. (See person in white shirt for
857 scale.) C. Large boulder in southern Sweden, Scania. D. A Blattnick moraine, a special kind
858 of Rogen moraine, displaying large boulders (Markgren and Lassila, 1980).

859 *2.3.2.2. Jigsaw puzzle texture*

860 A jigsaw-puzzle texture, where sediment has been pressed in between separate pieces of
861 fractured clasts, are often present in mass flow deposits (Costa, 1984; Scott, 1988b; Stoope
862 and Sheridan, 1992; Schneider and Fisher, 1998; Legros et al., 2000; Capra and Macias,
863 2002; Thompson, 2009; Thompson et al., 2010; Dufresne et al., 2018, 2021). These have also
864 been documented from “tillites” that display SGF facies (Harker and Giegengack, 1989; Bose
865 et al., 1992; Harker, 1993; Arnaud and Eyles, 2006; Ali et al., 2018; Molén, 2021). Jigsaw-
866 puzzle textures have not been reported from basal tills (Ui, 1989; Thompson, 2009). In stony
867 tills clasts have been single fractured with pieces still nearly in place, and soft or weathered
868 clasts have been transported with glaciers, but these do not display a typical jigsaw-puzzle
869 texture (Broster and Seaman, 1991; Piotrowski et al., 2004).

870 In areas that may be interpreted to be subglacial, the basal unconformity below diamictites
871 may be highly irregular and heterogenous, with areas of sediment injections into sedimentary
872 bedrock, and “elongated boulders” of sediment displaying jigsaw-puzzle texture, but all these
873 features are common in SGFs (Dufresne et al., 2021; Molén 2021; Le Heron et al., 2021b).

874 *2.4. Polished, faceted and striated clasts*

875 It is often assumed that glacially transported clasts exhibit more striations than clasts that
876 have been transported by SGFs. This assumption is not well documented as there is a great

877 difference in the frequency of striated clasts reported from different kinds of environments
878 (Table S1, Supplementary material).

879 Polished, faceted and striated clasts can form by different kinds of mass movements and by
880 tectonic movements including by folding (Crowell, 1957; Flint, 1961; Schermerhorn and
881 Stanton, 1963; Winterer, 1964; Schermerhorn, 1974a; Doré, 1981; Eisbacher, 1981; Rehmer,
882 1981; Hambrey, 1983; Martin et al., 1985; Eyles and Boyce, 1998; Atkins, 2003; Dakin et al.,
883 2013). In SGFs there may be more striated clasts where there are more clasts (Kennedy and
884 Eyles, 2021). Even hard quartzite can be striated in SGFs (Van Houten, 1957; Schermerhorn
885 1974a; Eyles, 1993), but usually most striations are exhibited by sedimentary clasts
886 (Winterer, 1964). Clasts formed under these circumstances may be impossible to distinguish
887 from clasts polished, faceted and striated by the action of ice-movement.

888 In the LPIA “tillites” of South Africa the shapes and sizes of clasts exhibit a very complex
889 pattern which do not give any independent support to a glaciogenic origin (Hall and Visser,
890 1984). “Glacially shaped” so-called flat-iron clasts in the Gowganda Formation are slightly
891 concave or convex “para-flat” with many small protuberances which shows that they cannot
892 have been shaped by ice, and the deposits having an appearance more like a breccia that has
893 been transported a short distance (Miall, 1985; Molén, 2021).

894 Even if there may be differences between striations on clasts from different environments,
895 there are many similarities, and not all environments have been compared (Atkins, 2003,
896 2004). Striations on clasts in SGFs may be random and also curve around corners. Striations
897 on glacially striated clasts may display one or more sub-parallel, or parallel, directions,
898 usually on a flat side of the clast. But, glacially transported clasts may display striations that
899 turn around edges or curvatures (Hicock, 1991; Hicock and Dreimanis, 1992a). Clasts that are
900 tectonically scratched usually display strictly parallel striations, and occasionally in more than

901 one direction (Frakes, 1979; Kennedy et al., 2019). Photographs and reports on striated clasts
902 in SGFs reveal that they usually have random but frequently parallel to sub-parallel striations
903 (Winterer, 1964; Lindsay, 1966; Winterer and von der Borch, 1968; Atkins, 2004) similar to
904 clasts from “tillites” which have striations that are random (Kulling, 1951), bend around
905 corners (Frakes, 1979; Deynoux, 1985b) display single parallel (du Toit, 1926; Deynoux and
906 Trompette, 1981b), and crossing parallel and sub-parallel striations (Deynoux, 1985b).
907 Occasionally clasts in “tillites” display both tectonic and “glacial” striations so the evidence is
908 equivocal (Aitken, 1991).

909 Occasionally clasts displaying “glaciogenic” climate features, like einkanter, “flutes” and
910 ventifacts, may be described from conglomerates and interpreted to have been formed at an
911 earlier time by glaciers (Williams, 2005). The internal structure of clasts may display an
912 appearance of being striated, some clasts appear to be faceted after having been cleaved in flat
913 planes, including bullet shaped clasts, and as a result, mistakes have been made in the
914 interpretation of ancient deposits as “tillites” (Vellutini and Vicat, 1983; Rowe and
915 Backeberg, 2011). Stoss and lee-forms on clasts may be formed in different environments
916 where there is mechanical erosion, but in lodgement tills clasts may have double stoss-lee
917 forms (Krüger, 1984, Benn and Evans, 1996). Double stoss-lee forms on clasts may be the
918 only unequivocal criteria for glaciation (Krüger, 1984).

919 In “tillites” soft sedimentary clasts may be subangular, fresh and commonly striated, while
920 harder basement clasts are rounded, commonly weathered and rarely striated (Schermerhorn,
921 1976b; Deynoux and Trompette, 1981b; Eisbacher, 1981; Deynoux, 1985b). This may be an
922 indication for SGFs which transport older pre-weathered and pre-rounded basement clasts
923 together with newly ripped up sedimentary clasts.

924 *2.5. Striated, grooved and polished surfaces/pavements*

925 *2.5.1. Presence of striated, grooved and polished surfaces/pavements*

926 Pavements/striated surfaces can form by many different processes, including by glaciers, sea
927 ice (Hume and Schalk, 1964; Flint, 1971; Hoppe, 1981), icebergs (section 2.7), mass
928 transport and tectonism (Sandberg, 1928; Flint, 1961; Schermerhorn and Stanton, 1963;
929 Frakes et al., 1969; Hambrey, 1983; Iverson, 1991; Eyles and Boyce, 1998; Legros et al.,
930 2000; Vandyk et al., 2021). Subaqueous flow tills may generate tool marks, but these would
931 be very restricted (Evenson et al., 1977). There are many similarities displayed by surfaces
932 produced by these diverse processes. There are also many differences in appearance which
933 usually, if they are thoroughly documented, may be sufficient to reveal the origin of various
934 striated/grooved surfaces.

935 Erosional marks are almost always formed beneath glaciers, but it is not always recognized
936 how commonly these form by different kinds of mass flows (e.g., Scott, 1988b; Dakin et al.,
937 2013; Peakall et al., 2020). Striated, grooved and polished bedrock, including chevron
938 structures/crescentic gouges/chattermarks, grooves, nailhead striae (which may be labeled
939 prod marks by SGF researchers), and deposition of fluted ridges, form as a result of different
940 kinds of mass movements. These have been documented in both ancient and recent
941 formations, including from debris flows, volcanic flows, avalanches, earth slides, tectonism
942 and other kinds of mass movements (Pettijohn and Potter, 1964; Glicken, 1996; Shepard and
943 Dill, 1966; Enos, 1969; Wilson, 1969; Harrington, 1971; Daily et al., 1973; Allen, 1984;
944 Scott, 1988b; Waitt, 1989; Blatt, 1992; Schneider and Fisher, 1998; Eyles and Boyce, 1998;
945 Atkins, 2003; Draganits et al., 2008; Dakin et al., 2013; Hu and McSaveney, 2018; Sobiesiak
946 et al., 2018; Peakall et al., 2020; Vandyk et al., 2021). Cohesive SGFs may move plastically,
947 sometimes almost like a glacier, and therefore striations, grooves and polishing will appear
948 more similar to erosion by glacier ice, at least on a local scale. This may also happen from
949 pure tectonic movements, i.e. slickensides or fault grooves which locally may display an

950 appearance very similar to glaciogenic striated and abraded formations including presence of
951 crescentic fractures, flute ridges, nail head striations and striated clasts (Eyles and Boyce,
952 1998; Atkins, 2003; Vandyk et al., 2021). The most common tools producing marks in soft
953 sediment, including striations and grooves, appear to be shale clasts (Hampton, 1972;
954 Middleton and Hampton, 1976; Lowe, 1979; Clark, 1991; Peakall et al., 2020).

955 Debris flows may overlie grooved surfaces that are tens of kilometers long, 15 m deep and 25
956 m wide (Posamentier and Kolla, 2003; Peakall et al., 2020). Detailed studies of grooves
957 formed by SGFs, have documented flows covering distances in excess of 40 km and areas of
958 c. 300 km² (Peakall et al., 2020). That may explain why most pre-Pleistocene pavements are
959 in soft sediments (e.g., Le Heron et al., 2020), as opposite to the Pleistocene and Holocene.

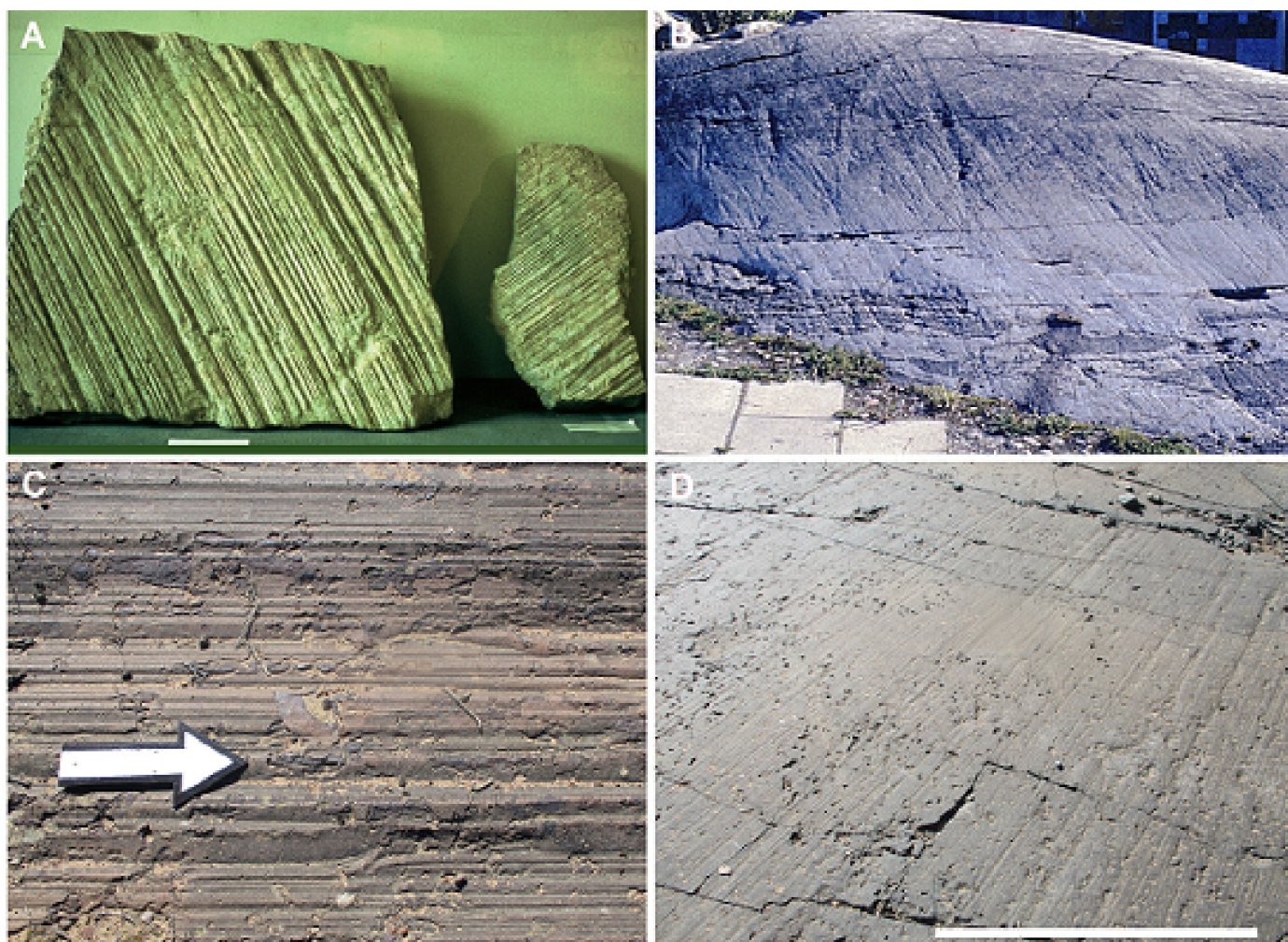
960 Examples of misidentified pavements include several meters long grooves and striations in
961 the Triassic of Australia, which are clearly non-glacial (Gore and Taylor, 2003). On the island
962 of Svalbard 2-3 m long striations and “ice-polished bedrock” (sandstone and shale) have been
963 formed under the action of sea-ice and waves (Hoppe, 1981). Other “glaciogenic” surfaces
964 exhibiting nail-head striae and “possible” crescentic gouges (Schenk, 1965) have been
965 reinterpreted as tectonic in origin (e.g., Miall, 1985). In certain cases pavements are
966 mentioned as evidence of glaciation, but upon investigation the descriptions appear to be
967 erroneous and there are not even any indications of pavements (Dey et al., 2020).

968 *2.5.2. Formation of striated, grooved and polished surfaces/pavements*

969 Striations formed by clasts frozen to the bottom of glaciers consist of sub-parallel sets,
970 commonly accompanied by chattermarks and/or nailhead striae (Anderson, 1983). Similar
971 striations can, however, also be formed by SGFs, and be both parallel/sub-parallel and
972 somewhat curved and show crosscutting to 90° but commonly < 40°, both on rock surfaces

973 and on soft sediment (Pettijohn and Potter, 1964; Enos, 1969; Harrington, 1971; Middleton
974 and Hampton, 1976; Allen, 1984; Ricci Lucchi, 1995; Hu and McSaveney, 2018; Peakall et
975 al., 2020). Tectonic striations will mostly be parallel. Soft sediment slickensides may form
976 internally in tills (Evans et al., 2006), but commonly the appearance of slickensides is very
977 different from striations and grooves.

978 At the sole of warm-based glaciers clasts gradually reorient, horizontally and vertically, such
979 that striations and grooves will always change their appearances (Iverson, 1991). There is a
980 debate concerning whether cold-based glaciers move, but a clast at the bottom of a glacier is
981 never frozen with no internal movement within the ice and striations are varied in appearance
982 (Atkins, 2004, 2013). Glacial striations of Pleistocene age, on sedimentary bedrock may
983 display a superficial appearance similar to striated surfaces below SGFs, as they are parallel
984 and straight for short distances (Fig. 2A). But such glaciogenic striations bear evidence of
985 sideways horizontal and vertical movements (Iverson, 1991), and commonly are short (e.g.,
986 0.05-1 m; Sokołowski and Wysota, 2020), even if the features are not incompatible with
987 some mass flow striations.



988 Fig. 2. Pavements. A and B are Pleistocene (Weichselian), C and D are LPIA. A. Glacial
 989 striations in Silurian limestone (Gotland, Sweden). The striations in the limestone show
 990 superficial similarities to some striations from SGFs in soft sediments. But, the evidence of
 991 horizontal and vertical wobbles of the clasts from within the glacier is clearly apparent, if
 992 only looking a little bit more in detail on the picture. (Gotlands Museum, 1986. Pieces of
 993 paper are c. 10 cm.) B. Glacial striations on the stoss side of a roche moutonnée in magmatic
 994 bedrock (University of Stockholm, Sweden). At the roche moutonnée the striations and
 995 grooves are short, irregular, and subparallel. C. Soft sediment LPIA “glaciogenic” striations
 996 which are perfectly similar to those formed by SGFs, i.e. straight and parallel and no or little
 997 evidence of vertical or sideways wobbles of the tools making the striations and grooves
 998 (Oorlogskloof, South Africa, arrow is 25 cm) (Draganits et al., 2008; Peakall et al., 2020;
 999 Molén and Smit, 2022). D. LPIA striations on Precambrian andesitic lava (marker is c. 1 m)
 1000 (Douglas, South Africa). The striations are almost exactly parallel for a distance of more than

1001 50 m (variation is reported as approximately 1° by Stratten and Humphreys, 1974).

1002 *2.5.3. Differences displayed by striated, grooved and polished surfaces/pavements*

1003 SGFs and slides generate a number of features on surfaces, including different grooves and
1004 striations, which are seldom or never generated with similar appearances below glaciers.

1005 Striated and grooved surfaces displaying such appearances, i.e. those that are generated by
1006 mass flows, are common in areas where there are pre-Pleistocene “tillites.” For example,
1007 during the Paleozoic the majority of “subglacially formed pavements” are in unlithified sand
1008 (Le Heron et al., 2020; Fig. 2C), whereas similar surfaces are very rare or non-existent in
1009 Pleistocene and more recent deposits. A number of the appearances of striated surfaces
1010 displayed by SGFs are documented in the list below. Most of these appearances are
1011 documented by Peakall et al. (2020) and Baas et al. (2021).

1012 a) SGFs commonly display straight movements, often for hundreds of meters or more, and
1013 extensive striated and grooved surfaces may be generated in time periods of only seconds or
1014 minutes (Piper et al., 1999; Peakall et al., 2020; Baas et al., 2021). Debris flows have traveled
1015 at a speed of 500 km/h (Shanmugam, 2002).

1016 b) Grooves are often parallel, display constant rounding, depth and width, may display
1017 parallel internal striae, and occasionally raised lateral ridges (Peakall et al., 2020, Baas et al.,
1018 2021).

1019 c) SGFs may pass areas without leaving much traces. This is shown by the presence of bypass
1020 zones, which can be tens of kilometers, where there is no erosion (Moscardelli et al., 2006;
1021 Georgiopoulou et al., 2010; Talling et al., 2012; Stevenson et al., 2014; Cardona et al., 2020;
1022 Peakall et al., 2020; Baas et al., 2021).

1023 d) Stacked striated surfaces are common in SGFs, with more or less vertical and horizontal
1024 distance between these surfaces, i.e. in some areas the striated surfaces even shift

1025 stratigraphic position and move up and down through the beds as a result of different
1026 movements during deposition (Enos, 1969; Petit and Laville, 1987; Draganits et al., 2008; Le
1027 Heron et al., 2014; Peakall et al., 2020). (Fig. 3.) Similar stacked striated surfaces are not
1028 observed from Pleistocene or more recent deposits where it is known that glaciers were the
1029 depositional agent (Trosdorf et al., 2005a). Stacked striated/grooved surfaces commonly
1030 display similarities to what has been labeled “tectonic hydroplastic slickensides” or “internal
1031 grooves and striations” in SGFs that form in soft sand (Enos, 1969; Petit and Laville, 1987;
1032 Deynoux and Ghienne, 2004, 2005; Le Heron et al., 2005, 2014), while some are stacked
1033 slickensided (or slickenlined) clay or mud (Simms, 2007; Cesta, 2015; Rodrigues et al.,
1034 2020). Woodworth-Lynas and Dowdeswell (1994), Vesely and Assine (2014), and Rosa et al.
1035 (2019) interpreted single and stacked soft sediment surfaces as evidence for ice-keel scouring
1036 by icebergs. Such an interpretation was not accepted for “glaciogenic” striated surfaces in the
1037 Ordovician of northern Africa, that was interpreted as hydroplastic and formed
1038 simultaneously by tectonics and pressure from below thick glaciers (Deynoux and Ghienne,
1039 2004, 2005; Le Heron et al., 2005, 2014). (Iceberg keel grooves are discussed in section 2.7.)

1040 e) Traction carpet sediments are common between striated surfaces and superposed diamictite
1041 debrites. The sediments may be striated, and may be a stratigraphic plane where clasts
1042 commonly glide (Moscardelli et al., 2006; Georgiopoulou et al., 2010; Talling et al., 2012;
1043 Dakin et al., 2013; Cardona et al., 2020; Peakall et al., 2020; Molén and Smit, 2022). Thin
1044 basal layers of sediment are not present between Quaternary tills and pavements, even if a
1045 process for the origin of such sediments could be hypothesized during special circumstances
1046 in rare and confined environments.

1047 f) Contacts below “tillites” may display overhanging walls (Miall, 1985; Molén 2021) or
1048 channels (Moncrieff and Hambrey, 1988) which may exhibit striations (Frakes and Crowell,
1049 1970; Armentrout, 1983). This may result from erosion by SGFs rather than from glaciation,
1050 with or without striations (Scott, 1966; Shepard and Dill, 1966; section 1.4.).

1051 Table S2 (Supplementary material) lists striated surfaces which display similar appearances
1052 as mass flows, from striated surfaces/pavements which had been interpreted to have formed
1053 by glacial ice. Even though all appearances of pre-Pleistocene striated surfaces have not been
1054 observed in recent deposits, and some are difficult to fully explain, the evidence documented
1055 in Table S2 display similarities to striated surfaces which have a mass transport or a tectonic
1056 origin, rather than a glaciogenic origin. In conclusion, similar pavement features commonly
1057 do not form, or have never formed, by Pleistocene or younger glaciers, and therefore these
1058 “pavements” are better explained by a mass transport origin rather than by glaciation.



1059 Fig. 3. Four soft sediment stacked sandstone striated surfaces, LPIA, Dwyka Group,
1060 Oorlogskloof, South Africa. These surfaces are perfectly similar to those made by SGFs
1061 (Draganits et al., 2008; Peakall et al., 2020). The regular appearance of the grooves show no
1062 similarity with glaciogenic surfaces.

1063 *2.6. Striated, grooved and polished surfaces, rock polish*

1064 Mechanically abraded rock surfaces formed beneath glaciers may display a thin glossy
1065 coating layer. Such glacial polish is typically a few micrometers thick, consisting of minute
1066 transported clasts and mineral fragments in a fine-grained amorphous matrix of nano-sized
1067 phyllosilicates. The observations suggest bending and fracturing of the uppermost part of the
1068 original bedrock, followed by smearing of clast fragments and amorphous material on top of
1069 the bedrock surfaces (Siman-Tov et al., 2017). Variants of such surfaces may also be
1070 generated in fault zones. Except for formation by mechanical shearing, an appearance of rock
1071 polish may result from purely chemical precipitation (Bussert, 2010; Molén, 2017).

1072 Striated and grooved surfaces below Neoproterozoic diamictites, commonly interpreted to be
1073 “tillites,” have been shown to be at least partly formed by post-depositional chemical
1074 modification, and there is “polish” even on striations with rugged surfaces (Molén, 2017).

1075 Surfaces on Ordovician “glaciogenic” soft sandstone surfaces display cataclasis of mineral
1076 grains, but not amorphization and smearing of clast fragments (Denis et al., 2010). Ichno-
1077 fossil *Tigillites* burrows at this striated surface remains undeformed, which would be quite
1078 exceptional if a glacier would have passed the soft sediment area (Denis et al., 2010). In
1079 Chinese Ediacarian-Cambrian sediments “glaciogenic” polish is mentioned to occur on
1080 apparently soft sediment surfaces, where striations also have been formed inside the
1081 diamictite, above a surface displaying perfectly straight striations in two directions, but
1082 occasionally curvilinear (Le Heron et al., 2018b). None of these polished surfaces displays
1083 more than superficial similarities to polish on Quaternary pavements.

1084 A recent rock avalanche in China, initially moving as a “water-saturated, dense grain flow,”
1085 passing over dolomitic black shale, formed a surface “highly reminiscent of a classical
1086 striated rock pavement from beneath a glacier,” displaying polish and chemical precipitation
1087 (Hu and McSaveney, 2018). Polish, melting and precipitation are formed in realistic
1088 mechanical experiments and from landslides (Legros et al., 2000; Hu and McSaveney, 2018).

1089 Heat is always produced by friction, and large mass flows or slides could under certain
1090 circumstances probably generate high temperatures, capable of creating polish and lithifying
1091 the underlying surface (compare to a pavement where temperatures of c. 1000°C have been
1092 suggested below an outcrop commonly interpreted to have been deposited below glaciers;
1093 Bestmann et al., 2006; Molén, 2017).

1094 *2.7. Striated, grooved and polished surfaces, iceberg keel scour marks*

1095 Ice scour marks form when keels of icebergs and sea or lake ice press up ridges and plough
1096 through unconsolidated sediments. Some of the pre-Pleistocene soft sediment surfaces which
1097 have been interpreted to be formed by glaciers, had been interpreted to be from icebergs or
1098 sea ice (Woodworth-Lynas, 1992; Woodworth-Lynas and Dowdeswell, 1994; Vesely and
1099 Assine, 2014, who reinterpreted 17 soft sediment surfaces as generated by icebergs;
1100 Rodríguez-López et al., 2021: Table S2, Supplementary material) while others refrain from
1101 such an interpretation (Deynoux and Ghienne, 2004, 2005; Le Heron et al., 2005, 2014,
1102 2020). Similarities between SGFs, single moving clasts, and iceberg scours, include cases
1103 where the underlying sediments become depressed. Similarities also include berms that may
1104 be pushed up next to iceberg scours, in size from a few centimeters to many meters high, and
1105 similar linear ridges which may form by SGFs next to single clasts which are moving at the
1106 bottom, and even sometimes by running water. Non-glacial push up and sedimentary linear
1107 structures may be labeled lateral ridges, flowbands, or sometimes levees (e.g., Dufresne and
1108 Davies, 2009; Kneller et al., 2016; Peakall et al., 2020; Procter et al., 2021).

1109 Quaternary ice keel scour marks may be more than 20 km long, depth may be 80 m, and they
1110 may be up to 1 km wide. They may form at depths of more than 600 m, but are more common
1111 at depths of 60-400 m or less (Woodworth-Lynas, 1992; Woodworth-Lynas and Dowdeswell,
1112 1994; Dowdeswell and Hogan, 2016). In SGFs isolated outrunner blocks, up to many

1113 hundreds of square meters in size, are common, and have traveled many kilometers over very
1114 low gradients e.g., $0.3\text{-}0.4^\circ$, and have made long glide tracks and scour marks in the sea
1115 bottom (Prior et al., 1982; Nissen et al., 1999; Ilstad et al., 2004; Moscardelli et al., 2006;
1116 Festa et al., 2016, Nwoko et al, 2020b, Kumar et al., 2021). Larger outrunner blocks, in
1117 kilometer-sizes, have outrun the main slide deposits for c. 10 km and have excavated
1118 megascours that, including the basal erosion within the main slide deposit, are 1 km wide,
1119 150 m deep and 70 km long (Soutter et al., 2018). SGFs may make deep scours that turn
1120 through about 45° , and then split into many smaller <10 m deep scours (Moscardelli et al.,
1121 2006). There may therefore be at least superficial similarities between ice keel scour marks
1122 and mass flow processes, and in at least one case they are known to have formed in a non-
1123 glacial turbidity current environment (Scott, 1966). “Iceberg grooves” in the Paleoproterozoic
1124 of India were only between 1.2-7.8 cm wide, and 9.2-13.1 cm deep, and pointing in the
1125 direction of $66\text{-}68^\circ$ from the surface (instead of close to 90°) (Rodríguez-López et al., 2021).
1126 This gives them an appearance of small fractures induced only by short sediment movement,
1127 and these were later (quickly) filled with sandy laminated sediments.

1128 In a few instances grooves below “tillites” are curved (Bryan, 1983), up to an angle of 90° in
1129 one meter (Fairbridge, 1979), and they may still be parallel after they changed direction
1130 (Allen, 1975). This is believed to result from overturning of iceblocks, or from changed wind
1131 or current direction that diverted icebergs with clasts frozen to their bottom. However, from
1132 different mechanisms, SGFs may turn, at occasions even 180° , and therefore the direction of
1133 sole structures also will change (Enos, 1969; Kneller et al., 1991; Pickering et al., 1992;
1134 Butler and Tavarnelli, 2006; Draganits et al., 2008; Peakall et al., 2020).

1135 Woodworth-Lynas (1996) published a detailed list of features generated by icebergs, and an
1136 update of a few of the more important of these which can be readily studied in ancient
1137 lithified restricted outcrops in the field, are mentioned below:

1138 a) In the Quaternary there is an abundance of ice-keel scours generated by icebergs over a
1139 total approximate area of $10 \times 10^6 \text{ km}^2$ (Woodworth-Lynas and Dowdeswell, 1994). The
1140 complete bottom surface may be covered by a network of ice-scour marks, occasionally
1141 displaying straight directions but commonly curvilinear and often in many different directions
1142 (Woodworth-Lynas, 1992; Woodworth-Lynas and Dowdeswell, 1994; Batchelor et al., 2020).
1143 Because of e.g. tides, there are examples of looped or spiralling iceberg scour marks
1144 (Woodworth-Lynas et al., 1985; Newton et al., 2016). Different from Quaternary sediments,
1145 large grooves which have been interpreted as ice scour marks in pre-Pleistocene
1146 environments (commonly in sand) are often single, but if many soft sediment surfaces are
1147 superposed or next to each other they are pointing in the same direction (different from
1148 stacked soft striated surfaces in recent tidal mud sediments; Woodworth-Lynas, 1996), and
1149 they often display exactly parallel grooves and striations within the scour.

1150 b) There may be grooves and striations within ice-scour marks (Batchelor et al., 2020), and if
1151 so these are subparallel, i.e. different to parallel grooves and striations commonly generated
1152 beneath SGFs (section 2.5.).

1153 c) Commonly pre-Pleistocene surfaces which have been interpreted to be iceberg keel scours,
1154 are horizontal, while more recent marks may be undulous in cross-section and display small
1155 scale faults induced by iceberg loading (Thomas and Connell, 1985; Woodworth-Lynas and
1156 Guigné, 1990). Wave action and diurnal tides are documented from ice-berg keel scour marks
1157 in Quaternary sediments (Woodworth-Lynas and Guigné, 1990; Bennett and Bullard, 1991),
1158 and there should be evidence of constant changing vertical movements below icebergs. There
1159 is also documentation of up to 2 m high and 20-40 m wide orthogonal or perpendicular
1160 ridges, asymmetric in cross-profile, that are interpreted to have been produced from tides
1161 during the Quaternary (Dowdeswell and Hogan, 2016; Batchelor et al., 2020).

1162 d) Ring structures, a few decimeters high and wide, made from up to 50 m large chunks of
1163 shore ice, are formed today in Canada (Dionne, 1992). Similar forms produced by icebergs,
1164 i.e. grounding pits, may be 10 m deep and 50 m in diameter (Dowdeswell and Ottesen, 2013;

1165 Batchelor et al., 2020). Similar structures have not been reported from the pre-Pleistocene.
1166 e) There are micromorphological criteria for iceberg keel scours (Linch and Dowdeswell,
1167 2016) which have been used to interpret the origin of a pre-Pleistocene soft-sediment striated
1168 pavement as not formed by icebergs but by a grounded icemass (Le Heron et al., 2020).
1169 f) There are grounding-zone wedges showing clear evidence of still-stands or re-advances of
1170 glaciers, up to 15 m high, which have not been registered from the pre-Pleistocene (Batchelor
1171 et al., 2020).
1172 g) Large areas (kilometers) display up to 2 m high asymmetric or sinuous corrugation ridges
1173 that are transverse to the strike of the glaciers, which are easily explained by tide-water
1174 fluctuations during glacial retreat (Batchelor et al., 2020). Similar structures have not been
1175 documented in the pre-Pleistocene.

1176 In conclusion, if there is evidence of a series of vertical and sideway movements, from tides,
1177 waves wind or currents, and subparallel grooves/striations, an iceberg keel origin of scour
1178 marks may be a better option of interpretation than other processes. Other data may be of
1179 help, as mentioned above, but the evidence from movement is diagnostic.

1180 *2.8. Boulder pavements*

1181 There are many boulder accumulations with a more or less flat upper surface which geologists
1182 have described as boulder pavements. Hansom (1983) described boulder pavements which
1183 probably originated by winnowing out of fine material from glacial till on beaches. Close to
1184 the continental shelf/continental slope boundary (Boulton, 1990), or anywhere below sea
1185 level where there is net erosion, the fine material will be winnowed out and leave the
1186 boulders. In other places, pavements originated where sea ice had forced boulders into the
1187 underlying substrate (Hansom, 1983). Hara and Thorn (1982) described fluvial boulder beds
1188 which had been modified by periglacial processes as “subnival boulder pavements,” and frost

1189 heaved boulders that display “flat” tops because of gravity but not paving. During drainage of
1190 dammed lakes, boulders can accumulate to form a deposit exhibiting a flat upper surface,
1191 called a boulder delta (Elfström, 1987). The Mount St. Helens eruption generated a lahar that
1192 cut volcanic boulders and produced “... a surface similar to a glacial pavement cut in
1193 conglomerate” (Scott, 1988a), and more or less planar boulder accumulations are present in
1194 other SGF deposits (Best, 1992). What appears to be boulder or pebble trains (which may be
1195 described as boulder pavements) may be formed by SGFs, but are often present in “tillites”
1196 (Bussert, 2014; Kennedy and Eyles, 2019).

1197 The Pleistocene “classical” inter- and intra-till boulder pavements are usually only one layer
1198 thick (Clark, 1991; Hicock, 1991). These have been suggested to originate possible by a
1199 process slightly similar to debris flows, where boulders sink down into fine-grained till and
1200 after that deforms by overriding glaciers (Clark, 1991; Hicock, 1991). It would therefore be
1201 difficult to differentiate this kind of pavement from boulders that have accumulated from
1202 debris flows (Lowe, 1979, 1982).

1203 Boulder pavements are common in pre-Pleistocene “tillites” (e.g., Lindsay, 1970a; Gravenor,
1204 1979; Rocha-Campos and Santos, 1981; Martin, 1981a; Von Brunn and Stratten, 1981;
1205 Visser, 1983b; Caputo and Crowell, 1985; Visser and Hall, 1985, López-Gamundí et al.,
1206 2016). but are more seldom reported from the Pleistocene (Derbyshire, 1979).

1207 Pre-Pleistocene boulder pavements are often located at the base or top of “tillites.” Boulder
1208 pavements have been a) traced back to channel deposits (Lindsay, 1970a), b) described as
1209 bevelled dropstones (Moncrieff and Hambrey, 1988), c) formed by a local fault and covered
1210 by calcite (González and Glasser, 2008), and d) described as boulders lined up after each
1211 other, with a decrease in size both upstream and downstream, thus showing affinities to
1212 pebble trains in streams (Dal Cin, 1968). Boulder pavements are most common in the Dwyka

1213 Group in South Africa, and display many different appearances. The basal “tillite” in the
1214 southern part of the Dwyka Group commonly is capped with a bed of boulder “tillite” at the
1215 top of an upwards coarsening sequence (Visser and Loock, 1982), and boulder accumulations
1216 may grade upwards into conglomerates labeled boulder rudites. One boulder pavement
1217 displays single imbricated beds (Visser and Hall, 1985) more typical of debris flow, tsunami
1218 or cyclone deposits (Shanmugam, 2012, 2021b). Boulder beds may be up to 12 m thick, and
1219 display moderate sorting (Visser and Hall, 1985). In places boulders have accumulated on the
1220 lee side of an obstacle (Visser and Loock, 1988) or are described as a lag deposit of a single
1221 layer of boulders at the base of sandstones (Visser et al., 1987).

1222 An origin of boulder pavements by SGFs seems at least as possible as an origin beneath a
1223 glacier, by winnowing out of material, by reversed grading, or simply by the common
1224 upwards movement of large clasts which takes place in SGFs (section 2.13.1.1.). The
1225 differences between ancient and Pleistocene inter/intra-till boulder pavements may be
1226 considerable.

1227 *2.9. Erosional landforms, lineations*

1228 There will always be superficial similarities between landforms generated by different
1229 processes, including at the boundary layer in different environments (Stokes, 2018), whether
1230 it be glaciers, running water or mass movements. The direction of movement and the
1231 cohesiveness or plasticity of the moving medium will generate features which may display
1232 different appearances.

1233 Commonly sea bottoms are sculptured and grooved over large areas by SGFs or slides. Ice
1234 streams mold large areas into streamlined landforms, i.e. lineations, sediment into drumlin-
1235 like forms, and through erosion of bedrock they produce linear landforms (Eyles et al., 2018).

1236 Lucchitta (2001) studied subaqueous (glaciogenic) lineations at the Antarctic shelf, and
1237 concluded that they were similar to glaciogenic lineations on Mars. However, the lineations
1238 on Mars, including gigantic outflow channels, are probably formed by catastrophic water
1239 release from subsurface groundwater reservoirs, i.e. large scale tectonism and fissures
1240 releasing water, and not by glaciers (Baker and Milton, 1974; Baker and Kochel, 1979; Burr
1241 et al., 2002; Plescia, 2003; Rodriguez, 2005; Leask et al., 2007). Similar lineations were
1242 produced by catastrophic release of water and debris flows triggered by the failure of Mount
1243 St Helens stratocone (Major et al., 2005), the formation of the English Channel and the
1244 Channeled Scablands in Washington (Plescia, 2003; Gupta, 2007; Gupta et al., 2007, 2017).
1245 Other landforms in unconsolidated sediments or bedrock, heading in different directions,
1246 formed subaqueously or subaerially, including 60 km long channels/megascours and
1247 lineations with dimensions of up to many tens of km long, 6-8 km wide, and 600 m deep,
1248 from SGFs, and in places they are U-shaped (Best, 1992; Moscardelli et al., 2006; Robinson
1249 et al., 2017; Ortiz-Karpf et al., 2017; Nwoko et al., 2020a, 2020b). Lineations, tens of
1250 kilometers long, up to 10 m high, and with wavelengths of 100 m, also are formed by density-
1251 driven sediment and water movement, during seasonal weather conditions (Canals et al.,
1252 2006). A slide generated c. 30-120 km long, 100-600 m wide and 10-30 m deep grooves (Gee
1253 et al., 2007), which may be labeled lineations, but such forms may be labeled striations by
1254 marine geologists (e.g., de Blasio, 2006; Gee et al., 2007; Nwoko et al., 2020a). Smaller
1255 lineations, e.g., only 0.4-1.5 m high and spaced at 5-7 m, may also be formed by SGFs (Piper
1256 et al., 1999).

1257 In the Quaternary, there are megalineations that excessively outnumber those that are
1258 interpreted from the Paleozoic, both in areal size and evidence of large-scale energy impact
1259 during geological processing. These cover extensive areas, both subaqueously and
1260 subaerially, with both soft (drumlinised sediment) and hard (rock drumlinoid) forms
1261 (Margold et al., 2015; Dowdeswell et al., 2016a, 2016b; Eyles et al., 2018; Stokes, 2018;

1262 Bukhari et al., 2021), contrasting with Paleozoic surfaces which are interpreted to be
1263 megalineations. In some areas there are also numerous, up to kilometers long and wide,
1264 transverse ridges (Stokes, 2018; Batchelor et al., 2020). The present author knows of no
1265 transverse ridges on lineations interpreted from the pre-Pleistocene. Pre-Pleistocene ice
1266 streams and lineations appear to be more sinuous, partly anastomosing or amalgamated,
1267 follow an outline similar to a SGF where they also change direction, are often parallel to the
1268 strike of the underlying bedrock, and are shorter and wider (see figures and descriptions in
1269 Andrews et al., 2019). Similar structures form by SGFs and slides, but may be labeled
1270 striations (Gee et al., 2005, 2007; Macdonald et al., 2011). Other areas displaying
1271 megalineations interpreted from Google Earth from sandstone plateaus in Chad (Le Heron,
1272 2018), display many different surface structures when investigated at greater detail including
1273 an underlying “dipping substrate” (Le Heron, 2018), rather than ice streams.

1274 Single linear landforms, including those which are drop formed, which display similarities to
1275 landforms that are interpreted to be glaciogenic (Assine et al., 2018), form by catastrophic
1276 outbursts of water which may or may not have any connection to glaciation (Burr et al., 2002;
1277 Plescia, 2003; Gupta, 2007; Gupta et al., 2007, 2017; Robinson et al., 2017), and also from
1278 SGFs (Dufresne and Davies, 2009), and may be labeled “whaleback bars” (Scott, 1988a) or
1279 “shadow remnants” (Moscardelli et al., 2006).

1280 Pre-Pleistocene roches moutonnées have often been reported, but these often display steep
1281 stoss sides and gentle lee sides (e.g., Frakes and Crowell, 1970; Visser and Loock, 1988;
1282 Bussert, 2010; Assine et al., 2018), as opposed to Pleistocene roches moutonnées. They may
1283 therefore be interpreted to be whalebacks or rock drumlins. Some “roches moutonnées” seem
1284 to have their stoss side undercut by erosion (Frakes and Crowell, 1970, their Fig. 6C) – a
1285 more likely phenomenon to take place below a SGF or in running water than below a glacier.
1286 Others have been shown to be a product of tectonics and fluvial erosion on structurally

1287 controlled bedrock features (Vandyk et al., 2021). There is a large difference between the
1288 number of “roches moutonnées” and other small scale erosional landforms in pre-Pleistocene
1289 formations compared to younger formations, as they are almost all-present in Pleistocene and
1290 Holocene glaciogenic formations.

1291 Bedrock forms, especially those in magmatic rocks, should be better preserved than
1292 sediments in the rock record, but there is no extensive record evident from ancient “tillites.”

1293 *2.10. Erosional landforms – plucking*

1294 A process similar to glacial plucking may be caused by SGFs and fluvial action, including on
1295 the surface of magmatic bedrock (Dill, 1964, 1966; Shepard and Dill, 1966; Carter, 1975;
1296 Tinkler, 1993; Whipple et al., 2000; Stock and Dietrich, 2006; Dakin et al., 2013; Lamb et al.,
1297 2014; Hodgson et al., 2018; Vandyk et al., 2021). So-called p-forms (or s-forms) may be
1298 formed by non-glacial fluvial currents (Tinkler, 1993, Vandyk et al., 2021), even though they
1299 often are interpreted to be formed subglacially (Le Heron et al., 2019a; Chen et al., 2020;
1300 Vandyk et al., 2021). Additionally, there is a debate whether fluvial landforms which are
1301 similar to glaciofluvial landforms, have been produced by tsunamis or storm waves (Bryant
1302 and Young 1996; Burgeois, 2009; Shanmugam, 2012; Lascelles and Lowe, 2021). Cavitation
1303 may be one process responsible for plucking (Falvey, 1990). Another process that display
1304 slight similarities to glacial plucking is more like delamination, i.e. detachment of soft
1305 sediments or clasts and entrainment into SGFs (e.g., Butler and Tavarnerelli, 2006; Clark and
1306 Stanbrook, 2009; Butler and McCaffrey, 2010; Dykstra et al., 2011; Fonnesu et al., 2016;
1307 Sobiesiak et al., 2016; Eggenhuisen et al., 2011; Hodgson et al., 2018; Ogata et al., 2019;
1308 Cardona et al., 2020; Kennedy and Eyles, 2021), and where the delaminated sediments have
1309 later been lithified (which is what commonly takes place, as can be seen almost everywhere in
1310 the complete geologic rock record). If plucking leaves a jagged and uneven surface, and no

1311 later polishing (Miall, 1985), this indicate plucking by SGFs and not by glaciers (Molén,
1312 2021).

1313 *2.11. Glacial and non-glacial valleys and fjords*

1314 *2.11.1. Glacial and non-glacial valleys – general appearance*

1315 Many processes create valleys. Steep incisions hundreds of meters deep may be consistent
1316 both with glacial action and fluvial erosion driven by pure tectonic rift uplift (Vandyk et al.,
1317 2021). Hanging valleys are surprisingly common in non-glaciated areas, including in
1318 magmatic and metamorphic rocks, both subaqueously and subaerially (Dill, 1964; Sheppard
1319 and Dill, 1966; Erginal and Ertek, 2002; Mitchell, 2006; Wobus et al., 2006; Crosby et al.,
1320 2007; Lamb, 2008; Amblas et al., 2011; Harris et al., 2014; Normandeau et al., 2015). Such
1321 valleys could be the equivalent of “glacial” hanging valleys that have been interpreted from
1322 the Dwyka Group in South Africa (Visser, 1982; Hancox and Götz, 2014). “Glacial valleys”
1323 an basins in the LPIA of Namibia and Brazil, are “pre-glacial” in places including with
1324 examples of streamlined and striated landforms that are interpreted to be e.g. roches
1325 moutonnées (Martin, 1981b, Santos et al., 1996; Dietrich et al., 2021; Rosa et al., 2021).

1326 Submarine canyons are preferentially eroded in “resistant bedrock” (i.e., metamorphic,
1327 igneous and lithified sedimentary bedrock; Moosdorf et al., 2018) and next to the coast, and
1328 c. 1000 canyons are present at the Last Glacial Maximum and later shorelines (Bernhardt and
1329 Schwanghart, 2021). Isostatic movements could have elevated pre-Pleistocene submarine
1330 canyons above the present sea surface, giving these an appearance of having been carved by
1331 glaciers.

1332 Approximately a thousand non-glacial channels or scours, on slopes as low as 0.02°, which

1333 are up to kilometers in depth and many kilometers in width and length, have been
1334 documented, and this is only from the northeast Atlantic margin (Macdonald et al., 2011).
1335 Channels are common in mass transport deposits (Kneller et al., 2016; sections 2.2.8, 2.7.-
1336 2.9.). Smaller channels are common on fan deposits (Shanmugam, 2016). Initial V-shaped
1337 grooves or “megalineaments” up to tens of kilometers long, 6-8 km wide and 600 m deep,
1338 formed by mass flow transport, may turn into larger U-shaped valleys during movement
1339 (pictures in Ortiz-Karpf et al., 2017). Megascours, up to 1 km wide, 150 m deep and 70 km in
1340 length, some with a basal slide surface of 7000 km² and moving down slopes of c. 1.1° for
1341 290 km, some formerly interpreted as submarine channels, some with extremely irregular
1342 basal boundary geometry, had originated by erosion from debris flows and slides (Dakin et
1343 al., 2013; Sobiesiak et al., 2018; Soutter et al., 2018).

1344 All this variation and similarities need to be acknowledged when the origin of ancient valleys is
1345 the question for study.

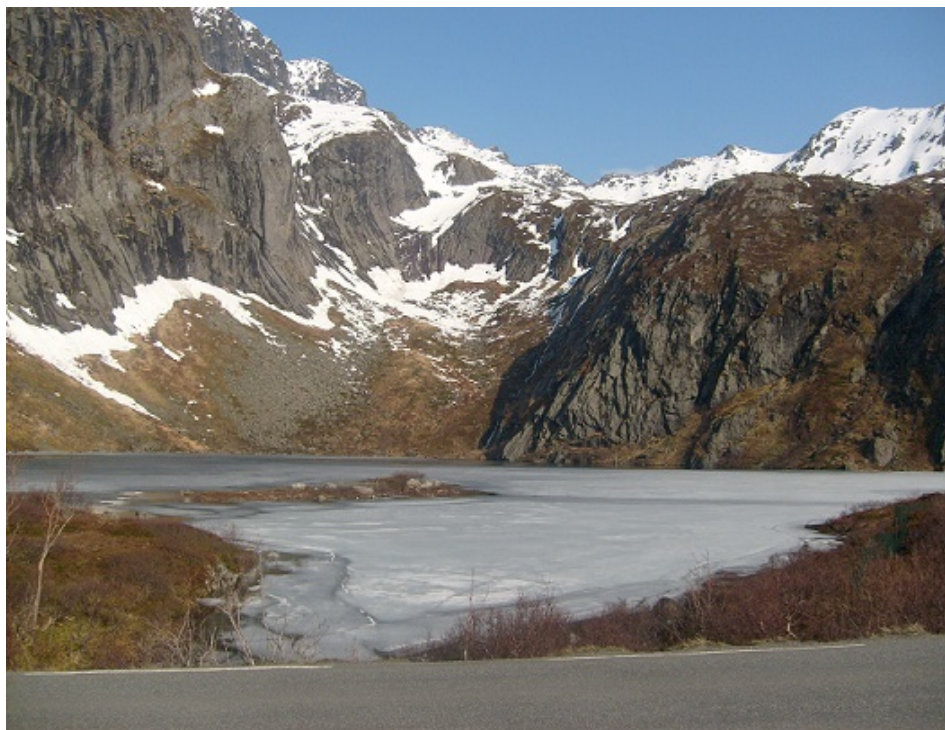
1346 *2.11.2. Glacial and non-glacial valleys – shape*

1347 Glaciated valleys are commonly U-shaped, and fluvial valleys are commonly V-shaped
1348 (Montgomery, 2002; Prasicek et al., 2014). But glaciogenic tunnel valleys may be both V-
1349 shaped and U-shaped (van der Vegt et al., 2012). And U-shaped valleys are produced by
1350 many non-glacial processes and in different environments, i.e. in pull-apart basins (Gürbüz,
1351 2010; Fedorchuk et al., 2019), by slides, rivers and SGFs (Woolfe, 1994; Ebert, 1996; Lamb,
1352 2008; Giddings et al., 2010; Amblas et al., 2011; Macdonald et al., 2011; Clarke et al., 2012;
1353 He et al., 2013; Vachtman et al., 2013; Coles, 2014; Ortiz-Karpf et al., 2017; Pauls et al.,
1354 2019; Isbell et al., 2021), in submarine canyons (Imbo et al., 2003; He et al., 2013; Gales et
1355 al., 2014; Pehlivan, 2019; Puga Bernabéu et al., 2020; see also Kumar et al., 2021), and by
1356 lowering of the sea level (compare descriptions in Germs and Gaucher, 2012 to Sial et al.,

1357 2015; and also Giddings et al., 2010 to Bechstädt et al., 2018). Coles (2014) wrote: “In fact
1358 fluvial valleys occupied a wide range of valley shapes, not simply the V-shape referred to in
1359 previous, particularly glacial orientated, literature. This means these idealized forms cannot
1360 be solely used to distinguish between glacial and fluvial valleys.”

1361 *2.11.3. Glacial and non-glacial valleys – fjords*

1362 Fjords are distinctive overdeepened narrow valleys. They are most shallow at the outlet where
1363 there is a “sill” or ridge of any material, but commonly bedrock (Fig. 4), which can be more
1364 than 1 km higher than the deepest parts of the fjords (Mangerud et al., 2019). Fjords are very
1365 common in the Pleistocene and Holocene, almost 1800 are recorded (Syvitski and Shaw,
1366 1995), and these would easily be preserved in the rock record. However, there is a very poor
1367 record of ancient fjords. The few examples reported in the literature mainly document
1368 sedimentary infill of valleys, they do not display the typical fjord appearance with e.g., a ridge
1369 at the outlet, and may display uneven and irregular floors (Bowen, 1969; Visser, 1987;
1370 Kneller et al., 2004; Bussert, 2010; Alonso-Muruaga et al., 2018; Bechstädt et al., 2018;
1371 Moxness et al., 2018; Fedorchuk et al., 2019; Dietrich et al., 2021; Vesely et al., 2021).
1372 Landforms interpreted as fjords/glaciated valleys, including documented striated and abraded
1373 landforms, may have been formed by tectonics combined with SGFs and fluvial erosion
1374 (sections 2.5, 2.9-2.11.1).



1375 Fig. 4. The smallest fjord observed by the present author, Vassdalsvatnet, Lofoten Peninsula,
 1376 Norway. The length of this fjord is around 400 m, but it has the same appearance as all other
 1377 fjords, i.e. it is deepest in the middle and displays a ridge at the outlet. There are actually two
 1378 ridges in this fjord, similar to what may be present in some larger fjords. One is next to the
 1379 road and another one is sticking up through the ice as a small island (in the middle of the
 1380 picture). In the same area there are more small fjords with slightly greater lengths and depths.

1381 *2.12. Glaciofluvial deposits*

1382 Any strong water currents produce similar features, e.g., compare González and Glasser
 1383 (2008) to Lamb et al. (2014). Lang et al. (2020) described bedforms in glaciogenic settings
 1384 generated by “supercritical” currents and wrote: “individual bedform types are generally not
 1385 indicative of any specific depositional environment.” Further, they stated that glaciogenic
 1386 “upper-flow regime bedforms” are rare in pre-Pleistocene deposits, and provided only five
 1387 examples from pre-Pleistocene environments and all from Upper Ordovician “glaciogenic”

1388 sandstone areas (Lang et al., 2020).

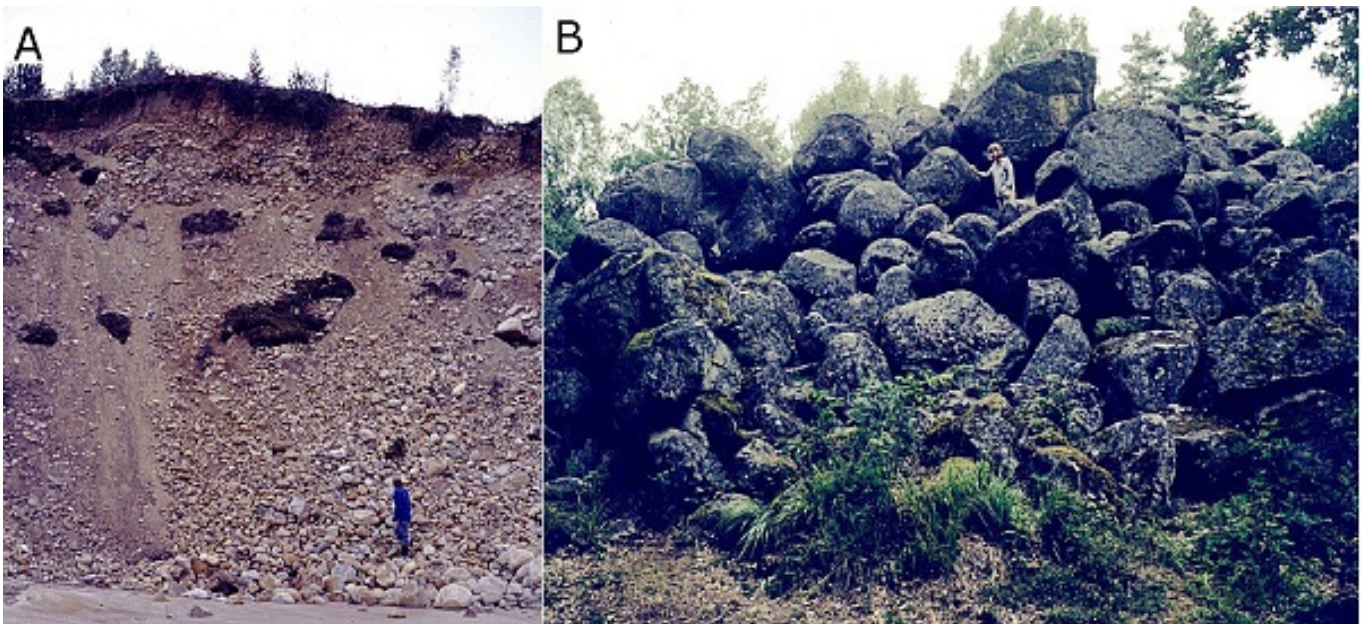
1389 Only when water flow is restricted by ice, and no other obstacles are present, there may be
1390 differences. All kinds of glaciofluvial deposits where ice restricted the flow of water, e.g., in
1391 kames (Fig. 5B), englacial and supraglacial eskers, lateral channels, crevasse fillings, etc., are
1392 missing from ancient deposits. These structures ought to be the more diagnostic features, as
1393 opposed to the often documented “glaciofluvial” or fluvial outwash and channel sandstones
1394 which can form in a wide variety of environments.

1395 *2.12.1. Eskers*

1396 Pleistocene eskers are commonly well sorted, often large boulders at the bottom center, then
1397 followed by finer clasts and sand (Fig. 5A). Their appearance is like linear conglomerates, but
1398 mostly sand higher up in the stratigraphic sequence. This general and most important
1399 structural configuration of eskers is the most significant difference compared to pre-
1400 Pleistocene linear landforms which are interpreted to be eskers. Furthermore, there are no
1401 reports of erratics on top of or close to the top of pre-Pleistocene “eskers,” which is a
1402 common phenomenon for Pleistocene eskers (Frakes, 1979). Only a few reports mention
1403 “glacial” tectonic disturbances in pre-Pleistocene “eskers” or “tunnel valleys,” similar to ice-
1404 push structures, ice-block load structures and lateral slump and slide structures displayed by
1405 Pleistocene eskers (Allen, 1975; Biju-Duval et al., 1981).

1406 Sediments which are interpreted to be pre-Pleistocene eskers are rarely reported (Vesely et al.,
1407 2021). There are, however, sandstone channels in many places which show superficial
1408 similarities to eskers. These are mainly present in the Upper Ordovician and many may have
1409 been reinterpreted to be tunnel valleys (see below). LPIA linear sandstone bodies in South
1410 America which had been interpreted to be eskers are commonly short but may be up to 100 m

1411 long and display about the same width (1.5-2 m) as height (1-2.5 m) (González and Glasser,
 1412 2008), while common width/depth ratios for eskers lie between 2 and 20 (Vesely et al., 2021).
 1413 These “eskers” display occasional thin layers of pebbles, and are covered by “tillite”
 1414 (González and Glasser, 2008). There are also debris-filled (e.g., conglomerates) channels in
 1415 the same area which earlier had been interpreted to be eskers (González and Glasser, 2008).



1416 Fig. 5. A. Esker in Västerbotten county, Sweden. Boulders of different sizes and sand are
 1417 sorted into different zones. Upper zone is winnowed out (below highest coastline).
 1418 Commonly eskers consist of more sand and smaller boulders than the esker in the picture. B.
 1419 A kame, i.e. a “short esker hill.” This one is exceptional as it mainly consists of very large
 1420 boulders. Antamála rör, Småland county, Sweden (Lundqvist, 1979).

1421 2.12.2. Tunnel valleys

1422 Ordovician and LPIA geologic features which have been interpreted as tunnel valleys (but
 1423 sometimes may be interpreted as ice stream valleys) are commonly made up of sandstone.

1424 These may be tens of kilometers long, tens of meters to occasionally more than 300 m deep,
1425 more than 1 km wide, linear or slightly sinuous, and may display amalgamation or an
1426 anastomosing network (Le Heron et al., 2004; Le Heron. 2010; Vesely et al., 2021). These
1427 tunnel valleys display many similarities to other types of valleys with which they can be
1428 confused. They are in many respects similar to fluvially eroded valleys (e.g., Baker and
1429 Milton, 1974; Gupta et al., 2017; Zaki et al., 2018, 2020, 2021). In some ways, they are
1430 similar to quickly formed slump-generated recent megachannels, but the sedimentary material
1431 is almost only sand in the Paleozoic valleys but richer in clay in recent valleys which may
1432 explain structural differences in appearance (Eyles and Lagoe, 1998). Tunnel valleys also
1433 resemble tidal channels (except for depth, up to 60 km long, 3 km wide and 22 m deep;
1434 Aliotta and Perillo, 1987), non-glacial sandstone channels (lacustrine or marine, tens of
1435 kilometers long, tens of meters deep, more than 1 km wide, linear or slightly sinuous and
1436 often amalgamated, but if exhumed may show up as positive landforms; e.g., Bell et al.,
1437 2020; Dou et al., 2021), and submarine channels and canyons (e.g., compare to Covault and
1438 Romans, 2009; Covault et al., 2016; Shanmugam, 2016). Some researchers have interpreted
1439 tunnel valleys to be fluvial even if glaciers have been close by (Keller et al., 2011).

1440 Pleistocene tunnel valleys are somewhat more outstanding than more ancient “tunnel
1441 valleys,” up to 100 km long, 400 m deep and 5 km wide, but most common is c. 10 km, 100
1442 m and 1.5 km, respectively, displaying a typical width/depth ratio around 10 (Vesely et al.,
1443 2021). While van der Vegt et al. (2012) mix descriptions of Ordovician “tunnel valleys” and
1444 Pleistocene tunnel valleys, cross-sections indicate that the Ordovician examples commonly
1445 are wider and not as deep. Furthermore, there are no intra-formal striated pavements in the
1446 Pleistocene, but these are common in the Ordovician tunnel valley sediments. Pleistocene
1447 tunnel valleys are better preserved but also display more of an appearance of a valley than
1448 pre-Pleistocene examples (Vesely et al., 2021, their Fig. 13).

1449 The control of the distribution of Ordovician tunnel valleys may partly be from the existence
1450 of older crustal lineaments, and the valleys are bounded by faulted and/or folded zones
1451 (Ghienne et al., 2003; Le Heron et al., 2006), which may add a tectonic component to their
1452 origin. Keller et al. (2011) wrote: “The genesis of these tunnel (?) valleys is still a matter of
1453 debate.” Le Heron et al. (2018a) wrote that there is an absence “of suitable modern
1454 analogues” to these tunnel valleys, even though they tried to solve the problem.

1455 *2.12.3. Raised channels, eskers and tunnel valleys*

1456 Except for the linear non-glacial landforms described in previous sections, there are more
1457 than 100 areas displaying inverted stream channels, i.e. wadis or other fluvial channels, which
1458 have been exhumed and stand out as long positive ridges (Zaki et al., 2021). These are present
1459 on almost all continents, from the Silurian until the Holocene, and these may be compared to
1460 Ordovician raised channels/eskers/tunnel valleys which are interpreted to be glaciogenic
1461 (Maizels, 1990a, 1990b; Zaki and Giegengack, 2016; Zaki et al. 2018, 2020, 2021). In Egypt,
1462 there are more than 7000 sinuous ridges, across ~40 000 km², up to 18 km in length, up to a
1463 few hundred meters in width and up to 33 m high, which are commonly interpreted to be
1464 inverted wadis (Zaki and Giegengack, 2016; Giegengack and Zaki, 2017; Zaki et al., 2018,
1465 2020). In different areas, ridges may be up to approximately 500 km long, the heights may be
1466 more than 40 m and the widths up to 4 km (Zaki et al., 2021). Such raised channels could
1467 easily be mistaken for eskers or tunnel valleys, especially if they would not show up clearly in
1468 stratigraphic sections. In the Plio-Pleistocene sediments of Oman, there is a complicated
1469 network of many generations of raised channel systems, but also many deeply buried, some of
1470 which have been labeled with the term “pseudo-esker” (Maizels, 1990a, 1990b). These are up
1471 to 250 km long, in some places more than 2 km wide, but commonly <30 m in height, and
1472 they display similarities to the Ordovician “tunnel valleys” in shape, length and composition
1473 (compare Maizels, 1990a, 1990b, to e.g., Vesely et al., 2021).

1474 In conclusion, there is a suggested similarity of pre-Pleistocene tunnel valleys and eskers to
1475 non-glacial channels, and a suggested difference to Pleistocene tunnel valleys and eskers.

1476 *2.13. Dropstones*

1477 *2.13.1. Dropstones, similarities*

1478 Dropstones are often assumed as prime evidence for glaciation, with the consequence that
1479 cold climates have been interpreted for many areas. For example, Rodríguez-López et al.
1480 (2016) interpreted lonestones in Cretaceous sediments as dropstones, even though there is no
1481 other demanding evidence for glaciation. Similarly, Frakes and Krassay (1992) interpreted
1482 lonestones in Jurassic and Cretaceous fine grained sediments as probably glaciogenic
1483 dropstones, because there was a shortage of fossil driftwood in the strata. However, Donovan
1484 and Pickerill (1997, 2008) considered lonestones in the early Cenozoic of Jamaica as non-
1485 glaciogenic, as there was no evidence or possibility for glaciation at that place and time. And
1486 Doublet and Garcia (2004) interpreted dropstones from Mesozoic sediments in Spain as
1487 dropped from floating trees. LPIA dropstones in Argentina had dropped as rock fall from
1488 steep valley walls (Moxness et al., 2018).

1489 Many different parameters are important for the appearance of clast penetration and sediment
1490 disturbance during impact. These parameters include water depth, properties of the bottom
1491 sediment, clast size and shape (Bronikowska et al., 2021), whether clasts are frozen to ice
1492 during sinking, simultaneous deposition of sediment by flowing water, and if the sediments
1493 are reworked by SGFs. Small dropstones, approximately a cm in size or smaller, may not
1494 produce much structures in bottom sediments (Bronikowska et al., 2021). Even if there are
1495 many unknowns, there are criteria which may help to determine if a lonestone has been
1496 dropped or has been transported by a SGF (see below).

1497 Any violent disturbance of the environment, like glaciation, earthquakes, mass movements,
1498 tsunamis, and even larger storms, may induce scenarios that transport clasts which may
1499 display an appearance of dropstones (Tachibana, 2013; see also Shanmugam, 2012). Recent
1500 tsunamis have documented runups up to 524 meter above sea level, i.e. in 1958 in Alaska
1501 (Paris et al., 2018). Clasts can also be transported in water by biological rafting, as projectiles,
1502 and occasionally by floatation or strong whirlwinds (Liu and Gastaldo, 1992; Oberbeck et al.,
1503 1993a; Bennett et al., 1994, 1996; de Lange et al., 2008; Bronikowska et al., 2021).
1504 Deposition of all these clasts may display an appearance similar to glaciogenic dropstones,
1505 like compaction of sediment both during deposition and later because of dewatering and/or
1506 compression from superimposed sediments.

1507 Iceberg dump mounds are accumulations of clasts dropped when icebergs overturn and
1508 release lots of material at once. These may be sorted, from the sinking of the sediments
1509 through the water column, may be conical or display different patterns of irregular outlines
1510 and different penetration of the underlying sediment (Thomas and Connell, 1985;
1511 Pisarska-Jamroży et al., 2018; Bronikowska et al., 2021). However, Aitken (1993) showed
1512 the mounds documented by Thomas and Connell (1985) to be small subaqueous fans and
1513 debris flows, even if they are in an area where there is deposition from icebergs. Another
1514 accumulation of sediments, labeled “till pellets,” can be found smeared out as if they have
1515 been molded by the overlying sediment (Miall, 1983; Visser, 1983a). Clast accumulations
1516 may be produced in any flowing media.

1517 *2.13.1.1. Transport by sediment gravity flows*

1518 Clasts transported with SGFs are often embedded in a clayey matrix (Bouma, 1964; Embley,
1519 1982). Single clasts, up to 20 meter in diameter (Shanmugam, 2016, 2021b), or clusters of

1520 clasts can be dragged along, slide on top of a sedimentary mass flow sequence, move upwards
1521 through the flow, or be winnowed out, and be deposited at different depths of a sedimentary
1522 sequence during single events (Postma et al., 1988; Scott, 1988b; Best, 1992; Pickering and
1523 Hiscott, 2015; Shanmugam, 2020, 2021b; Kennedy and Eyles, 2021). These clasts may
1524 display an appearance similar to clasts transported by icebergs, i.e. these are “left-overs” or
1525 lonestones, or “dumps” (Crowell, 1957, 1964; Schermerhorn, 1974a; Kim et al., 1995).
1526 Transport of lonestones by SGF deposits can be determined by fabric analyses (section 2.2.9).

1527 In lahar deposits in Utah the clasts are often locally concentrated in clots high up in the
1528 sedimentary beds (Walton and Palmer, 1988), thus showing similarities with “iceberg roll
1529 dumps” (e.g., in the LPIA of Tasmania; Powell, 1990). Clasts with diameters of up to 15 cm
1530 had been transported more than 400 km, probably by water currents and/or SGFs. After
1531 deposition, the clasts became incorporated in SGFs. These clasts were earlier thought to have
1532 been transported with icebergs (Jansa and Carozzi, 1970).

1533 *2.13.1.2. Transport by vegetation, animals and floatation*

1534 Especially during a catastrophe (e.g., a tsunami) much material can be transported with up-
1535 rooted trees. In Carboniferous coal seams, boulders with weights up to 70 kg are present
1536 (Price, 1932; Woolfe, 1994). Boulders in Cretaceous and Carboniferous sediments have been
1537 transported up to 100 km or more, by floating with plants (Hawkes, 1943; Liu and Gastaldo,
1538 1992). Boulders transported with contemporary tree roots have sizes up to 3 m (Bennett et al,
1539 1996). Fossils of land-living plants are present from the Ordovician, even if their affinities are
1540 largely unknown (Servais et al., 2019).

1541 Clasts dropped from kelp or vegetation may not display any differences to those dropped
1542 from icebergs (Doublet and Garcia, 2004). Probably hundreds of thousands of kelp rafts are

1543 transporting attached clasts of “dropstones-to-be” today in the Southern Ocean alone (Waters
1544 and Craw, 2017), and ancient transport with kelp or other algae is documented (Bennett et al.,
1545 1994; Zalasiewicz and Taylor, 2001). Species of green and red algae may float on the water
1546 surface (Thiel and Gutow, 2005). Red algae are present in the Precambrian (1.6 billion years,
1547 Bengtson et al., 2017; 1.0 billion years, Gibson et al., 2018) and in Ordovician sediments
1548 (Fry, 1983), but these are commonly smaller species which could not transport larger clasts
1549 than maybe a few centimeters. Unspecified macroalgae (incomplete specimens >2 cm in
1550 length which are small parts of much larger algae) are present in close connection to “glacial”
1551 diamictites in the Neoproterozoic (Ye et al., 2015; Chen et al., 2015). Green algae are known
1552 from the Cambrian (Servais et al., 2019), but their origin may be placed in the Meso- or
1553 Neoproterozoic (Del Cortona et al., 2020). Kelp, which commonly refers to brown algae, are
1554 considered to have diverged some 100 million years ago (Silberfeld et al., 2010), and most
1555 larger forms maybe not until 25 million years ago (Rothman et al., 2017), even if some
1556 Precambrian to Jurassic fossils are classified as possible brown algae (Hollick, 1930; Fry,
1557 1983; Zalasiewicz and Taylor, 2001; Silberfeld et al., 2010). Kelp transports much sediment
1558 onto beaches, including veneers of clasts, over distances of 5000 km, in sizes commonly up to
1559 83 kg, and a record estimated weight of a large clast of 365 kg (Emery and Tschudy, 1941;
1560 Garden and Smith, 2011).

1561 Microbial mats occasionally are lifted from the bottom surface and may transport clasts, sand
1562 clusters and clay fragments which are up to several cm long (Schieber, 1999; Thiel and
1563 Gutow, 2005). Pebbles up to 25 mm in length, can in rare instances float directly on the
1564 surface of the sea surface (Hume, 1963; Bennett et al., 1996). Gastroliths with weights up to
1565 2.5 kg, and clusters of gastroliths up to 70 kg. had been recorded from sedimentary sequences
1566 (Bennett et al., 1996). However, the appearance of gastroliths, commonly displaying a
1567 “polished” rounded form, in most cases would be easy to sort out from dropstones.

1568 *2.13.3. Dropstones, differences*

1569 The amount of material which has been dropped by ice in Quaternary sedimentary deposits
1570 may be “astounding” over extensive areas and can even create “pathways” of dropstones
1571 (Korstgård and Nielsen, 1989; Dionne, 1993; Pisarska-Jamroży et al., 2018), but pre-
1572 Pleistocene rafted material commonly is dispersed. Marine sedimentation from a large glacier
1573 would be more uniform over wider areas than deposition from SGFs (Clark and Hanson,
1574 1983; Boulton, 1990).

1575 Ancient dropstone-bearing strata often are deposited as blanketing layers on top of “tillites,”
1576 similar to turbidity deposits (compare, e.g., Talling et al., 2007; Shanmugam, 2016; Molén,
1577 2017, 2021; Rampino, 2017). The sediments commonly are not present close to the outermost
1578 border of diamictites, or in bowls in the upper surface of the “tillite,” where marine, brackish
1579 and lake sediments usually are deposited (Deynoux, 1985b).

1580 Thomas and Connell (1985) documented data and developed criteria for recognition of
1581 dropstones from a Pleistocene lake in Scotland, and these were further developed mainly by
1582 theoretical numerical process modeling by Bronikowska et al. (2021). The list below
1583 describes the most common features, and these are also those that are not commonly present
1584 in SGF deposits. The difference between the appearance of dropstones documented by
1585 Thomas and Connell (1985), in SGF deposits, and those in pre-Pleistocene strata, are
1586 mentioned in the comments.

1587 a) Penetration of dropstones 5-20 cm in diameter is commonly about 1/3 of the clast size, but
1588 2/3 if clasts display close to vertical orientation and are thin. Larger clasts penetrate more
1589 (Bronikowska et al., 2021). However, it is difficult to state anything conclusively concerning
1590 the magnitude of crushing and depressions in underlying laminae, because the firmness of the
1591 bottom sediments vary from hard to soft (Bronikowska et al., 2021).

1592 Comment 1: Clasts transported by SGFs may not penetrate laminae. Laminae below clasts are
1593 almost always bent just by the compaction of the sediments, but sharp rocks commonly
1594 penetrate. Single penetrations of laminae are always to be expected for SGFs. Some reef
1595 blocks transported by mass flows are interpreted to have sunk down >1 m into underlying soft
1596 sediments (Rigby, 1958).

1597 Comment 2: Dropstones in ancient diamictites do not usually cut through underlying laminae
1598 (Fig. 6), although a few authors report evidence of penetration (Binda and van Eden, 1972;
1599 Smith and Eriksson, 1979; Mustard and Donaldson, 1987a), and laminae that are not
1600 penetrated are not diagnostic of a dropstone origin (Thomas and Connell, 1985). Published
1601 photos and descriptions of ancient dropstones generally show that laminae have been bent
1602 around the clasts or slightly pressed down, not commonly cut or crushed (even if photos of
1603 such features are often chosen for publication, e.g., Molén, 2021), even though the clasts may
1604 be c. 0.6 m in diameter (Schenk, 1965; Visser and Kingsley, 1982; Gravenor et al., 1984; Kim
1605 et al., 1995; Craddock et al., 2019; Isbell et al., 2021; Table S3). The sediments thin out
1606 around clasts, both above and below, and the sediments are actually draping the clasts, which
1607 is what could be expected from SGFs (Dey et al., 2020; Molén, 2021). In some areas clast are
1608 “locally very abundant along bedding planes” (Kneller et al., 2004).

1609 b) Variable clast size.

1610 Comment 1: Clasts may be sorted in SGF deposits. In the Gowganda Formation dropstones
1611 are more common in coarse grained than in fine grained rhythmites (Mustard and Donaldson,
1612 1987a).

1613 Comment 2: Dropstones which have been transported by sea ice or vegetation will usually
1614 have a smaller size and better sorting and roundness than those which have been transported
1615 by glacier ice, the latter which may be up to 10 m in diameter (Gilbert, 1990). Diameters of
1616 Quaternary glaciogenic dropstones of diameters 0.5 m and larger are not uncommon (Dionne,
1617 1993; Meyer et al., 2016; Pisarska-Jamróży et al., 2018; Bronikowska et al., 2021). The
1618 maximum size of “left-overs” in SGFs should in general be smaller than dropstones (Clark

1619 and Hanson, 1983; Peakall et al., 2020), but as already documented (section 2.3.) the
1620 “erratics” in “tillites” are smaller than those in tills, and it is therefore necessary to compare
1621 relative sizes (Molén, 2021). While single supposed dropstones in pre-Pleistocene sediments
1622 may be up to 3 m in diameter (Rodríguez-López et al., 2016), and clasts many meters in size
1623 that are interpreted to be dropstones are present in massive debris flows or slides (Domack
1624 and Hoffman, 2011), pre-Pleistocene dropstones commonly are much smaller. As examples,
1625 dropstones in the Neoproterozoic outcrops are mostly pebble-sized (Schermerhorn, 1977) as
1626 opposed to common meter-sized dropstones of Precambrian affinity in Pleistocene and
1627 Holocene deposits (Dionne, 1993). In the Dwyka Group in South Africa dropstones are often
1628 only 2-5 cm, but may rarely be up to one meter across (Visser, 1982, 1983b), and in massive
1629 “glaciomarine” diamictites they may be a few meters (Haldorsen et al., 2001). Le Heron et al.
1630 (2017) mentioned “unequivocal” evidence for ice rafting, from the Neoproterozoic of Death
1631 Valley, but pictured dropstones were solely 2-3 cm in diameter and displaying only limited
1632 penetration, as would also be expected from lonestones. Maslov (2010) mentioned dropstones
1633 of sizes “up to 2 cm” in Paleoproterozoic sediments. It may be suspected that very small
1634 dropstones, with a diameter of only a few cm or smaller, will not penetrate much into
1635 sediments (Bronikowska et al. 2021), but in SGFs even the smallest clasts likely will disturb
1636 the laminations.

1637 c) Most clasts are oversized.

1638 Comment: In SGF deposits it is common that the clasts have a similar size or are smaller than
1639 the sediment beds within where they are buried. (Fig. 6, Table S3.)

1640 d) No correlation between the size of clasts and thicknesses of beds.

1641 Comment: SGF deposits may display correlation. (Fig. 6, Table S3.) In ancient “glaciogenic”
1642 deposits larger dropstones are often present in thicker layers, which suggest that they have
1643 been transported by SGFs (McCann and Kennedy, 1974, plate 2; Martin et al., 1985; Mustard
1644 and Donaldson, 1987a; Moncrieff and Hambrey, 1990, their Fig. 6C; Molén, 2021).

1645 e) Fabrics – only measured on 50 clasts (Thomas and Connell, 1985). Clast orientation

1646 seldom subparallel to stratification (4%), more often inclined (46%), but most are subvertical
1647 (50%).

1648 Comment: Fabrics variable in SGF deposits, but planar fabrics and vertical clasts are not
1649 uncommon. (Section 2.2.9. Also, see planar fabrics for outsized clasts and “dropstones” in
1650 Lindsay et al., 1970; Kim et al., 1995.)

1651 f) No current indicators.

1652 Comment 1: In a laminated or rhythmic sediment section, any horizontal movement in the
1653 bottom sediments may result in disturbances around clasts. Evidence of movements may
1654 indicate that the deposition was not slow, i.e. not within an environment displaying more or
1655 less stagnant bottom water. Clasts which are transported within SGFs, whether the sediments
1656 will be deposited as laminations or not, may show both external and internal (within the
1657 sediment) structures indicating horizontal movement. (Fig. 6.)

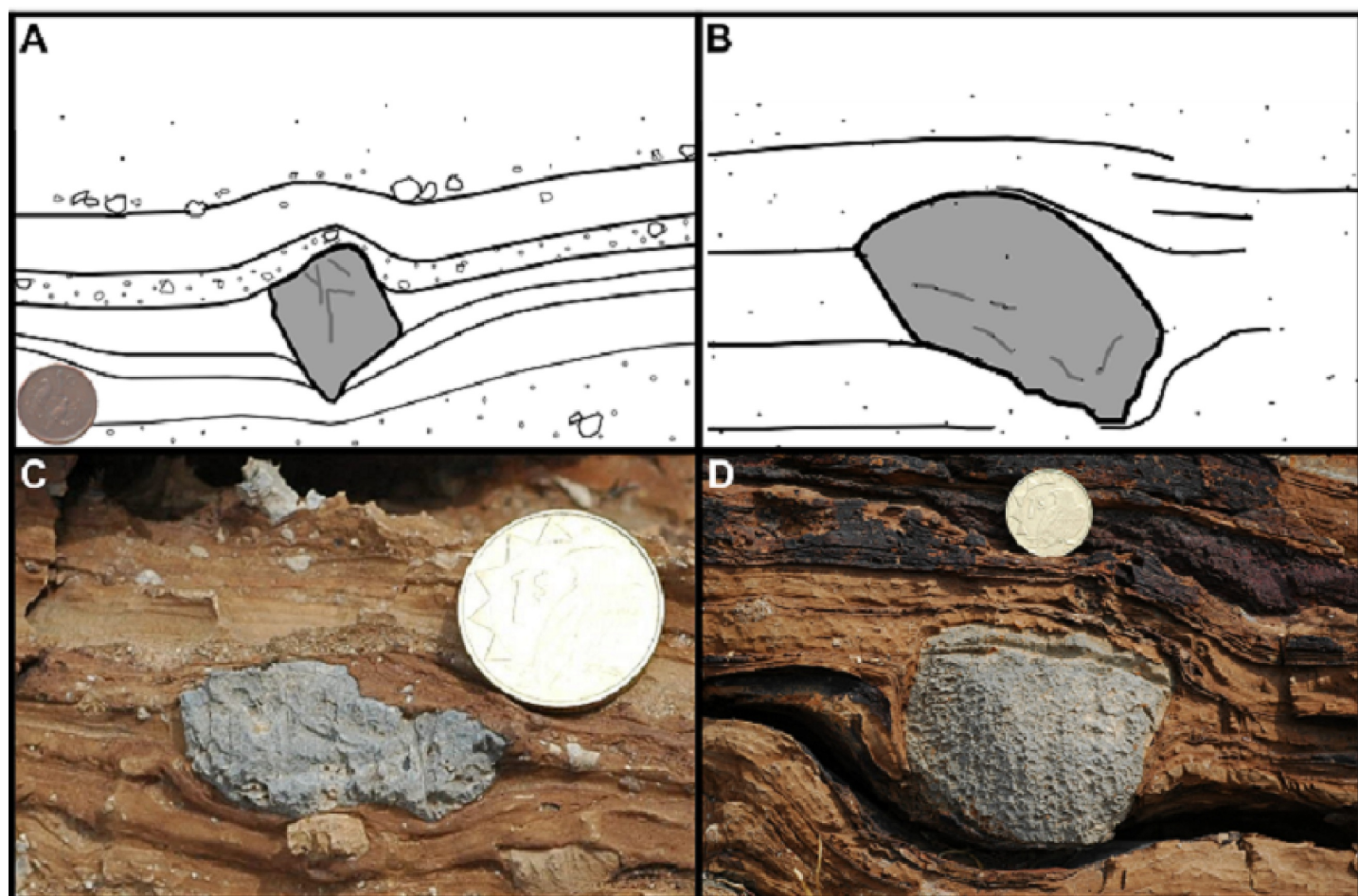
1658 Comment 2: There are often lee side structures connected with pre-Pleistocene “dropstones”
1659 (Lindsey, 1969; Ovenshine, 1970; Visser, 1983a; Aitken, 1991; Molén, 2017, 2021). In the
1660 Middle Permian of Australia brachiopod fossils are present on the lee sides of oversized
1661 clasts which are interpreted to be dropstones (Yang et al., 2018). In places the sediment has
1662 been pushed up in front of a dropstone, without any evidence of penetration of underlying
1663 beds, as if the clast has been moved along in a SGF (Mustard and Donaldson, 1987a, their
1664 Fig. 6G; Molén, 2017, 2021).

1665 g) Sediment around clasts are commonly rucked (pushed up on both sides, commonly sharp
1666 folds), ruptured (lamination in sediment next to, below and/or above clast is broken and
1667 mixed) and/or onlapped (covering sediment next to clasts not draped around the clast, but
1668 stops at the clast, except for those laminae that cover the clast).

1669 Comment: Draping is prevalent if clasts are transported by SGFs. Draping of clast may
1670 display laminae that commonly are covering the clasts on all sides, but the thickness of the
1671 sediments may change next to the clast. Some laminae may thicken next to the clasts, others
1672 may thin out. Some may only stop at the clast. Commonly there are not many sharp

1673 sedimentary structures around clasts transported by SGFs. Laminae may become diffuse or
 1674 split into more laminae, reflecting wake eddies (compare to Kim et al., 1995). (Fig. 6.)

1675 Table S3 (Supplementary material) document dropstones which display features which are
 1676 more compatible with transport by SGFs than to dropping from ice.



1677 Fig. 6. Clasts which have been interpreted as dropstones from the Ghaub and Chuos
 1678 Formations of Namibia. The irregularities and appearances displayed in the beds next to the
 1679 clasts indicate currents and a SGF origin. If clasts as small as these would have been dropped
 1680 from ice, they may not have disturbed the sediment much at all (Bronikowska et al., 2021). In
 1681 general, the appearances displayed in these pictures are common in ancient “glaciogenic”
 1682 sediments, but different from Quaternary dropstone bearing sections. A. The bed containing
 1683 the clast becomes thicker next to the clast on both sides. There may be penetration of strata,
 1684 but even if the clast is pointy it appears more that the sediment is slightly bent because of

1685 compression during transport and therefore thins out beneath the clast. (Drawing after
1686 Hoffman www.geol.umd.edu/~jmerck/geol342/lectures/06.html). B. There is a small
1687 “impact” structure to right of the clast, but nothing on the left side. Laminae on the left are
1688 straight. To the right, the beds above the clast bend down over the clast. The appearance is
1689 one of diffuse wake eddies on the right side of the clast. Clast is c. 1.5 cm in length. (Drawing
1690 after Le Heron et al., 2021a.) C. The sediment bed becomes thicker next to the clast. The clast
1691 is regularly enclosed by sediment above and below. This is the most common appearance of
1692 pre-Pleistocene clasts interpreted to be dropstones. D. This clast is inside a thicker sediment
1693 bed. The bed thickens next to the clast, which is especially evident on the right side of the
1694 clast where the sediment surface enclosing the clast is at a lower level than on the left side.
1695 To the left, both the bedding and the underlying sediment are bent, as would be the case if the
1696 clast was transported in that direction enclosed in a SGF. It can be discussed if there is much
1697 evidence of penetration, or if the sediments mostly thin out beneath the clast. (Photographs by
1698 T. Bechstädt; Bechstädt et al., 2018.)

1699 *2.14. Laminated sediments*

1700 “Varved sediments” (laminated beds) which may be interpreted as deposited on a yearly basis
1701 can form instantaneously by SGFs, including hyperpycnal flows, and also from contour
1702 currents (the latter commonly move with speeds up to 3 m/s, and including cyclone driven
1703 bottom flows with velocities of up to 70 m/s), in many different environments (Kuenen,
1704 1964; Pettijohn and Potter, 1964; Winterer, 1964; McKee et al., 1967; Lowe, 1982, 1988;
1705 Gravenor and Rocha-Campos, 1983; Domack, 1990; Dykstra, 2012; Zavala and Arcuri, 2016;
1706 Yawar and Schieber, 2017; Shanmugam, 2017a, 2021a; Tedesco et al., 2020; Isbell et al.,
1707 2021; Tian et al., 2021). There are criteria for distinguishing yearly varves from surge
1708 laminae, and also other rhythms, even though these criteria are not clear cut (Smith and
1709 Ashley, 1985), and there is a vigorous debate in this area (e.g., Andrews et al., 2018; Smith

1710 and Bailey, 2018a, 2018b; Da Silva et al., 2019; Matys Grygar, 2019; Smith, 2019). Marine
1711 couplets, with affinities to annual lacustrine varves, often form in response to tidal water if
1712 there is an abundance of suspended sediment available, and may display double mud layers
1713 (Cowan and Powell, 1990; Smith et al., 1990; Shanmugam, 2016, 2017a, 2021a, 2021b). A
1714 recorded maximum of 1000 couplets have been deposited in three to four years time (Molnia,
1715 1983b). In connection to the variation in differences in sedimentation in general, Shanmugam
1716 (2017a) concluded that “the grand ingrained principle of 'one deposit for one flow type' is
1717 nothing more than a misplaced optimism.”

1718 In pre-Pleistocene “glacial” deposits many rhythmites with an appearance of yearly varves
1719 occur in what must have been marine settings (Schermerhorn, 1977). Annual varves can only
1720 form in fresh water, for example in a lake or perhaps sometimes on a shallow shelf where an
1721 abundance of meltwater is constantly draining from a large glacier. Experiments show that
1722 clay flocculates and will deposit as quickly as sand, if there is no stirring (Schieber et al.,
1723 2007, 2013; Sutherland et al., 2015), and thin silt/clay laminae which are often interpreted to
1724 be yearly varves are deposited simultaneously in both fresh and salt water (Yawar and
1725 Schieber, 2017). The only known marine rhythmites form in response to tidal water (Cowan
1726 and Powell, 1990), or originate by turbidity currents.

1727 Pre-Pleistocene rhythmite sequences may exhibit features not shown by yearly varves.

1728 “Varves” in the Gowganda Formation may be very finely laminated as opposite to more
1729 thickly laminated Pleistocene yearly varves (Molén, 2021). They have been reinterpreted as
1730 non-annual (because of the rhythmite pattern) “distal” turbidites and may contain ripple
1731 marks (Jackson, 1965; Miall, 1983, 1985; Eyles et al., 1985; Smith and Bailey, 2018b).

1732 Rhythmites next to Precambrian “tillites” in the Appalachian mountains, and in the
1733 Gowganda Formation, have been put into question because the “winter layers” are thicker
1734 than the “summer layers” (Schwab, 1981; Molén, 2021), as this appearance is the opposite of

1735 normal varve deposition, but may be possible in rare instances if produced during glaciation.
1736 In the LPIA Dwyka Group of South Africa this is a common appearance (Tavener-Smith and
1737 Mason, 1983). Rhythmites in the Dwyka Group have been reinterpreted to be deposited from
1738 turbidites or tidal activity (Isbell et al., 2008), and LPIA “varves” in Brazil are no longer
1739 considered to be annual (Kochhann et al., 2020)..

1740 *2.15. Glaciomarine (and lake) diamictites*

1741 There is an astounding number and a great diversity of submarine glacial features, linear,
1742 transverse and irregular, covering large areas, which have been produced by glaciers, from the
1743 Pleistocene until today (Dowdeswell et al., 2016a, 2016b). In glaciomarine sediments there
1744 would be grounding zones displaying pushed up transverse till and sea-bottom mud ridges, as
1745 well as different kinds of subglacial, englacial and supraglacial submarine fans where the
1746 upflow part of the deposits shows evidence of having been bordered by an ice-shelf or a
1747 glacier (Boulton, 1990; Powell, 1990; Zecchin et al., 2015). There is nothing remotely similar
1748 to this in the pre-Pleistocene record. There is either no record at all of similar features, the
1749 features are different than those in the Quaternary record, or there are only single examples
1750 where it would be expected to be large areas covered by similar features (Molén, 2021). And,
1751 there are no reports of observational evidence of removal of material by erosion of large areas
1752 of former subaqueous glaciogenic features, i.e. erosion of areas which would be more
1753 protected than terrestrial environments.

1754 In pre-Pleistocene glaciomarine deposits, almost the only evidence given for glaciation is
1755 dropstones, especially if the clasts are found in rhythmites (Frakes et al., 1969; Binda and
1756 Eden, 1972; McCann and Kennedy, 1974; Anderson, 1983; Miall, 1983, 1985; Visser 1989a).
1757 But, if there are marine or lacustrine fossils close to or within sediments that are interpreted to
1758 be glaciogenic, interpretations should be regarded as tentative. As mentioned earlier c. 95%

1759 of ancient “glaciogenic” deposits are interpreted to be marine (section 1.3.), and there are
1760 often marine fossils close to or even (autochthonously) within such diamictites (e.g., Allen,
1761 1975; Bryan, 1983; González and Glasser, 2008; Caputo and Santos, 2020, Sterren et al.,
1762 2021; López-Gamundí et al., 2021). Marine fossils also are common in cyclone and tsunami
1763 deposits, which may trigger mass flows (Shanmugam, 2012).

1764 Neoproterozoic “tillites” usually are not bordered by marine till and a wide zone of ice-rafted
1765 material (Schermerhorn, 1977). Diamictites in general are draped with shale or rhythmites
1766 with lonestones (e.g., Rampino, 2017; Molén, 2017, 2021; López-Gamundí et al., 2021). A
1767 submarine subglacial fan has been inferred from the Carboniferous of Tasmania, but with no
1768 diagnostic ice-contact features present (Powell, 1990). None of the other geological features
1769 have been clearly identified with diagnostic geologic features from any ancient deposit, but
1770 some features may be interpreted from commonly more restricted sedimentary assemblages to
1771 try to integrate the data into a glaciogenic framework (e.g., Aquino et al., 2016; Rosa et al.,
1772 2019; Dietrich and Hofmann, 2019).

1773 *2.16. Periglacial structures*

1774 Periglacial look-alike structures, with the appearance of e.g. ice-wedges, can form by
1775 processes other than freezing and thawing, for example, wetting and drying, thermal
1776 contraction, sedimentary compaction, gravitational loading, small scale tectonics, flexure over
1777 an uneven surface, and almost any volume change in sediments (Yehle, 1954; Flint, 1961;
1778 Schermerhorn, 1974a; Black, 1976; Walters, 1978; Eyles and Clark, 1985; Shanmugam,
1779 2012; Robinson et al., 2017). In tropical waters, polygons originate by infilling of sediment
1780 from above, in fractures that form during cementation (SEPM, 2021). Sheeting joints in
1781 sandstones may display polygonal structures over large areas (Loope and Burberry, 2018).

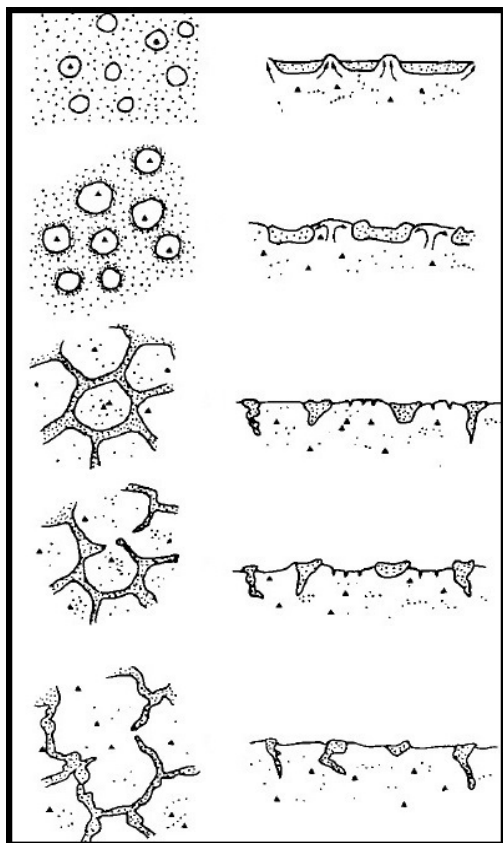
1782 Ice-wedges are normally filled with material from above and polygons frequently show stony
1783 margins (Frakes, 1979). This is not shown by pre-Pleistocene “permafrost” deposits. In
1784 Pleistocene to Holocene polygonal ice-wedge networks (or casts), polygon diameters may be
1785 between 1-46 m, wedge depth 0.25-50 m, and wedge width 0.1-10 m, while the same
1786 structures in the Neoproterozoic Port Askaig Formation were 0.35-1.5 m, 0.09-1.12 m and
1787 0.05-0.3 m, respectively (Eyles and Clark, 1985). The latter was explained as non-glacial and
1788 interpreted to have been generated by gravitational downfolding, and similar structures are
1789 widely reported in shallow marine sequences (Fig. 7).

1790 Clastic dykes have been documented in, for example, the Gowganda Formation in Canada
1791 (Young, 1981b) and the Dwyka Group in South Africa (Visser and Loock, 1982; Visser et al.,
1792 1987). “Ice wedges” from the Ordovician “glacial” in the Sahara likely are sandstone dykes
1793 radiating from sand volcanoes (Fairbridge, 1970; Bryan, 1983), and some sandstone dykes
1794 have been documented to cross each other with an appearance of polygons (Allen, 1975;
1795 Deynoux, 1985a). There are sandstone dykes also in, for example, the Neoproterozoic Port
1796 Askaig “tillites” in Scotland (Eyles and Clark, 1985) and the probable non-glacial diamictites
1797 in France (Eyles, 1990), and these have been interpreted as ice-wedges (Hambrey, 1983).

1798 In the Ordovician of Sahara there are up to 1 km long domes which had been interpreted as
1799 pingos (Bryan, 1983). Further research showed that these structures are tectonically uplifted
1800 diapiric structures in soft sediments, from vertical loading or maybe from upwelling basalts
1801 (Fairbridge, 1971, 1979; Le Blanc Smith and Eriksson, 1979; Le Heron et al., 2005).

1802 Other features which are present in periglacial sedimentary sequences are solifluction debris,
1803 loess, cover sands, ventifacted clasts, slope wash accumulations, frost shattered clasts,
1804 vertically aligned clasts, and size-sorting (Eyles and Clark, 1985), which are commonly not
1805 reported from the pre-Pleistocene.

1806 On the whole it seems that “periglacial” structures are quite rare in pre-Pleistocene “tillites.”
 1807 Instead, structures that mimic periglacial structures seem to be common, for example clastic
 1808 or sandstone dykes formed by loading (Eyles and Clark, 1985). Dykes may be present below
 1809 Quaternary tills but are not very common.



1810 Fig. 7. The figure shows how loading and diapirism in sand have created polygonal patterns,
 1811 superficially similar to permafrost polygons. Uppermost two pictures show diapirism and the
 1812 lower three show the appearance after erosion. (Figure from: Eyles and Clark, B.M., 1985.
 1813 Gravity induced soft sediment deformation in glaciomarine sequences of the Upper
 1814 Proterozoic Port Askaig Formation, Scotland. *Sedimentology* 32, 789-814.)

1815 2.17. *Soft sediment deformation, tectonism*

1816 In both glaciogenic and mass flow environments there are soft sediment tectonic deformation,

1817 both compressional and tensional (Sobiesiak et al., 2018). There are no simple specified
1818 criteria used to distinguish different environments from each other. Ancient deposits have
1819 commonly not been compared to data from Quaternary proved non-glaciogenic and
1820 glaciogenic sediments (Visser et al., 1984; Hart and Roberts, 1994; McCarroll and Rijdsdijk,
1821 2003), and the structures may be present in different sedimentary environments (Arnaud,
1822 2012). Dreimanis (1993) listed eight glaciotectonic structures, and wrote that most of them
1823 may be found in mass flow deposits. He concluded that it would be best to use multiple
1824 stress-related criteria, including e.g., glacial abrasion marks over an area of several hundred
1825 meters, to track down the origin of the deposit. Only conjugate sets of steep-dipping fractures
1826 are stated to be more common in glaciotectonic deposits (Dreimanis, 1993).

1827 A SGF origin may be more probable if there are (Visser et al., 1984; Dreimanis, 1993;
1828 Sobiesiak et al., 2018):

- 1829 a) tensional and compressional stress regimes in one single horizon,
- 1830 b) presence of dewatering structures,
- 1831 c) restriction of deformation to specific lithologies (even leaving other beds above and below
1832 intact and without deformation),
- 1833 d) intimate association with mass flow deposits,
- 1834 e) random orientation of microfold axes,
- 1835 f) sheared sediment lenses that usually are curved or bent in different ways,
- 1836 g) overturned recumbent flows which usually do not have their anticlines sheared off, and/or
1837 are occasionally flattened at their base, and/or have a bulbous terminus often pointing in the
1838 downflow direction,
- 1839 h) extension fractures which are filled by dykes that are localized on the distal side of the
1840 deposit and are accompanied by normal faults.

1841 Some of the structures tabulated above are also present in tills and are interpreted as evidence

1842 of glaciotectonic deformation, e.g., dewatering structures (Dreimanis, 1993).

1843 Any mass flow which loses its velocity and comes to a stop will display both compressional
1844 and tensional regimes, except if it all stops as one large slab. If it is glaciotectonic there
1845 should commonly be more similar tectonism all through the sediments (e.g., Bennett et al.,
1846 2003), but occasionally more at the top parts of the deposits compared to the bottom.

1847 Soft sediment deformation in diamictites in the LPIA of Brazil were interpreted to be
1848 glaciotectonically formed (Rosa et al., 2019), but there was no unequivocal evidence of
1849 glaciotectonics compared to tectonics formed by mass flows. Other soft sediment tectonics in
1850 the LPIA of Brazil is interpreted to be from mass flows, even if there are postulated glaciers
1851 nearby (Mottin et al., 2018), and some glaciotectonic features had been reinterpreted as non-
1852 glacial (Rodrigues et al., 2020).

1853 *2.18. SEM studies*

1854 SEM studies of surface microtextures on quartz sand grains is a quick method to easily
1855 distinguish glaciogenic sediments from other sediments (Mahaney, 2002; Molén, 2014,
1856 2017). Glaciogenic quartz sand grains are characterized by fresh fractures which have been
1857 irregularly abraded all over the grain surface (Molén, 2014). The processes of fracturing and
1858 abrasion may take place at the same instant, as it is grinding rather than impacting that creates
1859 the fractures. It is possible to follow how a glaciogenic grain, which later will be transported
1860 glaciofluvially, will be abraded so that the typical glaciogenic surface microtextures will
1861 slowly first change to microtextures similar to those present in rivers (Molén, 2014; Kalińska
1862 et al., 2022), and after that will continue to change depending on the environment of
1863 deposition.

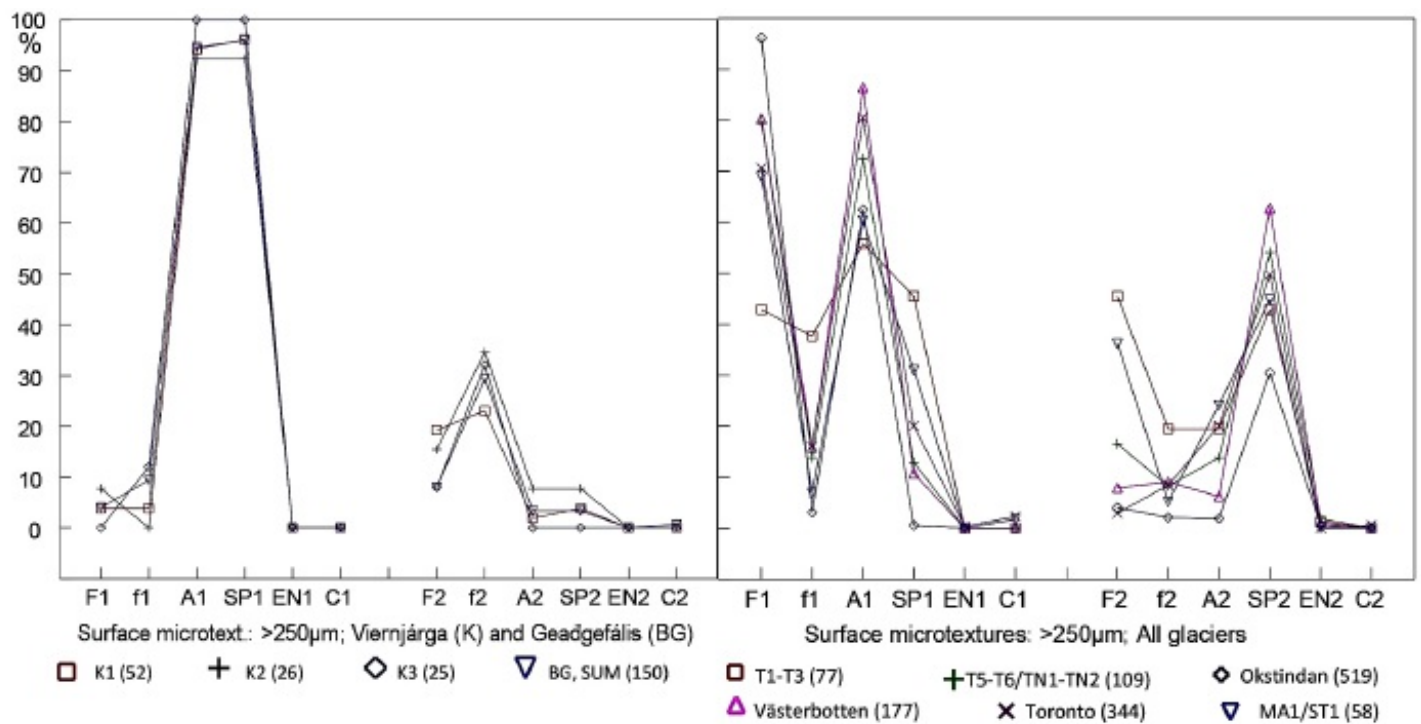
1864 Single surface microtextures produced by glaciers, like different varieties of fractures, may
1865 form in any environment (Mahaney, 2002; Molén, 2014, 2017). This is basic physics, as there
1866 is no difference from the impact of similar forces from different environments. Therefore,
1867 there needs to be a systematic combination of surface microtextures if the origin of a
1868 sediment is to be revealed. Subglacial transport is necessary if surface microtextures typical
1869 for a glacial environment shall be acquired. Supraglacial till and flow tills (if they never have
1870 been transported subglacially), and to a large part englacial till, will not acquire any or only
1871 very few surface microtextures typical for a subglacial environment (Kalińska et al., 2022).
1872 But as soon as a glacier processes rock material subglacially, glaciogenic surface
1873 microtextures form quickly. Supraglacial till, englacial till, and supraglacial flow till, are
1874 usually a minor part of glaciogenic sediments, and these sediments are often loosely packed
1875 and surficial and therefore easily removed by later erosion. This is in contrast to basal till.
1876 Periglacial environments also do not imprint glaciogenic surface microtextures on quartz sand
1877 grains (Kalińska-Nartiša et al., 2017).

1878 Surface microtextures often stand out more on sand grains >250 µm. Smaller grains retain
1879 older surface microtextures more easily which may therefore be preserved from the original
1880 environment, instead of the grain displaying more evidence of the latest environment or
1881 transport history (Molén, 2014).

1882 A method of sorting surface microtextures based on the appearance of the complete grain
1883 surfaces, and not a multitude of small scale surface microtextures which may originate in
1884 different environments, has been shown to be simple and quick (Molén 2014). The data is
1885 easily visualized in a “2-History-Diagram” (Fig. 8). This diagram shows both the last
1886 geological history and the former. The former may be e.g., the origin before release from
1887 bedrock, or glaciation followed by fluvial or eolian transport. The method is described in
1888 detail in Molén (2014) and is applied in Molén (2017) and Molén and Smit (2022).

1889 Soreghan et al. (2014) and Keiser et al. (2015), by referring to occurrences of single small-
1890 scale surface microtextures, misidentified grains that commonly originate from release from
1891 bedrock (compare to Mahaney, 2002; Molén, 2014), and interpreted these grains to be
1892 glaciogenic. This led them to suggest a glaciation at the Upper Paleozoic paleoequator.
1893 Immonen (2013) did not show any glacially abraded grains but only regular abrasion
1894 originating from movement by water, on e.g., fractures. Hore et al. (2020) and Alley et al.
1895 (2020) only showed unabraded fractures (some with regular rounding made from fluvial
1896 action) as evidence for glaciation in the Cretaceous of Australia. Le Heron et al. (2020)
1897 showed small fractures from Ordovician and LPIA sediments, which have no relevance to
1898 glaciation. Kalińska-Nartiša et al. (2017), Passchier et al. (2021) and Kut et al. (2021)
1899 correctly identified surface microtextures as not glaciogenic, in periglacial/permafrost
1900 climate. Reahl et al. (2021) could differentiate out non-glaciogenic grains.

1901 Some typical glaciogenic grains, and a few multicyclical grains, are displayed in Fig. 9. No
1902 other environment except the subglacial environment displays the combination of fresh
1903 irregularly abraded fractures. Based on more than 50 years of research (but commonly
1904 described in a more complicated, not so straightforward way), if the combination of fresh
1905 irregularly abraded fractures is not present, then the sediment is not glaciogenic. This
1906 combination of surface microtextures is displayed even by processing from a very thin
1907 probable only c. 10 m thick glacier (Molén, 2014). Multicyclical, beach and river sand grains
1908 display fewer and smaller fractures, regular abrasion and more weathering, when compared to
1909 glaciogenic quartz grains (Mahaney, 2002; Molén, 2014, 2017). Grains in high energy
1910 environments, where there is no grinding similar to that occurring at the bottom of glaciers,
1911 like in a rockfall, a conglomerate or a SGF, may acquire many fractures but not much
1912 abrasion, at least not irregular abrasion (Mahaney, 2002; Molén and Smit, 2022).

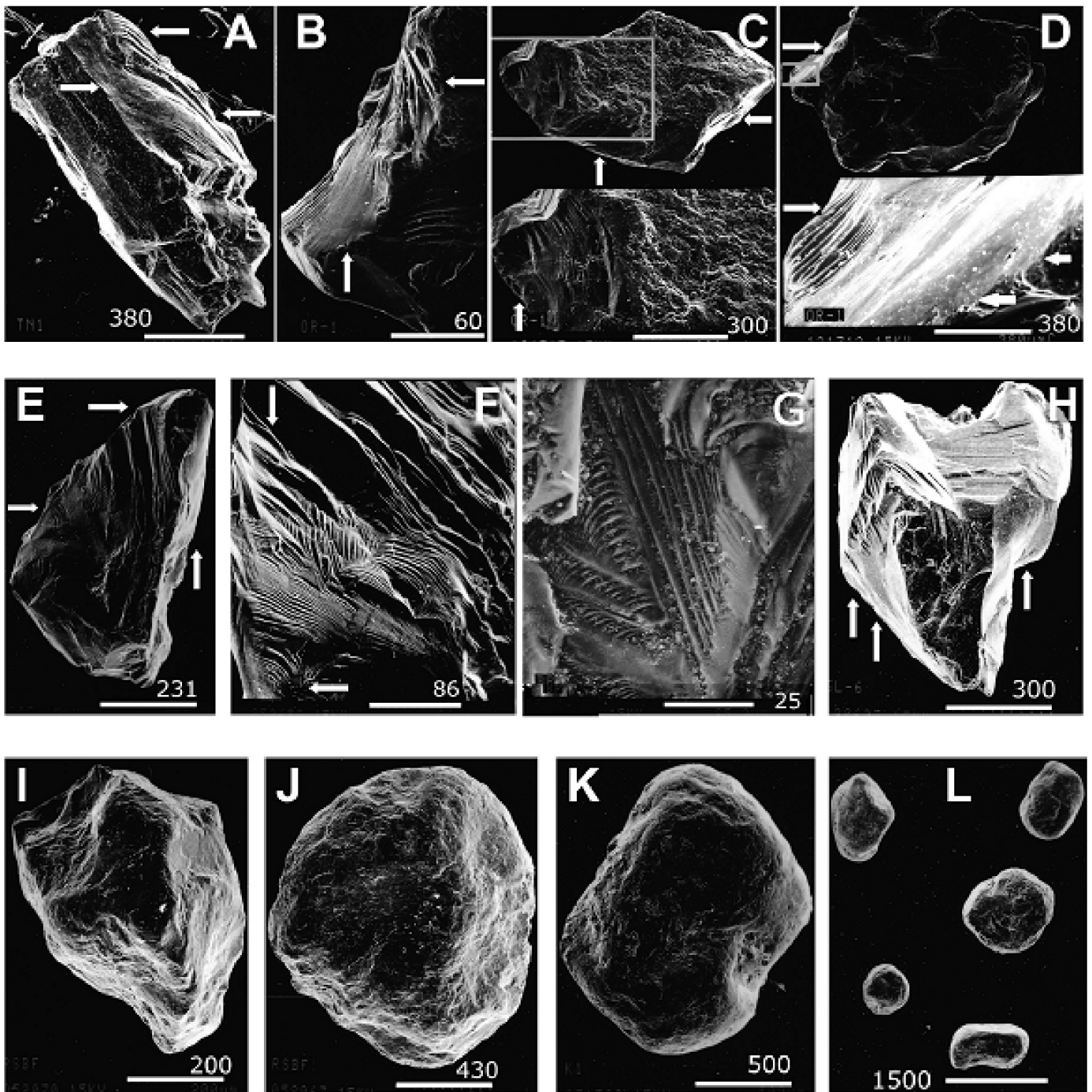


1913 Fig. 8. A 2-History-Diagram displays a “geological signature” from the appearance of surface
 1914 microtextures of quartz sand grains. The data is easily visualized, and the diagram is easy to
 1915 construct. The left diagram show surface microtextures from multicyclical grains from a
 1916 diamictite which commonly is interpreted to be glaciogenic (Neoproterozoic, northern
 1917 Norway; Molén, 2017). Grains from this area display regular abrasion (similar all over the
 1918 grain, whether the grain is round or angular in general shape) and weathering (A1 + SP1), and
 1919 a few fractures, but no glacial surface microtextures (F1+A1) (Molén, 2017). The right
 1920 diagram show data from Pleistocene and Neoglacial tills from Scandinavia and Ontario. T1-
 1921 T3, T5-T6/TN1-TN2 and Okstindan are samples from small Neoglacial glaciers. Västerbotten
 1922 (Sweden) and Toronto (Ontario) are samples from Pleistocene glaciers. MA1/ST1 are
 1923 samples from Pleistocene tills in Ontario which were composed of >95% crushed limestone.
 1924 The glaciogenic grains are easily identified by displaying fresh fractures which are irregularly
 1925 abraded (F1+A1) (Molén, 2014).

1926 F/f are large and small fractures, A is abrasion, EN are embayments/nodes where the grains
 1927 were in contact with other bedrock material during cooling and crystallization, and C is
 1928 chemically precipitated crystal surfaces. The number 1 displays the most recent surface

1929 microtextures, from the most recent geological process, and number 2 are older overlapped
1930 surface microtextures. Percentages are numbers of grains displaying the documented surface
1931 microtexture compared to the total number of grains in the samples.

1932 The connecting lines in the diagrams are drawn only to enhance visibility, as described in
1933 Molén (2014). These lines are important, as they visually indicate the general trend of the
1934 different surface microtextures, up or down, and therefore also display an easily
1935 distinguishable “geological signature” of the appearance of each sample. Number of studied
1936 quartz sand grains are within parentheses. (Figure from: Molén, M.O., 2017.)



1937 Fig. 9. SEM microphotographs of quartz sand grains from different environments. A is
 1938 Neoglacial till and B-F are Pleistocene tills, Västerbotten county, Sweden. G-H are
 1939 Pleistocene, Southern Ontario, Canada. I-L are multicyclic grains. Arrows point to fractures
 1940 that have been irregularly abraded, i.e. typical for glaciogenic grains. A. Large fractures all
 1941 over grain. On the upper surface all the fracture steps have been heavily abraded. B. Heavily
 1942 fractured and abraded grain. The fracture steps on the light left surface have been abraded. C.
 1943 Abrasion visible on fracture steps and in different parts of the grain surface. D. Large

1944 fractures. Most abrasion shown in the insert, i.e. uneven abraded surface all over and fracture
1945 steps have been abraded. E. Multiple fractured grain. Many fractures are sharp, but irregular
1946 abrasion is present in many places all over the grain. F. Closeup of fracture faces displaying
1947 steps on grain E. Abrasion is best visible in lower left corner, but most other rounded surfaces
1948 are probably curved fractures. G. Closeup of spectacular fractures showing linear and curved
1949 steps. As this grain from a till is much magnified, only small areas displaying possible
1950 abrasion are visible. H. Multiple fractured grain. Many fractures are still sharp, but some have
1951 been heavily irregularly abraded. This is a short transported glaciofluvial quartz grain, and
1952 therefore the grain has not yet acquired regular abrasion typical for transport with running
1953 water. I-J. Grains displaying weathering and regular abrasion. Ordovician sandstone, Canada.
1954 K-L. Rounded grains displaying weathering and regular abrasion. These grains are from
1955 diamictites, formerly interpreted to be tillites, but the surface microtextures display the same
1956 appearance as multicyclical grains similar to e.g., the sandstone in Figs. 9 I-J. Neoproterozoic,
1957 Norway (Molén, 2017). (Scale bars are in μm .)

1958 **3. Discussion**

1959 A feature of dubious origin present in a “tillite” may be interpreted as evidence for a
1960 glaciogenic origin. This feature may later be used as evidence for a glacial origin for similar
1961 features in other deposits. Maybe it was a slip of the tongue when Deynoux and Trompette
1962 (1981a) wrote the following about some Upper Ordovician sandstones in Guinea that were
1963 correlated with the “glacial” sediments in the Sahara: “There is no evidence for the glacial
1964 origin of these sandstones.” Similarly, Moncrieff and Hambrey (1990) acknowledged
1965 Schermerhorn’s (1974a) criticism of the glaciogenic interpretation of Neoproterozoic
1966 diamictites, but wrote that the glacial origin of many of the deposits has since then been
1967 confirmed, referring to Hambrey and Harland (1981). What they did not observe was the
1968 differences between what was reported in this extensive review volume of pre-Pleistocene

1969 “glaciogenic” deposits and Pleistocene glaciogenic deposits, as reported here. Their own
1970 work (Moncrieff and Hambrey, 1990), concerning Neoproterozoic “glaciomarine” deposits in
1971 Greenland, showed that these outcrops did “... not have a suitable modern analogue.” They
1972 also suggested that ancient glaciomarine deposits, including from the Neoproterozoic in
1973 Greenland, should be used to aid the interpretation of recent sediments instead of the
1974 opposite. More bluntly, Dey et al. (2020) wrote concerning the Neoproterozoic Blaini
1975 Formation in India “... that the idea of its glacial origin is more a belief than a scientific
1976 interpretation.”

1977 All this might end up as a philosophical problem. Actualism may be defined as the notion that
1978 physical natural laws do not change over time or space, or, uniformity of process (Gould
1979 1987). Uniformitarianism (classical) is the notion that the rates and intensities of all processes
1980 have always been the same as today, or the same as during non-catastrophic conditions, and
1981 this concept is definitively falsified (Gould, 1987; Romano, 2015).

1982 Instead of believing in uniformity of climatic changes (uniformitarianism), one should put
1983 stronger confidence in uniformity of physical natural laws and per se sedimentary processes
1984 (actualism). There is no natural law which states that the climate must have been cold and
1985 humid over large areas at many different occasions during earth history, just because there has
1986 been an ice-age quite recently. There is no evidence of uniformity of climatic change from the
1987 geological record even if it would be assumed that all “tillites” are glaciogenic or from
1988 theoretical considerations (the Milankovitch astronomical theory notwithstanding, e.g.,
1989 compare to Haldorsen et al., 2001). Bickert and Heinrich (2011) wrote “ ... we are far away
1990 from understanding the dynamics and processes of the Earth’s climatic change.” However, if
1991 the geological processes have changed during the ages (not only the rates or intensities), then
1992 also the natural laws must have changed.

1993 The “exceptional” features which are frequently documented from ancient “glacial” periods
1994 and have been “pushed” into a glacial framework, indicate a need for a change of
1995 interpretations. The research which describe and explain processes from Quaternary glaciers
1996 and glaciations are invaluable, but they need to be accompanied by similar rigorous research
1997 of “tillites” and compare these to deposits resulting from SGFs and other non-glacial
1998 processes. Although some of the processes discussed in this paper have only been studied
1999 either in restricted areas or very rarely, we cannot reject explanations only on the basis of
2000 uniformitarianism. Many kinds of “catastrophes” have occurred, and the processes we have
2001 seen only on a local scale might on a number of occasions have been more widespread (Ager,
2002 1981). But, there is no need for large catastrophes to explain the origin of diamictites, but
2003 only recent common processes and time.

2004 It is essential to hold on to the basic concept that the recent is the key to the past, i.e. that the
2005 framework for scientific research should be actualism and not uniformitarianism. In the
2006 current paper the discussion has been concerning diamictites, glaciation and mass flows. In
2007 this context it is informative to quote researchers who have documented “missing” sediments:
2008 a) By comparing ancient slides to Quaternary slides, Woodcock (1979) wrote “... where are
2009 the analogues of the larger continental margin slides in the ancient record?” (...) and “...
2010 submarine slides described from present day continental margins are on average several
2011 orders of magnitude larger in cross-sectional area than submarine slides described from
2012 ancient on-land sequences.” There are marine sediments covering large areas of recent
2013 cratonic land surfaces, and there is no reason that there should have been large differences in
2014 the appearance of submarine slides during ancient transgressions.

2015 b) Concerning the similarities of geological features which may originate by impacts followed
2016 by earthquakes and tsunamis and those in “tillites” (even if the interpretation of impacts was
2017 overstated initially) Oberbeck et al. (1993a) wrote: “How do ancient glacial deposits become
2018 preserved, while expected impact crater deposits equal to the thickest of the ancient tillites

2019 (and with the same appearance as tillites) become removed without a trace?”

2020 c) Shanmugam (2016) noted that “... the long-standing belief that submarine fans are
2021 composed of turbidites, in particular, of gravelly and sandy high-density turbidites, is a myth.
2022 This is because there are no empirical data ...” (from observations in the world’s oceans nor
2023 from experiments to validate this). “Mass-transport processes, which include slides, slumps,
2024 and debris flows (but no turbidity currents), are the most viable mechanisms for transporting
2025 gravels and sands into the deep sea.” He also noted that the “geologic reality is that frequent
2026 short-term events that lasts for only a few minutes to hours or days (e.g., earthquakes,
2027 meteorite impacts, tsunamis, tropical cyclones, etc.)” are the more important processes of
2028 transporting and depositing sediments. Or, as Kneller et al. (2016) stated: “Mass failures thus
2029 include the largest sedimentation events on earth.”

2030 d) And why, as the final and most important question, should it be that: “The dominant
2031 'glacial' facies in the rock record are subaqueous debris flow diamictites and turbidites
2032 recording the selective preservation of poorly-sorted glacioclastic sediment deposited in deep
2033 water basins by SGFs” (Eyles, 1993). Of course, the preservation potential is greatest in
2034 deeper basins, and therefore the question is if ancient glaciogenic material really has been
2035 preserved in any large abundance. It also appears that most “glaciations” can be correlated
2036 with tectonic movements (Eyles, 1993; Eyles and Januszczak, 2007; Kennedy and Eyles,
2037 2021; Molén, 2021; Molén and Smit, 2022), which would trigger SGFs but not per se long
2038 term cold climate, even though long term climatic changes connected to magmatism and
2039 tectonism were suggested by Youbi et al. (2021).

2040 Documented geological data indicate that many more diamictites than suspected may be mass
2041 flow deposits. SGF is the most abundant process of moving sediment today, both on land and
2042 in water, and would have been so even in ancient times (Moore et al., 1994; Moscardelli et
2043 al., 2006; Talling et al., 2015; Shanmugam, 2016, 2020; Ventra and Clarke, 2018).

2044 One can conclude with the words of Johan N. J. Visser, formerly of the University of the
2045 Orange Free State in South Africa, that: "... ancient deposits do not always correspond with
2046 Cenozoic glaciation models" (Visser, 1989a), or, as stated by Grotzinger et al. (2011) "...
2047 geology is about what happened – not what should have happened."

2048 **4. Conclusion**

2049 Many geologic features which are assumed to originate only during a cold climate or by the
2050 action of ice, also form in many other environments and by non-glacial processes, especially
2051 by SGFs. Furthermore, many features which are present in deposits from the pre-Pleistocene
2052 "glacial" record are not present in the Pleistocene glacial record (and vice versa). These
2053 missing features commonly indicate an origin by different kinds of SGFs, combined with
2054 tectonic uplift or subsidence (e.g., Maxwell, 1959; Wilson, 1969; Eyles and Eyles, 1989;
2055 Eyles 1990, 1993; Kennedy and Eyles, 2021), rather than glacial or periglacial erosion and
2056 deposition. "Ancient ice-ages" may be mainly deposits from different kinds of SGFs, instead
2057 of glaciogenic deposits.

2058 However, a glacial component can often not be excluded only on the basis of sedimentary and
2059 erosional structures. Glacial environments are often complex and it is therefore possible to
2060 argue for a glacial origin for many features present in an outcrop. But if all geological data
2061 from a formation are considered, even if nine out of ten features are consistent with glaciation
2062 but may also be formed by SGFs, a non-glaciogenic interpretation of many "tillites" may
2063 become a clear possibility.

2064 Thus, many researchers have become aware that sediments from SGFs form a large number
2065 of recent and ancient sedimentary deposits. Furthermore, even if there may still be debates,
2066 many "glaciations" have been reinterpreted completely or in part as SGF deposits or other

2067 non-glacial phenomena (e.g., Newell, 1957; van Houten, 1957; Dott, 1961; Schwarzbach,
2068 1961; Winterer, 1964; Lindsay, 1966; Scott, 1966; Condie, 1967; Frakes et al., 1969;
2069 Volkheimer, 1969; Frakes, 1979; Schermerhorn, 1974a, 1974b, 1981; Cecioni, 1981;
2070 Vellutini and Vicat, 1983; Martin et al., 1985; Mahaney, 1987; Eyles and Eyles, 1989; Eyles,
2071 1990, 1993; Bailey et al., 1990; Rampino, 1994, 2017; Eyles and Januszczak, 2007;
2072 Thompson, 2009; Carto and Eyles, 2012a, 2012b; Delpomdor et al., 2016; Isbell et al., 2016;
2073 Molén, 2017, 2021; Bechstädt et al., 2018; Moxness et al., 2018; Fedorchuk et al., 2019;
2074 Kennedy et al., 2019; Le Heron and Vandyk, 2019; Pauls et al., 2019; Dey et al., 2020;
2075 Kennedy and Eyles, 2019, 2021; Dufresne et al., 2021; Isbell et al., 2021; Vandyk et al.,
2076 2021; Molén and Smit, 2022). It appears that many diamictites which have been interpreted
2077 as “tillites” have been formed in a similar geological environment, but not in a similar
2078 climate.

2079 The documentation of features from the current paper is summed up in the Appendix, a
2080 Diamict Origin Table. This table may be used as a working tool, and also as a reference in
2081 publications (Molén 2017, 2021). The documentation in the current paper has sorted out
2082 unequivocal criteria. Even if the current paper have reviewed most recent literature, because
2083 of a general lack of work in some research areas that have been discussed, a few of the
2084 similarities and differences between deposits with a different origin are provisional, requiring
2085 further documentation. Many of the features described need both better qualification and
2086 quantification before they can be used more conclusively. The evidence from surface
2087 microtextures may be the quickest way to interpret the origin of deposits, as the evidence
2088 from different surface microtextures from Pleistocene and Holocene deposits are not
2089 equivocal (Mahaney, 2002; Molén, 2014, 2017).

2090 **Acknowledgments**

2091 Scholarships from York University, Toronto, and the University of Umeå, provided support
 2092 in writing parts of this paper. Thanks are due to a large number of geologists who have
 2093 provided critical and enhancing comments from their specialities. The current paper benefited
 2094 greatly from their assistance.

2095 5. Appendix Diamict Origin Table

2096	FEATURE	ORIGIN	
		Glaciog	Mass flow. Diamict
		.	Tect.
2097	Areally continuous	2	1
2098	Areally dispersed	1	2
2099	Large areal extent	2	1
2100	Warm climate sediments	0-1	2
2101	Warm climate fossils	0-1	2
2102	Matrix supported/fine grained	2	1-2
2103	Clast/bed thickness correlation	0-1	2
2104	Sorting/grading	0-1	2
2105	Streaks of different sediments/diamictites	1	2
2106	Unconsol. transport. sediment	1	2
2107	Soft substrate	1-2	2
2108	Fabrics	2	2
	Strong	2	1
	Weak	1	2
	Bimodal	2	1
	Planar	1	2
	Variable in sections	1	2
2109	Erratics	2	2
	>1-3 m diameter	2	1-(2)
	Smaller in "tillite" than in mass flow	0	2
	Jigsaw fractures	-	1
2110	Striated clasts	1-2	1-2
	Subparallel striae	2	1
	Parallel striae	1	2
	Curved/random striae	1	2
	Crossing striae	2	1
	Soft angular not striated, hard rounded striated	1	2
2111	Faceted/polished clasts	1-2	1-(2)
2112	Pavement/striae/grooves	2	1
	Subparallel striae	2	1
	Parallel striae	1	2
	Crossing striae	2	1
	Polished striae	2	1
	Soft sediment pavement	1	2
	Sediment pressed down	-	2

	Pressed up ridges	-	2
	Stacked	0-1	1-2
	Irregular horizontally and vertically	2	1-2
	Regular striations	0-1	1-2
	Continue over extensive areas	2	1
	Interlaminated sediment/traction carpet	-	1
	Ripples, laminae (etc.)	-	1
	Brecciation	1	1
	Overhanging walls (etc.)	0-1	1
	Rock polish chemical	(?)	1
2113	Iceberg keel scour marks and mimics	2	0-1
	Abundant where present	2	-
	Changing directions	2	0-1
	Superposed/stacked in same direction	-	1
	Parallel striations/grooves	1	2
	Undulous in cross-section	2	0-1
	Evidence of tides, wind and waves	2	0-1
	Grounding pits	2	(?)
	Glacier grounding-zone wedges	2	(1)
2114	Boulder pavements	2	1-2
2115	Roches moutonnés/plucking	2	(0-1)
	Uneven surface	0-1	1
2116	Fjords, overdeepened, regular, ridged outlet	2	(0-1)
2117	Eskers	2	(0-1)
	Sorting	2	1
	Large clasts on top	2	(?)
2118	Glaciofluvial restricted by ice, kames, etc.	2	-
2119	Dropstones/lonestones	2	2
	No fabric	2	1
	Weak fabric	1	2
	Varied size of clasts	2	1
	Small size	1	2
	Small size compared to other sediments	-	2
	Correlation: clast size and sediment thickness	-	2
	Larger clasts in thicker sediments	1	2
	Sorted	0-1	1-2
	Differently compressed laminae	1	2
	No/little penetration	1	2
	1/3 of clast penetrate	2	1
	Sediment thickness changes around clast	1	2
	Lee side structures/movement/wake eddies	1	2
	Rip-up clasts	0-1	1
2120	“Varves” (with dropstones) drape diamictite	1	2
2121	Rythmites, thick "winter layer"	0-1	2
2122	Small tectonics, e.g., clastic dikes/water escape structures,	1	2
2123	especially within rythmites		
2124	“Glaciomarine” deposits drape diamictite	1	2
2125	Submarine glacial features	2	1
2126	“Periglacial” features not formed by frost	1	2
2127	Surface microtextures a) only fractured, or b) both	-	2
2128	weathered and regularly abraded		

2129	Surface microtextures synchronously fractured and	2	-
2130	<u>irregularly abraded</u>		

2131 **GEOLOGICAL FEATURES WHICH DISPLAY NO CRITERIA TO**
 2132 **EASILY INTERPRET THE ORIGIN OF THESE FEATURES**

2133	Geochemistry	Too many exceptions and interpretations
2134	Transverse/irregular landforms	Criteria not fully documented
2135	Mass flows	Difficult to see evidence of glaciation
2136	Channels below "tillites"	Difficult to know the origin
2137	Flutes	Criteria not fully documented
2138	Impact structures	Irrelevant, except if misinterpreted
2139	Lineations	Too few criteria
2140	Glacial valleys	Too much variation
2141	Channels/tunnel valleys	Too few criteria
2142	<u>Large soft sediment tectonic structures</u>	<u>Too much variation</u>

2143 Diamict Origin Table of geologic features formed in environments of glaciation, mass flows
 2144 and tectonics. Columns display how common a feature may be, and if it has a glaciogenic
 2145 origin or a non-glacogenic origin (mass flows etc).

2146 Tabulated features in the upper part of the table differ substantially between glaciogenic and
 2147 non-glaciogenic deposits, and the more provisionally documented features are in the lower
 2148 part. Even though the absolute differences are not known between different processes,
 2149 relative values have been provided. Details of the origin of these structures are discussed in
 2150 the text. Included in the SGF/tectonic column are also other non-glacial processes which have
 2151 been discussed. Not all data discussed in the text are listed, but only those that more clearly
 2152 help in interpreting the origin of a diamictite. Hence, provisional or insignificant (not fully)
 2153 documented differences, and those that may be easily interpreted to have formed in different
 2154 environments, are not tabulated but only discussed in the text.

2155 In the column for glaciogenic origin, structures that form by non-glaciogenic processes in a
2156 glacial environment are not included, e.g., debris flows. However, if clasts in debrites are
2157 glacially striated, this may be evidence for glaciation. On the other hand, debrites, with no
2158 other evidence for a glacial environment than striations that may form by debris flows, is not a
2159 very helpful evidence for interpreting presence of a glacial climate.

2160 2 = more common, 1 = less common, 0 = very rare, - = no example known, parentheses = rare
2161 or commonly displaying a distinct appearance, ? = no well documented research known.

2162 The complete, or parts of this table may be copied and used directly in publications (e.g.
2163 Molén, 2017, 2021). (Last column is left open for the area/outcrop studied.)

2164 **6. References**

- 2165 Aalto, K.R., 1971. Glacial marine sedimentation and stratigraphy of the Toby Conglomerate
2166 (Upper Proterozoic), southeastern British Columbia, northwestern Idaho and northeastern
2167 Washington. *Canadian Journal of Earth Sciences* 8, 753-787.
- 2168 Abbott, D.H., Embley, R.W., 1982. Upslope flow of turbidity currents on abyssal hills in the
2169 eastern Nares abyssal plain. *EOS Transactions, American Geophysical Union* 63, 445.
- 2170 Adie, R.J., 1975. Permo-Carboniferous glaciation of the Southern Hemisphere, in: Wright,
2171 A.E., Moseley, F. (Eds.), *Ice Ages: Ancient and Modern*. Seal House Press, Liverpool, pp.
2172 287-300.
- 2173 Ager, D.V., 1981. *The Nature of the Stratigraphical Record*, second ed. John Wiley and Sons,
2174 New York, 151 pp.
- 2175 Aitken, J.D., 1991. Two Late Proterozoic glaciations, Mackenzie Mountains, northwestern
2176 Canada. *Geology* 19, 445-448.
- 2177 Aitken, J.F., 1993. A re-appraisal of supposed iceberg “dump” and “grounding” structures
2178 from Pleistocene glaciolacustrine sediments, Aberdeenshire. *Quaternary Newsletter* 71, 1-10.
- 2179 Ali, D.O., Spencer, A.M., Fairchild, I.J., Chew, K.J., Anderton, R., Levell, B.K., Hambrey,
2180 M.J., Dove, D., Le Heron, D.P., 2018. Indicators of relative completeness of the glacial
2181 record of the Port Askaig Formation, Garvellach Islands, Scotland. *Precambrian Research*
2182 319, 65-78. <https://doi.org/10.1016/j.precamres.2017.12.005>.

- 2183 Aliotta, S., Perillo, G.M.E., 1987. A sand wave field in the entrance to Bahia Blanca estuary,
2184 Argentina. *Marine Geology* 76, 1-14.
- 2185 Allen, J.R.L., 1984. *Sedimentary Structures: Their Character and Physical Basis*. Elsevier,
2186 Amsterdam vol. 1, pp. 267-268, vol. 2, pp. 513-519.
- 2187 Allen, P., 1975. Ordovician glacials of the Central Sahara, in: Wright, A.E., Moseley, F.
2188 (Eds.), *Ice Ages: Ancient and Modern*. Seal House Press, Liverpool, pp. 275-286.
- 2189 Alley, N.F., Hore, S.B., Frakes, L.A., 2020. Glaciations at high-latitude Southern Australia
2190 during the Early Cretaceous. *Australian Journal of Earth Sciences* 67, 1045-1095.
2191 <https://doi.org/10.1080/08120099.2019.1590457>.
- 2192 Alonso-Muruaga, P.J., Limarino, C.O., Spalletti, L.A., Piñol, F.C., 2018. Depositional
2193 settings and evolution of a fjord system during the carboniferous glaciation in Northwest
2194 Argentina. *Sedimentary Geology* 369, 28-45. <https://doi.org/10.1016/j.sedgeo.2018.03.002>.
- 2195 Alves, T.M., 2015. Submarine slide blocks and associated soft-sediment deformation in
2196 deep-water basins: A review. *Marine and Petroleum Geology* 67, 262-285.
2197 <https://doi.org/10.1016/j.marpetgeo.2015.05.010>.
- 2198 Alves, T.M., Gamboa, D., 2020. Mass transport deposits as markers of local tectonism in
2199 extensional basins, in: Kei Ogata, K., Festa, A., Pini, G.A. (Eds.), *Submarine Landslides:
2200 Subaqueous Mass Transport Deposits from Outcrops to Seismic Profiles*. Geophysical
2201 Monograph 246, American Geophysical Union. John Wiley and Sons, Inc., Washington D.C.,
2202 pp. 71-90.

- 2203 Amblas, D., Gerber, T.P., Canals, M., Pratson, L.F., Urgeles, R., Lastras, G., Calafat, A.M.,
2204 2011. Transient erosion in the Valencia Trough turbidite systems, NW Mediterranean Basin.
2205 *Geomorphology* 130, 173-184. <https://doi.org/10.1016/j.geomorph.2011.03.013>.
- 2206 Anderson, A.M., McLachlan, I.R., 1976. The plant record in the Dwyka and Ecca series
2207 (Permian) of the south-western half of the Great Karroo Basin, South Africa. *Palaeontologica*
2208 *Africana* 19, 31-42.
- 2209 Anderson, J.B., 1983. Ancient glacial-marine deposits: their spatial and temporal distribution,
2210 in: Molnia, B.F. (Ed.), *Glacial-Marine Sedimentation*, Plenum Press, New York, pp. 3-92.
- 2211 Andrews, S.D., Cornwell, D.G., Trewin, N.H., Hartley, A.J., Archer, S.G., 2018. Reply to the
2212 discussion on 'A 2.3 Million Year Lacustrine Record of Orbital Forcing from the Devonian of
2213 Northern Scotland', *Journal of the Geological Society, London* 173, 474–488. *Journal of the*
2214 *Geological Society* 175, 563. <https://doi-org.ezp.sub.su.se/10.1144/jgs2017-132>.
- 2215 Andrews, G.D., McGrady, A.T., Brown, S.R., Maynard, S.M., 2019. First description of
2216 subglacial megalineations from the late Paleozoic ice age in southern Africa. *PLoS ONE* 14,
2217 e0210673. <https://doi.org/10.1371/journal.pone.0210673>.
- 2218 Aquino, C.D., Buso, V.V., Faccini, U.F., Milana, J.P., Paim, P.S.G., 2016. Facies and
2219 depositional architecture according to a jet efflux model of a late Paleozoic tidewater
2220 grounding-line system from the Itararé Group (Paraná Basin), southern Brazil. *Journal of*
2221 *South American Earth Sciences* 67, 180-200. <https://doi.org/10.1016/j.jsames.2016.02.008>.

- 2222 Armentrout, J.M., 1983. Glacial lithofacies of the Neogene Yakataga Formation Robinson
2223 Mountains, Southern Alaska Coast Range, Alaska, in: Molnia, B.F. (Ed.), *Glacial-Marine*
2224 *Sedimentation*. Plenum Press, New York, pp. 629-665.
- 2225 Arnaud, E., 2008. Deformation in the Neoproterozoic Smalfjord Formation, northern
2226 Norway: an indicator of glacial depositional conditions? *Sedimentology* 55, 335–356.
- 2227 Arnaud, E., 2012. The paleoclimatic significance of deformation structures in Neoproterozoic
2228 successions. *Sedimentary Geology* 243–244, 33–56.
- 2229 Arnaud, E., Eyles, C.H., 2006. Neoproterozoic environmental change recorded in the Port
2230 Askaig Formation, Scotland: Climatic vs tectonic controls. *Sedimentary Geology* 183,
2231 99-124. <https://doi.org/10.1016/j.sedgeo.2005.09.014>.
- 2232 Assine, M.L., de Santa Ana, H., Veroslavsky, G., Vesely, F.F., 2018. Exhumed subglacial
2233 landscape in Uruguay: Erosional landforms, depositional environments, and paleo-ice flow in
2234 the context of the late Paleozoic Gondwanan glaciation. *Sedimentary Geology* 369, 1-12.
2235 <https://doi.org/10.1016/j.sedgeo.2018.03.011>.
- 2236 Atkins, C.B., 2003. Characteristics of Striae and Clast Shape in Glacial and Non-Glacial
2237 Environments (Ph.D. thesis). Victoria University of Wellington.
- 2238 Atkins, C.B., 2004. Photographic atlas of striations from selected glacial and non-glacial
2239 environments. Antarctic Data Series 28. Victoria University of Wellington.

- 2240 Atkins, C.B., 2013. Geomorphological evidence of cold-based glacier activity in South
2241 Victoria Land, Antarctica. Geological Society, London, Special Publications 381, 299-318.
2242 <https://doi.org/10.1144/SP381.18>.
- 2243 Baas, J.H., Tracey, N.D., Peakall, J., 2021. Sole marks reveal deep-marine depositional
2244 process and environment: Implications for flow transformation and hybrid-event-bed models.
2245 *Journal of Sedimentary Research* 91, 986–1009. <https://doi.org/10.2110/jsr.2020.104>.
- 2246 Bahlburg, H., Dobrzinski, N., 2011. A review of the Chemical Index of Alteration (CIA) and
2247 its application to the study of Neoproterozoic glacial deposits and climate transitions, in:
2248 Arnaud, E., Halverson, G.P., Shields-Zhou, G. (Eds.), *The Geological Record of*
2249 *Neoproterozoic Glaciations*, Geological Society, London, Memoirs 36, pp. 81-92.
2250 <https://doi.org/10.1144/M36.6>.
- 2251 Bailey, R.A., Huber, K.N., Curry, R.R., 1990. The diamicton at Deadman Pass, Central Sierra
2252 Nevada, California: A residual lag and colluvial deposit, not a 3 Ma glacial till. *GSA Bulletin*
2253 102, 1165-1173.
- 2254 Baioumy, H., Anuar, M.N.A.B., Nordin, M.N.M., Arifin, M.H., Al-Kahtany, K., 2020.
2255 Source and origin of Late Paleozoic dropstones from Peninsular Malaysia: First record of
2256 Mississippian glaciogenic deposits of Gondwana in Southeast Asia. *Geological Journal* 55,
2257 6361-6375. <https://doi.org/10.1002/gj.3809>.
- 2258 Baker, V.R., Kochel, C., 1979. Martian channel morphology: Maja and Kasei Valles, *Journal*
2259 *of Physical Research* 84, 7961-7983.

- 2260 Baker, V.R., Milton, D.J., 1974. Erosion by catastrophic floods on Mars and Earth. *Icarus* 23,
2261 27-41.
- 2262 Banerjee, I., 1966. Turbidites in a glacial sequence: A study from the Talchir Formation,
2263 Raniganj Coalfield, India. *Journal of Geology* 74, 593-606.
- 2264 Barbolini, N., 2014. Palynostratigraphy of the South African Karoo Supergroup and
2265 Correlations with Coeval Gondwanan Successions (Ph.D. thesis). University of the
2266 Witwatersrand, Johannesburg.
- 2267 Barbolini, N., Rubidge, B., Bamford, M.K., 2018. A new approach to biostratigraphy in the
2268 Karoo retroarc foreland system: utilising restricted-range palynomorphs and their first
2269 appearance datums for correlation. *Journal of African Earth Sciences* 140, 114-133.
2270 <https://doi.org/10.1016/j.jafrearsci.2017.11.031>.
- 2271 Batchelor, C.L., Montelli, A., Ottesen, D., Evans, J., Dowdeswell, E.K., Christie, F.D.W.,
2272 Dowdeswell, J.A., 2020. New insights into the formation of submarine glacial landforms
2273 from high-resolution Autonomous Underwater Vehicle data. *Geomorphology* 370, 107396.
2274 <https://doi.org/10.1016/j.geomorph.2020.107396>.
- 2275 Bauch, D., Hölemann, J., Andersen, N., Dobrotina, E., Nikulina, A., Kassens, H., 2011. The
2276 Arctic shelf regions as a source of freshwater and brine-enriched waters as revealed from
2277 stable oxygen isotopes. *Polarforschung* 80, 127-140.
2278 <https://doi.org/10.2312/polarforschung.80.3.127>.
- 2279 Bauska, T.K., Baggenstos, D., Brook, E.J., Mix, A.C., Marcott, S.A., Petrenko, V.V.,
2280 Schaefer, H., Severinghaus, J.P., Lee, J.E., 2016. Carbon isotopes characterize rapid changes

- 2281 in atmospheric carbon dioxide during the last deglaciation. PNAS 113, 3465-3470.
2282 <https://doi.org/10.1073/pnas.1513868113>.
- 2283 Bechstädt, T., Jäger, H., Rittersbacher, A., Schweisfurth, B., Spence, G., Werner, G., Boni,
2284 M., 2018. The Cryogenian Ghaub Formation of Namibia – New insights into Neoproterozoic
2285 glaciations. Earth-Science Reviews 177, 678–714.
2286 <https://doi.org/10.1016/j.earscirev.2017.11.028>.
- 2287 Bell, D., Hodgson, D.M., Pontén, A.S.M., Hansen, L.A.S., Flint, S.S., Kane, I.A., 2020.
2288 Stratigraphic hierarchy and three dimensional evolution of an exhumed submarine slope
2289 channel system. Sedimentology 67, 3259-3289. <https://doi.org/10.1111/sed.12746>.
- 2290 Bengtson, S., Sallstedt, T., Belivanova, V., Whitehouse, M., 2017. Three-dimensional
2291 preservation of cellular and subcellular structures suggests 1.6 billion-year-old crown-group
2292 red algae. PLoS Biology 15, e2000735. <https://doi.org/10.1371/journal.pbio.2000735>.
- 2293 Benn, D.I., Evans, D.J.A., 1996. The interpretation and classification of
2294 subglacially-deformed materials. Quaternary Science Reviews 15, 23-52.
2295 [https://doi.org/10.1016/0277-3791\(95\)00082-8](https://doi.org/10.1016/0277-3791(95)00082-8).
- 2296 Bennett, M.R., Bullard, J.E., 1991. Correspondence: Iceberg tool marks: An example from
2297 Heinabergsjökull, southeast Iceland. Journal of Glaciology 37, 181-183.
- 2298 Bennett, M.R., Doyle, P., Mather, A.E., Woodfin, J.L., 1994. Testing the climatic
2299 significance of dropstones: an example from southeast Spain. Geological Magazine 131, 845-
2300 848.

- 2301 Bennett, M.R., Doyle, P., Mather, A.E., 1996. Dropstones: their origin and significance.
2302 *Palaeogeography, Palaeoclimatology, Palaeoecology* 121, 331-339.
- 2303 Bennett, M.R., Waller, R.I., Midgley, N.G., Huddart, D., Gonzalez, S., Cook, S.J., Tomio, A.,
2304 2003. Subglacial deformation at sub-freezing temperatures? Evidence from
2305 Hagafellsjökull-Eystri, Iceland. *Quaternary Science Reviews* 22, 915–923.
- 2306 Bernardi, M., Petti, F.M., Benton, M.J., 2018. Tetrapod distribution and temperature rise
2307 during the Permian-Triassic mass extinction. *Proceedings of the Royal Society B* 285,
2308 20172331. <https://doi.org/10.1098/rspb.2017.2331>.
- 2309
- 2310 Bernhardt, A., Schwanghart, W., 2021. Where and why do submarine canyons remain
2311 connected to the shore during sea-level rise? Insights from global topographic analysis and
2312 Bayesian regression. *Geophysical Research Letters* 48, e2020GL092234.
2313 <https://doi.org/10.1029/2020GL092234>.
- 2314 Best, J.L., 1992. Sedimentology and event timing of a catastrophic volcanoclastic mass
2315 flow, Volcan Hudson, Southern Chile. *Bulletin of Volcanology* 54, 299-318.
- 2316 Bestmann, M., Rice, A.H.N., Langenhorst, F., Grasmann, B., Heidelbach, F., 2006.
2317 Subglacial bedrock welding associated with glacial earthquakes. *Journal of the Geological*
2318 *Society* 163, 417-420.
- 2319 Bickert, T., Heinrich, R., 2011. Climate records of deep-sea sediments: towards the Cenozoic
2320 ice house, in: Hüneke, H., Mulder, T. (Eds.), *Developments in Sedimentology* 63. Elsevier,
2321 Amsterdam, pp. 793-823.

- 2322 Bielenstein, H.U., Eisbacher, G.H., 1969. Tectonic interpretation of elastic-strain-recovery
2323 measurements at Elliot Lake, Ontario. Department of Energy, Mines and Resources Ottawa,
2324 Report R210, 64 pp.
- 2325 Bigarella, J.J., Salamuni, R., Fuck, R.A., 1967. Striated surfaces and related features,
2326 developed by the Gondwana ice sheets (State of Paraná, Brazil). *Palaeogeography,*
2327 *Palaeoclimatology, Palaeoecology* 3, 265-276.
- 2328 Biju-Duval, B., Deynoux, M., Rognon, P., 1981. Late Ordovician tillites of the Central
2329 Sahara, in: Hambrey, M.J., Harland, W.B. (Eds.), *Earth's Pre-Pleistocene Glacial Record.*
2330 Cambridge University Press, Cambridge, pp. 99-107.
- 2331 Binda, P.L., Van Eden, J.G., 1972. Sedimentological Evidence on the Origin of the
2332 Precambrian Great Conglomerate (Kundelungu Tillite), Zambia. *Palaeogeography,*
2333 *Palaeoclimatology, Palaeoecology* 12, 151-168.
- 2334 Bjørlykke, K., 1967. The Eocambrian "Reusch Moraine" at Bigganjargga and the geology
2335 around Varangerfjord; Northern Norway. *Norges Geologiske Undersøkelse* 251, 18-44.
- 2336 Black, R.F., 1976. Periglacial features indicative of permafrost: Ice and soil wedges.
2337 *Quaternary Research* 6, 3-26.
- 2338 Blatt, H., 1992. *Sedimentary Petrology*, second ed. W.H. Freedman and Co, New York, pp.
2339 56-58.
- 2340 Blauw, M., 2012. Out of tune: the dangers of aligning proxy archives. *Quaternary Science*
2341 *Reviews* 36, 38-49.

- 2342 Blomenkemper, P., Kerp, H., Bomfleur, B., 2020. A treasure trove of peculiar Permian plant
2343 fossils. *PalZ* 94, 409–412. <https://doi.org/10.1007/s12542-019-00489-4>.
- 2344 Bond, G., 1981a. Late Paleozoic (Dwyka) glaciation in the Middle Zambezi Region, in:
2345 Hambrey, M.J., Harland, W.B. (Eds.), *Earth's Pre-Pleistocene Glacial Record*. Cambridge
2346 University Press, Cambridge, pp. 55-57.
- 2347 Bond, G., 1981b. Late Paleozoic (Dwyka) glaciation in the Sabi-Limpopo Region,
2348 Zimbabwe, in: Hambrey, M.J., Harland, W.B. (Eds.), *Earth's Pre-Pleistocene Glacial Record*.
2349 Cambridge University Press, Cambridge, pp. 58-60.
- 2350 Bose, P.K., Mukhopadhyay, G., Bhattacharyya, H.N., 1992. Glaciogenic coarse clastics in a
2351 Permo-Carboniferous bedrock through in India: A sedimentary model. *Sedimentary Geology*
2352 76, 79-97.
- 2353 Boulton, G.S., 1990. Sedimentary and sea level changes during glacial cycles and their
2354 control on glacial marine facies architecture, in: Dowdeswell, J.A., Scourse, J.D. (Eds.),
2355 *Glacial Marine Environments: Processes and Sediments*. Geological Society, London, Spec.
2356 Publ. 53, pp. 15-52.
- 2357 Boulton, G.S., Deynoux, M., 1981. Sedimentation in glacial environments and the
2358 identification of tills and tillites in ancient sedimentary sequences. *Precambrian Research* 15,
2359 397-422.
- 2360 Bouma, A.H., 1962. *Sedimentology of some flysch deposits: A graphic approach to facies*
2361 *interpretation*. Elsevier, Amsterdam, 168 pp..

- 2362 Bouma, A.H., 1964. Turbidites, in: Bouma, A.H., Brouwer, A. (Eds.), Turbidites. Elsevier,
2363 Amsterdam, pp. 251-256.
- 2364 Bourgeois, J., 2009. Geologic effects and records of tsunamis, in: Robinson, A.R., Bernard,
2365 E.N. (Eds.), The Sea, vol 15, Tsunamis. Harvard University Press, Cambridge, pp 53-91.
- 2366 Bowen, R.L., 1969. Late Paleozoic glaciations – the Parana Basin of South America, in:
2367 Amos, A.J. (Ed.), Gondwana Stratigraphy. IUGS Symposium in Buenos Aires 1967,
2368 UNESCO, pp. 589-597.
- 2369 Bronikowska, M., Pisarska-Jamroży, M., van Loon, A.J.T., 2021. Dropstone deposition:
2370 Results of numerical process modeling of deformation structures, and implications for the
2371 reconstruction of the water depth in shallow lacustrine and marine successions. *Journal of*
2372 *Sedimentary Research* 91, 507–519. <https://doi.org/10.2110/jsr.2020.111>.
- 2373 Broster, B.E., Seaman, A.A., 1991. Glacigenic rafting of weathered granite: Charlie Lake,
2374 New Brunswick. *Canadian Journal of Earth Sciences* 28, 649-654.
2375 <https://doi.org/10.1139/e91-056>.
- 2376 Bryan, M., 1983. Of shales and schists and ignimbrites, and other Rocky things (a report on
2377 the talks given at the 1983 Conference at Bradford University). *OUGS Journal* 4 (2), 31-53
2378 (Review of Prof. P. Allens lecture: Ice Ages in the Central Sahara, pp. 51-53.)
- 2379 Bryant, E.A, Young, R.W., 1996. Bedrock-sculpting by tsunami, south coast New South
2380 Wales, Australia. *Journal of Geology* 104, 565–582.

- 2381 Bukhari, S., Eyles, N., Sookhan, S., Mulligan, R., Paulen, R., Krabbendam, M., Putkinen, N.,
2382 2021. Regional subglacial quarrying and abrasion below hard-bedded palaeo-ice streams
2383 crossing the Shield–Palaeozoic boundary of central Canada: the importance of substrate
2384 control. *Boreas*. <https://doi.org/10.1111/bor.12522>.
- 2385 Burr, D.M., Grier, J.A., McEwen, A.S., Keszthelyi, L.P., 2002. Repeated aqueous flooding
2386 from the Cerberus Fossae: evidence for very recently extant, deep groundwater on Mars.
2387 *Icarus* 159, 53-73.
- 2388 Bussert, R., 2010. Exhumed erosional landforms of the Late Palaeozoic glaciation in northern
2389 Ethiopia: Indicators of ice-flow direction, palaeolandscape and regional ice dynamics.
2390 *Gondwana Research* 18, 356-369. <https://doi.org/10.1016/j.gr.2009.10.009>.
- 2391 Bussert, R., 2014. Depositional environments during the Late Palaeozoic ice age (LPIA) in
2392 northern Ethiopia, NE Africa. *Journal of African Earth Sciences* 99, 386-407.
2393 <https://doi.org/10.1016/j.jafrearsci.2014.04.005>.
- 2394 Butler, R.W.H, McCaffrey, W.D., 2010. Structural evolution and sediment entrainment in
2395 mass-transport complexes: outcrop studies from Italy. *Journal of the Geological Society* 167,
2396 617–631. <https://doi.org/10.1144/0016-76492009-041>.
- 2397 Butler, R.W.H., Tavarnelli, E., 2006. The structure and kinematics of substrate entrainment
2398 into high-concentration sandy turbidites: a field example from the Gorgoglione ‘flysch’ of
2399 southern Italy. *Sedimentology* 53, 655–670. [https://doi.org/10.1111/j.1365-](https://doi.org/10.1111/j.1365-3091.2006.00789.x)
2400 [3091.2006.00789.x](https://doi.org/10.1111/j.1365-3091.2006.00789.x).

- 2401 Caetano-Filho, S., Sansjofre, P., Ader, M., Paula-Santos, G.M., Guacaneme, C., Babinski,
2402 M., Bedoya-Rueda, C., Kuchenbecker, M., Reis, H.L.S., Trindade, R.I.F., 2021. A large
2403 epeiric methanogenic Bambuí sea in the core of Gondwana supercontinent? *Geoscience*
2404 *Frontiers* 12, 203-218. <https://doi.org/10.1016/j.gsf.2020.04.005>.
- 2405 Cahen, L., Lepage, J., 1981. Proterozoic diamictites of Lower Zaire, in: Hambrey, M.J.,
2406 Harland, W.B. (Eds.), *Earth's Pre-Pleistocene Glacial Record*. Cambridge University Press,
2407 Cambridge, pp.153-157.
- 2408 Canals, M., Puig, P., de Madron, X.D., Heussner, S., Palanques, A., Fabres, J., 2006.
2409 Flushing submarine canyons. *Nature* 444, 354-357. <https://doi.org/10.1038/nature05271>.
- 2410 Capra, L., Macias, J.L., 2002. The cohesive Naranjo debris-flow deposit (10 km³): A dam
2411 breakout flow derived from the Pleistocene debris-avalanche deposit of Nevado de Colima
2412 Volcano (México). *Journal of Volcanology and Geothermal Research* 117, 213-235.
- 2413 Caputo, M.V., Crowell, J.C., 1985. Migration of glacial centers across Gondwana during
2414 Paleozoic Era. *GSA Bulletin* 96, 1020-1036.
- 2415 Caputo, M.V., Santos, R.O.B. dos, 2020. Stratigraphy and ages of four Early Silurian through
2416 Late Devonian, Early and Middle Mississippian glaciation events in the Parnaíba Basin and
2417 adjacent areas, NE Brazil. *Earth-Science Reviews* 207, 103002.
2418 <https://doi.org/10.1016/j.earscirev.2019.103002>.
- 2419 Cardona, S., Wood, L.J., Dugan, B., Jobe, Z., Strachan, L.J., 2020. Characterization of the
2420 Rapanui mass-transport deposit and the basal shear zone: Mount Messenger Formation,

- 2421 Taranaki Basin, New Zealand. *Sedimentology* 67, 2111-2148.
- 2422 <https://doi.org.10.1111/sed.12697>.
- 2423 Caron, V., Mahieux, G., Ekomane, E., Moussango, P., Babinski, M., 2011. One, two or no
2424 record of Late Neoproterozoic glaciation in South-East Cameroon? *Journal of African Earth*
2425 *Sciences* 59, 111-124. <https://doi.org/10.1016/j.jafrearsci.2010.09.004>.
- 2426 Carter, R. M., 1975. A discussion and classification of subaqueous mass-transport with
2427 particular application to grain-flow, slurry-flow, and fluxoturbidites. *Earth-Science Reviews*
2428 11, 145-177.
- 2429 Carto, S.L., Eyles, N., 2012a. Identifying glacial influences on sedimentation in tectonically-
2430 active, mass flow dominated arc basins with reference to the Neoproterozoic Gaskiers
2431 glaciation (c. 580 Ma) of the Avalonian-Cadomian Orogenic Belt. *Sedimentary Geology*
2432 261–262, 1–14.
- 2433 Carto, S.L., Eyles, N., 2012b. Sedimentology of the Neoproterozoic (c. 580 Ma) Squantum
2434 “Tillite,” Boston Basin, USA: Mass flow deposition in a deep-water arc basin lacking direct
2435 glacial influence. *Sedimentary Geology* 269, 1–14.
- 2436 Cecioni, G.O., 1957. Cretaceous Flysch and Molasse in Departamento Ultima Esperanza,
2437 Magallanes Province, Chile. *Bulletin of the American Association of Petroleum Geologists*
2438 41, 538-564.
- 2439 Cecioni, G.O., 1981. Cretaceous Lago Sofia Formation, Chilean Patagonia, in: Hambrey,
2440 M.J., Harland, W.B. (Eds.), *Earth’s Pre-Pleistocene Glacial Record*. Cambridge University
2441 Press, Cambridge, p. 834.

- 2442 Cerda, I.A., Carabajal, A.P., Salgado, L., Coria, R.A., Reguero, M.A., Tambussi, C.P, Moly,
2443 J.J., 2012. The first record of a sauropod dinosaur from Antarctica. *Naturwissenschaften* 99,
2444 83-87.
- 2445 Cernusak, L.A., Winter, K., Aranda, J., Turner, B.L., 2008. Conifers, angiosperm trees, and
2446 lianas: growth, whole-plant water and nitrogen use efficiency, and stable isotope composition
2447 ($\delta^{13}\text{C}$ and $\delta^{18}\text{O}$) of seedlings grown in a tropical environment. *Plant Physiology* 148, 642–659.
2448 www.plantphysiol.org/cgi/doi/10.1104/pp.108.123521.
- 2449 Cesta, J.M., 2015. Soft-sediment slickensides in the Stockton Formation, Stockton, New
2450 Jersey. Geological Society of America, Northeastern Section – 50th Annual Meeting (23-25
2451 March 2015), Paper 45-1.
2452 https://gsa.confex.com/gsa/2015NE/finalprogram/abstract_253490.htm.
- 2453 Charrier, R., 1986. The Gondwana glaciation in Chile: Description of alleged glacial deposits
2454 and paleogeographic conditions bearing on the extension of the ice cover in Southern South
2455 America. *Palaeogeography, Palaeoclimatology, Palaeoecology* 56, 151-175.
2456 [https://doi.org/10.1016/0031-0182\(86\)90111-2](https://doi.org/10.1016/0031-0182(86)90111-2).
- 2457 Chen, X., Kuang, H., Liu, Y., Wang, Y., Yang, Z., Vandyk, T.M., Le Heron, D.P., Wang, S.,
2458 Geng, Y., Bai, H., Peng, N., Xia, X., 2020. Subglacial bedforms and landscapes formed by an
2459 ice sheet of Ediacaran-Cambrian age in west Henan, North China. *Precambrian Research* 344,
2460 105727. <https://doi.org/10.1016/j.precamres.2020.105727>.
- 2461 Chen, X., Kuang, H., Liu, Y., Le Heron, D.P., Wang, Y., Peng, N., Wang, Z., Zhong, Q., Yu,
2462 H., Chen, J., 2021. Revisiting the Nantuo Formation in Shennongjia, South China: A new
2463 depositional model and multiple glacial cycles in the Cryogenian. *Precambrian Research* 356,

- 2464 106132. <https://doi.org/10.1016/j.precamres.2021.106132>.
- 2465 Clark, D., Stanbrook, D.A., 2001. Formation of large scale shear structures during deposition
2466 from high density turbidity currents, Grès d'Annot Formation, South East France, in:
2467 McCaffrey, W., Kneller, B. and Peakall, J. (Eds.), Particulate Gravity Currents. International
2468 Association of Sedimentologists, Special Publication 31, Blackwell Science Ltd., London, pp.
2469 219-232.
- 2470 Clark, D.L., Hanson, A., 1983. Central Arctic Ocean Sediment Texture: A Key to Ice
2471 Transport Mechanisms, in: Molnia, B.F. (Ed.), Glacial-Marine Sedimentation. Plenum Press,
2472 New York, pp. 301-330.
- 2473 Clark, P.U., 1991. Striated clast pavements: Products of deforming subglacial sediment?
2474 *Geology* 19, 530-533.
- 2475 Clarke, S., Hubble, T., Airey, D., Yu, P., Boyd, R., Keene, J., Exon, N., Gardner, J.,
2476 Shipboard Party SS12/2008, 2012. Submarine landslides on the upper southeast Australian
2477 passive continental margin – preliminary findings, in: Yamada, Y., Kawamura, K., Ikehara,
2478 K., Ogawa, Y., Urgeles, R., Mosher, D., Chaytor, J., Strasser, M. (Eds.), Submarine Mass
2479 Movements and Their Consequences. Springer International Publ., Switzerland, pp. 55-66.
2480 <https://doi.org/10.1007/978-94-007-2162-3>.
- 2481 Coats, R.P., Preiss, W.V., 1987. Stratigraphy of the Umberatana Group, in: Drexel, J.F. (Ed.),
2482 Preiss, W.V. (compiler), The Adelaide geosyncline – Late Proterozoic Stratigraphy,
2483 Sedimentation, Palaeontology and Tectonics. Bulletin of the Geological Survey of South
2484 Australia 53, pp. 125-209.

- 2485 Coles, R.J., 2014. The Cross-sectional Characteristics of Glacial Valleys and Their Spatial
2486 Variability (Ph.D. thesis). Geography Department, University of Sheffield, 335 pp..
- 2487 Condie, K.C., 1967. Petrology of the Late Precambrian tillite(?) Association in Northern
2488 Utah. GSA Bulletin 78, 1317-1343.
- 2489 Costa, J.E., 1984. Physical geomorphology of debris flows, in: Costa, J.E., Fleisher, P.J.
2490 (Eds.), Developments and Applications of Geomorphology. Springer-Verlag, Berlin, pp. 268-
2491 317.
- 2492 Covault, J.A., Romans, B.W., 2009. Growth patterns of deep-sea fans revisited: Turbidite-
2493 system morphology in confined basins, examples from the California Borderland. Marine
2494 Geology 265, 51-66.
- 2495 Covault, J.A., Sylvester, Z., Hubbard, S.M., Jobe, Z.R., Sech, R.P., 2016. The stratigraphic
2496 record of submarine-channel evolution. The Sedimentary Record 14, 4-11.
2497 <https://doi.org/10:2110/sedred.2016.3>.
- 2498 Cowan, E.A., Powell, R.D., 1990. Suspended sediment transport and deposition of cyclically
2499 interlaminated sediment in a temperate glacial fjord, Alaska, U.S.A., in: Dowdeswell, J.A.,
2500 Scurce, J.D. (Eds.), Glacimarine Environments: Processes and Sediments. Geological
2501 Society, London, Spec. Publ. 53, pp. 75-89.
- 2502 Craddock, J.P., Ojakangas, R.W., Malone, D.V., Konstantinou, A., Mory, A., Bauer, W.,
2503 Thomas, R.J., Affinati, S.C., Pauls, K., Zimmerman, U., Botha, G., Rochas-Campos, A., dos
2504 Santos, P.R., Tohver, E., Riccomini, C., Martin, J., Redfern, J., Horstwood, M., Gehrels, G.,
2505 2019. Detrital zircon provenance of Permo-Carboniferous glacial diamictites across

- 2506 Gondwana. *Earth-Science Reviews* 192, 285-316.
2507 <https://doi.org/10.1016/j.earscirev.2019.01.014>.
- 2508 Creixell, C., Sepúlveda, F., Álvarez, J., Vásquez, P., Velásquez, R., 2021. The Carboniferous
2509 onset of subduction at SW Gondwana revisited: Sedimentation and deformation processes
2510 along the late Paleozoic forearc of north Chile (21°–33° S). *Journal of South American Earth
2511 Sciences* 107, 103149. <https://doi.org/10.1016/j.jsames.2020.103149>.
- 2512 Crosby, B.T., Whipple, K.X., Gasparini, N.M., Wobus, C.W. 2007. Formation of fluvial
2513 hanging valleys: Theory and simulation, *Journal of Geophysical Research* 112, F03S10.
2514 <https://doi.org/10.1029/2006JF000566>.
- 2515 Crowell, J.C., 1957. Origin of pebbly mudstones. *Bulletin of the Geological Society of
2516 America* 68, 993-1010.
- 2517 Cuneo, R.N., Isbell, J., Taylor, E.D., Taylor, T.M., 1993. The *Glossopteris* flora from
2518 Antarctica: taphonomy and paleoecology. *Comptes Rendus XII ICC-P 2*, 13-40.
- 2519 Da, J., Zhang, Y.G., Li, G., Meng, X., Ji, J., 2019. Low CO₂ levels of the entire Pleistocene
2520 epoch. *Nature Communications* 10, 4342. <https://doi.org/10.1038/s41467-019-12357-5>.
- 2521 Da Silva, A.C., Dekkers, M.J., De Vleeschouwer, D., Hladil, J., Chadimova, L., Slavík, L.,
2522 Hilgen, F.J., 2019. Millennial-scale climate changes manifest Milankovitch combination
2523 tones and Hallstatt solar cycles in the Devonian greenhouse world: Reply. *Geology* 47, e489-
2524 e490. <https://doi.org/10.1130/G46732Y.1>.

- 2525 Daily, B., Gostin, V.A., Nelson, C.A., 1973. Tectonic origin for an assumed glacial pavement
2526 of Late Proterozoic age, South Australia. *Journal of the Geological Society of Australia* 20,
2527 75-78. <https://doi.org/10.1080/14400957308527896>.
- 2528 Dakin, N., Pickering, K.T., Mohrig, D., Bayliss, N.J., 2013. Channel-like features created by
2529 erosive submarine debris flows: field evidence from the Middle Eocene Ainsa Basin, Spanish
2530 Pyrenees. *Marine and Petroleum Geology* 41, 62-71.
- 2531 Dal Cin, R., 1968. "Pebble clusters": Their origin and utilization in the study of
2532 paleocurrents. *Sedimentary Geology* 2, 233-241.
2533 [https://doi.org/10.1016/0037-0738\(68\)90001-8](https://doi.org/10.1016/0037-0738(68)90001-8).
- 2534 Dasgupta, P., 2003. Sediment gravity flow – the conceptual problems. *Earth-Science Reviews*
2535 62, 265-281.
- 2536 De Blasio, F.V., Engvik, L.E., Elverhøi, A., 2006. Sliding of outrunner blocks from
2537 submarine landslides. *Geophysical Research Letters* 33, L06614.
2538 <https://doi.org/10.1029/2005GL025165>.
- 2539 de Lange, W.P., de Lange, P.J., Moon, V.G., 2006. Boulder transport by waterspouts: An
2540 example from Aorangi Island, New Zealand. *Marine Geology* 230,115–125.
2541 <https://doi.org/10.1016/j.margeo.2006.04.006>.

- 2542 de Wit, M.C.J., 2016a. Dwyka eskers along the northern margin of the main Karoo Basin, in:
2543 Linol, B., de Wit, M.J. (Eds.), Origin and Evolution of the Cape Mountains and Karoo Basin,
2544 Regional Geology Reviews. Springer International Publishing, Switzerland, pp. 87-99.
2545 https://doi.org/10.1007/978-3-319-40859-0_9.
- 2546 de Wit, M.C.J., 2016b. Early Permian diamond-bearing proximal eskers in the
2547 Lichtenburg/Ventersdorp area of the North West Province, South Africa. South African
2548 Journal of Geology 119, 585-606. <https://doi.org/10.2113/gssajg.119.4.585>.
- 2549 Decombeix, A.-L., Durieux, T., Harper, C.J., Serbet, R., Taylor, E.L., 2021. A Permian nurse
2550 log and evidence for facilitation in high latitude Glossopteris forests. Lethaia 54, 96–105.
2551 <https://doi.org/10.1111/let.12386>.
- 2552 Del Cortona, A., Jackson, C.J., Bucchini, F., Van Bel, M., D'hondt, S., Škaloud, P.,
2553 Delwiche, C.F., Knoll, A.H., Raven, J.A., Verbruggen, H., Vandepoele, K., De Clerck, O.,
2554 Leliaert, F., 2020, Neoproterozoic origin and multiple transitions to macroscopic growth in
2555 green seaweeds: PNAS 117, 2551–2559. <https://doi.org/10.1073/pnas.1910060117>.
- 2556 Delpomdor, F., Eyles, N., Tack, L., Pr at, A., 2016. Pre- and post-Marinoan carbonate facies
2557 of the Democratic Republic of the Congo: Glacially- or tectonically-influenced deep-water
2558 sediments? Palaeogeography, Palaeoclimatology, Palaeoecology 457, 144–157.
2559 <https://doi.org/10.1016/j.palaeo.2016.06.014>.
- 2560 Denis, M., Guiraud, M., Konat , M., 2010. Subglacial deformation and water-pressure cycles
2561 as a key for understanding ice stream dynamics: evidence from the Late Ordovician

- 2562 succession of the Djado Basin (Niger). *International Journal of Earth Sciences* 99,
2563 1399–1425. <https://doi.org/10.1007/s00531-009-0455-z>.
- 2564 Derbyshire, E., 1979. Glaciers and environment, in: John, B.S. (Ed.), *The Winters of the*
2565 *World*. Davies and Charles, Newton Abbot, pp. 58-106.
- 2566 DeVore, M.L., Pigg, K.B., 2020. The Paleocene-Eocene thermal maximum: plants as
2567 paleothermometers, rain gauges, and monitors, in: Martinetto, E., Tschopp, E., Gastaldo, R.
2568 (Eds.), *Nature through Time*. Springer Textbooks in Earth Sciences, Geography and
2569 Environment. Springer, Cham, pp. 109-128. https://doi.org/10.1007/978-3-030-35058-1_4.
- 2570 Dey, S., Dasgupta, P., Das, K., Matin, A., 2020. Neoproterozoic Blaini Formation of Lesser
2571 Himalaya, India: fiction and fact. *GSA Bulletin* 132, 2267-2281.
2572 <https://doi.org/10.1130/B35483.1>.
- 2573 Deynoux, M., 1983. Late Precambrian and Upper Ordovician glaciations in the Taoudeni
2574 Basin, West Africa, in: Deynoux, M. (Ed.), *Till Mauretania* 83. Centre National de la
2575 Recherche Scientifique, Paris, pp. 44-86.
- 2576 Deynoux, M., 1985a. Les Glaciations du Sahara. *La Recherche* 16, 986-997.
- 2577 Deynoux, M., 1985b. Terrestrial or waterlain glacial diamictites? Three case studies from the
2578 Late Precambrian and Late Ordovician glacial drifts in West Africa. *Palaeogeography,*
2579 *Palaeoclimatology, Palaeoecology* 51, 97-141.
2580 [https://doi.org/10.1016/0031-0182\(85\)90082-3](https://doi.org/10.1016/0031-0182(85)90082-3).

- 2581 Deynoux, M., Ghienne, J.-F., 2004. Late Ordovician glacial pavements revisited: a
2582 reappraisal of the origin of striated surfaces. *Terra Nova* 16, 95-101.
2583 <https://doi.org/10.1111/j.1365-3121.2004.00536.x>.
- 2584 Deynoux, M., Ghienne, J.-F., 2005. Reply. Late Ordovician glacial pavements revisited: a
2585 reappraisal of the origin of striated surfaces. *Terra Nova* 17, 488-491.
- 2586 Deynoux, M., Trompette, R., 1976. Discussion: Late Precambrian mixtites: glacial and/or
2587 nonglacial? Dealing especially with the mixtites of West Africa. *American Journal of Science*
2588 276, 1302-1315.
- 2589 Deynoux, M., Trompette, R., 1981a. Late Ordovician Tillites of the Taoudeni Basin, West
2590 Africa, in: Hambrey, M.J., Harland, W.B. (Eds.), *Earth's Pre-Pleistocene Glacial Record*.
2591 Cambridge University Press, Cambridge, pp. 89-96.
- 2592 Deynoux, M., Trompette, R., 1981b. Late Precambrian tillites of the Taoudeni Basin, West
2593 Africa, in: Hambrey, M.J., Harland, W.B. (Eds.), *Earth's Pre-Pleistocene Glacial Record*.
2594 Cambridge University Press, Cambridge, pp. 123-131.
- 2595 Dietrich, P., Hofmann, A., 2019. Ice-margin fluctuation sequences and grounding zone
2596 wedges: The record of the Late Palaeozoic ice age in the eastern Karoo Basin (Dwyka Group,
2597 South Africa). *Depositional Record* 5, 247–271. <https://doi.org/10.1002/dep2.74>.
- 2598 Dietrich, P., Franchi, F., Setlhabi, L., Prevec, R., Bamford, M., 2019. The nonglacial
2599 diamictite of Toutswe Mogala Hill (Lower Karoo Supergroup, Central Botswana):

- 2600 Implications on the extent of the Late Paleozoic ice age in the Kalahari-Karoo Basin. *Journal*
2601 *of Sedimentary Research* 89, 875–889. <https://doi.org/10.2110/jsr.2019.48>.
- 2602 Dietrich, P., Griffis, N.P., Le Heron, D.P., Montañez, I.P., Kettler, C., Robin, C.,
2603 Guillocheau, F., 2021. Fjord network in Namibia: A snapshot into the dynamics of the late
2604 Paleozoic glaciation. *Geology* 49. <https://doi.org/10.1130/G49067.1>.
- 2605 Dill, R.F., 1964. Sedimentation and erosion in Scripps Submarine Canyon head, in: Miller,
2606 R.L. (Ed.), *Papers in Marine Geology*. Macmillan, New York, pp. 23-41.
- 2607 Dill, R.F., 1966. Sand Flows and Sand Falls, in: Fairbridge, R.W. (Ed.), *The Encyclopedia of*
2608 *Oceanography*. Reinhold Publ., New York, pp. 763-765.
- 2609 Dionne, J.-C., 1992. Ring structures made by shore ice in muddy tidal flat, St. Lawrence
2610 estuary, Canada. *Sedimentary Geology* 76, 285-292.
- 2611 Dionne, J.-C., 1993. Sediment load of shore ice and ice rafting potential, upper St. Lawrence
2612 Estuary, Québec, Canada. *Journal of Coastal Research* 9, 628-646.
- 2613 Domack, E.W., 1990. Laminated terrigenous sediments from the Antarctic Peninsula: the role
2614 of subglacial and marine processes, in: Dowdeswell, J.A., Scource, J.D. (Eds.), *Glacimarine*
2615 *Environments: Processes and Sediments*. Geological Society, London, Special Publications
2616 53, pp. 91-103.

- 2617 Domack, E.W., Hoffman, P.F., 2011. An ice grounding-line wedge from the Ghaub glaciation
2618 (635 Ma) on the distal foreslope of the Otavi carbonate platform, Namibia, and its bearing on
2619 the snowball Earth hypothesis. *GSA Bulletin* 123, 1448-1477.
2620 <https://doi.org/10.1130/B30217.1>.
- 2621 Donovan, S.K., Pickerill, R.K., 1997. Dropstones: their origin and significance: a comment.
2622 *Palaeogeography, Palaeoclimatology, Palaeoecology* 131, 175-178.
- 2623 Donovan, S.K., Pickerill, R.K., 2008. The Paleogene Richmond Formation of Jamaica: Not
2624 an impact-related succession. *Scripta Geologica* 136, 107-111.
- 2625 Doré, F., 1981. Late Precambrian tilloids of Normandy (Armorican Massif), in: Hambrey,
2626 M.J., Harland, W.B. (Eds.), *Earth's Pre-Pleistocene Glacial Record*. Cambridge University
2627 Press, Cambridge, pp. 643-646.
- 2628 Dott, R.H., 1961. Squantum "tillite," Massachusetts – evidence of glaciation or subaqueous
2629 mass movements? *GSA Bulletin* 72, 1289-1305.
- 2630 Dott, R.H., 1963. Dynamics of subaqueous gravity depositional processes. *Bulletin of the*
2631 *American Association of Petroleum Geologists* 47, 104-128.
- 2632 Dott, R.H., Batten, R.L., 1976. *Evolution of the Earth*, second ed. McGraw-Hill, New York,
2633 p. 285.

- 2634 Dou, L., Best, J., Bao, Z., Hou, J., Zhang, L., Liua, Y., 2021. The sedimentary architecture of
2635 hyperpycnites produced by transient turbulent flows in a shallow lacustrine environment.
2636 *Sedimentary Geology* 411, 105804. <https://doi.org/10.1016/j.sedgeo.2020.105804>.
- 2637 Doublet, S., Garcia, J.P., 2004. The significance of dropstones in a tropical lacustrine setting,
2638 eastern Cameros Basin (Late Jurassic-Early Cretaceous, Spain). *Sedimentary Geology* 163,
2639 293-309.
- 2640 Dow, D.B., Beyth, M., Hailu, T., 1971. Palaeozoic glacial rocks recently discovered in
2641 northern Ethiopia. *Geological Magazine* 108, 53-60.
- 2642 Dowdeswell, J.A., Hogan, K.A., 2016. Huge iceberg ploughmarks and associated corrugation
2643 ridges on the northern Svalbard shelf, in: Dowdeswell, J.A., Canals, M., Jakobsson, M.,
2644 Todd, B.J., Dowdeswell, E.K., Hogan, K.A. (Eds.), *Atlas of Submarine Glacial Landforms:
2645 Modern, Quaternary and Ancient*. Geological Society, London, Memoirs 46, pp. 269-270.
2646 <https://doi.org/10.1144/M46.4>.
- 2647 Dowdeswell, J.A., Ottesen, D., 2013. Buried iceberg ploughmarks in the early Quaternary
2648 sediments of the central North Sea: A two-million year record of glacial influence from 3D
2649 seismic data. *Marine Geology* 344, 1-9. <https://doi.org/10.1016/j.margeo.2013.06.019>.
- 2650 Dowdeswell, J.A., Canals, M., Jakobsson, M., Todd, B.J., Dowdeswell, E.K., Hogan, K.A.,
2651 2016a. The variety and distribution of submarine glacial landforms and implications for
2652 ice-sheet reconstruction, in: Dowdeswell, J.A., Canals, M., Jakobsson, M., Todd, B.J.,
2653 Dowdeswell, E.K., Hogan, K.A. (Eds.), *Atlas of Submarine Glacial landforms: Modern,*

- 2654 Quaternary and Ancient. Geological Society, London, Memoirs, 46, pp. 519-552.
2655 <https://doi.org/10.1144/M46.183>.
- 2656 Dowdeswell, J.A., Canals, M., Jakobsson, M., Todd, B.J., Dowdeswell, E.K., Hogan, K.A.
2657 (Eds.), 2016b. Atlas of Submarine Glacial landforms: Modern, Quaternary and Ancient.
2658 Geological Society, London, Memoirs 46, 618 pp. <https://doi.org/10.1144/M46>.
- 2659 Draganits, E., Schlaf, J., Grasemann, B., Argles, T., 2008. Giant submarine landslide grooves
2660 in the Neoproterozoic/Lower Cambrian Phe Formation, northwest Himalaya: Mechanisms of
2661 formation and palaeogeographic implications. *Sedimentary Geology* 205, 126–141.
2662 <https://doi.org/10.1016/j.sedgeo.2008.02.004>.
- 2663 Dreimanis, A., 1993. Small to medium-sized glacitectonic structures in till and in its
2664 substratum and their comparison with mass movement structures. *Quaternary International*,
2665 18, 69-79.
- 2666 du Toit, A.L., 1926. *The Geology of South Africa*. Oliver and Boyd, Edinburgh, pp. 205-215.
- 2667 Dufresne, A., Davies, T.R., 2009. Longitudinal ridges in mass movement deposits.
2668 *Geomorphology* 105, 171-181.
- 2669 Dufresne, A., Geertsema, M., Shugar, D.H., Koppes, M., Higman, B., Haeussler, P.J., Stark,
2670 C., Venditti, J.G., Bonno, D., Larsen, C., Gulick, S.P.S., McCall, N., Walton, M., Loso, M.G.,
2671 Willis, M.J., 2018. Sedimentology and geomorphology of a large tsunamigenic landslide,

- 2672 Taan Fiord, Alaska. *Sedimentary Geology* 364, 302-318.
- 2673 <https://doi.org/10.1016/j.sedgeo.2017.10.004>.
- 2674 Dufresne, A., Zernack, A., Bernard, K., Thouret, J.-C., Roverato, M., 2021. Sedimentology of
2675 volcanic debris avalanche deposits, in: Roverato, M., Dufresne, A., Procter, J. (Eds.),
2676 Volcanic Debris Avalanches. *Advances in Volcanology*. Springer, Cham, pp. 175-210.
2677 https://doi.org/10.1007/978-3-030-57411-6_8.
- 2678 Dykstra, M., 2012. Deep-water tidal sedimentology, in: Davies, R.A., Jr., Dalrymple, R.W.
2679 (Eds.), *Principles of Tidal Sedimentology*. Springer, Dordrecht, pp. 371-395.
2680 https://doi.org/10.1007/978-94-007-0123-6_14.
- 2681 Dykstra, M., Garyfalou, K., Kertznus, V., Kneller, B., Milana, J.P., Molinaro, M., Szuman,
2682 M., Thompson, P., 2011. Mass-transport deposits: Combining outcrop studies and seismic
2683 forward modeling to understand lithofacies distributions, deformation, and their seismic
2684 stratigraphic expression, in: Shipp, R.C., Weimer, P., Posamentier, H.W. (Eds.), *Mass-*
2685 *Transport Deposits in Deepwater Settings*. SEPM Special Publication 96, pp. 293–310.
- 2686 Ebert, D.A., 1996. Origin and significance of mud-filled incised valleys (Upper Cretaceous)
2687 in southern Alberta, Canada. *Sedimentology* 43, 459-477.
- 2688 Eggenhuisen, J.T., McCaffrey, W.D., Haughton, P.D.W., Butler, R.W.H., 2011. Shallow
2689 erosion beneath turbidity currents and its impact on the architectural development of turbidite
2690 sheet systems. *Sedimentology* 58, 936–959, [https://doi.org/10.1111/j.1365-](https://doi.org/10.1111/j.1365-3091.2010.01190.x)
2691 [3091.2010.01190.x](https://doi.org/10.1111/j.1365-3091.2010.01190.x).

- 2692 Eisbacher, G.H., 1981. The Late Precambrian Mount Lloyd George diamictites, northern
2693 British Columbia, in: Hambrey, M.J., Harland, W.B. (Eds.), Earth's Pre-Pleistocene Glacial
2694 Record. Cambridge University Press, Cambridge, pp. 728-729.
- 2695 Elfström, Å., 1987. Large boulder deposits and catastrophic floods. *Geografiska Annaler*
2696 *69A*, 101-121.
- 2697 El-Makhrouf, A.A. 1988. Tectonic interpretation of Jabal Eghei area and its regional
2698 application to Tibesti orogenic belt, south central Libya (S.P.L.A.J.). *Journal of African Earth*
2699 *Sciences* 7, 945-967.
- 2700 Embleton, C., King, C.A.M., 1968. *Glacial and Periglacial Geomorphology*. Edward Arnold,
2701 London, p. 304.
- 2702 Embley, R.W., 1976. New Evidence for occurrence of debris flow deposits in the deep sea.
2703 *Geology* 4, 371-374.
- 2704 Embley, R.W., 1980. The role of mass transport in the distribution and character of deep-
2705 ocean sediments with special reference to the North Atlantic. *Marine Geology* 38, 23-50.
- 2706 Embley, R.W., 1982. Anatomy of some Atlantic margin sediment slides and some comments
2707 on ages and mechanisms, in: Saxov, S., Nieuwenhuis, J.K. (Eds.), *Marine Slides and Other*
2708 *Mass Movements*. Plenum Press, New York, pp. 189-213.

- 2709 Embley, R.W., Morley, J.J., 1980. Quaternary sedimentation and paleoenvironmental studies
2710 off Namibia (South-West Africa). *Marine Geology* 36, 183-204.
- 2711 Emery, K.O., Tschudy, R.H., 1941. Transportation of rock by kelp. *Bulletin of the Geological*
2712 *Society of America* 52, 855-862.
- 2713 Enos, P., 1969. Anatomy of flysch. *Journal of Sedimentary Research* 39, 680-723.
- 2714 Eriksson, P.G., 1991. A note on coarse-grained gravity-flow deposits within Proterozoic
2715 Lacustrine sedimentary rocks, Transvaal Sequence, South Africa. *Journal of African Earth*
2716 *Sciences* 12, 549-553.
- 2717 Erginal, A.E., Ertek, T.A., 2002. Geomorphology of Hereke-Körfez area and its relation to
2718 the submarine morphology of the centre basin of the Gulf of Izmit. *Turkish Journal of Marine*
2719 *Sciences* 8, 67-89.
- 2720 Evans, D.J.A., Roberts, D.H., Evans, S.C., 2016. Multiple subglacial till deposition: A
2721 modern exemplar for Quaternary palaeoglaciology. *Quaternary Science Reviews* 145,
2722 183-203. <https://doi.org/10.1016/j.quascirev.2016.05.029>.
- 2723 Evans, D.J.A., Phillips, E.R., Hiemstra, J.F., Auton, C.A., 2006. Subglacial till: Formation,
2724 sedimentary characteristics and classification. *Earth-Science Reviews* 78, 115-176.
2725 <https://doi.org/10.1016/j.earscirev.2006.04.001>.

- 2726 Evenson, E.B., Dreimanis, A., Newsome, J.W., 1977. Subaquatic flow tills: a new
2727 interpretation for the genesis of some laminated deposits. *Boreas*, 6 115-133.
2728 <https://doi.org/10.1111/j.1502-3885.1977.tb00341.x>.
- 2729 Eyles, C.H., Eyles, N., 1989. The Upper Cenozoic White River “tillites” of Southern Alaska:
2730 subaerial slope and fan-delta deposits in a strike-slip setting. *GSA Bulletin* 101, 1091-1102.
- 2731 Eyles, C.H., Eyles, N., 2000. Subaqueous mass flow origin for Lower Permian diamictites
2732 and associated facies of the Grant Group, Barbwire Terrace, Canning Basin, Western
2733 Australia. *Sedimentology* 47, 343-356.
- 2734 Eyles, C.H., Lagoe, M.-B., 1998. Slump-generated megachannels in the Pliocene-Pleistocene
2735 glaciomarine Yakataga Formation, Gulf of Alaska. *GSA Bulletin* 110, 395-408.
- 2736 Eyles, C.H., Eyles, N., Miall A.D., 1985. Models of glaciomarine sediment and their
2737 application to the interpretation of ancient glacial sequences. *Palaeogeography,*
2738 *Palaeoclimatology, Palaeoecology* 51, 15-84.
- 2739 Eyles, N., 1990. Marine debris flows: Late Precambrian “tillites” of the Avalonian-Cadomian
2740 orogenic belt. *Palaeogeography, Palaeoclimatology, Palaeoecology* 79, 73-98.
- 2741 Eyles, N., 1993. Earth’s glacial record and its tectonic setting. *Earth-Science Reviews* 35,
2742 1-248.

- 2743 Eyles, N., Boyce, J.I., 1998. Kinematic indicators in fault gouge: tectonic analog for
2744 soft-bedded ice sheets. *Sedimentary Geology* 116, 1-12.
- 2745 Eyles, N., Clark, B.M., 1985. Gravity induced soft sediment deformation in glaciomarine
2746 sequences of the Upper Proterozoic Port Askaig Formation, Scotland. *Sedimentology* 32,
2747 789-814. <https://doi.org/10.1111/j.1365-3091.1985.tb00734.x>.
- 2748 Eyles, N., Januszczak, N., 2007. Syntectonic subaqueous mass flows of the Neoproterozoic
2749 Otavi Group, Namibia: where is the evidence of global glaciation? *Basin Research* 19, 179-
2750 198.
- 2751 Eyles, N., Dearman, W.R., Douglas, T.D., 1983. The Distribution of glacial landsystems in
2752 Britain and North America, in: Eyles, N. (Ed.), *Glacial Geology*. Pergamon Press, pp.
2753 213-228. <https://doi.org/10.1016/B978-0-08-030263-8.50015-4>.
- 2754 Eyles, N., Moreno, L.A., Sookhan, S., 2018. Ice streams of the Late Wisconsin Cordilleran
2755 Ice Sheet in western North America. *Quaternary Science Reviews* 179, 87-122.
2756 <https://doi.org/10.1016/j.quascirev.2017.10.027>.
- 2757 Ezpeleta, M., Rustán, J.J., Balseiro, D., Dávila, F.M., Dahlquist, J.A., Vaccari, N.E., Sterren,
2758 A.F., Prestianni, C., Cisterna, G.A., Basei, M., 2020. Glaciomarine sequence stratigraphy in
2759 the Mississippian Río Blanco Basin, Argentina, southwestern Gondwana. Basin analysis and
2760 palaeoclimatic implications for the Late Paleozoic Ice Age during the Tournaisian. *Journal of*
2761 *the Geological Society* 177, 1107-1128. <https://doi-org.ezp.sub.su.se/10.1144/jgs2019-214>.

- 2762 Fairbridge, R.W., 1970. South Pole reaches the Sahara. *Science* 168, 878-881.
- 2763 Fairbridge, R.W., 1971. Upper Ordovician glaciation in Northwest Africa? Reply. *GSA*
2764 *Bulletin* 82, 269-274.
- 2765 Fairbridge, R.W., 1979. Traces from the desert: Ordovician, in: John, Brian S. (Ed.), *The*
2766 *Winters of the World*. Davies and Charles, Newton Abbot, pp. 131-153.
- 2767 Fairbridge, R.W., Finkl, C.W. Jr., 1980. Cratonic erosional unconformities and peneplains.
2768 *Journal of Geology* 88, 69-86.
- 2769 Fairchild, I.J., Fleming, E.J., Bao, H., Benn, D.I., Boomer, I., Dublyansky, Y.V., Halverson,
2770 G.P., Hambrey, M., Hendy, C., Mcmillan, E.A., Spötl, C., Stevenson, C.T.E., Wynn, P.M.,
2771 2016. Continental carbonate facies of a Neoproterozoic panglaciation, north-east Svalbard.
2772 *Sedimentology* 63, 443-497. <https://doi.org/10.1111/sed.12252>.
- 2773 Falvey, H.T., 1990. *Cavitation in Chutes and Spillways*. A Water Resources Technical
2774 Publication Engineering Monograph 42. United States Department of the Interior Bureau of
2775 Reclamation, Denver, 163 pp.
- 2776 Fedorchuk, N.D., Isbell, J.L., Griffis, N.P., Montañez, I.P., Vesely, F.F., Iannuzzi, R., Mundil,
2777 R., Yin, Q-Z., Pauls, K.N., Rosa; E.L.M., 2019. Origin of paleovalleys on the Rio Grande do
2778 Sul Shield (Brazil): Implications for the extent of late Paleozoic glaciation in west-central
2779 Gondwana. *Palaeogeography, Palaeoclimatology, Palaeoecology* 531, Part B, 108738.
2780 <https://doi.org/10.1016/j.palaeo.2018.04.013>.

- 2781 Fedorchuk, N.D., Griffis, N.P., Isbell, J.L., Goso, C., Rosa, E.L.M., Montañez, I.P., Yin, Q.-
2782 Z., Huyskens, M.H., Sanborn, M.E., Mundil, R., Vesely, F.F., Iannuzzi, R., 2021. Provenance
2783 of late Paleozoic glacial/post-glacial deposits in the eastern Chaco-Paraná Basin, Uruguay and
2784 southernmost Paraná Basin, Brazil. *Journal of South American Earth Sciences* 106, 102989.
2785 <https://doi.org/10.1016/j.jsames.2020.102989>.
- 2786 Festa, A., Ogata, K., Pini, G.A., Dilek, Y., Alonso, J.L., 2016. Origin and significance of
2787 olistostromes in the evolution of orogenic belts: a global synthesis. *Gondwana Research*
2788 39, 180–203. <https://doi.org/10.1016/j.gr.2016.08.002>.
- 2789 Festa, A., Pini, G.I., Ogata, K., Dilek, Y., 2019. Diagnostic features and field-criteria in
2790 recognition of tectonic, sedimentary and diapiric mélanges in orogenic belts and exhumed
2791 subduction-accretion complexes. *Gondwana Research* 74, 7-30.
2792 <https://doi.org/10.1016/j.gr.2019.01.003>.
- 2793 Finkl, C.W. Jr., Fairbridge, R.W., 1979. Paleogeographic evolution of a rifted cratonic
2794 margin: S.W. Australia. *Palaeogeography, Palaeoclimatology, Palaeoecology* 26, 221-252.
- 2795 Fiorillo, A.R., Kobayashi, Y., McCarthy, P.J., Tanaka, T., Tykoski, R.S., Lee, Y.-N.,
2796 Takasaki, R., Yoshida, J., 2019. Dinosaur ichnology and sedimentology of the Chignik
2797 Formation (Upper Cretaceous), Aniakchak National Monument, southwestern Alaska;
2798 Further insights on habitat preferences of high-latitude hadrosaurs. *PLoS ONE* 14, e0223471.
2799 <https://doi.org/10.1371/journal.pone.0223471>.

- 2800 Fleisher, P.J., Lachniet, M.S., Muller, E.H., Bailey, P.K., 2006. Subglacial deformation of
2801 trees within overridden foreland strata, Bering Glacier, Alaska. *Geomorphology* 75, 201-211.
2802 <https://doi.org/10.1016/j.geomorph.2005.01.013>.
- 2803 Flint, R.F., 1961. Geological evidence of cold climate, in: Nairn, A.E.M. (Ed.), *Descriptive*
2804 *Palaeoclimatology*. Interscience Publ., New York, pp. 140-155.
- 2805 Flint, R.F., 1971. *Glacial and Quaternary Geology*. John Wiley and Sons, New York, 892 pp..
- 2806 Flint, R.F., 1975. Features other than diamicts as evidence of ancient glaciations, in: Wright,
2807 A.E., Moseley, F. (Eds.), *Ice Ages: Ancient and Modern*. Seal House Press, Liverpool, pp.
2808 121-136.
- 2809 Fonnesu, M., Patacci, M., Haughton, P.D.W., Felletti, F., McCaffrey, W.D., 2016. Hybrid
2810 event beds generated by local substrate delamination on a confined-basin floor. *Journal of*
2811 *Sedimentary Research* 86, 929–943. <https://doi.org/10.2110/jsr.2016.58>.
- 2812 Frakes, L.A., 1979. *Climates through Geologic Time*. Elsevier, Amsterdam, 304 pp.
- 2813 Frakes, L.A., Crowell, J.C., 1969. Late Paleozoic glaciation: I, South America. *GSA Bulletin*
2814 80, 1007-1042.
- 2815 Frakes, L.A., Crowell, J.C., 1970. Late Paleozoic glaciation: II, Africa exclusive of the Karoo
2816 Basin. *GSA Bulletin* 81, 2261-2286.

- 2817 Frakes, L.A., Krassay, A.A., 1992. Discovery of probable ice-rafting in the Late Mesozoic of
2818 the Northern Territory and Queensland. *Australian Journal of Earth Sciences* 39, 115-119.
2819 <https://doi.org/10.1080/08120099208728006>.
- 2820 Frakes, L.A., Amos, A.A., Crowell, J.C., 1969. Origin and stratigraphy of Late Paleozoic
2821 diamictites in Argentina and Bolivia, in: Amos, A.J. (Ed.), *Gondwana Stratigraphy*. IUGS
2822 Symposium in Buenos Aires 1967, UNESCO, pp. 821-843.
- 2823 Francis, J.E., 1990. Polar fossil forests. *Geology Today* 6, May-June, 92-95.
- 2824 Frimmel, H.E., 2010. On the reliability of stable carbon isotopes for Neoproterozoic
2825 chemostratigraphic correlation. *Precambrian Research* 182, 239-253.
2826 <https://doi.org/10.1016/j.precamres.2010.01.003>.
- 2827 Frimmel, H.E., 2018. The Gariep Belt, in: Siegesmund, S., Basei, M., Oyhantçabal, P.,
2828 Oriolo, S. (Eds.), *Geology of Southwest Gondwana*. Regional Geology Reviews. Springer,
2829 Cham. https://doi.org/10.1007/978-3-319-68920-3_13.
- 2830 Fry, W.L., 1983. An algal flora from the Upper Ordovician of the Lake Winnipeg Region,
2831 Manitoba, Canada. *Review of Palaeobotany and Palynology* 39, 313-341.
- 2832 Gales, J.A., Leat, P.T., Larter, R.D., Kuhn, G., Hillenbrand, C.-D., Graham, A.G.C., Mitchell,
2833 N.C., Tate, A.J., Buys, G.B., Jokat W., 2014. Large-scale submarine landslides, channel and
2834 gully systems on the southern Weddell Sea margin, Antarctica. *Marine Geology* 348, 73–87.
2835 <https://doi.org/10.1016/j.margeo.2013.12.002>.

- 2836 Garden, C.J., Smith, A.M., 2011. The role of kelp in sediment transport: Observations from
2837 southeast New Zealand. *Marine Geology* 281, 35-42.
- 2838 Garzanti, E., Resentini, A., 2016. Provenance control on chemical indices of weathering
2839 (Taiwan river sands). *Sedimentary Geology* 336, 81-95.
2840 <https://doi.org/10.1016/j.sedgeo.2015.06.013>.
- 2841 Gastaldo, F.A., Bamford, M., Calder, J., DiMichele, W.A., Iannuzzi, R., Jasper, A., Kerp, H.,
2842 McLoughlin, S., Opluštil, S., Pfefferkorn, H.W., Rößler, R., Wang, J., 2020a. The non-analog
2843 vegetation of the Late Paleozoic icehouse–hothouse and their coal-forming forested
2844 environments, in: Martinetto, E., Tschopp, E., Gastaldo, R. (Eds.), *Nature through Time*.
2845 Springer Textbooks in Earth Sciences, Geography and Environment. Springer, Cham, pp.
2846 291-316. https://doi.org/10.1007/978-3-030-35058-1_12.
- 2847 Gastaldo, F.A., Bamford, M., Calder, J., DiMichele, W.A., Iannuzzi, R., Jasper, A., Kerp, H.,
2848 McLoughlin, S., Opluštil, S., Pfefferkorn, H.W., Rößler, R., Wang, J., 2020b. The coal farms
2849 of the Late Paleozoic, in: Martinetto, E., Tschopp, E., Gastaldo, R. (Eds.), *Nature through*
2850 *Time*. Springer Textbooks in Earth Sciences, Geography and Environment. Springer, Cham,
2851 pp. 317-343. https://doi.org/10.1007/978-3-030-35058-1_13.
- 2852 Gateway to the Paleobiology Database. <http://fossilworks.org/> (accessed 29 January 2020).
- 2853 Gaucher, C., Sial, A.N., Frei, R., 2015. Chemostratigraphy of Neoproterozoic banded iron
2854 formation (BIF): types, age and origin, in: Ramkumar, M. (Ed.), *Chemostratigraphy:*

- 2855 Concepts, Techniques, and Applications. Elsevier, Amsterdam, pp. 433-449.
2856 <https://doi.org/10.1016/B978-0-12-419968-2.00017-0>.
- 2857 Gee, M.J.R., Gawthorpe, R.L., Friedmann, J.S., 2005. Giant striations at the base of a
2858 submarine landslide. *Marine Geology* 214, 287–294.
- 2859 Gee, M.J.R., Uy, H.S., Warren, J., Morley, C.K., Lambiase, J.J., 2007. The Brunei slide: A
2860 giant submarine landslide on the North West Borneo Margin revealed by 3D seismic data.
2861 *Marine Geology* 246, 9–23. <https://doi.org/10.1016/j.margeo.2007.07.009>.
- 2862 Georgiopoulou, A., Masson, D.G, Wynn, R.B., Krastel, S., 2010. Sahara Slide: Age,
2863 initiation, and processes of a giant submarine slide. *Geochemistry, Geophysics, Geosystems*
2864 11, Q07014. <https://doi.org/10.1029/2010GC003066>.
- 2865 Germs, G.J.B., Gaucher, C., 2012. Nature and extent of a late Ediacaran (c. 547 Ma)
2866 glacial erosion surface in southern Africa. *South African Journal of Geology* 115, 91–102.
- 2867 Gibson, T.M., Shih, P.M., Cumming, V.M., Fischer, W.W., Crockford, P.W., Hodgskiss,
2868 M.S.W., Wörndle, S., Creaser, R.A., Rainbird, R.H., Skulski, T.M., Halverson, G.P., 2018.
2869 Precise age of *Bangiomorpha pubescens* dates the origin of eukaryotic photosynthesis.
2870 *Geology* 46, 135–138. <https://doi.org/10.1130/G39829.1>.
- 2871 Ghienne, J.-F., 2003. Late Ordovician sedimentary environments, glacial cycles, and
2872 post-glacial transgression in the Taoudeni Basin, West Africa. *Palaeogeography,*
2873 *Palaeoclimatology, Palaeoecology* 189, 117-145.

- 2874 Ghienne, J.-F., Deynoux, M., Manatschal, G, Rubino, J.L., 2003. Palaeovalleys and fault-
2875 controlled depocentres in the Late-Ordovician glacial record of the Murzuq Basin (central
2876 Libya). *Comptes Rendus Geoscience* 335, 1091-1100.
- 2877 Ghienne, J.-F., Le Heron, D.P., Moreau, J., Denis, M., Deynoux, M., 2007. The Late
2878 Ordovician glacial sedimentary system of the North Gondwana platform, in: Hambrey, M.J.,
2879 Christoffersen, P., Glasser, N.F., Hubbard, B. (Eds) *Glacial Sedimentary Processes and*
2880 *Products*. International Association of Sedimentologists Special Publication 39, Blackwell
2881 Publishing, Victoria, pp. 295-319.
- 2882 Ghuma, M.A., Rogers, J.J.W., 1978. Geology geochemistry, and tectonic setting of the
2883 Ben Ghnema batholith, Tibesti massif, southern Libya. *GSA Bulletin* 89, 1351-1358.
- 2884 Giddings, J.A., Wallace, M.W., Haines, P.W., Mornane, K., 2010. Submarine origin for the
2885 Neoproterozoic Wonoka canyons, South Australia. *Sedimentary Geology* 223, 35–50.
- 2886 Giegengack, R.F., Zaki, A.S., 2017. Inverted topographic features, now submerged beneath
2887 the water of Lake Nasser, document a morphostratigraphic sequence of high-amplitude late-
2888 Pleistocene climate oscillation in Egyptian Nubia. *Journal of African Earth Sciences* 136,
2889 176-187. <https://doi.org/10.1016/j.jafrearsci.2017.06.027>.
- 2890 Gilbert, R., 1990. Rafting in glacialmarine environments, in: Dowdeswell, J.A., Scource, J.D.
2891 (Eds.), *Glacialmarine Environments: Processes and Sediments*. Geological Society, London,
2892 *Spec. Publ.* 53, pp. 105-120.

- 2893 Glicken, H., 1996. Rockslide-debris avalanche of May 18, 1980, Mount St. Helens Volcano,
2894 Washington. US Geological Survey, Open-File Report 96-677.
- 2895 Glock, W.D., Studhalter, R.A., Agerter, S.R., 1960. Classification and multiplicity of growth
2896 layers in the branches of trees at the extreme lower forest border. Smithsonian Miscellaneous
2897 Collections 140, Smithsonian Institution, Washington, 294 pp.
- 2898 Gómez-Peral, L.E., Sial, A.N., Arrouy, M.J., Richiano, S., Ferreira, V.P., Kaufman, A.J.,
2899 Poiré, D.G., 2017. Paleo-climatic and paleo-environmental evolution of the Neoproterozoic
2900 basal sedimentary cover on the Río de La Plata Craton, Argentina: Insights from the $\delta^{13}\text{C}$
2901 chemostratigraphy. *Sedimentary Geology* 353, 139-157.
- 2902 González, C.R., Glasser, N.F., 2008. Carboniferous glacial erosional and depositional
2903 features in Argentina. *Geologica et Palaeontologica* 48, 39-54.
- 2904 Gore, D.B., Taylor M.P. 2003. Discussion and Reply: Grooves and striations on the
2905 Stanthorpe Adamellite: Evidence for a possible late Middle – Late Triassic age glaciation.
2906 *Australian Journal of Earth Sciences* 50, 467-470.
- 2907 Götz, A.E., Ruckwied, K., Wheeler, A., 2018. Marine flooding surfaces recorded in Permian
2908 black shales and coal deposits of the Main Karoo Basin (South Africa): implications for basin
2909 dynamics and cross-basin correlation. *International Journal of Coal Geology* 190, 178–190.
2910 <https://doi.org/10.1016/j.coal.2017.10.014>.

- 2911 Gould, S.J., 1987. *Time's Arrow, Time's Cycle*. Harvard University Press, Cambridge, 222
2912 pp.
- 2913 Gravenor, C.P., 1979. The nature of the Late Paleozoic glaciation in Gondwana as determined
2914 from an analysis of garnets and other heavy minerals. *Canadian Journal of Earth Sciences* 16,
2915 1137-1153.
- 2916 Gravenor, C.P., 1986. Magnetic and pebble fabrics in subaquatic debris-flow deposits.
2917 *Journal of Geology* 94, 683-698.
- 2918 Gravenor, C.P., Rocha-Campos, A.C., 1983. Patterns of Late Paleozoic glacial sedimentation
2919 on the southeast side of the Paraná Basin, Brazil. *Palaeogeography, Palaeoclimatology,*
2920 *Palaeoecology* 43, 1-39.
- 2921 Gravenor, C.P., Von Brunn, V., 1987. Aspects of Late Paleozoic glacial sedimentation in
2922 parts of the Paraná Basin, Brazil, and the Karoo Basin, South Africa, with special reference to
2923 the origin of massive diamictite, in: McKenzie, G.D. (Ed.), *Gondwana Six: Stratigraphy,*
2924 *Sedimentology and Paleontology*. Geophysical Monograph 41, pp. 103-111.
- 2925 Gravenor, C.P., Von Brunn, V., Dreimanis, A., 1984. Nature and classification of waterlain
2926 glaciogenic sediments, exemplified by Pleistocene, Late Paleozoic and Late Precambrian
2927 deposits. *Earth-Science Reviews* 20, 105-166.
- 2928 Griffis, N.P., Montañez, I.P., Fedorchuk, N., Isbell, J., Mundil, R., Vesely, F., Weinshultz, L.,
2929 Iannuzzi, R., Gulbransen, E., Taboada, A., Pagani, A., Sanborn, M.E., Huyskens, M.,

- 2930 Wimpenny, J., Linol, B., Yin, Q.-Z., 2019. Isotopes to ice: Constraining provenance of glacial
2931 deposits and ice centers in west-central Gondwana. *Palaeogeography, Palaeoclimatology,*
2932 *Palaeoecology* 531, 108745. <https://doi.org/10.1016/j.palaeo.2018.04.020>.
- 2933 Grotzinger, J.P., Fike, D.A., Fischer, W.W., 2011. Enigmatic origin of the largest-known
2934 carbon isotope excursion in Earth's history. *Nature Geoscience* 4, 285-292.
2935 <https://doi.org/10.1038/NGEO1138>.
- 2936 Gulbranson, E.L., Ryberg, P.E., Decombeix, A.-L., Taylor, E.L., Taylor, T.N., Isbell, J.L.,
2937 2014. Leaf habit of Late Permian *Glossopteris* trees from high-palaeolatitude forests. *Journal*
2938 *of the Geological Society* 171, 493-507.
- 2939 Gupta, S., 2007. Making the paper. *Nature* 448, xv.
- 2940 Gupta, S., Collier, J.S., Palmer-Felgate1, A., Graeme Potter, G., 2007. Catastrophic flooding
2941 origin of shelf valley systems in the English Channel. *Nature* 448, 342-346.
- 2942 Gupta, S., Collier, J.S., Garcia-Moreno, D., Oggioni, F., Trentesaux, A., Vanneste, K., De
2943 Batist, M., Camelbeek, T., Potter, G., Van Vliet-Lanoe, B., Arthur, J.C.R., 2017. Two-stage
2944 opening of Dover Strait and the origin of island Britain. *Nature Communications* 8, 1-12.
- 2945 Gürbüz, A., 2010. Geometric characteristics of pull-apart basins. *Lithosphere* 2, 199-206.
2946 <https://doi.org/10.1130/L36.1>.

- 2947 Haflidason, H., Sejrup, H.P., Nygård, A., Mienert, J., Bryn, P., Lien, R., Forsberg, C.F., Berg,
2948 K., Masson, D., 2004. The Storegga Slide: architecture, geometry and slide development.
2949 *Marine Geology* 213, 201–234. <https://doi.org/10.1016/j.margeo.2004.10.007>.
- 2950 Haldorsen, S., 1983. The characteristics and genesis of Norwegian tills, in: Ehlers, J. (Ed.),
2951 *Glacial Deposits in North-west Europe*. A. A. Balkema, Rotterdam, pp. 11-17.
- 2952 Haldorsen, S., Von Brunn, V., Maud, R., Truter, E.D., 2001. A Weichselian deglaciation
2953 model applied to the early Permian glaciation in the northeast Karoo Basin, South Africa.
2954 *Journal of Quaternary Science* 16, 583-593. <https://doi.org/10.1002/jqs.637>.
- 2955 Hall, K.J., 1989. Clast shape, in: Barrett, P.J. (Ed.), *Antarctic Cenozoic History from the*
2956 *CIROS-1 Drillhole, McMurdo Sound*. DSIR Bulletin 245, pp. 63-66.
- 2957 Hall, K.J., Visser, J.N.J., 1984. Observations on the relationship between clast size, shape,
2958 and lithology from the Permo-Carboniferous glaciogenic Dwyka Formation in the western
2959 part of Karoo Basin. *Transactions of the Geological Society of South Africa* 87, 225-232.
- 2960 Hambrey, M.J., 1983. Correlation of Late Proterozoic tillites in the North Atlantic region and
2961 Europe. *Geological Magazine* 120, 209-232.
- 2962 Hambrey, M.J., Harland, W.B. (Eds.), 1981. *Earth's Pre-Pleistocene Glacial Record*.
2963 Cambridge University Press, Cambridge. (Reissued edition in 2011.)

- 2964 Hambrey, M.J., Harland, W.B., 1981. Criteria for the identification of glacial deposits, in:
2965 Hambrey, M.J., Harland, W.B. (Eds.), *Earth's Pre-Pleistocene Glacial Record*. Cambridge
2966 University Press, Cambridge, 14-20.
- 2967 Hampton, M.A., 1972. The role of subaqueous debris flow in generating turbidity currents.
2968 *Journal of Sedimentary Petrology* 42, 775-793.
- 2969 Hancox, P.J., Götz, A.E., 2014. South Africa's coalfields – A 2014 perspective. *International*
2970 *Journal of Coal Geology* 132, 170–254. <https://doi.org/10.1016/j.coal.2014.06.019>.
- 2971 Hansen, L.A.S., Hodgson, D.M., Pontén, A., Bell, D., Flint, S., 2019. Quantification of basin-
2972 floor fan pinchouts: examples from the Karoo Basin, South Africa. *Frontiers in Earth Science*
2973 7, article 12. <https://doi.org/10.3389/feart.2019.00012>.
- 2974 Hansom, J.D., 1983. Ice-formed intertidal boulder pavements in the Sub-Antarctic. *Journal of*
2975 *Sedimentary Petrology* 53, 135-145.
- 2976 Hara, Y., Thorn, C.E., 1982. Preliminary quantitative study of alpine subnival boulder
2977 pavements, Colorado, Front Range, U.S.A. *Arctic and Alpine Research* 14, 361-367.
- 2978 Harker, R.I., 1993. Fracture patterns in clasts of diamictites (? tillites). *Journal of the*
2979 *Geological Society* 150, 251-254. <https://doi.org/10.1144/gsjgs.150.2.0251>.
- 2980 Harker, R.I., Giegengack, R., 1989. Brecciation of clasts in diamictites of the Gowganda
2981 Formation, Ontario, Canada. *Geology* 17, 123-126.

- 2982 Harland, W.B., Herod, K.N., 1975. Glaciations through time, in: Wright, A.E., Moseley, F.
2983 (Eds.), *Ice Ages: Ancient and Modern*. Seal House Press, Liverpool, pp. 189-216.
- 2984 Harrington, H.J., 1971. Glacial-like “striated floor” originated by debris-laden torrential water
2985 flows. *AAPG Bulletin* 55, 1344-1347.
- 2986 Harris, P.T., Barrie, J.V., Conway, K.W., Greene, H.G., 2014. Hanging canyons of Haida
2987 Gwaii, British Columbia, Canada: Fault-control on submarine canyon geomorphology along
2988 active continental margins. *Deep Sea Research Part II: Topical Studies in Oceanography* 104,
2989 83-92. <http://dx.doi.org/10.1016/j.dsr2.2013.06.017>.
- 2990 Hart, J.K., Roberts, D.H., 1994. Criteria to distinguish between subglacial glaciotectonic and
2991 glaciomarine sedimentation, I. Deformation styles and sedimentology. *Sedimentary Geology*
2992 91, 191-213. [https://doi.org/10.1016/0037-0738\(94\)90129-5](https://doi.org/10.1016/0037-0738(94)90129-5).
- 2993 Hartley, A., Kurjanski, B., Pugsley, J., Armstrong, J., 2020, Ice-rafting in lakes in the early
2994 Neoproterozoic: dropstones in the Diabaig Formation, Torridon Group, NW Scotland.
2995 *Scottish Journal of Geology* 56, 47–53. <https://doi.org/10.1144/sjg2019-017>.
- 2996 Hawkes, L., 1943. The erratics of the Cambridge Greensand – their nature provenance and
2997 mode of transport. *Quarterly Journal of the Geological Society of London* 99, 93-104.
- 2998 He, Y., Xie, X., Kneller, B.C., Wang, Z., Li, X., 2013. Architecture and controlling factors of
2999 canyon fills on the shelf margin in the Qiongdongnan Basin, northern South China Sea.

- 3000 Marine and Petroleum Geology 41, 264-276.
- 3001 <https://doi.org/10.1016/j.marpetgeo.2012.03.002>.
- 3002 Heezen, B.C., Hollister, C.D., 1971. The Face of the Deep. Oxford University Press, New
3003 York, pp. 293-304.
- 3004 Hicock, S.R., 1991. On subglacial stone pavements in till. Journal of Geology 99, 607-619.
- 3005 Hicock, S.R., Dreimanis, A., 1992a. Sunnybrook drift in the Toronto area, Canada:
3006 Reinvestigation and reinterpretation, in: Clark, P.U., Lea, P.D. (Eds.), The Last Interglacial
3007 Transition in North America. Geological Society of America Special Paper 270, Boulder,
3008 Colorado, pp. 139-161. <https://doi.org/10.1130/SPE270-p139>.
- 3009 Hicock, S.R., Dreimanis, A., 1992b. Deformation till in the Great Lakes region: implications
3010 for rapid flow along the south-central margin of the Laurentide Ice Sheet. Canadian Journal of
3011 Earth Sciences 29, 1565-1579.
- 3012 Hill, P., Aksu, A.E., Piper, D.J.W., 1982. The deposition of thin bedded subaqueous debris
3013 flow deposits, in: Saxov, S., Nieuwenhuis, J.K. (Eds.), Marine Slides and Other Mass
3014 Movements. Plenum Press, New York, pp. 273-287.
- 3015 Hodgson, D.M., Brooks, H.L., Ortiz-Karpf, A., Sychala, Y., Lee, D.R., Jackson, C.A.-L.,
3016 2018. Entrainment and abrasion of megaclasts during submarine landsliding and their impact
3017 on flow behaviour, in: Lintern, D.G., Mosher, D.C., Moscardelli, L.G., Bobrowsky, P.T.,
3018 Campbell, C., Chaytor, J.D., Clague, J.J., Georgiopoulou, A., Lajeunesse, P., Normandeau,

- 3019 A., Piper, D.J.W., Scherwath, M., Stacey, C., Turmel, D. (Eds.), Subaqueous Mass
3020 Movements and Their Consequences: Assessing Geohazards, Environmental Implications
3021 and Economic Significance of Subaqueous Landslides. Geological Society, London, Special
3022 Publications 477, 223-240. <https://doi.org/10.1144/SP477.26>.
- 3023 Hoffman, P.F., 2011. A history of Neoproterozoic glacial geology, 1871–1997, in: Arnaud,
3024 E., Halverson, G.P., Shields-Zhou, G. (Eds.), The Geological Record of Neoproterozoic
3025 Glaciations. Geological Society, London, Memoirs 36, pp. 17-37.
3026 <https://doi.org/10.1144/M36.2>
- 3027 Hoffman, P.F., Kaufman, A.J., Halverson, G.P., 1998. Comings and goings of global
3028 glaciations on a Neoproterozoic tropical platform in Namibia. Geological Society of America
3029 Today 8, 1-9.
- 3030 Hoffman, P.F., Halverson, G.P., 2008. Otavi Group of the Northern Platform and the
3031 Northern Margin Zone, in: Miller, R.McG. (Ed.), The Geology of Namibia. Neoproterozoic to
3032 Lower Paleozoic, vol. 2. Geological Survey of Namibia, Windhoek, pp. 13.69-13.136.
- 3033 Hoffman, P.F., Calver, C.R., Halverson, G.P., 2009. Cottons breccia of King Island,
3034 Tasmania: Glacial or non-glacial, Cryogenian or Ediacaran? Precambrian Research 172,
3035 311-322. <https://doi.org/10.1016/j.precamres.2009.06.003>.
- 3036 Hoffman, P.F., Halverson, G.P., Schrag, D.P., Higgins, J.A., Domack, E.W., Macdonald,
3037 F.A., Pruss, S.B., Blättler, C.L., Crockford, P.W., Hodgkin, E.B., Bellefroid, E.J., Johnson,
3038 B.W., Hodgskiss, M.S.W., Lamothe, K.G., LoBianco, S.J.C., Busch, J.F., Howes, B.J.,

- 3039 Greenman, J.W., Nelson, L.L., 2021. Snowballs in Africa: Sectioning a long-lived
3040 Neoproterozoic carbonate platform and its bathyal foreslope (NW Namibia). *Earth-Science*
3041 *Reviews* 219, 103616. <https://doi.org/10.1016/j.earscirev.2021.103616>.
- 3042 Hollick, A., 1930. *The Upper Cretaceous Floras of Alaska*, U.S. Geological Survey
3043 Professional Paper 159, 214 pp (including plates).
- 3044 Holme, C., Gkinis, V., Lanzky, M., Morris, V., Olesen, M., Thayer, A., Vaughn, B.H.,
3045 Vinther, B.M., 2019. Varying regional $\delta^{18}\text{O}$ -temperature relationship in high-resolution stable
3046 water isotopes from east Greenland. *Climate of the Past* 15, 893–912.
3047 <https://doi.org/10.5194/cp-15-893-2019>.
- 3048 Hoppe, G., 1981. Glacial traces on the Island of Hopen, Svalbard: A correction. *Geografiska*
3049 *annaler* 63A, 67-68.
- 3050 Horan, K., 2015. Falkland Islands (Islas Malvinas) in the Permo-Carboniferous. Springer
3051 *Earth System Sciences*, Springer, Cham, pp. 45-70. [https://doi.org/10.1007/978-3-319-08708-](https://doi.org/10.1007/978-3-319-08708-5_4)
3052 [5_4](https://doi.org/10.1007/978-3-319-08708-5_4).
- 3053 Hore, S.B., Hill, S.M., Alley, N.F., 2020. Early Cretaceous glacial environment and
3054 paleosurface evolution within the Mount Painter Inlier, northern Flinders Ranges, South
3055 Australia. *Australian Journal of Earth Sciences* 67, 1117-1160.
3056 <https://doi.org/10.1080/08120099.2020.1730963>.

- 3057 Hu, W., McSaveney, M.J., 2018. A polished and striated pavement formed by a rock
3058 avalanche in under 90 s mimics a glacially striated pavement. *Geomorphology* 320, 154-161.
- 3059 Huber, H., Koeberl, C., McDonald, I., Reimold, W.U., 2001. Geochemistry and petrology of
3060 Witwatersrand and Dwyka diamictites from South Africa: search for an extraterrestrial
3061 component. *Geochimica et Cosmochimica Acta* 65, 2007-2016.
- 3062 Hume, J.D., 1963. Floating sand and pebbles near Barrow, Alaska. *Geological Society of*
3063 *America, Memoir* 73, Abstracts for 1962, New York, p. 176.
- 3064 Hume, J.D., Schalk, M., 1964. The effects of ice-push in Arctic beaches. *American Journal of*
3065 *Science* 262, 267-273.
- 3066 Iltad, T., De Blasio, F.V., Elverhøi, A., Harbitz, C.B., Engvik, L., Longvad, O., Marr, J.G.,
3067 2004. On the frontal dynamics and morphology of submarine debris flows. *Marine Geology*
3068 213, 481–497.
- 3069 Imbo, Y., De Batist, M., Canals, M., Prieto, M.J., Baraza, J., 2003. The Gebra Slide: a
3070 submarine slide on the Trinity Peninsula Margin, Antarctica. *Marine Geology* 193, 235–252.
- 3071 Immonen, N., 2013. Surface microtextures of ice-rafted quartz grains revealing glacial ice
3072 in the Cenozoic Arctic. *Palaeogeography, Palaeoclimatology, Palaeoecology* 374, 293-302.
- 3073 Isbell, J.L., 2010. Environmental and paleogeographic implications of glaciotectonic
3074 deformation of glaciomarine deposits within Permian strata of the Metschel Tillite, southern

- 3075 Victoria Land, Antarctica, in: López-Gamundí, O.R., Buatois, L.A. (Eds.), Late Paleozoic
3076 Glacial Events and Postglacial Transgressions in Gondwana. Geological Society of America
3077 Special Paper 468, pp. 81–100. [https://doi.org/10.1130/2010.2468\(03\)](https://doi.org/10.1130/2010.2468(03)).
- 3078 Isbell, J.L., Miller, M.F., Babcock, L.E., Hasiotis, S.T., 2001. Ice-marginal environment and
3079 ecosystem prior to initial advance of the late Palaeozoic ice sheet in the Mount Butters area of
3080 the central Transantarctic Mountains, Antarctica. *Sedimentology* 48, 953-970.
- 3081 Isbell, J.L., Cole, D.I., Catuneanu, O., 2008. Carboniferous-Permian glaciation in the main
3082 Karoo Basin, South Africa: Stratigraphy, depositional controls, and glacial dynamics, in:
3083 Fielding, C.R., Frank, T.D., Isbell, J.L. (Eds.), *Resolving the Late Paleozoic Ice Age in Time
3084 and Space*. Geological Society of America Special Paper 441, pp. 71–82.
3085 [https://doi.org/10.1130/2008.2441\(05\)](https://doi.org/10.1130/2008.2441(05)).
- 3086 Isbell, J.L., Henry, L.C., Gulbranson, E., Limarino, C.O., Fraiser, M.L., Koch, Z.J., Ciccioli,
3087 P.L., Dineen, A.A., 2012. Glacial paradoxes during the late Paleozoic ice age: Evaluating the
3088 equilibrium line altitude as a control on glaciation. *Gondwana Research* 22, 1–19.
- 3089 Isbell, J.L., Henry, L.C., Reid, C.M, Fraiser, M.L., 2013. Sedimentology and palaeoecology
3090 of lonestone-bearing mixed clastic rocks and cold-water carbonates of the Lower Permian
3091 basal beds at Fossil Cliffs, Maria Island, Tasmania (Australia): Insight into the initial decline
3092 of the late Palaeozoic ice age, in: Gasiewicz, A., Słowakiewicz, M. (Eds.), *Palaeozoic
3093 Climate Cycles: Their Evolutionary and Sedimentological Impact*. Geological Society,
3094 London, Special Publications 376, pp. 307–341. <https://doi.org/10.1144/SP376.2>.

- 3095 Isbell, J.L., Biakov, A.S., Vedernikov, I.L., Davydov, V.I., Gulbranson, E.L., Fedorchuk,
3096 N.D., 2016. Permian diamictites in northeastern Asia: Their significance concerning
3097 the bipolarity of the late Paleozoic ice age. *Earth-Science Reviews* 154, 279–300.
3098 <https://doi.org/10.1016/j.earscirev.2016.01.007>.
- 3099 Isbell, J.L., Vesely, F.F., Rosa, E.L.M., Pauls, K.N., Fedorchuk, N.D., Ives, L.R.W., McNall,
3100 N.B., Litwin, S.A., Borucki, M.K., Malone, J.E., Kusick, A.R., 2021. Evaluation of physical
3101 and chemical proxies used to interpret past glaciations with a focus on the late Paleozoic Ice
3102 Age. *Earth-Science Reviews* 221, 103756. <https://doi.org/10.1016/j.earscirev.2021.103756>.
- 3103 Isotta, C.A.L., Rocha-Campos, A.C., Yoshida, R., 1969. Striated pavement of the Upper Pre-
3104 Cambrian glaciation in Brazil. *Nature* 222, 466-468.
- 3105 Iverson, N.R., 1991. Morphology of glacial striae: Implications for abrasion of glacier beds
3106 and fault surfaces. *GSA Bulletin* 103, 1308-1316.
- 3107 Ives, L.R.W., Isbell, J.L., 2021. A lithofacies analysis of a South Polar glaciation in the Early
3108 Permian: Pagoda Formation, Shackleton Glacier region, Antarctica. *Journal of Sedimentary*
3109 *Research* 91, 611–635. <https://doi.org/10.2110/jsr.2021.004>.
- 3110 Jackson, T.A., 1965. Power-spectrum analysis of two “varved” argillites in the Huronian
3111 Cobalt Series (Precambrian) of Canada. *Journal of Sedimentary Petrology* 35, 877-886.
- 3112 Jansa, L.F., Carozzi, A.V., 1970. Exotic pebbles in La Salle limestone (Upper
3113 Pennsylvanian), La Salle, Illinois. *Journal of Sedimentary Petrology* 40, 688-694.

- 3114 John, B.S., 1979. The great ice age: Permo-Carboniferous, in: John, B.S. (Ed.), *The Winters*
3115 *of the World*. Davies and Charles, Newton Abbot, pp.154-172.
- 3116 Johnson, M.R., Van Vuuren, C.J., Visser, J.N.J., Cole, D.I., Wickens, H.D.V., Christie,
3117 A.D.M., Roberts, D.L., 1997. The foreland Karoo Basin, South Africa, in: Selley, R.C. (Ed.),
3118 *African Basins, Sedimentary Basins of the World 3*. Elsevier, Amsterdam, pp. 269-317.
- 3119 Kalińska-Nartiša, E., Woronko, B., Ning, W., 2017. Microtextural inheritance on quartz sand
3120 grains from Pleistocene periglacial environments of the Mazovian Lowland, Central Poland.
3121 *Permafrost and Periglacial Processes* 28, 741-756. <https://doi.org/10.1002/ppp.1943>.
- 3122 Kalińska, E., Lamsters, K., Karušs, J., Krievāns, M., Rečs, A., Ješkis, J., 2022. Does glacial
3123 environment produce glacial mineral grains? Pro- and supra-glacial Icelandic sediments in
3124 microtextural study. *Quaternary International* 617, 101-111..
3125 <https://doi.org/10.1016/j.quaint.2021.03.029>.
- 3126 Karlsrud, K., Edgers, L., 1982. Some aspects of slope stability, in: Saxov, S., Nieuwenhuis, J.
3127 K. (Eds.), *Marine Slides and Other Mass Movements*. Plenum Press, New York, pp. 61-81.
- 3128 Keiser, L.J., Soreghan, G.S., Kowalewski, M., 2015. Use of quartz microtextural analysis to
3129 assess possible proglacial deposition for the Pennsylvanian-Permian Cutler Formation
3130 (Colorado, U.S.A.). *Journal of Sedimentary Research* 85, 1310-1322.

- 3131 Keller, M., Hinderer, M., Al-Ajmi, H., Rausch, R., 2011. Palaeozoic glacial depositional
3132 environments of SW Saudi Arabia: process and product. Geological Society, London, Special
3133 Publications 354, 129-152. <https://doi.org/10.1144/SP354.8> .
- 3134 Kennedy, K., Eyles, N., 2019. Subaqueous debrites of the Grand Conglomérat Formation,
3135 Democratic Republic of Congo: A model for anomalously thick Neoproterozoic: “Glacial”
3136 diamictites. *Journal of Sedimentary Research* 89, 935–955.
3137 <https://doi.org/10.2110/jsr.2019.51>.
- 3138 Kennedy, K., Eyles, N., 2021. Syn-rift mass flow generated ‘tectonofacies’ and
3139 ‘tectonosequences’ of the Kingston Peak Formation, Death Valley, California, and their
3140 bearing on supposed Neoproterozoic panglacial climates. *Sedimentology* 68, 352-381.
3141 <https://doi.org/10.1111/sed.12781>.
- 3142 Kennedy, K., Eyles, N., Broughton, D., 2019. Basinal setting and origin of thick (1.8 km)
3143 mass-flow dominated Grand Conglomérat diamictites, Kamoia, Democratic Republic of
3144 Congo: Resolving climate and tectonic controls during Neoproterozoic glaciations.
3145 *Sedimentology* 66, 556–589. <https://doi.org/10.1111/sed.12494>.
- 3146 Kent, D.V., Muttoni, G., 2020. Pangea B and the Late Paleozoic ice age. *Palaeogeography,*
3147 *Palaeoclimatology, Palaeoecology* 553, 109753.
3148 <https://doi.org/10.1016/j.palaeo.2020.109753>.
- 3149 Kerr, R.A., 1993. Fossils tell of mild winters in an ancient hothouse. *Science* 261, 682.

3150 Kerr, R.A., 2008. More climate wackiness in the Cretaceous supergreenhouse? *Science* 319,
3151 145.

3152 Kilfeather, A.A., Ó Cofaigh, C., Dowdeswell, J.A., van der Meer, J.J.M., Evans, D.J.A.,
3153 2010. Micromorphological characteristics of glacimarine sediments: implications for
3154 distinguishing genetic processes of massive diamicts. *Geo-Marine Letters* 30, 77–97 .
3155 <https://doi.org/10.1007/s00367-009-0160-8>.

3156 Kim, S.B., Chough, S.K., Chun, S.S., 1995. Bouldery deposits in the lowermost part of the
3157 Cretaceous Kyokpori Formation, SW Korea: cohesionless debris flows and debris falls on a
3158 steep-gradient delta slope. *Sedimentary Geology* 98, 97-119.
3159 [https://doi.org/10.1016/0037-0738\(95\)00029-8](https://doi.org/10.1016/0037-0738(95)00029-8).

3160 Klein, T., Ramon, U., 2019. Stomatal sensitivity to CO₂ diverges between angiosperm and
3161 gymnosperm tree species. *Functional Ecology* 33, 1411-1424.
3162 <https://doi.org/10.1111/1365-2435.13379>.

3163 Kneller, B.C., Edwards, D., McCaffrey, W.D., Moore, R., 1991. Oblique reflection of
3164 turbidity currents. *Geology* 14, 250-252.

3165 Kneller, B., Milana, J.P., Buckee, C., al Ja'aidi, O., 2004. A depositional record of
3166 deglaciation in a paleofjord (Late Carboniferous [Pennsylvanian] of San Juan Province,
3167 Argentina): The role of catastrophic sedimentation. *GSA Bulletin* 116, 348–367.
3168 <https://doi.org/10.1130/B25242.1>.

- 3169 Kneller, B., Dykstra, M., Fairweather, L., Milana, J.P., 2016. Mass-transport and slope
3170 accommodation: Implications for turbidite sandstone reservoirs. AAPG Bulletin 100,
3171 213-235. <https://doi.org/10.1306/09011514210>.
- 3172 Kochhann, M.V.L., Cagliari, J., Kochhann, K.G.D., Franco, D.R., 2020. Orbital and
3173 millennial-scale cycles paced climate variability during the Late Paleozoic Ice Age in the
3174 southwestern Gondwana. *Geochemistry, Geophysics, Geosystems* 21, e2019GC008676.
3175 <https://doi.org/10.1029/2019GC008676>.
- 3176 Kohn, M.W., 2010. Carbon isotope compositions of terrestrial C3 plants as indicators of
3177 (paleo)ecology and (paleo)climate. *PNAS* 107, 19691-19695.
3178 <https://doi.org/10.1073/pnas.1004933107>.
- 3179 Komar, P.D., 1970. The competence of turbidity current flow. *GSA Bulletin* 81, 1555-1562.
- 3180 Korstgård, J.A., Nielsen, O.B., 1989. Provenance of dropstones in Baffin Bay and Labrador
3181 Sea, Leg 105, in: Srivastava, S.P., Arthur, M.L, Clement, B., Aksu, A., Baldauf, J.,
3182 Bohrmann, G., Busch, W., Cederberg, T., Cremer, M., Dadey, K., De Vernal, A., Firth, J.,
3183 Hall, F., Head, M., Hiscott, R., Jarrard, R., Kaminski, M., Lazarus, D., Monjanel, A.L.,
3184 Nielsen, O.B., Stein, R., Thiebault, F., Zachos, J., Zimmerman, H. (Eds.), *Proceedings of the*
3185 *Ocean Drilling Program, Scientific Results 105*. Texas A&M University, College Station, pp.
3186 65-69. <https://doi.org/10.2973/odp.proc.sr.105.200.1989>.
- 3187 Krüger, J., 1984. Clasts with stoss-lee form in lodgement tills: a discussion. *Journal of*
3188 *Glaciology* 30:241-243.

- 3189 Kuenen, P.H., 1964. Deep sea sands and ancient turbidites, in: Bouma, A.H., Brouwer, A.
3190 (Eds.), *Turbidites*. Elsevier Publ., Amsterdam, pp. 3-33.
- 3191 Kuhn, T.S., 1970. Science does not develop by accumulation (excerpts from *The Structure of*
3192 *Scientific Revolutions*), in: Neurath, O. (Ed.), *International Encyclopedia of Unified Science*
3193 *2*. The University of Chicago Press, Chicago, pp. 219-228.
- 3194 Kulling, O., 1951. Spår av Varangeristiden i Norrbotten. SGU C503, Stockholm, 44 pp.
- 3195 Kumar, P.C., Omosanya, K.O., Eruteya, O.E., Sain, K., 2021. Geomorphological
3196 characterization of basal flow markers during recurrent mass movement: A case study from
3197 the Taranaki Basin, offshore New Zealand. *Basin Research*, 00:1–25.
3198 <https://doi.org/10.1111/bre.12560>.
- 3199 Kurtz, D.D., Anderson, J.B., 1979. Recognition and sedimentologic description of recent
3200 debris flow deposits from the Ross and Weddel Seas, Antarctica. *Journal of Sedimentary*
3201 *Petrology* 49, 1159-1170.
- 3202 Kut, A.A., Woronko, B., Spektor, V.V., Klimova, I.V., 2021. Grain-surface microtextures in
3203 deposits affected by periglacial conditions (Abalakh High-Accumulation Plain, Central
3204 Yakutia, Russia). *Micron* 146, 103067. <https://doi.org/10.1016/j.micron.2021.103067>.
- 3205 Kyser, K.T., 1986. Stable isotope variations in the mantle, in: Valley, J.W., Taylor, H.P.,
3206 O'Neil, J.R. (Eds.), *Stable Isotopes in High Temperature Geologic Processes*. Reviews in

- 3207 Mineralogy and Geochemistry 16, De Gruyter, Washington, pp. 141–164.
3208 <https://doi.org/10.1515/9781501508936>.
- 3209 LaMarche, V.C. Jr., 1969. Environment in relation to age of Bristlecone pines. *Ecology* 50,
3210 53-59. <https://doi.org/10.2307/1934662>.
- 3211 Lamb, M.P., 2008. Formation of Amphitheater-Headed Canyons (Ph.D. thesis). University of
3212 California, Berkeley, 311 pp.
- 3213 Lamb, M.P., Mackey, B.H., Farley, K.A., 2014. Amphitheater-headed canyons formed by
3214 megaflooding at Malad Gorge, Idaho. *PNAS* 111, 57-62.
3215 <https://doi.org/10.1073/pnas.1312251111>.
- 3216 Lang, J., Le Heron, D.P., Van den Berg, J.H., Winsemann, J., 2020. Bedforms and
3217 sedimentary structures related to supercritical flows in glacial settings. *Sedimentology* 68,
3218 1539-1579. <https://doi.org/10.1111/sed.12776>.
- 3219 Larsen, V., Steel, R.J., 1978. The sedimentary history of a debris-flow dominated, Devonian
3220 alluvial fan—a study of textural inversion. *Sedimentology* 25, 37-59.
- 3221 Lascelles, D.F., Lowe, R.J., 2021. Tsunami deposits on a Paleoproterozoic unconformity?
3222 The 2.2 Ga Yerrida marine transgression on the northern margin of the Yilgarn
3223 Craton, Western Australia. *Journal of Marine Science and Engineering* 9, 213.
3224 <https://doi.org/10.3390/jmse9020213>.

- 3225 Lawson, D.E., 1979. A comparison of the pebble orientations in ice and deposits of the
3226 Matanuska Glacier, Alaska. *Journal of Geology* 87, 629-645.
- 3227 Le Blanc Smith, G., Eriksson, K.A., 1979. A fluvio-glacial and glaciolacustrine deltaic
3228 depositional model for Permo-Carboniferous coals of the northeastern Karoo Basin, South
3229 Africa. *Palaeogeography, Palaeoclimatology, Palaeoecology* 27, 67-84.
- 3230 Le Heron, D.P., 2010. Interpretation of Late Ordovician glaciogenic reservoirs from 3-D
3231 seismic data: an example from the Murzuq Basin, Libya. *Geological Magazine* 147, 28-41.
- 3232 Le Heron, D.P., 2018. An exhumed Paleozoic glacial landscape in Chad. *Geology* 46, 91-94.
3233 <https://doi.org/10.1130/G39510.1>.
- 3234 Le Heron, D.P., Vandyk, T., 2019. A slippery slope for Cryogenian diamictites? *Depositional*
3235 *Record* 5, 306-321. <https://doi.org/10.1002/dep2.67>.
- 3236 Le Heron, D., Sutcliffe, O., Bourqig, K., Craig, J., Visentin, C., Whittington, R., 2004.
3237 Sedimentary architecture of Upper Ordovician tunnel valleys, Gargaf Arch, Libya:
3238 Implications for the genesis of a hydrocarbon reservoir. *GeoArabia* 9, 137-160.
- 3239 Le Heron, D.P., Sutcliffe, O.E., Whittington, R.J., Craig, J., 2005. The origins of glacially
3240 related soft-sediment deformation structures in Upper Ordovician glaciogenic rocks:
3241 implication for ice-sheet dynamics. *Palaeogeography, Palaeoclimatology, Palaeoecology* 218,
3242 75-103.

- 3243 Le Heron, D.P., Craig, J., Sutcliffe, O., Whittington, R., 2006. Late Ordovician glaciogenic
3244 reservoir heterogeneity: an example from the Murzuq Basin, Libya. *Marine and Petroleum*
3245 *Geology* 23, 655-677.
- 3246 Le Heron, D.P., Armstrong, H.A., Wilson, C., Howard, J.P., Gindre, L., 2010. Glaciation and
3247 deglaciation of the Libyan Desert: The Late Ordovician record. *Sedimentary Geology* 223,
3248 100-125. <https://doi.org/10.1016/j.sedgeo.2009.11.002>.
- 3249 Le Heron, D.P., Busfield, M.E., Collins, A.S., 2014. Bolla Bollana boulder beds: A
3250 Neoproterozoic trough mouth fan in South Australia? *Sedimentology* 61, 978–995.
3251 <https://doi.org/10.1111/sed.12082>.
- 3252 Le Heron, D.P., Tofaif, S., Vandyk, T., Ali, D.O., 2017. A diamictite dichotomy: Glacial
3253 conveyor belts and olistostromes in the Neoproterozoic of Death Valley, California, USA.
3254 *Geology* 45, 31-34.
- 3255 Le Heron, D.P., Tofaif, S., Melvin, J., 2018a. The Early Palaeozoic glacial deposits of
3256 Gondwana: overview, chronology, and controversies, in: Menzies, J., van der Meer, J.J.M.
3257 (Eds.), *Past Glacial Environments*, second ed. Elsevier, Amsterdam, pp. 47-73.
3258 <https://doi.org/10.1016/B978-0-08-100524-8.00002-6>.
- 3259 Le Heron, D.P., Vandyk, T.M., Wu, G., Li, M., 2018b. New perspectives on the Luoquan
3260 Glaciation (Ediacaran Cambrian) of North China. *The Depositional Record* 4, 274-292.
3261 <https://doi.org/10.1002/dep2.46>.

- 3262 Le Heron, D.P., Vandyk, T.M., Kuang, H., Liu, Y., Chen, X., Wang, Y., Yang, Z.,
3263 Scharfenberg, L., Davies, B., Shields, G., 2019a. Bird's-eye view of an Ediacaran subglacial
3264 landscape. *Geology* 47, 705–709. <https://doi.org/10.1130/G46285.1>.
- 3265 Le Heron, D.P., Dietrich, P., Busfield, M.E., Kettler, C., Bermanschläger, S., Grasemann, B.,
3266 2019b. Scratching the surface: footprint of a late Carboniferous ice sheet. *Geology* 47, 1034-
3267 1038. <https://doi.org/10.1130/G46590.1>.
- 3268 Le Heron, D.P., Heninger, M., Baal, C., Bestmann, M., 2020. Sediment deformation and
3269 production beneath soft-bedded Palaeozoic ice sheets. *Sedimentary Geology* 408, 105761.
3270 <https://doi.org/10.1016/j.sedgeo.2020.105761>.
- 3271 Le Heron, D.P., Busfield, M.E., Kettler, C., 2021a, Ice-rafted dropstones in “postglacial”
3272 Cryogenian cap carbonates: *Geology* 49, 263–267. <https://doi.org/10.1130/G48208.1>.
- 3273 Le Heron, D.P., Kettler, C., Griffis, N.P., Dietrich, P., Montañez, I.P., Osleger, D.A.,
3274 Hofmann, A, Douillet, G., Mundil, R., 2021b. The Late Palaeozoic Ice Age unconformity in
3275 southern Namibia viewed as a patchwork mosaic. *Depositional Record* 00:1-17.
3276 <https://doi.org/10.1002/dep2.163>.
- 3277 Leask, H.J., Wilson, L., Mitchell, K.L., 2007. Formation of Mangala Valles outflow channel,
3278 Mars: Morphological development and water discharge and duration estimates. *Journal of*
3279 *Geophysical Research* 112, E08003. <https://doi.org/10.1029/2006JE002851>.

- 3280 Legros, F., Cantagrel, J.-M., Devouard, B., 2000. Pseudotachylyte (Frictionite) at the base of
3281 the Arequipa Volcanic landslide deposit (Peru): Implications for emplacement mechanisms.
3282 *Journal of Geology* 108, 601–611.
- 3283 Leonard, J.E., Cameron, B., Pilkey, O.H., Friedman, G.M., 1981. Evaluation of cold-water
3284 carbonates as a possible paleoclimatic indicator. *Sedimentary Geology* 28, 1-28.
- 3285 Liégeois, J.-P., 2006. The Hoggar swell and volcanism, Tuareg shield, Central Sahara:
3286 Intraplate reactivation of Precambrian structures as a result of Alpine convergence.
3287 <http://www.mantleplumes.org/WebpagePDFs/Hoggar.pdf> (accessed 20 March 2021).
- 3288 Limarino, C.O., López-Gamundí, O.R., 2021. Late Paleozoic basins of South America:
3289 Insights and progress in the last decade. *Journal of South American Earth Sciences* 107,
3290 103150. <https://doi.org/10.1016/j.jsames.2020.103150>.
- 3291 Linch, L.D., Dowdeswell, J.A., 2016. Micromorphology of diamicton affected by iceberg-
3292 keel scouring, Scoresby Sund, East Greenland. *Quaternary Science Reviews* 152, 169–196.
3293 <https://doi.org/10.1016/j.quascirev.2016.09.013>.
- 3294 Lindsay, J.F., 1966. Carboniferous subaqueous mass-movement in the Manning-Macleay
3295 Basin, Kempsey, New South Wales. *Journal of Sedimentary Petrology* 36, 719-732.
- 3296 Lindsay, J.F., 1968. The development of clast fabric in mudflows. *Journal of Sedimentary*
3297 *Petrology* 38, 1242-1253.

- 3298 Lindsay, J.F., 1970a. Depositional environment of Paleozoic glacial rocks in the Central
3299 Transantarctic Mountains. *GSA Bulletin* 81, 1149-1171.
- 3300 Lindsay, J.F., 1970b. Clast fabrics of till and its development. *Journal of Sedimentary*
3301 *Petrology* 40, 629-641.
- 3302
- 3303 Lindsay, J.F., Summerson, C.H., Barrett, P.J., 1970. A long-axis clast fabric comparison of
3304 Squantum "Tillite," Massachusetts and the Gowganda Formation, Ontario. *Journal of*
3305 *Sedimentary Petrology* 40, 475-479.
- 3306 Lindsey, D.A., 1969. Glacial sedimentology of the Precambrian Gowganda Formation,
3307 Ontario, Canada. *GSA Bulletin* 80, 1685-1701 and plate section.
- 3308 Liu, E., Wang, H., Pan, S., Qin, C., Jiang, P., Chen, S., Yan, D., Lü, X., Jing, Z.. 2021.
3309 Architecture and depositional processes of sublacustrine fan systems in structurally active
3310 settings: An example from Weixinan Depression, northern South China Sea. *Marine and*
3311 *Petroleum Geology* 134, 105380. <https://doi.org/10.1016/j.marpetgeo.2021.105380>.
- 3312 Liu, Y., Gastaldo, R.A., 1992. Characteristics and provenance of log-transported gravels in a
3313 Carboniferous channel deposit. *Journal of Sedimentary Petrology* 62, 1072-1083.
- 3314 Loope, D.B., Burberry, C.M., 2018. Sheeting joints and polygonal patterns in the Navajo
3315 Sandstone, southern Utah: Controlled by rock fabric, tectonic joints, buckling, and gullyng.
3316 *Geosphere* 14, 1818–1836. <https://doi.org/10.1130/GES01614.1>.

- 3317 López-Gamundí, O.R., 2010. Transgressions related to the demise of the Late Paleozoic Ice
3318 Age: Their sequence stratigraphic context, in: López-Gamundí, O.R., Buatois, L.A. (Eds.),
3319 Late Paleozoic Glacial Events and Postglacial Transgressions in Gondwana. Geological
3320 Society of America Special Paper 468, pp. 1-35. [https://doi.org/10.1130/2010.2468\(01\)](https://doi.org/10.1130/2010.2468(01)).
- 3321 López-Gamundí, O., Sterren, A.F., Cisterna, G.A., 2016. Inter- and intratill boulder
3322 pavements in the Carboniferous Hoyada Verde Formation of West Argentina: An insight on
3323 glacial advance/retreat fluctuations in Southwestern Gondwana. *Palaeogeography,*
3324 *Palaeoclimatology, Palaeoecology* 447, 29-41. <https://doi.org/10.1016/j.palaeo.2016.01.038>.
- 3325 López-Gamundí, G., Limarino, C.O., Isbell, J.L., Pauls, K., Césari, S.N., Alonso-Muruaga,
3326 P.J., 2021. The late Paleozoic Ice Age along the southwestern margin of Gondwana: Facies
3327 models, age constraints, correlation and sequence stratigraphic framework. *Journal of South*
3328 *American Earth Sciences* 107, 103056. <https://doi.org/10.1016/j.jsames.2020.103056>.
- 3329 Lowe, D.R., 1979. Sediment gravity flows: Their Classification and some Problems of
3330 Application to Natural Flows and Deposits. *SEPM Special Publication* 27, 75-82.
- 3331 Lowe, D.R., 1982. Sediment gravity flows: II. Depositional models with special reference to
3332 the deposits of high-density turbidity currents. *Journal of Sedimentary Petrology* 52, 279-297.
- 3333 Lowe, D.R., 1988. Suspended-load fallout rate as an independent variable in the analysis of
3334 current structures. *Sedimentology* 35, 765-776.

- 3335 Lucchitta, B.K., 2001. Antarctic ice streams and outflow channels on Mars. *Geophysical*
3336 *Research Letters* 28, 403-406.
- 3337 Lundqvist, J., 1979. Morphogenetic classification of glaciofluvial deposits, SGU 767C,
3338 Uppsala, 72 pp.
- 3339 Macdonald, F.A., 2020. Deep-time paleoclimate proxies, *AGU Advances* 1,
3340 e2020AV000244. <https://doi.org/10.1029/2020AV000244>.
- 3341 Macdonald, H.A., Wynn, R.B., Huvenne, V.A.I., Peakall, J., Masson, D.G., Weaver, P.P.E,
3342 McPhail, S.D., 2011. New insights into the morphology, fill, and remarkable longevity (>0.2
3343 m.y.) of modern deep-water erosional scours along the northeast Atlantic margin. *Geosphere*
3344 7, 845-867. <https://doi.org/10.1130/GES00611.1>.
- 3345 Maghfouri, S., Hosseinzadeh. M.R., Lentz, D.R., Choulet, F., 2020. Geological and
3346 geochemical constraints on the Farahabad vent-proximal sub-seafloor replacement SEDEX-
3347 type deposit, Southern Yazd basin, Iran. *Journal of Geochemical Exploration* 209, 106436.
- 3348 Mahaney, W.C., 1987. Pleistocene glaciation on Le Mont Aigoual, Massif Central Français:
3349 Fact or fiction? *Zeitschrift für Geomorphologie* 31, 371-377.
- 3350 Mahaney, W.C., 1990. *Ice on the Equator: Quaternary Geology of Mount Kenya, East Africa.*
3351 Wm Caxton Ltd., Ellison Bay, 386 pp.

- 3352 Mahaney, W.C., 2002. Atlas of Sand Grain Surface Textures and Applications. Oxford
3353 University Press, New York, 237 pp.
- 3354 Maizels, J., 1990a. Raised channel systems as indicators of palaeohydrologic change: a case
3355 study from Oman. *Palaeogeography, Palaeoclimatology, Palaeoecology* 76, 241-277.
- 3356 Maizels, J., 1990b. Long-term palaeochannel evolution during episodic growth of an
3357 exhumed Plio-Pleistocene alluvial fan, Oman, in: Rachocki, A.H., Michael, C. (Eds.),
3358 *Alluvial Fans: A Field Approach*. John Wiley and Sons Ltd., Chichester, pp. 271-304.
- 3359 Major, J.J., 1998. Pebble orientation on large, experimental debris-flow deposits.
3360 *Sedimentary Geology* 117, 151-164. [https://doi.org/10.1016/S0037-0738\(98\)00014-1](https://doi.org/10.1016/S0037-0738(98)00014-1).
- 3361 Major, J.J., Pierson, T.C., Scott, K.M., 2005. Debris flows at Mount St. Helens, Washington,
3362 USA, in: Jakob, M., Hungr, O. (Eds.), *Debris-Flow Hazards and Related Phenomena*.
3363 Praxis/Springer, Berlin/Heidelberg, pp. 685-731.
- 3364 Malahoff, A., Embley, R.W., Fornari, D.J., 1979. Geological observations from alvin of the
3365 continental margin from Baltimore Canyon to Norfolk Canyon. *EOS Transactions, American*
3366 *Geophysical Union* 60, 287.
- 3367 Mangerud, J., Hughes, A.L.C., Sæle, T.H., Svendsen, J.I., 2019. Ice-flow patterns and precise
3368 timing of ice sheet retreat across a dissected fjord landscape in western Norway. *Quaternary*
3369 *Science Reviews* 214, 139-163. <https://doi.org/10.1016/j.quascirev.2019.04.032>.

- 3370 Margold, M., Stokes, C.R., Clark, C.D., 2015. Ice streams in the Laurentide Ice Sheet:
3371 Identification, characteristics and comparison to modern ice sheets. *Earth-Science Reviews*
3372 143, 117-146. <https://doi.org/10.1016/j.earscirev.2015.01.011>.
- 3373 Markgren, M., Lassila, M., 1980. Problems of moraine morphology: Rogen moraine and
3374 Blattnick moraine. *Boreas* 9, 271-274. <https://doi.org/10.1111/j.1502-3885.1980.tb00704.x>.
- 3375 Marshall, J.D., Brooks, J.R., Lajtha, K., 2007. Sources of variation in the stable isotopic
3376 composition of plants, in: Michener, R., Lajtha, K. (Eds.), *Stable Isotopes in Ecology and*
3377 *Environmental Science*, second ed. Blackwell Publishing Ltd., Malden, Oxford, Victoria, pp.
3378 22-60. <https://doi.org/10.1002/9780470691854.ch2>.
- 3379 Martin, H., 1981a. The Late Paleozoic Dwyka Group of the South Kalahari Basin in Namibia
3380 and Botswana, and the subglacial valleys of the Kaokoveld in Namibia, in: Hambrey, M.J.,
3381 Harland, W.B. (Eds.), *Earth's Pre-Pleistocene Glacial Record*. Cambridge University Press,
3382 Cambridge, pp. 61-66.
- 3383 Martin, H., 1981b. The late Palaeozoic Gondwana glaciation. *Geologische Rundschau* 70,
3384 480-496.
- 3385 Martin, H., Porada, H., Walliser, O.H., 1985. Mixtite deposits of the Damara sequence,
3386 Namibia, Problems of interpretation. *Palaeogeography, Palaeoclimatology, Palaeoecology* 51,
3387 159-196.
- 3388 Maslov, A.V., 2010. Glaciogenic and related sedimentary rocks: Main lithochemical

- 3389 features. Communication 1. Late Archean and Proterozoic. *Lithology and Mineral Resources*
3390 45, 377–397. <https://doi.org/10.1134/S0024490210040061>.
- 3391 Matys Grygar, T., 2019. Millennial-scale climate changes manifest Milankovitch combination
3392 tones and Hallstatt solar cycles in the Devonian greenhouse world: Comment. *Geology* 47,
3393 e487. <https://doi.org/10.1130/G46452C.1>.
- 3394 Maxwell, J.C., 1959. Turbidite, tectonic and gravity transport, Northern Appenine Mountains,
3395 Italy. *Bulletin of the American Association of Petroleum Geologists* 43, 2701-2719.
- 3396 Mays, C., Vajda, V., Frank, T.D., Fielding, C.R., Nicoll, R.S., Tevyaw, A.P., McLoughlin, S.,
3397 2020. Refined Permian–Triassic floristic timeline reveals early collapse and delayed recovery
3398 of south polar terrestrial ecosystems. *GSA Bulletin* 132, 1489–1513.
3399 <https://doi.org/10.1130/B35355.1>.
- 3400 McCann, A.M., Kennedy, M.J., 1974. A probable glacio-marine deposit of Late Ordovician –
3401 Early Silurian age from the north central Newfoundland Appalachian Belt. *Geological*
3402 *Magazine* 111, 549-563.
- 3403 McCarroll, D., Rijdsdijk, K.F., 2003. Deformation styles as a key for interpreting glacial
3404 depositional environments. *Journal of Quaternary Science* 18, 473-489.
- 3405 McClure, H.A., 1980. Permian-Carboniferous glaciation in the Arabian Peninsula. *GSA*
3406 *Bulletin* 91, 707-712.

- 3407 McKee, E.D., Crosby, E.J., Berryhill, H.L. Jr., 1967. Flood deposits, Bijou Creek, Colorado,
3408 June 1965. *Journal of Sedimentary Petrology* 37, 829-851.
- 3409 McLoughlin, S., 2011. *Glossopteris* – insights into the architecture and relationships of an
3410 iconic Permian Gondwanan plant. *Journal of the Botanical Society of Bengal* 65, 1-14.
- 3411 Menard, H.W., 1955. Deep-sea channels, topography, and sedimentation. *AAPG Bulletin* 39,
3412 236-255.
- 3413 Meyer, K.S., Young, C.M., Sweetman, A.K., Taylor, J., Soltwedel, T., Bergmann, M., 2016.
3414 Rocky islands in a sea of mud: biotic and abiotic factors structuring deep-sea dropstone
3415 communities. *Marine Ecology Progress Series* 556, 45-57.
3416 <https://doi.org/10.3354/meps11822>.
- 3417 Meyerhoff, A.A., Boucot, A.J., Meyerhoff Hull, D., Dickins, J.M., 1996. Phanerozoic faunal
3418 and floral realms of the Earth: the intercalary relations of the Malvinokaffric and Gondwana
3419 faunal realms with the Tethyan faunal realm. *Geological Society of America, Memoir* 189,
3420 Boulder, 69 pp. <https://doi.org/10.1130/MEM189>.
- 3421 Miall, A.D., 1983. Glaciomarine Sedimentation in the Gowganda Formation (Huronian),
3422 Northern Ontario. *Journal of Sedimentary Petrology* 53, 477-491.
- 3423 Miall, A.D., 1985. Sedimentation on an early Proterozoic continental margin under glacial
3424 influence: the Gowganda Formation (Huronian), Elliot Lake area, Ontario, Canada.
3425 *Sedimentology* 32, 763-788.

- 3426 Middleton, G.V., Hampton, M.A., 1976. Subaqueous sediment transport and deposition by
3427 sediment gravity flows, in: Stanley, D.J., Swift, D.J.P. (Eds.), *Marine Sediment Transport and*
3428 *Environmental Management*. John Wiley, New York, pp. 197-218.
- 3429 Middleton, G.V., Neal, W.J., 1989. Experiments on the thickness of beds deposited by
3430 turbidity currents. *Journal of Sedimentary Petrology* 59, 297-307.
- 3431 Mikhailova, K., Rogov, M.A., Ershova, V.B., Vasileva, K.Y., Pokrovsky, B.G., Baraboshkin,
3432 E.Y., 2021. New data on stratigraphy and distributions of glendonites from the Carolinefjellet
3433 Formation (Middle Aptian – Lower Albian, Cretaceous), Western Spitsbergen. *Stratigraphy*
3434 *and Geological Correlation* 29, 21–35.
- 3435 Miller, M.F., Kneprath, N.E., Cantrill, D.J., Francis, J.E., Isbell, J.L., 2016. Highly
3436 productive polar forests from the Permian of Antarctica. *Palaeogeography,*
3437 *Palaeoclimatology, Palaeoecology* 441, 292-304.
3438 <https://doi.org/10.1016/j.palaeo.2015.06.016>.
- 3439 Mitchell, N.C., 2006. Morphologies of knickpoints in submarine canyons. *GSA Bulletin* 18,
3440 589–605. <https://doi.org/10.1130/B25772.1>.
- 3441 Molén, M.O., 2014. A simple method to classify diamicts by scanning electron microscope
3442 from surface microtextures. *Sedimentology* 61, 2020-2041.
3443 <https://doi.org/10.1111/sed.12127>.

- 3444 Molén, M.O., 2017. The origin of Upper Precambrian diamictites; Northern Norway: A case
3445 study applicable to diamictites in general, *Geologos* 23, 163-181.
3446 <https://doi.org/10.1515/logos-2017-0019>.
- 3447 Molén, M.O., 2021. Field evidence suggests that the Palaeoproterozoic Gowganda Formation
3448 in Canada is non-glacial in origin. *Geologos* 27, 73-91.
3449 <https://doi.org/10.2478/logos-2021-0009>.
- 3450 Molén, M.O., Smit, J.J., 2022. Reconsidering the glaciogenic origin of Gondwana
3451 diamictites, Dwyka Group, South Africa. ***
- 3452 Molnia, B.F. (Ed.), 1983a. *Glacial-Marine Sedimentation*. Plenum Press, New York, preface.
- 3453 Molnia, B.F., 1983b. Subarctic Glacial-Marine Sedimentation: A Model, in: Molnia, B.F.
3454 (Ed.), *Glacial-Marine Sedimentation*. Plenum Press, New York, pp. 95-144.
- 3455 Moncrieff, A.C.M., Hambrey, M.J., 1988. Late Precambrian glacially-related grooved and
3456 striated surfaces in the tillite group of central east Greenland. *Palaeogeography,*
3457 *Palaeoclimatology, Palaeoecology* 65, 183-200.
- 3458 Moncrieff, A.C.M., Hambrey, M.J., 1990. Marginal-marine glacial sedimentation in the Late
3459 Precambrian succession of east Greenland, in: Dowdeswell, J.A., Scource, J.D. (Eds.),
3460 *Glacimarine Environments: Processes and Sediments*. Geological Society, London, Spec.
3461 Publ. 53, pp. 387-410.

- 3462 Montañez, I.P., Poulsen, C.J., 2013. The Late Paleozoic Ice Age: An evolving paradigm.
3463 Annual Review of Earth and Planetary Sciences 41, 629-656.
3464 <https://doi.org/10.1146/annurev.earth.031208.100118>.
- 3465 Montgomery, D.R., 2002. Valley formation by fluvial and glacial erosion. *Geology* 30, 1047-
3466 1050. [https://doi-org.ezp.sub.su.se/10.1130/0091-7613\(2002\)030<1047:VFBFAG>2.0.CO;2](https://doi-org.ezp.sub.su.se/10.1130/0091-7613(2002)030<1047:VFBFAG>2.0.CO;2).
- 3467 Moore, J.G., Clague, D.A., Holcomb, R.T., Lipman, P.W., Normark, W.R., Torres, M.E.,
3468 1989. Prodigious submarine landslides on the Hawaiian Ridge. *Journal of Geophysical*
3469 *Research* 94 (B12), 17465-17484. <https://doi.org/10.1029/JB094iB12p17465>.
- 3470 Moore, J.G., Normark, W.R., Holcomb, R.T., 1994. Giant Hawaiian underwater landslides.
3471 *Science* 264, pp. 46-47.
- 3472 Moore, J.G., Bryan, W.B., Beeson, M.E., Normark, W.R., 1995. Giant blocks in the South
3473 Kona landslide, Hawaii. *Geology* 23, 125-128.
- 3474 Moosdorf, N., Cohen, S., von Hagke, C., 2018. A global erodibility index to represent
3475 sediment production potential of different rock types. *Applied Geography* 101, 36-44.
3476 <https://doi.org/10.1016/j.apgeog.2018.10.010>.
- 3477 Mori, H., Druckenmiller, P.S., Erickson, G.M., 2016. A new Arctic hadrosaurid from the
3478 Prince Creek Formation (lower Maastrichtian) of northern Alaska. *Acta Palaeontologica*
3479 *Polonica* 61, 15-32. <https://doi.org/10.4202/app.00152.2015>.

- 3480 Mörner, N.-A., 2008. Paleoseismicity and Uplift of Sweden. 33 IGC excursion No 11, 109
3481 pp.
- 3482 Morris, S.C., 1985. Polar forests of the past. *Nature* 318, 739.
- 3483 Moscardelli, L., Wood, L., 2016. Morphometry of mass-transport deposits as a predictive
3484 tool. *GSA Bulletin* 128, 47-80. <https://doi.org/10.1130/B31221.1>.
- 3485 Moscardelli, L., Wood, L., Mann, P., 2006. Mass-transport complexes and associated
3486 processes in the offshore area of Trinidad and Venezuela. *AAPG Bulletin* 90, 1059–1088.
3487 <https://doi.org/10.1306/02210605052>.
- 3488 Mottin, T.E., Vesely, F.F., Rodrigues, M.C.N.L., Kipper, F., Souza, P.A., 2018. The paths
3489 and timing of late Paleozoic ice revisited: New stratigraphic and paleo-ice flow
3490 interpretations from a glacial succession in the upper Itararé Group (Paraná Basin, Brazil).
3491 *Palaeogeography, Palaeoclimatology, Palaeoecology* 490, 488-504.
3492 <https://doi.org/10.1016/j.palaeo.2017.11.031>.
- 3493 Mountjoy, E.W., Cook, H.E., Pray, L.C., McDaniel, P.N., 1972. Allochthonous carbonate
3494 debris flow – worldwide indicators of reef complexes, banks or shelf margins, in: McLaren,
3495 D.J., Middleton, G.V. (Eds.), *Stratigraphy and Sedimentology*. 24th International Geological
3496 Congress, Section 6, Montreal, pp. 172-189.
- 3497 Mountjoy, J.J., Howarth, J.D., Orpin, A.R., Barnes, P.M., Bowden, D.A., Rowden, A.A.,
3498 Schimel, A.C.G., Holden, C., Horgan, H.J., Nodder, S.D., Patton, J.R., Lamarche, G.,

3499 Gerstenberger, M., Micallef, A., Pallentin, A., Kane, T., 2018. Earthquakes drive large-scale
3500 submarine canyon development and sediment supply to deep-ocean basins. *Science Advances*
3501 *4*, eaar3748.

3502 Moxness, L.D., Isbell, J.A., Pauls, K.N., Limarino, C.O., Schencman, J., 2018.
3503 Sedimentology of the mid-Carboniferous fill of the Olta paleovalley, eastern Paganzo Basin,
3504 Argentina: Implications for glaciation and controls on diachronous deglaciation in western
3505 Gondwana during the late Paleozoic Ice Age. *Journal of South American Earth Sciences* *84*,
3506 127-148. <https://doi.org/10.1016/j.jsames.2018.03.015>.

3507 Mustard, P.S., Donaldson, J.A., 1987a. Early Proterozoic ice-proximal glaciomarine
3508 deposition: The Lower Gowganda Formation at Cobalt, Ontario, Canada. *GSA Bulletin* *98*,
3509 373-387.

3510 Mustard, P.S., Donaldson, J.A., 1987b. Substrate quarrying and subglacial till deposition by
3511 Early Proterozoic ice sheet: evidence from the Gowganda Formation at Cobalt, Ontario,
3512 Canada. *Precambrian Research* *34*, 347-368.

3513 Naugolnykh, S.V., Uranbileg, L., 2018. A new discovery of *Glossopteris* in southeastern
3514 Mongolia as an argument for distant migration of Gondwanan plants. *Journal of Asian Earth*
3515 *Sciences* *154*, 142-148. <https://doi.org/10.1016/j.jseaes.2017.11.039>.

3516 Newell, N.D., 1957. Supposed Permian tillites in northern Mexico are submarine slide
3517 deposits. *Bulletin of the Geological Society of America* *68*, 1569-1576.

- 3518 Newton, A., Huuse, M., Brocklehurst, S., 2016. Buried iceberg scours reveal reduced North
3519 Atlantic Current during the stage 12 deglacial. *Nature Communications* 7, 10927.
3520 <https://doi.org/10.1038/ncomms10927>.
- 3521 Nissen, S.E., Haskell, N.L., Steiner, C.T., Coterill, K.L., 1999. Debris flow outrunner blocks,
3522 glide tracks, and pressure ridges identified on the Nigerian continental slope using 3-D
3523 seismic coherency. *Leading Edge* 18, 595–599.
- 3524 Normandeau, A., Lajeunesse, P., St-Onge, G., 2015. Submarine canyons and channels in the
3525 Lower St. Lawrence Estuary (Eastern Canada): Morphology, classification and recent
3526 sediment dynamics. *Geomorphology* 241, 1-18.
3527 <https://doi.org/10.1016/j.geomorph.2015.03.023>.
- 3528 Nugraha, H.D., Jackson A.-L., Johnson, H.D., Hodgson, D.A., 2020. Lateral variability in
3529 strain along the toewall of a mass transport deposit: a case study from the Makassar Strait,
3530 offshore Indonesia. *Journal of the Geological Society* 177, 1261-1279.
3531 <https://doi.org/10.1144/jgs2020-071>.
- 3532 Nwoko, J., Kane, I., Huuse, M., 2020a. Megaclasts within mass-transport deposits: their
3533 origin, characteristics and effect on substrates and succeeding flows. *Geological Society,*
3534 *London, Special Publications* 500, 515-530. <https://doi.org/10.1144/SP500-2019-146>.
- 3535 Nwoko, J., Kane, I., Huuse, M., 2020b. Mass transport deposit (MTD) relief as a control on
3536 post-MTD sedimentation: Insights from the Taranaki Basin, offshore New Zealand. *Marine*
3537 *and Petroleum Geology* 120, 104489. <https://doi.org/10.1016/j.marpetgeo.2020.104489>.

- 3538 Oberbeck, V.R, Marshall, J.B., Aggarwal, H., 1993a. Impacts, tillites and the breakup of
3539 Gondwanaland. *Journal of Geology* 101, 1-19.
- 3540 Oberbeck, V.R, Marshall, J.B., Aggarwal, H., 1993b. Impacts, tillites and the breakup of
3541 Gondwanaland: A reply. *Journal of Geology* 101, 679-683.
- 3542 Oberbeck, V.R., Hörz, F., Bunch, T., 1994. Impacts, tillites, and the breakup of
3543 Gondwanaland: A second reply. *Journal of Geology* 102, 485-489.
- 3544 Ogata, K., Festa, A., Pini, G.A., Pogačnik, Ž., Lucente, C.C., 2019. Substrate deformation and
3545 incorporation in sedimentary mélanges (olistostromes): Examples from the northern
3546 Apennines (Italy) and northwestern Dinarides (Slovenia). *Gondwana Research* 74, 101-125.
- 3547 Ortiz-Karpf, A., Hodgson, D.M., Jackson, C.A.-L., McCaffrey, W.D., 2017. Influence of
3548 seabed morphology and substrate composition on mass-transport flow processes and
3549 pathways: insights from the Magdalena Fan, offshore Colombia. *Journal of Sedimentary
3550 Research* 87, 189-209. <https://doi.org/10.2110/jsr.2017.10>.
- 3551 Ovenshine, A.T., 1970. Observations of iceberg rafting in Glacier Bay, Alaska, and the
3552 identification of ancient ice-rafted deposits. *GSA Bulletin* 81, 891-894.
- 3553 Paris, R., Ramalho, R.S., Madeira, J., Ávila, S., May, S.M., Rixhon, G., Engel, M., Brückner,
3554 H., Herzog, M., Schukraft, G., Perez-Torrado, F.J., Rodriguez-Gonzalez, A., Carracedo, J.C.,
3555 Giachetti, T., 2018. Mega-tsunami conglomerates and flank collapses of ocean island
3556 volcanoes. *Marine Geology* 395, 168-187. <https://doi.org/10.1016/j.margeo.2017.10.004>.

- 3557 Passchier, S., Hansen, M.A., Rosenberg, J., 2021. Quartz grain microtextures illuminate
3558 Pliocene periglacial sand fluxes on the Antarctic continental margin. *Depositional Record* 7,
3559 564-581. <https://doi.org/10.1002/dep2.157>.
- 3560 Pauls, K.N., Isbell, J.L., McHenry, L., Limarino, C.O., Moxness, L.D., Schencman, L.J.,
3561 2019. A paleoclimatic reconstruction of the Carboniferous-Permian paleovalley fill in the
3562 eastern Paganzo Basin: Insights into glacial extent and deglaciation of southwestern
3563 Gondwana. *Journal of South American Earth Sciences* 95, 102236.
3564 <https://doi.org/10.1016/j.jsames.2019.102236>.
- 3565 Pauls, K.N., Isbell, J.L., Limarino, C.O., Alonso-Murauga, P.J., Moxness, L.D., 2021.
3566 Constraining late paleozoic ice extent in the Paganzo basin of western Argentina: Provenance
3567 of the lower Paganzo group strata. *Journal of South American Earth Sciences* 105, 102899.
3568 <https://doi.org/10.1016/j.jsames.2020.102899>.
- 3569 Pazos, P.J., Bettucci, L.S., Loureiro, J., 2008. The Neoproterozoic glacial record in the Río de
3570 la Plata Craton: a critical reappraisal, in: Pankhurst, R.J., Trouw, R.A.J., De Brito Neves,
3571 B.B., de Wit, M.J. (Eds.), *West Gondwana: Pre-Cenozoic Correlations Across the South
3572 Atlantic Region*. Geological Society, London, Special Publications 294, pp. 343–364.
3573 <https://doi.org/10.1144/SP294.18>.
- 3574 Peakall, J., Best, J., Baas, J.H., Hodgson, D.M., Clare, M.A., Talling, P.J., Dorrell, R.M., Lee,
3575 D.R., 2020. An integrated process-based model of flutes and tool marks in deep-water
3576 environments: Implications for palaeohydraulics, the Bouma sequence and hybrid event beds.
3577 *Sedimentology* 67, 1601–1666. <https://doi.org/10.1111/sed.12727>.

- 3578 Pehlivan, V., 2019. Slope Channels on an Active Margin; A 3D Study of the Variability,
3579 Occurrence, and Proportions of Slope Channel Geomorphology in the Taranaki Basin, New
3580 Zealand (M.Sc. thesis). Colorado School of Mines, Golden.
- 3581 Permenter, J.L., Oppenheimer, C., 2007. Volcanoes of the Tibesti massif (Chad, northern
3582 Africa). *Bulletin of Volcanology* 69, 609–626. <https://doi.org/10.1007/s00445-006-0098-x>.
- 3583 Petit, J.P., Laville, E., 1987. Morphology and microstructures of hydroplastic slickensides in
3584 sandstone, in: Jones, M.E., Preston, R.M. (Eds.), *Deformation of Sediments and Sedimentary*
3585 *Rocks*. Geological Society, London, Special Publications 29, pp. 107-121.
- 3586 Pettijohn, F.J., Potter, P.E., 1964. *Atlas and Glossary of Primary Sedimentary Structures*.
3587 Springer-Verlag, New York, 424 pp.
- 3588 Peyrot, D., Playford, G., Mantle, D.J., Backhouse, J., Milne, L.A., Carpenter, R.J., Foster, C.,
3589 Mory, A.J., McLoughlin, S., Vitacca, J., Scibiorski, J., Mack, C.L., Bevan, J., 2019. The
3590 greening of Western Australian landscapes: the Phanerozoic plant record. *Journal of the*
3591 *Royal Society of Western Australia* 102, 52-82.
- 3592 Pickering, K.T., Corregidor, J., 2005. Mass-transport complexes (MTCs) and tectonic control
3593 on basin-floor submarine fans, Middle Eocene, south Spanish Pyrenees. *Journal of*
3594 *Sedimentary Research* 75, 761–783. <https://doi.org/10.2110/jsr.2005.062>.
- 3595 Pickering, K.T., Hiscott, R.N., 2015. *Deep Marine Systems: Processes, Deposits,*
3596 *Environments, Tectonics and Sedimentation*. John Wiley and Sons, Oxford, 672 pp.

- 3597 Pickering, K.T., Underwood, M.B., Taira, A., 1992. Open-ocean to trench turbidity-current
3598 flow in the Nankai Trough: flow collapse and reflection. *Geology* 20, 1099-1102.
- 3599 Pierson, T.C., Janda, R.J., Thouret, J.-C., Borrero, A.C., 1990. Perturbation and melting of
3600 snow and ice by the 13 November 1985 eruption of Nevado del Ruiz, Colombia, and
3601 consequent mobilization, flow and deposition of lahars. *Journal of Volcanology and
3602 Geothermal Research* 41, 17-66.
- 3603 Piotrowski, J.A., Mickelson, D.M., Tulaczyk, S. Krzyszkowski, D., Junge, F.W., 2001. Were
3604 deforming subglacial beds beneath past ice sheets really widespread? *Quaternary International*
3605 86, 139–150.
- 3606 Piotrowski, J.A., Mickelson, D.M., Tulaczyk, S. Krzyszkowski, D., Junge, F.W., 2002. Reply
3607 to the comments by G.S. Boulton, K.E. Dobbie, S. Zatsepin on: Deforming soft beds under
3608 ice sheets: how extensive were they? *Quaternary International* 97-98, 173-177.
- 3609 Piotrowski, J.A., Larsen, N.K., Junge, F.W., 2004. Reflections on soft subglacial beds as a
3610 mosaic of deforming and stable spots. *Quaternary Science Reviews* 23, 993–1000.
- 3611 Piper, D.J.W., Cochonat, P., Morrison, M.L., 1999. The sequence of events around the
3612 epicentre of the 1929 Grand Banks earthquake: initiation of debris flows and
3613 turbidity current inferred from sidescan sonar. *Sedimentology* 46, 79–97.

- 3614 Pisarska-Jamrózy, M., van Loon, A.J.T., Bronikowska, M., 2018. Dumpstones as records of
3615 overturning ice rafts in a Weichselian proglacial lake (Rügen Island, NE Germany).
3616 *Geological Quarterly* 62, 917-924. <http://dx.doi.org/10.7306/gq.1448>.
- 3617 Plafker, G., Richter, D.H., Hudson, T., 1977. Reinterpretation of the origin of inferred
3618 Tertiary tillite in the northern Wrangell Mountains, Alaska. U.S. Geological Survey Circular
3619 751-B, B52-B54.
- 3620 Plescia, J.B., 2003. Cerberus Fossae, Elysium, Mars: a source for lava and water. *Icarus* 164,
3621 79–95.
- 3622 Plumstead, E.P., 1964. Palaeobotany of Antarctica, in: Adie, Raymond J. (Ed.), *Antarctic*
3623 *Geology*. North-Holland Publ. Co., Amsterdam, pp. 643-652.
- 3624 Porter, A.S., Yiotis, C., Montañez, I.P., McElwain, J.C., 2017. Evolutionary differences in
3625 $\Delta^{13}\text{C}$ detected between spore and seed bearing plants following exposure to a range of
3626 atmospheric $\text{O}_2:\text{CO}_2$ ratios; implications for paleoatmosphere reconstruction. *Geochimica et*
3627 *Cosmochimica Acta* 213, 517–533. <https://doi.org/10.1016/j.gca.2017.07.007>.
- 3628 Posamentier, H.W., Kolla, V., 2003. Seismic geomorphology and stratigraphy of depositional
3629 elements in deep-water settings. *Journal of Sedimentary Research* 73, 367-388.
- 3630 Postma, G., Nemeč, W., Kleinspehn K.L., 1988. Large floating clasts in turbidites: a
3631 mechanism for their emplacement. *Sedimentary Geology* 58, 47-61.

- 3632 Powell, R.D., 1990. Glacimarine processes at grounding-line fans and their growth to ice-
3633 contact deltas, in: Dowdeswell, J.A., Scource, J.D. (Eds.), *Glacimarine Environments:*
3634 *Processes and Sediments*. Geological Society, London, Special Publications 53, pp. 53-73.
- 3635 Prasicek, G., Otto, J.-C., Montgomery, D.R., Schrott, L., 2014. Multi-scale curvature for
3636 automated identification of glaciated mountain landscapes. *Geomorphology* 209, 53–65.
3637 <https://doi.org/10.1016/j.geomorph.2013.11.026>.
- 3638 Price, P.H., 1932. Erratic boulders in Sewell Coal of West Virginia. *Journal of Geology* 40,
3639 62-73.
- 3640 Prior, D.B., Coleman, J.M., Bornhold, B.D., 1982. Results of known seafloor instability
3641 event. *Geo-Marine Letters* 2, 117-122.
- 3642 Procter, J.N., Zernack, A.V., Cronin, S.J., 2021. Computer simulation of a volcanic debris
3643 avalanche from Mt. Taranaki, New Zealand, in: Roverato, M., Dufresne, A., Procter, J.
3644 (Eds.), *Volcanic Debris Avalanches*. *Advances in Volcanology*. Springer, Cham, pp. 281-310.
3645 https://doi.org/10.1007/978-3-030-57411-6_11.
- 3646 Prothero, D.R., Dott, R.H. Jr., 2003. *Evolution of the Earth*, seventh ed. McGraw-Hill, New
3647 York.
- 3648 Puga Bernabéu, Á., Webster, J.M., Beaman, R.J., Thran, A., López Cabrera, J., Hinestrosa,
3649 G., Daniell, J., 2020. Submarine landslides along the mixed siliciclastic carbonate margin of
3650 the great barrier reef (offshore Australia), in: Ogata, K., Festa, A., Pini, G.A. (Eds.),

- 3651 Submarine Landslides: Subaqueous Mass Transport Deposits from Outcrops to Seismic
3652 Profiles. Geophysical Monograph 246, American Geophysical Union. John Wiley and Sons,
3653 Inc., pp. 313-337. <https://doi.org/10.1002/9781119500513.ch19>.
- 3654 Rainbird, R.H., 1993. The sedimentary record of mantle plume uplift preceding eruption of
3655 the Neoproterozoic Natkusiak flood basalt. *Journal of Geology* 101, 305-318.
- 3656 Rampino, M.R., 1994. Tillites, diamictites, and ballistic ejecta of large impacts. *Journal of*
3657 *Geology* 102, 439-456.
- 3658 Rampino, M.R., 2017. Are some tillites impact-related debris-flow deposits? *Journal of*
3659 *Geology* 125, 155-164. <https://doi.org/10.1086/690212>.
- 3660 Reahl, J.N., Cantine, M.D., Wilcots, J., Mackey, T.J., Bergmann, K.D., 2021. Meta-analysis
3661 of Cryogenian through modern quartz microtextures reveals sediment transport histories.
3662 *Journal of Sedimentary Research*, accepted. <https://doi.org/10.1002/essoar.10504352.1>.
- 3663 Rees-Owen, R.L., Gill, F.L., Newton, R.N., Ivanović, R.F., Francis, J.E., Riding, J.B., Vane,
3664 C.H., Lopes dos Santos, R.A., 2018. The last forests on Antarctica: Reconstructing flora and
3665 temperature from the Neogene Sirius Group, Transantarctic Mountains. *Organic*
3666 *Geochemistry* 118, 4-14. <https://doi.org/10.1016/j.orggeochem.2018.01.001>.
- 3667 Rehmer, J., 1981. The Squantum Tilloid Member of the Roxbury Conglomerate of Boston,
3668 Massachusetts, in: Hambrey, M.J., Harland, W.B. (Eds.), *Earth's Pre-Pleistocene Glacial*
3669 *Record*. Cambridge University Press, Cambridge, pp. 756-759.

- 3670 Retallack, G.J., Broz, A.P., Lai, L.S.-H., Gardner, K., 2021. Neoproterozoic marine
3671 chemostratigraphy, or eustatic sea level change? *Palaeogeography, Palaeoclimatology,*
3672 *Palaeoecology* 562, 110155. <https://doi.org/10.1016/j.palaeo.2020.110155>.
- 3673 Ricci Lucchi, F., 1995. *Sedimentographica: Photographic Atlas Of Sedimentary Structures,*
3674 second ed. New York, Columbia University Press, digital version.
3675 <http://www.columbia.edu/dlc/cup/ricci/index.html>.
- 3676 Rice, A.H.N., Hofmann, C.C., 2000. Evidence for a glacial origin of Neoproterozoic III
3677 striations at Oaibaččannjar'ga, Finnmark, northern Norway. *Geological Magazine* 137,
3678 355–366.
- 3679 Rigby, J.K., 1958. Mass movements in Permian rocks of Trans-Pecos Texas. *Journal of*
3680 *Sedimentary Petrology* 28, 298-315.
- 3681 Robinson, J.E., Bacon, C.R., Major, J.J., Wright, H.M., Vallance, J.M., 2017. Surface
3682 morphology of caldera-forming eruption deposits revealed by lidar mapping of Crater Lake
3683 National Park, Oregon – Implications for deposition and surface modification. *Journal of*
3684 *Volcanology and Geothermal Research* 342, 61-78.
- 3685 Rocha-Campos, A.C., Santos, P.R. dos, 1981. The Itararé Subgroup, Aquidauana Group and
3686 San Gregório Formation, Paraná Basin, Southeastern South America, in: Hambrey, M.J.,
3687 Harland, W.B. (Eds.), *Earth's Pre-Pleistocene Glacial Record*. Cambridge University Press,
3688 Cambridge, pp. 842-852.

- 3689 Rodrigues, M.C.N.d.L., Trzaskos, B., Alsop, G.I., Vesely, F.F., 2020. Making a homogenite:
3690 An outcrop perspective into the evolution of deformation within mass-transport deposits.
3691 *Marine and Petroleum Geology* 112, 104033.
3692 <https://doi.org/10.1016/j.marpetgeo.2019.104033>.
- 3693 Rodriguez, J.A.P., Sasaki, S., Kuzmin, R.O., Dohm, J.M., Tanaka, K.L., Miyamoto, H.,
3694 Kurita, K., Komatsu, G., Fairéni, A.G., Ferris, J.C., 2005. Outflow channel sources,
3695 reactivation, and chaos formation, Xanthe Terra, Mars. *Icarus* 175, 36–57.
- 3696 Rodríguez-López, J.P., Liesa, C.L., Pardo, G., Melénde, N., Soria, A.R., Skilling, I., 2016.
3697 Glacial dropstones in the western Tethys during the late Aptian–early Albian cold snap:
3698 Palaeoclimate and palaeogeographic implications for the mid-Cretaceous. *Palaeogeography,*
3699 *Palaeoclimatology, Palaeoecology* 452, 11–27. <https://doi.org/10.1016/j.palaeo.2016.04.004>.
- 3700 Rodríguez-López, J.P., Van Vliet-Lanoë, B., López-Martínez, J., Martín-García, R., 2021.
3701 Scouring by rafted ice and cryogenic patterned ground preserved in a Palaeoproterozoic
3702 equatorial proglacial lagoon succession, eastern India, Nuna supercontinent. *Marine and*
3703 *Petroleum Geology* 123, 104766. <https://doi.org/10.1016/j.marpetgeo.2020.104766>.
- 3704 Rogov, M., Ershova, V., Vereshchagin, O., Vasileva, K., Mikhailova, K., Krylov, A., 2021.
3705 Database of global glendonite and ikaite records throughout the Phanerozoic. *Earth System*
3706 *Science Data* 13, 343-356. <https://doi.org/10.5194/essd-13-343-2021>.
- 3707 Romano, M., 2015. Reviewing the term uniformitarianism in modern Earth sciences.
3708 *Earth-Science Reviews* 148, 65-76. <https://doi.org/10.1016/j.earscirev.2015.05.010>.

- 3709 Rosa, E.L.M., Isbell, J.L., 2021. Late Paleozoic glaciation, in: Alderton, D., Elias, S.A.
3710 (Eds.), *Encyclopedia of Geology*, second ed. Elsevier, Amsterdam, pp. 534-545.
3711 <https://doi.org/10.1016/B978-0-08-102908-4.00063-1>.
- 3712 Rosa, E.L.M., Vesely, F.F., França, A.B., 2016. A review on late Paleozoic ice-related
3713 erosional landforms in the Paraná Basin: origin and paleogeographical implications. *Brazilian*
3714 *Journal of Geology* 46, 147-166. <https://doi.org/10.1590/2317-4889201620160050>.
- 3715 Rosa, E.L.M., Vesely, F.F., Isbell, J.L., Kipper, F., Fedorchuk, N.D., Souza, P.A., 2019.
3716 Constraining the timing, kinematics and cyclicity of Mississippian-Early Pennsylvanian
3717 glaciations in the Paraná Basin, Brazil. *Sedimentary Geology* 384, 29-49.
3718 <https://doi.org/10.1016/j.sedgeo.2019.03.001>.
- 3719 Rosa, E., Vesely, F., Isbell, J., Fedorchuk, N., 2021. As geleiras carboníferas no sul do Brasil.
3720 *Boletim Paranaense de Geociencias* 78, 24-43. <https://doi.org/10.5380/geo.v78i0.78669>.
- 3721 Rose, K.C., Ferraccioli, F., Jamieson, S.S.R., Bell, R.E., Corr, H., Creyts, T.T., Braaten, D.,
3722 Jordan, T.A., Fretwell, P.T., Damaske, D., 2013. Early East Antarctic Ice Sheet growth
3723 recorded in the landscape of the Gamburtsev Subglacial Mountains. *Earth and Planetary*
3724 *Science Letters* 375, 1-12. <https://doi.org/10.1016/j.epsl.2013.03.053>.
- 3725 Rothman, M.D., Mattio, L., Anderson, R.J., Bolton, J.J., 2017. A phylogeographic
3726 investigation of the kelp genus *Laminaria* (Laminariales, Phaeophyceae), with emphasis on
3727 the South Atlantic Ocean. *Journal of Phycology* 53, 778–789.

- 3728 Rowe, C.D., Backeberg, N.R., 2011. Discussion on: reconstruction of the Ordovician
3729 Pakhuis ice sheet, South Africa by H.J. Blignault, J.N. Theron. *South African Journal of*
3730 *Geology* 114, 95-102. <https://doi.org/10.2113/gssajg.114.1.95>.
- 3731 Runkel, A.C., Mackey, T.J., Cowan, C.C., Fox, D.L., 2010. Tropical shoreline ice in the late
3732 Cambrian: Implications for Earth's climate between the Cambrian Explosion and the Great
3733 Ordovician Biodiversification Event, *Geological Society of America Today* 20, 4-10.
3734 <https://doi.org/10.1130/GSATG84A.1>.
- 3735 Ryder, J.M., Thomson, B., 1986. Neoglaciation in the southern Coast Mountains of British
3736 Columbia: chronology prior to the late Neoglacial maximum. *Canadian Journal of Earth*
3737 *Science* 23, 273 -287.
- 3738 Sandberg, C.G.S., 1928. The origin of the Dwyka Conglomerate of South Africa and other
3739 "glacial" deposits. *Geological Magazine* 65, 117-138.
- 3740 Sanders, J.E., Cecioni, G.O., 1957. Discussion: "Flysch and Molasse". *Bulletin of the*
3741 *American Association of Petroleum Geologists* 41, 2136-2139.
- 3742 Santos, P.R. dos, Rocha-Campos, A.C., Canuto, J.R., 1996. Patterns of late Palaeozoic
3743 deglaciation in the Paraná Basin, Brazil. *Palaeogeography, Palaeoclimatology, Palaeoecology*
3744 125, 165-184.

- 3745 Schatz, E.R., Mángano, M.G., Buatois, L.A., Limarino, C.O., 2011. Life in the Late Paleozoic
3746 ice age: Trace fossils from glacially influenced deposits in a Late Carboniferous fjord of
3747 western Argentina. *Journal of Paleontology* 85, 502-518. <https://doi.org/10.1666/10-046.1>.
- 3748 Scheffler, K., Hoernes, S., Schwark, L.: 2003. Global changes during Carboniferous–Permian
3749 glaciation of Gondwana: Linking polar and equatorial climate evolution by geochemical
3750 proxies. *Geology* 31, 605–608.
3751 [https://doi.org/10.1130/0091-7613\(2003\)031<0605:GCDCGO>2.0.CO;2](https://doi.org/10.1130/0091-7613(2003)031<0605:GCDCGO>2.0.CO;2).
- 3752 Schenk, P.E., 1965. Depositional environment of the Gowganda Formation (Precambrian) at
3753 the south end of Lake Timagami, Ontario. *Journal of Sedimentary Petrology* 35, 309-318.
- 3754 Schenk, P.E., 1972. Possible Late Ordovician glaciation of Nova Scotia. *Canadian Journal of*
3755 *Earth Sciences* 9, 95-107.
- 3756 Schermerhorn, L.J.G., 1970. Saharan ice. *Geotimes* 15, 7-8.
- 3757 Schermerhorn, L.J.G., 1971. Upper Ordovician glaciation in Northwest Africa? Discussion.
3758 *GSA Bulletin* 82, 265-268.
- 3759 Schermerhorn, L.J.G., 1974a. Late Precambrian mixtites: glacial and/or nonglacial? *American*
3760 *Journal of Science* 274, 673-824.
- 3761 Schermerhorn, L.J.G., 1974b. No evidence for glacial origin of Late Precambrian tilloids in
3762 Angola. *Nature* 252, 114-115.

- 3763 Schermerhorn, L.J.G., 1975. Tectonic framework of Late Precambrian supposed glacials, in:
3764 Wright, A.E., Moseley, F. (Eds.), *Ice Ages: Ancient and Modern*. Seal House Press,
3765 Liverpool, pp. 241-274.
- 3766 Schermerhorn, L.J.G., 1976a. Reply. *American Journal of Science* 276, 375-384.
- 3767 Schermerhorn, L.J.G., 1976b. Reply. *American Journal of Science* 276, 1315-1324.
- 3768 Schermerhorn, L.J.G., 1977. Late Precambrian glacial climate and the Earth's obliquity – a
3769 discussion. *Geological Magazine* 114, 57-64.
- 3770 Schermerhorn, L.J.G., 1981. Late Precambrian tilloids of northwest Angola, in: Hambrey,
3771 M.J., Harland, W.B. (Eds.), *Earth's Pre-Pleistocene Glacial Record*. Cambridge University
3772 Press, Cambridge, pp. 158-161.
- 3773 Schermerhorn, L.J.G., Stanton, W.I., 1963. Tilloids in the West Congo Geosyncline.
3774 *Quarterly Journal of the Geological Society of London* 119, 201-241.
- 3775 Schieber, J., 1999. Microbial mats in terrigenous clastics: the challenge of identification in
3776 the rock record. *Palaios* 14, 3-12. <https://doi.org/10.2307/3515357>.
- 3777 Schieber, J., Southard, J., Thaisen, K., 2007. Accretion of mudstone beds from migrating
3778 floccule ripples. *Science* 318, 1760-1763. <https://doi.org/10.1126/science.1147001>.

- 3779 Schieber, J., Southard, J.B., Kissling, P., Rossman, B., Ginsburg, R., 2013. Experimental
3780 deposition of carbonate mud from moving suspensions: importance of flocculation and
3781 implications for modern and ancient carbonate mud deposition. *Journal of Sedimentary*
3782 *Research* 83, 1025-1031. <https://doi.org/10.2110/jsr.2013.77>.
- 3783 Schipper, C.I., Moussallam, Y., Curtis, A., Peters, N., Barnie, T., Bani, P., Jost, H.J.,
3784 Hamilton, D., Aiuppa, A., Tamburello, G., Giudice, G., 2017. Isotopically ($\delta^{13}\text{C}$ and $\delta^{18}\text{O}$)
3785 heavy volcanic plumes from Central Andean volcanoes: a field study. *Bulletin of*
3786 *Volcanology* 79, 65. <https://doi.10.1007/s00445-017-1146-4>.
- 3787 Schneebeli-Hermann, E., Kürschner, W.M., Kerp, H., Bomfleur, B., Hochuli, P.A., Bucher,
3788 H., Ware, D., Roohi, G., 2015. Vegetation history across the Permian-Triassic boundary in
3789 Pakistan (Amb section, Salt Range). *Gondwana Research* 27, 911-824.
3790 <https://doi.org/10.1016/j.gr.2013.11.007>.
- 3791 Schneider, J.L., Fisher, R.V., 1998. Transport and emplacement mechanisms of large
3792 volcanic debris avalanches: evidence from the northwest sector of Cantal Volcano (France).
3793 *Journal of Volcanology and Geothermal Research* 83, 141–165.
- 3794 Schwab, F.L., 1981. Late Precambrian tillites of the Appalachians, in: Hambrey, M.J.,
3795 Harland, W.B. (Eds.), *Earth's Pre-Pleistocene Glacial Record*. Cambridge University Press,
3796 Cambridge, pp. 751-755.

- 3797 Schwarzbach, M., 1961. The climatic history of Europe and North America, in: Nairn,
3798 A.E.M. (Ed.), *Descriptive Palaeoclimatology*. Interscience Publ. Inc., New York, pp.
3799 255-291.
- 3800 Scotese, C.R., Song, H., Mills, B.J.W., van der Meer, D.G., 2021. Phanerozoic
3801 paleotemperatures: The earth's changing climate during the last 540 million years. *Earth-*
3802 *Science Reviews* 215, 103503. <https://doi.org/10.1016/j.earscirev.2021.103503>.
- 3803 Scott, K.M., 1966. Sedimentology and dispersal pattern of a Cretaceous flysch sequence,
3804 Patagonian Andes, Southern Chile. *AAPG Bulletin* 50, 72-107.
- 3805 Scott, K.M., 1988a. Origin, Behavior and Sedimentology of Lahars and Lahar-runout Flows
3806 in the Toutle-Cowlitz River System. U.S. Geological Survey Professional Paper 1447A.
- 3807 Scott, K.M., 1988b. Origin, behavior and sedimentology of prehistoric catastrophic lahars at
3808 Mount St. Helens, Washington, in: Clifton, H.E. (Ed.), *Sedimentologic Consequences of*
3809 *Convulsive Geologic Events*. Geological Society of America Special Paper 229, pp. 23-36.
- 3810 Sensula, B., Böttger, T., Pazdur, A., Piotrowska, N., Wagner, R., 2006. Carbon and oxygen
3811 isotope composition of organic matter and carbonates in recent lacustrine sediments.
3812 *Geochronometria* 25, 77-94.
- 3813 SEPM, 2021. Diagenesis and Porosity. <http://www.sepmstrata.org/page.aspx?pageid=92>
3814 (accessed 2 January, 2021).

- 3815 Servais, T. Cascales-Miñana, B., Cleal, C.J., Gerrienne, P., Harper, D.A.T., Neumann, M.,
3816 2019. Revisiting the Great Ordovician Diversification of land plants: Recent data and
3817 perspectives. *Palaeogeography, Palaeoclimatology, Palaeoecology* 534, 109280.
3818 <https://doi.org/10.1016/j.palaeo.2019.109280>.
- 3819 Seward, A.C., 1932. A Persian *Sigillaria*. *Philosophical Transactions of the Royal Society of*
3820 *London. Series B, Containing Papers of a Biological Character* 221, 377-390.
- 3821 Shanmugam, G., 2002. Ten turbidite myths. *Earth-Science Reviews* 58, 311-341.
- 3822 Shanmugam, G., 2012. Process-sedimentological challenges in distinguishing paleo-tsunami
3823 deposits. *Natural Hazards* 63, 5–30. <https://doi.org/10.1007/s11069-011-9766-z>.
- 3824 Shanmugam, G., 2016. Submarine fans: a critical retrospective (1950-2015). *Journal of*
3825 *Palaeogeography* 5, 110-184.
- 3826 Shanmugam, G., 2017a. The contourite problem, in: Mazumder, R. (Ed.), *Sediment*
3827 *Provenance Influences on Compositional Change from Source to Sink*. Elsevier Inc., pp. 183-
3828 254. <https://doi.org/10.1016/B978-0-12-803386-9.00009-5>.
- 3829 Shanmugam, G., 2017b. Global case studies of soft-sediment deformation structures (SSDS):
3830 Definitions, classifications, advances, origins, and problems. *Journal of Palaeogeography* 6,
3831 251-320. <http://dx.doi.org/10.1016/j.jop.2017.06.004>.

- 3832 Shanmugam, G., 2019. Reply to discussions by Zavala (2019) and by Van Loon, Hüeneke,
3833 and Mulder (2019) on Shanmugam, G. (2018, *Journal of Palaeogeography*, 7 (3): 197–238):
3834 'the hyperpycnite problem'. *Journal of Palaeogeography* 8, 31.
3835 <https://doi.org/10.1186/s42501-019-0047-1>.
- 3836 Shanmugam, G., 2020. Gravity flows: Types, definitions, origins, identification markers, and
3837 problems. *Journal of the Indian Association of Sedimentologists* 37, 61-90.
3838 <https://doi.org/10.51710/jias.v37i2.117>.
- 3839 Shanmugam, G., 2021a. Deep-water processes and deposits, in: Alderton, D., Elias, S.A.
3840 (Eds.), *Encyclopedia of Geology*, second ed., 2. Academic Press, United Kingdom, pp. 965-
3841 1009. <https://doi.org/10.1016/B978-0-12-409548-9.12541-2>.
- 3842 Shanmugam, G., 2021b. *Mass Transport, Gravity Flows, and Bottom Currents*. Elsevier, 571
3843 pp. <https://doi.org/10.1016/C2019-0-03665-5>.
- 3844 Shanmugam, G., Lehtonen, L.R., Straume, T., Syvertsen, S.E., Hodgkinson, R.J., Skibej, M.,
3845 1994. Slump and debris-flow dominated upper slope facies in the Cretaceous of the
3846 Norwegian and northern North Seas (61-67°N): implications for sand distribution, *AAPG*
3847 *Bulletin*, 78, 910-937.
- 3848 Sharp, M., 1982. Modification of clasts in lodgement tills by glacial erosion. *Journal of*
3849 *Glaciology* 28, 475-481.

- 3850 Shepard, F.P., Dill, R.F., 1966. Submarine Canyons and Other Sea Valleys, Rand McNally,
3851 Chicago, 381 pp.
- 3852 Shields, G.A., Strachan, R.A., Porter, S.M., Halverson, G.P., Macdonald, F.A., Plumb, K.A.,
3853 Alvarenga, C.J. de, Banerjee, D.M., Bekker, A., Bleeker, W., Brasier, A., Chakraborty, P.P.,
3854 Collins, A.S., Condie, K., Das, K., Rvans, D.A.D., Ernst, R., Fallick, A.E., Frimmel, H.,
3855 Fuck, R.A., Hoffman, P.F., Kamber, B.S., Kuznetsov, A.B., Mitchell, R.N., Poiré, D.G.,
3856 Poulton, S.W., Riding, R., Sharma, M., Storey, C., Stueeken, E., Tostevin, R., Turner, E.,
3857 Xiao, S., Zhang, S., Zhou, Y., Zhu, M., 2022. A template for an improved rock-based
3858 subdivision of pre-Cryogenian time. *Journal of the Geological Society* 179, jgs2020-222.
3859 <https://doi.org/10.1144/jgs2020-222>.
- 3860 Sial, A.N., Gaucher, C., Ferreira, V.P., Pereira, N.S., Cezario, J.S., Chiglino, L., Lima, H.M.,
3861 2015. Isotope and elemental chemostratigraphy, in, Ramkumar, M. (Ed.), *Chemostratigraphy:
3862 Concepts, Techniques, and Applications*. Elsevier, Amsterdam, pp.23-64.
3863 <https://doi.org/10.1016/B978-0-12-419968-2.00002-9>.
- 3864 Silberfeld, T., Leigh, J.W., Verbruggen, H., Cruaud, C., de Reviers, B., Rousseau, F., 2010. A
3865 multi-locus time-calibrated phylogeny of the brown algae (Heterokonta, Ochrophyta,
3866 Phaeophyceae): Investigating the evolutionary nature of the “brown algal crown radiation”.
3867 *Molecular Phylogenetics and Evolution* 56, 659-674.
- 3868 Siman-Tov, S., Stock, G.M., Brodsky, E.E., White, J.C., 2017. The coating layer of glacial
3869 polish. *Geology* 45, 987-990. <https://doi.org/10.1130/G39281.1>.

- 3870 Simms, M.J., 2007. Uniquely extensive soft-sediment deformation in the Rhaetian of the
3871 UK: Evidence for earthquake or impact? *Palaeogeography, Palaeoclimatology, Palaeoecology*
3872 244, 407–423.
- 3873 Sloan, L.C., Barron, E.J., 1990. “Equable” climates during Earth history? *Geology* 18, 489-
3874 492.
- 3875 Smith, D.G., 2019. Millennial-scale climate changes manifest Milankovitch combination
3876 tones and Hallstatt solar cycles in the Devonian greenhouse world: Comment. *Geology* 47,
3877 e488. <https://doi.org/10.1130/G46475C.1>.
- 3878 Smith, D.G., Bailey, R.J., 2018a. Discussion on ‘A 2.3 million year lacustrine record of
3879 orbital forcing from the Devonian of northern Scotland’. *Journal of the Geological Society*
3880 173, 474- 488. *Journal of the Geological Society* 175, 561.
3881 <https://doi.org/10.1144/jgs2016-137>.
- 3882 Smith, D.G., Bailey, R.J., 2018b. Discussion: Howe, T.S., Corcoran, P.L., Longstaffe, F.J.,
3883 Webb, E.A, Pratt, R.G., 2016. Climatic cycles recorded in glacially influenced rhythmites of
3884 the Gowganda Formation, Huronian Supergroup, *Precambrian Research*, 286, 269-280.
3885 *Precambrian Research* 316, 324-326. <https://doi.org/10.1016/j.precamres.2017.04.022>.
- 3886 Smith, G.L.B., Eriksson, K.A., 1979. A fluvio-glacial and glaciolacustrine deltaic depositional
3887 model for Permo-Carboniferous coals of the Northeastern Karoo Basin, South Africa.
3888 *Palaeogeography, Palaeoclimatology, Palaeoecology* 27, 67-84.

- 3889 Smith, N.D., Ashley, G., 1985. Proglacial lacustrine environment, in: Ashley, C.M., Shaw, J.,
3890 Smith, N.D. (Eds.), *Glacial Sedimentary Environments*. SEPM Short Course Notes 16, pp.
3891 135-216. <https://doi.org/10.2110/scn.85.02.0135>.
- 3892 Smith, N.D., Phillips, A.C., Powell, R.D., 1990. Tidal drawdown: A mechanism for
3893 producing cyclic sediment laminations in glaciomarine deltas. *Geology* 18, 10-13.
- 3894 Sobiesiak, M.S., Kneller, B., Alsop, G.I., Milana, J.P., 2016. Inclusion of substrate blocks
3895 within a mass transport deposit: A case study from Cerro Bola, Argentina, in: Lamarche, G.,
3896 Mountjoy, J., Bull, S., Hubble, T., Krastel, S., Lane, E., Micallef, A., Moscardelli, L.,
3897 Mueller, C., Pecher, I., Woelz, S. (Eds.), *Submarine Mass Movements and Their
3898 Consequences*. Springer International Publ., Switzerland, pp. 487-496.
- 3899 Sobiesiak, M.S., Kneller, B., Alsop, G.I., Milana, J.P., 2018. Styles of basal interaction
3900 beneath mass transport deposits. *Marine and Petroleum Geology* 98, 629–639.
3901 <https://doi.org/10.1016/j.marpetgeo.2018.08.028>.
- 3902 Sokołowski, R.J., Wysota, W., 2020. Differentiation of subglacial conditions on soft and hard
3903 bed settings and implications for ice sheet dynamics: a case study from north.central Poland.
3904 *International Journal of Earth Sciences* 109, 2699–2717. [https://doi.org/10.1007/s00531-020-
3905 01920-x](https://doi.org/10.1007/s00531-020-01920-x).
- 3906 Soreghan, G.S., Sweet, D.S., Heavens, N.G., 2014. Upland glaciation in tropical Pangaea:
3907 Geologic evidence and implications for Late Paleozoic climate modeling. *Journal of Geology*
3908 122, 137-163. <https://doi.org/10.1086/675255>.

- 3909 Soutter, E.L., Kane, I.A., Huuse, M., 2018. Giant submarine landslide triggered by Paleocene
3910 mantle plume activity in the North Atlantic. *Geology* 46, 511–514.
3911 <https://doi.org/10.1130/G40308.1>.
- 3912 Spiekermann, R., Jasper, A., Benício, J.R.W., Guerra-Sommer, M., Ricardi-Branco, F.S.,
3913 Uhl, D., 2020. Late Palaeozoic lycopsid macrofossils from the Paraná Basin, South America
3914 – an overview of current knowledge. *Journal of South American Earth Sciences* 101, 102615.
3915 <https://doi.org/10.1016/j.jsames.2020.102615>.
- 3916 Srivastava, A.K., Agnihotri, D., 2010. Dilemma of late Palaeozoic mixed floras in
3917 Gondwana. *Palaeogeography, Palaeoclimatology, Palaeoecology* 298, 54–69.
3918 <https://doi.org/10.1016/j.palaeo.2010.05.028>.
- 3919 Stalker, A.M., 1975. The Large Interdrift Bedrock Blocks of the Canadian Prairies.
3920 Geological Survey of Canada, Paper 75-1, Part A, 421-422.
- 3921 Stalker, A.M., 1976. Megablocks, or the Enormous Erratics of the Albertan Prairies.
3922 Geological Survey of Canada, Paper 76-1C, 185-188.
- 3923 Stavrakis, N., 1986. Sedimentary environments and facies of the Orange Free State coalfield,
3924 in: Anhaeusser, C.R., Maske, S. (Eds.), *Mineral Deposits of Southern Africa* vols. I and II.
3925 Geological Society of South Africa, Johannesburg, pp. 1939–1952.
- 3926 Stavrakis, N., Smyth, M., 1991. Clastic sedimentary environments and organic petrology of
3927 coals in the Orange Free State, South Africa. *International Journal of Coal Geology* 18, 1-16.

- 3928 Stein, R.A., Sheldon, N.D., Smith, S.Y., 2021. C₃ plant carbon isotope discrimination does
3929 not respond to CO₂ concentration on decadal to centennial timescales. *New Phytologist* 229,
3930 2576-2585. <https://doi.org/10.1111/nph.17030>.
- 3931 Sterren, A.F., Cisterna, G.A., Rustán, J.J., Vaccari, N.E., Balseiro, D., Ezpeleta, M.,
3932 Prestianni, C., 2021. New invertebrate peri-glacial faunal assemblages in the Agua de Lucho
3933 Formation, Río Blanco Basin, Argentina. The most complete marine fossil record of the early
3934 Mississippian in South America. *Journal of South American Earth Sciences* 106, 103078.
3935 <https://doi.org/10.1016/j.jsames.2020.103078>.
- 3936 Stevenson, C.J., Talling, P.J., Sumner, E.J., Masson, D.G., Frenz, M., Wynn, R.B., 2014. On
3937 how thin submarine flows transported large volumes of sand for hundreds of kilometres
3938 across a flat basin plain without eroding the sea floor. *Sedimentology* 61, 1982-2019.
3939 <https://doi.org/10.1111/sed.12125>.
- 3940 Stock, J.D., Dietrich, W.E., 2006. Erosion of steepland valleys by debris flows. *GSA Bulletin*
3941 118, 1125-1148.
- 3942 Stokes, C.R., 2018. Geomorphology under ice streams: Moving from form to process. *Earth*
3943 *Surface Processes and Landforms* 43, 85-123. <https://doi.org/10.1002/esp.4259>.
- 3944 Stoopes, G.R., Sheridan, M.F., 1992. Giant debris avalanches from the Colima Volcanic
3945 Complex, Mexico: Implications for long-runout landslides (> 100 km) and hazard
3946 assessment. *Geology* 20, 299-302.

- 3947 Stratten, T., Humphreys, A.J.B., 1974. Extensive glacial pavement of Dwyka age near
3948 Douglas, Cape Province. *South African Journal of Science* 70, 44-45.
- 3949 Studer, B., 1827. Remarques géognostiques sur quelques parties de la chaîne septentrionale
3950 des Alpes. *Annales Des Sciences Naturelles*, Paris 11, 1-47.
- 3951 Sugden, D.E., John, B.S., 1982. *Glaciers and Landscape*. Edward Arnold, London, p. 161.
- 3952 Sutherland, B.R., Barrett, K.J., Gingras , M.K., 2015. Clay settling in fresh and salt water.
3953 *Environmental Fluid Mechanics* 15, 147-160. <https://doi.org/10.1007/s10652-014-9365-0>.
- 3954 Syvitski, J.P.M., Shaw, J., 1995. Sedimentology and geomorphology of fjords, in: Perillo,
3955 G.M.E. (Ed.), *Geomorphology and Sedimentology of Estuaries*. Developments in
3956 *Sedimentology* 53, Elsevier Science B.V., Amsterdam, pp. 113-178.
3957 [https://doi.org/10.1016/S0070-4571\(05\)80025-1](https://doi.org/10.1016/S0070-4571(05)80025-1).
- 3958 Tachibana, T., 2013. Lonestones as indicators of tsunami deposits in deep-sea sedimentary
3959 rocks of the Miocene Morozaki Group, central Japan. *Sedimentary Geology* 289, 62-73.
- 3960 Takasaki, R., Fiorillo, A.R., Kobayashi, Y., McCarthy, P.J., 2019. The first definite
3961 Lambeosaurine bone from the Liscomb Bonebed of the Upper Cretaceous Prince Creek
3962 Formation, Alaska, United States. *Scientific Reports* 9, 5384.
3963 <https://doi.org/10.1038/s41598-019-41325-8>.

- 3964 Talling, P.J., Wynn, R.B., Masson, D.G., Frenz, M., Cronin, B.T., Schiebel, R.,
3965 Akhmetzhanov, A.M., Dallmeier-Tiessen, S., Benetti, S., Weaver, P.P.E., Georgiopoulou, A.,
3966 Zühlsdorff, C., Amy, L.A., 2007. Onset of submarine debris flow deposition far from original
3967 giant landslide. *Nature* 450, 541-544.
- 3968 Talling, P.J., Masson, D.G., Sumner, E.J., Malgesini, G., 2012. Subaqueous sediment density
3969 flows: depositional processes and deposit types. *Sedimentology* 59, 1937-2003.
- 3970 Talling, P.J., Allin, J., Armitage, D.A. et al., and 27 more authors, 2015. Key future directions
3971 for research on turbidity currents and their deposits. *Journal of Sedimentary Research* 85,
3972 153-169. <https://doi.org/10.2110/jsr.2015.03>.
- 3973 Tavener-Smith, T., Mason, T.R., 1983. A late Dwyka (early Permian) varvite sequence near
3974 Isandlwana, Zululand, South Africa. *Palaeogeography, Palaeoclimatology, Palaeoecology* 41,
3975 233-249.
- 3976 Tedesco, J., Cagliari, J., Aquino, C.D., 2020. Late Paleozoic Ice-Age rhythmites in the
3977 southernmost Paraná Basin: A sedimentological and paleoenvironmental analysis. *Journal of*
3978 *Sedimentary Research* 90, 969–979. <https://doi.org/10.2110/jsr.2020.54>.
- 3979 Taylor, T.N., Taylor, N.R., Cúneo, N.R., 1992. The present is not the key to the past: a polar
3980 forest from the Permian of Antarctica. *Science* 257, 1675-1677.

- 3981 Thiel, M., Gutow, L., 2005. The ecology of rafting in the marine environment. I. The floating
3982 substrata, in: Gibson, R.N., Atkinson, R.J.A., Gordon, J.D.M. (Eds.), *Oceanography and*
3983 *Marine Biology: An Annual Review* 42, pp. 181–264.
- 3984 Thomas, G.S.P., Connell, R.J., 1985. Iceberg drop, dump and grounding structures from
3985 Pleistocene glacio-lacustrine sediments, Scotland. *Journal of Sedimentary Petrology* 55, 243-
3986 249. <https://doi.org/10.1306/212F8689-2B24-11D7-8648000102C1865D>.
- 3987 Thompson, N.D., 2009. *Distinct Element Numerical Modelling of Volcanic Debris*
3988 *Avalanche Emplacement Geomechanics* (Ph.D. Thesis). Bournemouth University,
3989 Bournemouth.
- 3990 Thompson, N., Matthew R., Bennett, M.D. Petford, N., 2010. Development of characteristic
3991 volcanic debris avalanche deposit structures: New insight from distinct element simulations.
3992 *Journal of Volcanology and Geothermal Research* 192, 191-200.
- 3993 Tian, X., Gao, Y., Li, Z., Zavala, C., Chen, Z., Huang, Y., Yu, E., Wang, C., 2021. Fine
3994 grained gravity flow deposits and their depositional processes: A case study from the
3995 Cretaceous Nenjiang Formation, Songliao Basin, NE China. *Geological Journal* 56, 1496-
3996 1509. <https://doi.org/10.1002/gj.4017>.
- 3997 Tinkler, K.J., 1993. Fluvially sculpted rock bedforms in Twenty Mile Creek, Niagara
3998 Peninsula, Ontario. *Canadian Journal of Earth Sciences* 30, 945-953.
3999 <https://doi.org/10.1139/e93-079>.

- 4000 Tripathy, G., Goswami, S., Das, P.P., 2021. Late Permian species diversity of the genus
4001 *Glossopteris* in and around Himgir, Ib River Basin, Odisha, India, with a clue on
4002 palaeoclimate and palaeoenvironment. *Arabian Journal of Geosciences* 14, 703.
4003 <https://doi.org/10.1007/s12517-021-07019-0>.
- 4004 Trompette, R., 1981. Late Precambrian tillites of the Volta Basin and the Dahomeyides
4005 Orogenic Belt (Benin, Ghana, Niger, Togo and Upper-Volta), in: Hambrey, M.J., Harland,
4006 W.B. (Eds.), *Earth's Pre-Pleistocene Glacial Record*. Cambridge University Press,
4007 Cambridge, pp. 135-139.
- 4008 Trostdorf Jr. I., Rocha-Campos, A.C., Santos, P.R. dos, Tomio, A., 2005a. Origin of Late
4009 Paleozoic, multiple, glacially striated surfaces in northern Paraná Basin (Brazil): Some
4010 implications for the dynamics of the Paraná glacial lobe. *Sedimentary Geology* 181, 59-71.
4011 <https://doi.org/10.1016/j.sedgeo.2005.07.006>.
- 4012 Trostdorf, I., Assine, M.L., Vesely, F.F., Rocha-Campos, A.C., Santos, P.R. dos, Tomio, A.,
4013 2005b. Glacially striated, soft sediment surfaces on late Paleozoic tillite at São Luiz do
4014 Purunã, PR. *Anais da Academia Brasileira de Ciências* 77, 367–378.
- 4015 Tucholke, B.E., 1992. Massive submarine rockslide in the rift-valley wall of the Mid-Atlantic
4016 Ridge. *Geology* 20, 129-132.
- 4017 Ui, T., 1989. Discrimination between debris avalanche and other volcanoclastic deposits, in:
4018 Latter, J.H. (Ed.), *Volcanic Hazards*. Springer, Berlin, pp. 201-209.

- 4019 Vachtman, D., Mitchell, N.C., Gawthorpe, R., 2013. Morphologic signatures in submarine
4020 canyons and gullies, central USA Atlantic continental margins. *Marine and Petroleum*
4021 *Geology* 41, 250-263. <https://doi.org/10.1016/j.marpetgeo.2012.02.005>.
- 4022 Valdez Buso, V., Milana, J.P., di Pasquo, M., Aburto, J.E., 2021. The glacial paleovalley of
4023 Vichigasta: Paleogeomorphological and sedimentological evidence for a large continental
4024 ice-sheet for the mid-Carboniferous over central Argentina. *Journal of South American Earth*
4025 *Sciences* 106, 103066. <https://doi.org/10.1016/j.jsames.2020.103066>.
- 4026 van der Vegt, P., Janszen, A., Moscariello, A., 2012. Tunnel valleys: current knowledge and
4027 future perspectives, in: Huuse, M., Redfern, J., Le Heron, D.P., Dixon, R. J., Moscariello, A.,
4028 Craig, J. (Eds.), *Glaciogenic Reservoirs and Hydrocarbon Systems*. Geological Society,
4029 London, Special Publications 368. <https://doi.org/10.1144/SP368.13>.
- 4030 van der Meer, J.J.M., Menzies, J., Rose, J., 2003. Subglacial till: the deforming glacier bed,
4031 *Quaternary Science Reviews* 22, 1659-1685.
4032 [https://doi.org/10.1016/S0277-3791\(03\)00141-0](https://doi.org/10.1016/S0277-3791(03)00141-0)
- 4033 Van Houten, F.B., 1957. Appraisal of Ridgway and Gunnison "Tillites," Southwestern
4034 Colorado. *Bulletin of the Geological Society of America* 66, 383-388.
- 4035 Vandyk, T.M., Kettler, C., Davies, B.J., Shields, G.A., Candy, I., Le Heron, D.P., 2021.
4036 Reassessing classic evidence for warm-based Cryogenian ice on the western Laurentian
4037 margin: The "striated pavement" of the Mineral Fork Formation, USA. *Precambrian Research*
4038 363, 106345. <https://doi.org/10.1016/j.precamres.2021.106345>.

- 4039 Vellutini, P., Vicat, J.-P., 1983. Sur L'Origine Des Formation Conglomératiques de Base du
4040 Geosynclinal Ouest-Congolien (Gabon, Congo, Zaire, Angola). *Precambrian Research* 23,
4041 87-101.
- 4042 Ventra, D., Clarke, L.E., 2018. Geology and geomorphology of alluvial and fluvial fans:
4043 current progress and research perspectives, in: Ventra, D., Clarke, L.E. (Eds.), *Geology and*
4044 *Geomorphology of Alluvial and Fluvial Fans: Terrestrial and Planetary Perspectives*.
4045 Geological Society, London, Special Publications 440, pp. 1–21.
4046 <https://doi.org/10.1144/SP440.16>.
- 4047 Veroslavsky, G., Rossello, E.A., López-Gamundí, O., de Santa Ana, H., Perinotto, A.J., 2021.
4048 Late Paleozoic tectono-sedimentary evolution of eastern Chaco-Paraná Basin (Uruguay,
4049 Brazil, Argentina and Paraguay). *Journal of South American Earth Sciences* 106, 102991.
4050 <https://doi.org/10.1016/j.jsames.2020.102991>.
- 4051 Vesely, F.F., Assine, M.L., 2014. Ice-keel scour marks in the geological record: evidence
4052 from Carboniferous soft-sediment striated surfaces in the Paraná Basin, southern Brazil.
4053 *Journal of Sedimentary Research* 84, 26–39. <https://doi.org/10.2110/jsr.2014.4>.
- 4054 Vesely, F.F., Rodrigues, M.C.N.L, Rosa, E.L.M., Amato, J.A., Trzaskos, B., Isbell, J.L.,
4055 Fedorchuk, N.D., 2018. Recurrent emplacement of non-glacial diamictite during the late
4056 Paleozoic ice age. *Geology* 46, 615-618. <https://doi.org/10.1130/G45011.1>.
- 4057 Vesely, F.F., Assine, M.L., França, A.B., Paim, P.S.G., Rostirolla, S.P., 2021. Tunnel-valley
4058 fills in the Paraná Basin and their implications for the extent of late Paleozoic glaciation in

- 4059 SW Gondwana. *Journal of South American Earth Sciences* 106, 102969.
4060 <https://doi.org/10.1016/j.jsames.2020.102969>.
- 4061 Visser, J.N.J., 1981. Carboniferous topography and glaciation in the North-Western part of
4062 the Karoo Basin, South Africa. *Annals of the Geological Survey of South Africa* 15, 13-24.
- 4063 Visser, J.N.J., 1982. Upper Carboniferous glacial sedimentation in the Karoo Basin near
4064 Prieska, South Africa. *Palaeogeography, Palaeoclimatology, Palaeoecology* 38, 63-92.
- 4065 Visser, J.N.J., 1983a. The problems of recognizing ancient subaqueous debris flow deposits
4066 in glacial sequences. *Transactions of the Geological Society of South Africa* 86, 127-135.
- 4067 Visser, J.N.J., 1983b. Glacial marine sedimentation in the Late Paleozoic Karoo Basin,
4068 Southern Africa, in: Molnia, B.F. (Ed.), *Glacial-Marine Sedimentation*. Plenum Press, New
4069 York, pp. 667-701.
- 4070 Visser, J.N.J., 1987. The palaeogeography of part of southwestern Gondwana during the
4071 Permo-Carboniferous glaciation. *Palaeogeography, Palaeoclimatology, Palaeoecology* 61,
4072 205-219.
- 4073 Visser, J.N.J., 1988. A Permo-Carboniferous tunnel valley system east of Barklay West,
4074 Northern Cape Province. *South African Journal of Geology* 91, 350-357.

- 4075 Visser, J.N.J., 1989a. The Permo-Carboniferous Dwyka Formation of Southern Africa:
4076 deposition by a predominantly subpolar marine ice sheet. *Palaeogeography,*
4077 *Palaeoclimatology, Palaeoecology* 70, 377-391.
- 4078 Visser, J.N.J., 1989b. Stone orientation in basal glaciogenic diamictite: four examples from
4079 the Permo-Carboniferous Dwyka Formation, South Africa. *Journal of Sedimentary Petrology*
4080 59, 935-943.
- 4081 Visser, J.N.J., 1996. A Late Carboniferous subaqueous glacial valley fill complex:
4082 Fluctuations in meltwater output and sediment flux. *South African Journal of Geology* 99,
4083 285-291.
- 4084 Visser, J.N.J., 1997. Deglaciation sequences in the Permo-Carboniferous Karoo and
4085 Kalahari basins of southern Africa: a tool in the analysis of cyclic glaciomarine basin fills.
4086 *Sedimentology* 44, 507-521.
- 4087 Visser, J.N.J., Hall, K.J., 1985. Boulder beds in the glaciogenic Permo-Carboniferous Dwyka
4088 Formation in South Africa. *Sedimentology* 32, 281-294.
4089 <https://doi.org/10.1111/j.1365-3091.1985.tb00510.x>.
- 4090 Visser, J.N.J., Kingsley, C.S., 1982. Upper Carboniferous glacial valley sedimentation in the
4091 Karoo Basin, Orange Free State. *Transactions of the Geological Society of South Africa* 85,
4092 71-79.

- 4093 Visser, J.N.J., Loock, J.C., 1982. An investigation of the basal Dwyka tillite in the southern
4094 part of the Karoo Basin, South Africa. Transactions of the Geological Society of South Africa
4095 85, 179-187.
- 4096 Visser, J.N.J., Loock, J.C., 1988. Sedimentary facies of the Dwyka Formation associated with
4097 the Nooitgedacht Glacial Pavements, Barkly West District. South African Journal of Geology
4098 91, 38-48.
- 4099 Visser, J.N.J., Colliston, W.P., Terblanche, J.C., 1984. The origin of soft-sediment
4100 deformation structures in Permo-Carboniferous glacial and proglacial beds, South Africa.
4101 Journal of Sedimentary Petrology 54, 1183-1196.
- 4102 Visser, J.N.J., Loock, J.C., Colliston, W.P., 1987. Subaqueous outwash fan and esker
4103 sandstones in the Permo-Carboniferous Dwyka Formation of South Africa. Journal of
4104 Sedimentary Petrology 57, 467-478.
- 4105 Visser, J.N.J., van Niekerk, B.N., van der Merwe, S.W., 1997. Sediment transport of the late
4106 Palaeozoic glacial Dwyka Group in the southwestern Karoo Basin. South African Journal of
4107 Geology 100, 223-236.
- 4108 Volkheimer, W., 1969. Palaeoclimatic Evolution in Argentina and Relations with Other
4109 Regions of Gondwana, in: Amos, A.J. (Ed.), Gondwana Stratigraphy. IUGS Symposium in
4110 Buenos Aires 1967, UNESCO, pp. 551-587.

- 4111 Von Brunn, V., 1977. A furrowed intratillite pavement in the Dwyka Group of northern
4112 Natal. Transactions of the Geological Society of South Africa 80, 125-130.
- 4113 Von Brunn, V., 1994. Glaciogenic deposits of the Permo-Carboniferous Dwyka Group in the
4114 eastern region of the Karoo Basin, South Africa, in: Deynoux, M., Miller, J.M.G., Domack,
4115 E.W., Eyles, N., Fairchild, I.J., Young, G.M. (Eds.), Earth's Glacial Record, Cambridge
4116 University Press, Cambridge, pp. 60-69.
- 4117 Von Brunn, V., 1996. The Dwyka Group in the northern part of Kwazulu/Natal, South
4118 Africa: sedimentation during late Palaeozoic deglaciation. Palaeogeography,
4119 Palaeoclimatology, Palaeoecology 125, 141-163.
- 4120 Von Brunn, V., Stratten, T., 1981. Late Paleozoic tillites of the Karoo Basin of South Africa,
4121 in: Hambrey, M.J., Harland, W.B. (Eds.), Earth's Pre-Pleistocene Glacial Record. Cambridge
4122 University Press, Cambridge, pp. 71-79.
- 4123 Von Gaertner, H.R. 1943. Bemerkungen über den Tillite von Bigganiargga am Varangerfjord,
4124 Geologische Rundschau, 34, 226-231. (Quoted by Bjørlykke, K. 1967. The Eocambrian
4125 "Reusch Moraine" at Bigganjargga and the Geology Around Varangerfjord; Northern
4126 Norway. Norges Geologiske Undersøkelse 251, Oslo, 18-44.)
- 4127 Waitt, R.B., 1989. Swift snowmelt and floods (lahars) caused by great pyroclastic surge at
4128 Mount St Helens volcano, Washington, 18 May 1980. Bulletin of Volcanology 52, 138-157.

- 4129 Walters, J.C., 1978. Polygonal Patterned Ground in Central New Jersey. *Quaternary Research*
4130 10, 42-54.
- 4131 Walton, A.W., Palmer, B.A., 1988. Lahar facies of the Mount Dutton Formation (Oligocene-
4132 Miocene) in the Marysville Volcanic Field, Southwestern Utah. *GSA Bulletin* 100, 1078-
4133 1091.
- 4134 Waters, J.M., Craw, D., 2017. Large kelp-rafted rocks as potential dropstones in the Southern
4135 Ocean. *Marine Geology* 391, 13-19.
- 4136 Watt, S.F.L., Talling, P.J., Vardy, M.E., Masson, D.G., Henstock, T.J., Hühnerbach, V.,
4137 Minshull, T.A., Urlaub, M., Lebas, E., Le Friant, A., Berndt, C., Crutchley, G.J., Karstens, J.,
4138 2012. Widespread and progressive seafloor-sediment failure following volcanic debris
4139 avalanche emplacement: landslide dynamics and timing offshore Montserrat, Lesser Antilles.
4140 *Marine Geology* 323, 69–94.
- 4141 Whipple, K.X., Hancock, G.S., Anderson, R.S., 2000. River incision into bedrock: Mechanics
4142 and relative efficacy of plucking, abrasion and cavitation. *GSA Bulletin* 112, 490-503.
4143 [https://doi.org/10.1130/0016-7606\(2000\)112<490:RIIBMA>2.0.CO;2](https://doi.org/10.1130/0016-7606(2000)112<490:RIIBMA>2.0.CO;2).
- 4144 White, W.M., 2015. *Isotope geochemistry*. John Wiley and Sons, Ltd., Chichester, pp. 277-
4145 363.
- 4146 Whiteside, J.H., Lindström, S., Irmis, R.B., Glasspool, I.J., Schaller, M.F., Dunlavey, M.,
4147 Nesbitt, S.J., Smith, N.D., Turner, A.H., 2015. Extreme ecosystem instability suppressed

- 4148 tropical dinosaur dominance for 30 million years. PNAS 112, 7909-7913.
4149 <https://doi.org/10.1073/pnas.1505252112>.
- 4150 Wilf, P., Little, S.A., Iglesias, A., Del Carmen Zamalao, M., Gandolfo, M.A., Cúneo, N.R.,
4151 Johnson, K.R., 2009. *Papuacedrus* (Cupressaceae) in Eocene Patagonia: a new fossil link to
4152 Australasian rainforests. *American Journal of Botany* 96, 2031-2047.
- 4153 Williams, G.E., 2005. Subglacial meltwater channels and glaciofluvial deposits in the
4154 Kimberley Basin, Western Australia: 1.8 Ga low-latitude glaciation coeval with continental
4155 assembly. *Journal of the Geological Society* 162, 111-124.
- 4156 Wilson, H.H., 1969. Late Cretaceous eugeosynclinal sedimentation, gravity tectonics, and
4157 ophiolite emplacement in Oman Mountains, Southeast Arabia. *AAPG Bulletin* 53, 626-671.
- 4158 Wilson, J.P., White, J.D., Montañez, I.P., DiMichele, W.A., McElwain, J.C., Poulsen, C.J.,
4159 Hren, M.T., 2020. Carboniferous plant physiology breaks the mold. *New Phytologist* 227,
4160 667-679. <https://doi.org/10.1111/nph.16460>.
- 4161 Winterer, E.L., 1964. Late Precambrian pebbly mudstone in Normandy, France: tillite or
4162 tilloid?, in: Nairn, A.E.M. (Ed.), *Problems in Palaeoclimatology*. John Wiley and Sons,
4163 London, pp. 159-178.
- 4164 Winterer, E.L., von der Borch, C.C., 1968. Striated pebbles in a mudflow deposit, South
4165 Australia. *Palaeogeography, Palaeoclimatology, Palaeoecology* 5, 205-211.

- 4166 Wobus, C.W., Crosby, B.T., Whipple, K.X., 2006. Hanging valleys in fluvial systems:
4167 Controls on occurrence and implications for landscape evolution. *Journal of Geophys.*
4168 *Research* 111, F02017. <https://doi.org/10.1029/2005JF000406>.
- 4169 Wohlfarth, B., 2013. A Review of Early Weichselian Climate (MIS 5d-a) in Europe.
4170 Technical Report TR-13-03, Svensk Kärnbränslehantering AB, Stockholm.
4171 <https://skb.se/upload/publications/pdf/TR-13-03.pdf>.
- 4172 Wolfe, J.A., 1977. Paleogene Floras from the Gulf of Alaska Region. U.S. Geological Survey
4173 Professional Paper 997. <https://doi.org/10.3133/pp997>.
- 4174 Woodcock, N.H., 1979. Sizes of submarine slides and their significance. *Journal of Structural*
4175 *Geology* 1, 137–142.
- 4176 Woodworth-Lynas, C.M.T., 1992. The Geology of Ice Scour (Ph.D. thesis). University of
4177 Wales, Bangor.
- 4178 Woodworth-Lynas, C.M.T., 1996. Ice scour as an indicator of glaciolacustrine environments,
4179 in: Menzies, J. (Ed.), *Past Glacial Environments: Sediments, Forms and Techniques*.
4180 Butterworth Heinemann, Oxford, pp. 161-178.
- 4181 Woodworth-Lynas, C.M.T., Dowdeswell, J.A., 1994. Soft-sediment striated surfaces and
4182 massive diamicton facies produced by floating ice, in: Deynoux, M., Miller, J.M.G., Domack,
4183 E.W., Eyles, N., Fairchild, I.J., Young, G.M. (Eds.), *Earth's Glacial Record*. Cambridge
4184 University Press, Cambridge, pp. 241-259. <https://doi.org/10.1017/CBO9780511628900.019>.

- 4185 Woodworth-Lynas, C.M.T., Guigné, J.Y., 1990. Iceberg scours in the geological record:
4186 examples from glacial Lake Agassiz, in: Dowdeswell, J.A., Scource, J.D. (Eds.), *Glacimarine*
4187 *Environments: Processes and Sediments*. Geological Society, London, Spec. Publ. 53, pp.
4188 217-223.
- 4189 Woodworth-Lynas, C.M.T., Simms, A., Rendell, C.M., 1985. Iceberg grounding and scouring
4190 on the Labrador Continental Shelf. *Cold Regions Science and Technology* 10, 163-186.
- 4191 Woolfe, K.J., 1994. Cycles of erosion and deposition during the Permo-Carboniferous
4192 glaciation in the Transantarctic Mountains. *Antarctic Science* 6, 93-104.
- 4193 Wright, R., Anderson, J.B., Fisco, P.P., 1983. Distribution and association of sediment
4194 gravity flow deposits and glacial/glacial-marine sediments around the continental margin of
4195 Antarctica, in: Molnia, B.F. (Ed.), *Glacial-Marine Sedimentation*. Plenum Press, New York,
4196 pp. 265-300.
- 4197 Yang, B., Shi, G.R., Lee, S., Luo, M., 2018. Co-occurrence patterns of ice-rafted dropstones
4198 and brachiopods in the Middle Permian Wandrawandian Siltstone of the southern Sydney
4199 Basin (southeastern Australia) and palaeoecological implications. *Journal of the Geological*
4200 *Society* 175, 850-864. <https://doi.org/10.1144/jgs2018-010>.
- 4201 Yassin, M.A., Abdullatif, O.M., 2017. Chemostratigraphic and sedimentologic evolution of
4202 Wajid Group (Wajid Sandstone): An outcrop analog study from the Cambrian to Permian,
4203 SW Saudi Arabia. *Journal of African Earth Sciences* 126, 159-175.

- 4204 Yawar, Z., Schieber, J., 2017. On the origin of silt laminae in laminated shales. *Sedimentary*
4205 *Geology* 360, 22-34.
- 4206 Ye, Q., Tong, J., Xiao, S., Zhu, S., An, Z., Tian, L., Hu, J., 2015. The survival of benthic
4207 macroscopic phototrophs on a Neoproterozoic snowball Earth. *Geology* 43, 507–510.
4208 <https://doi.org/10.1130/G36640.1>.
- 4209 Yehle, L.A., 1954. Soil tongues and their confusion with certain indicators of periglacial
4210 climate. *American Journal of Science* 252, 532-546.
- 4211 Yincan., Y. et al., 2017. *Marine Geo-Hazards in China*. China Ocean Press, Elsevier Inc., pp.
4212 193-194. <https://doi.org/10.1016/B978-0-12-812726-1.00006-1>.
- 4213 Youbi, N., Ernst, R.E., Mitchell, R.N., Boumehdi, M.A., Moume, W.E., Lahna, A.A.,
4214 Bensalah, M.K., Söderlund, U., Doblus, M., Tassinari, C.C.G., 2021. Preliminary appraisal of
4215 a correlation between glaciations and large igneous provinces over the past 720 million years,
4216 in: Ernst, R.E., Dickson, A.J., Bekker, A (Eds.), *Large Igneous Provinces: A Driver of Global*
4217 *Environmental and Biotic Changes*. Geophysical Monograph 255, The American Geophysical
4218 Union and John Wiley and Sons, Inc., pp. 169-190.
4219 <https://doi.org/10.1002/9781119507444.ch8>.
- 4220 Young, G.M., 1981a. The Early Proterozoic Gowganda Formation, Ontario, Canada, in:
4221 Hambrey, M.J., Harland, W.B. (Eds.), *Earth's Pre-Pleistocene Glacial Record*. Cambridge
4222 University Press, Cambridge, pp. 807-812.

- 4223 Young, G.M., 1981b. Diamictites of the Early Proterozoic Ramsay Lake and Bruce
4224 Formations, north shore of Lake Huron, Ontario, Canada, in: Hambrey, M.J., Harland, W.B.
4225 (Eds.), Earth's Pre-Pleistocene Glacial Record. Cambridge University Press, Cambridge, pp.
4226 813-816.
- 4227 Young, G.M., 2013. Precambrian supercontinents, glaciations, atmospheric oxygenation,
4228 metazoan evolution and an impact that may have changed the second half of Earth history.
4229 *Geoscience Frontiers* 4, 247-261.
- 4230 Young, G.M., Minter, W.E.L., Theron, J.N., 2004a. Geochemistry and palaeogeography of
4231 upper Ordovician glaciogenic sedimentary rocks in the Table Mountain Group, South Africa.
4232 *Palaeogeography, Palaeoclimatology, Palaeoecology* 214, 323–345.
- 4233 Young, G.M., Shaw, C.S.J., Fedo, C.M., 2004b. New evidence favouring an endogenic origin
4234 for supposed impact breccias in Huronian (Paleoproterozoic) sedimentary rocks. *Precambrian*
4235 *Research* 133, 63-74. <https://doi.org/10.1016/j.precamres.2004.03.013>.
- 4236 Zaki, A.S., Giegengack, R., 2016. Inverted topography in the southeastern part of the Western
4237 Desert of Egypt. *Journal of African Earth Sciences* 121, 56-61.
4238 <https://doi.org/10.1016/j.jafrearsci.2016.05.020>.
- 4239 Zaki, A.S., Pain, C.F., Edgett, K.E., Giegengack, R., 2018. Inverted stream channels in the
4240 Western Desert of Egypt: Synergistic remote, field observations and laboratory analysis on
4241 Earth with applications to Mars. *Icarus* 309, 105-124.
4242 <https://doi.org/10.1016/j.icarus.2018.03.001>.

- 4243 Zaki, A.S., Giegengack, R., Castellort, S., 2020. Inverted channels in the Eastern Sahara –
4244 distribution, formation, and interpretation to enable reconstruction of paleodrainage
4245 networks, in: Herget, J., Fontana, A. (Eds.), *Palaeohydrology, Geography of the Physical*
4246 *Environment*. Springer, Cham, pp. 117-134. https://doi.org/10.1007/978-3-030-23315-0_6.
- 4247 Zaki, A.S., Pain, C.F., Edgett, K.E., Castellort, S., 2021. Global inventories of inverted
4248 stream channels on Earth and Mars. *Earth-Science Reviews* 216, 103561.
4249 <https://doi.org/10.1016/j.earscirev.2021.103561>.
- 4250 Zalasiewicz, J., Taylor, L., 2001. Deep-basin dropstones in the early Silurian of Wales: a clue
4251 to penecontemporaneous, near-shore algal forests. *Proceedings of the Geologists' Association*
4252 112, 63-66. [https://doi.org/10.1016/S0016-7878\(01\)80050-X](https://doi.org/10.1016/S0016-7878(01)80050-X).
- 4253 Zavala, C., 2019. The new knowledge is written on sedimentary rocks – a comment on
4254 Shanmugam’s paper ‘The hyperpycnite problem’. *Journal of Palaeogeography* 8, 23.
4255 <https://doi.org/10.1186/s42501-019-0037-3>.
- 4256 Zavala, C., 2020. Hyperpycnal (over density) flows and deposits. *Journal of Palaeogeography*
4257 9, 17. <https://doi.org/10.1186/s42501-020-00065-x>.
- 4258 Zavala, C., Arcuri, M., 2016. Intrabasinal and extrabasinal turbidites: origin and distinctive
4259 characteristics. *Sedimentary Geology* 337, 36–54.
4260 <https://doi.org/10.1016/j.sedgeo.2016.03.008>.

- 4261 Zecchin, M., Catuneanu, O., Rebesco, M., 2015. High-resolution sequence stratigraphy of
4262 clastic shelves IV: High-latitude settings. *Marine and Petroleum Geology* 68A, 427-437.
4263 <https://doi.org/10.1016/j.marpetgeo.2015.09.004>.
- 4264 Zimmermann, U., Tait, J., Crowley, Q.G., Pashley, V., Straathof, G., 2011. The Witputs
4265 diamictite in southern Namibia and associated rocks: constraints for a global glaciation?
4266 *International Journal of Earth Sciences*, 100, 511-526.
4267 <https://doi.org/10.1007/s00531-010-0621-3>.

4268 **Supplementary material: Tables**

4269	Place and/or environment	Percentage striated clasts	Interpretation or comment	Reference
4271	Sediment gravity flow	19 of 19 clasts were striated.	One chert and the rest softer sedimentary clasts.	Winterer, 1964.
4273	Sediment gravity flow	Almost 50%.	Ca. 1% of the grains were larger than sand, so one would not expect to find many striated clasts, even if all the striated clasts were sedimentary.	Winterer and von der Borch, 1968.
4275	Tills and “tillites”	1-5% or 10-20%.		Anderson, 1983; Schermerhorn, 1974a.
4276	Carboniferous “glacial” conglomerate	15-20% striated.		Anderson, 1983.
4279	Late Paleozoic, “glaciogenic”	48% striated.	Mostly sub-parallel but also scattered.	Rocha-Campos and Santos, 1981.
4281	Paleoproterozoic “glaciogenic”	Rare striations, and a few clasts that display facets.	Conglomerate above grooved soft sand surfaces.	Williams, 2005.
4283	Carboniferous, “glaciogenic”	5-20% and up to 80%.		Visser, 1982; Hall and Visser, 1984; Visser et al., 1987.

4285	East Antarctica,	12% striated.		Anderson, 1983.
4286	continental shelf			
4287	Ross Sea shelf	60% striated or faceted;		Hall, 1989.
4288	area	in redeposited conglomerate 21% were striated and 4% faceted.		
4289	Antarctic shelf,	57% striated, 80%		Hall, 1989.
4290	McMurdo Sound	faceted.		
4291	Many different	0.1% - 80%, mostly 10-		Atkins, 2003, 2004.
4292	Quaternary	40%.		

4293 Table S1. Striations on clasts from different environments.

4294	Location in	Structure, comment	Reference
4295	ancient “glacial”		
4296	environments		
4297	Very common in	Soft sediment striations and surfaces, within	Bigarella et al., 1967; Lindsay, 1970a;
4298	pre-Pleistocene	or on top of sediments, including within	Schermerhorn, 1970, 1971; Fairbridge, 1971;
4299	diamictites from	“tillites.” Striations/grooves on all bedrock	Deynoux and Trompette, 1976; Frakes, 1979;
4300	all ages,	surfaces are commonly perfectly parallel.	Visser and Loock, 1982; Visser, 1983b; Visser
4301	worldwide (a, b		et al., 1987, Deynoux and Ghienne, 2004; Le
4302	and c from the		Heron et al., 2005, 2010, 2018a, 2018b, 2019b,
4303	list, and these are		2020; Keller et al., 2011; Vesely and Assine,
4304	all displayed by		2014, list of 17 places; Rosa et al., 2016, 2019;
4305	most of these		Molén, 2017; Alonso-Muruaga et al., 2018;
4306	striated surfaces		Assine et al., 2018; Dietrich and Hofmann,
4307	that is referred		2019; Caputo and Santos, 2020; Isbell et al.,
4308	to).		2021; López-Gamundí et al., 2021; Molén and
4309	Common (as	Striations and grooves superimposed,	Frakes and Crowell, 1969, 1970; Lindsay,
4310	described in list,	stacked, on many beds above each other,	1970a; Flint, 1975; Deynoux and Trompette,
4311	letter d).	commonly in soft sand.	1976; Von Brunn, 1977; Biju-Duval et al.,
			1981; Moncrieff and Hambrey, 1988; Visser and
			Loock, 1988; Visser, 1988, 1989b; Deynoux
			and Ghienne, 2004; Le Heron et al., 2004, 2005,
			2006, 2010, 2018b, 2020; Keller et al., 2011;
			Vesely and Assine, 2014; Assine et al., 2018;
			Caputo and Santos, 2020; Molén and Smit,
			2022.

4312	South Africa,	Sediment strings turn into grooves or	Molén and Smit, 2022.
4313	LPIA (a, b, c, d	striations. Three of four studied striated	
4314	and e in list.)	surfaces did not display any diamictites in the surrounding areas.	
4315	Brazil, LPIA (a,	Many striated surfaces, the largest covers	Rosa et al., 2019.
4316	b, c and f).	2500 m ² . Displaying soft sediment slickensides from sliding (similar to Isbell et al., 2001), flutes and grooved tops of diamictites, sand slumps (interpreted to be from “icebergs”; but compare to Molén and Smit, 2022) and “anastomosing shear planes,” inside diamictite or at surfaces.	
4317	Brazil, LPIA (a,	In one or more triple stacked striated	Trosdorf et al., 2005a, 2005b.
4318	b, c, d and e).	surfaces: Straight, parallel, bypass zones, stacked, small sand flows cover striations, ripples next to striations. Interpreted to be a tidal water glacier.	
4319	China (a, b, c, d.)	Bifurcating striae	Le Heron et al., 2018b, 2019a; Chen et al., 2020; compare to Molén and Smit, 2022.
4320	Botswana, LPIA	The “original ground moraine” is interpreted	Frakes and Crowell, 1970.
4321	(c in list).	to have been “stripped off” from striated surface before mudflows were deposited.	
4322	Antarctica,	Soft sediment surfaces are grooved or	Lindsay, 1970a.
4323	Permian (b, d, e	striated only if a thin veneer of sorted	
4324	in list).	sediment is lying directly on top of the surfaces. At places where the sorted sediment disappear the striations also disappear.	

4325	South Africa,	1) Striations continued unbroken from the	1) Flint, 1961. 2) Visser, 1988. 3) Visser, 1988;
4326	LPIA and Sahara,	top of a “tillite” into the striations on the	Visser and Loock, 1988; Deynoux and Ghienne,
4327	Ordovician (a, b,	surface below. 2) Striations passed from lava	2004 (Sahara, Ordovician). 4) Von Brunn, 1977.
4328	c, d and e in list).	to a triple stacked soft sediment surface. 3) Thin beds of sand, mud or laminated sediment directly overlying striated surface. 4) Stratigraphy is: Grooved “tillite” surface, mudstone, “tillite.” 5) Soft sediment surface cut in ripple laminated siltstone. 6) Fossil plants between striated surface and “tillite.” 7) A soft sediment surface, draped with mudrock displaying crustacean track ways, which transforms upwards to diamictite. Comment: All these structures may form by SGFs, but not below glaciers.	5) Visser, 1983b. 6) du Toit, 1926; Sandberg, 1928. 7) Von Brunn, 1996.
4329	Ethiopia, LPIA	Traction carpet on a polished surface,	Bussert, 2010.
4330	(b, c and e).	stacked striated surfaces (but this was not recognized in article, their Fig. 6A.)	
4331	Argentina (b, d).	Intertill and intratill soft sediment surfaces, occasionally tectonic and glacial striations on the same surfaces.	González and Glasser, 2008.
4332	South America in	1) Striations display the same direction as	1-2) Frakes and Crowell, 1969. 3) Isotta et al.,
4333	1-2) LPIA and 3)	foliation in underlying gneiss. 2)	1969; Frakes, 1979.
4334	Upper	Slickensides pass straight into the striations	
4335	Precambrian (a, c,	on a surface. 3) A 180 000 m ² surface show	
4336	g).	parallel “glacial” grooves which occasionally exhibit “overhanging” walls. Comment: Appear to be at least partly tectonic.	

4337	Cameroon,	Stacked (“staircase”), no glaciogenic	Caron et al., 2011.
4338	Neoproterozoic	deposits, on siltstone and limestone.	
4339	(a, b, c, d).		
4340	Sahara, Saudi	1) Abundance of striations and grooves in	1) Schermerhorn, 1970, 1971. 2) Fairbridge,
4341	Arabia,	spite of the fact that there are very few clasts	1971, 1979. 3) Le Heron et al., 2004.
4342	Ordovician (a, b,	in the “tillite.” 2) At right angles or oblique	
4343	c, d).	to grooves; there are in places minor ripples.	
		3) Striations within current rippled and	
		laminated sandstone.	
		Comment: Would be possible if the origin is	
		by SGF.	
4344	Saudi Arabia,	One picture shows striations that are very	Keller et al., 2011, their Fig 12e.
4345	Ordovician.	irregular.	
		Comment: These display similarities to	
		striations made by volcanic flows or tectonic	
		movements (e.g., Pierson et al., 1990,	
		Rainbird 1993, Glicken 1996, Eyles and	
		Boyce 1998, Atkins 2003).	
4346	West Africa, Late	One 1 cm layer of sandstone with ripple-	Trompette, 1981.
4347	Precambrian (e).	marks is interposed in between the “tillite”	
		and the striated surface.	
		Comment: This can be suspected from	
		deposition of debris flows in water.	
4348	Canada,	Striated surfaces and boulders are probably	Bielenstein and Eisbacher, 1969; Harker and
4349	Gowganda Fm,	of tectonic origin.	Giegengack, 1989; Miall, 1985.
4350	Paleoproterozoic		
4351	(g).		
4352	Canada and South	Occasionally the “tillite” is stratified	Schenk, 1965; Isotta et al., 1969.
4353	America,	immediately above the surfaces.	
4354	Precambrian.	Comment: This indicates deposition from	
		SGFs.	

4355	Australia,	Comment: Some believe that these surfaces	Daily et al., 1973; Coats and Preiss, 1987.
4356	Paleoproterozoic.	are tectonic, others that they are partially tectonic and partially glacial.	
4357	Australia, Late	Grooves etc. in soft sediment sand are	Williams, 2005.
4358	Proterozoic (c).	interpreted to be formed by meltwater or glaciers. Conglomerate deposited on top of the sand display the same transport direction as the grooves. No evidence of any other glaciogenic proxies. Comment: Except for a few examples, similar grooves do not form by meltwater and glaciers, but all may be from SGFs.	
4359	Chile, Cretaceous.	Surface/contact zone exhibit both striations and ripple-marks. Comment: Has been reinterpreted as formed by turbidity currents or mudflows.	Cecioni, 1957, 1981; Sanders and Cecioni, 1957; Scott, 1966.
4360	Norway, Late	2 mm push up rinds around striations,	1) Molén, 2017. 2) Rice and Hofmann, 2000. 3)
4361	Proterozoic.	recently weathered out clasts, mud-flake imprints. Comment: 1) The evidence suggests a soft surface. Point 2-4 below are explanations based on a glaciogenic interpretation. 2). "... the striated platform (...) is c. 150 Ma older than the overlying diamictite." 3) Quick melting and "instantaneous" lithification at a temperature > 1000°C. 4) A piece of till dropped from an iceberg and landed on top of the striations.	Bestmann et al., 2006. 4) Mentioned by Bjørlykke, 1967; as interpreted by von Gaertner, 1943.
4362	Worldwide.	Glaciogenic striations. Displaying changing vertically and horizontally movement directions.	Not clearly documented before the Pleistocene.

4363 Table S2. Striated surfaces/pavements which are all commonly interpreted to be from
 4364 glaciation. All these surfaces conform well with an origin from mass transport, mainly from
 4365 cohesive SGFs, but not with a glaciogenic origin. The table is not documenting every single
 4366 occurrence of any surface structure from all mentioned areas, because then it would be very
 4367 extensive. Some striated surfaces are referred to in more than one row, if many features are
 4368 documented. The letters, a-g, are the criteria described in the list in section 2.5.

Place	Age	1/3-2/3 penetration	Small size of dropstones (cm)	Small compared to other sediments size of dropst	Clasts within single bed	Correlation between clast on top and sediment thickness	Fabrics transport in	Relative horizontal measurements of sediments	Push structures next to clast	Sediment thickens next to clasts	Dips out much penetrated	around Reference and/or
		a	b	b	c	d	e	f	f, g	f, g	f, g	
4369 Brazil	LPIA	N	<1 to 40	Y	Y					Y	Y	1
4370 Argen-	LPIA	N			Y			Y		Y	Y	2
4371 tina												
4372 Ethiopia	LPIA	N	Often cm		Y					Y	Y	3
4373 Malaysia	LPIA	N	0.5-20							Y	Y	4
4374 S-Africa,	LPIA	N	>2-5, but	Y	Y					Y	Y	5
4375 Namibia			> meter									
4376 Brazil	Dev	N	2							Y		6
4377 China	Cam	N	Few cm				Y		Y	Y	Y	7
4378 China	Neo	N	Y	Y							Y	8
4379 Namibia	Neo	N	Y (N)	Y (N)	Y	Y		Y		Y	Y	9
4380 Namibia	Neo	N			Y			Y	Y	Y	Y	10
4381 Namibia	Neo	N	Y		Y					Y	Y	11
4382 Namibia	Neo	N	< 2	Y	Y			Y		Y	Y	12
4383 Scotland	Neo	N	3.5-9		Y		Y			Y	Y	13
4384 Canada	Neo	N	most 1-4	Y	Y	Y		Y	Y	Y	Y	14

lasts but not

4386	Tasma-	Neo	N	most cm	Y							Y	15
4387	nia												
4388	India	Pal	N	Few cm			Y						16

4389 Table S3. The table document examples of areas displaying clasts from pre-Pleistocene
4390 formations which had been interpreted as glaciogenic dropstones in the papers which are
4391 referred to, or in the majority of published papers describing the same formation. Lonestones
4392 from sedimentary sequences which have been fully explained as from SGFs, even if there
4393 may be some different opinions, are not in the table. Often reports of dropstones only mention
4394 just that word. In other reports only superficial similarities between dropstones and observed
4395 clast are mentioned, and commonly there are no detailed descriptions of the clasts which are
4396 interpreted to be dropstones. Therefore, it is difficult to find extensive data for this table, and
4397 some interpretations may be conjectural, only because too little data have been documented in
4398 the original reports. In the table appearances of dropstones which may not be mentioned in
4399 the original publication, but which are evident from published photographs, are tabulated.

4400 Examples of appearances of dropstones and sedimentary structures displayed around these
4401 clasts, from each research area, are documented in the different columns of the table. Not all
4402 lonestones from each area display all the appearances documented (which would be
4403 impossible), but may be predominant examples. The letters a-g in the columns refers to the
4404 descriptions in the list of features, with comments (section 2.13.3.). There may be clasts in the
4405 research areas which may display appearances that are compatible with any kind of transport,
4406 but the tabulated structures are those better compatible with transport by SGFs but less
4407 common or highly implausible from simple rafting in slowly moving or standing water. The
4408 data in the table do not show examples of exceptions of single or a few clasts which may have
4409 been deposited by any agent, if there is an abundance of clasts. Instead, the documented clasts

4410 display the structures which may be in majority, or are otherwise reported in the referred
4411 articles, or possible only are photographed as typical for the area or formation. Therefore the
4412 table is partly conjectural and does not display definite documentation from each area. And
4413 further, the documentation from the different research areas does not include all data which
4414 may be of relevance, e.g., not the difference between the clast size of dropstones compared to
4415 clast size in other sediments, or other features which could be documented in the table,
4416 because such data is seldom published.

4417 Despite the shortcomings in the documentation from different research areas, the sedimentary
4418 structures in the table are more or less incompatible with an interpretation of simple rafting by
4419 ice or any other rafting agent. It is possible to draw the conclusion that too many clasts have
4420 been reported as dropstones even if the full evidence for this interpretation is not available. In
4421 conclusion, the data in the table are as well documented as the descriptions provided in the
4422 original reports and therefore may be possible to use in evaluation of different interpretations.

4423 Dev = Devonian.

4424 Cam = Cambrian.

4425 Neo = Neoproterozoic.

4426 Pal = Paleoproterozoic.

4427 N = Not documented as present. (Within paranthesis = exceptions.)

4428 Y = Documented, present.

4429 No sign = not mentioned or shown in the original publications.

4430

4431 References: 1. Aquino et al, 2016; Vesley et al., 2018, 2021; Tedesco et al., 2020. 2. Schatz et
4432 al., 2011; Valdez Buso et al., 2021. 3. Bussert, 2014. 4. Baioumy, et al., 2020. 5. Commonly
4433 2-5 cm, rarely up to one meter, but in massive “glaciomarine” diamictites they may be a few
4434 meters. Visser, 1982, 1983b; Visser and Kingsley, 1982; Tavener-Smith and Mason, 1983;
4435 Haldorsen et al., 2001; Isbell et al., 2021. 6. Caputo and Santos, 2020. 7. Le Heron et al.,
4436 2018b. 8. Chen et al., 2021. 9. Hoffman and Halversen, 2008; Hoffman et al., 2021 (Ghaub).
4437 10. Domack and Hoffman, 2011 (Ghaub). 11. Bechstädt et al., 2018 (Ghaub). 12. Hoffman
4438 and Halversen, 2008; Le Heron et al., 2021a (Chuosi); see also Martin et al., 1985. 13. Hartley
4439 et al., 2020. 14. Molén, 2021. 15. Hoffman et al., 2009. 16. Rodríguez-López et al., 2021.